Chemotherapy of candidiasis: study of ABC transporter-mediated azole resistance and identification of a novel antifungal therapeutic strategy

Tan Ning (Sarah) TSAO

Department of Biochemistry

McGill University, Montreal

December, 2010

A thesis submitted to McGill University in partial fulfillment of the requirements of the degree of Ph.D.

Acknowledgement

First of all, I would like to give a big thank to my supervisor, Dr. Martine Raymond, for giving me an opportunity to pursue my PhD study on ABC transporters in her lab. I also thank her for her valuable suggestions, guidance and encouragement during my study. I have learned about perseverance and precision from her throughout these years, which are invaluable lessons to a PhD student. I would also like to thank my co-director, Dr. Bernard Turcotte and my thesis committee members Drs. Philippe Gros and Michel Bouvier, for providing clear and constructive comments on my projects.

Thanks to all past and present members of the Raymond lab for many fruitful discussions on ideas of both scientific and sociological interests. A big thank to Sandra Weber, for keeping the lab in order and for too many other things that are too long to list here. Thanks to members from the Verreault's lab, especially Dr. Alain Verreault, Dr. Hugo Wurtele and Eun-Hye Lee, with whom I had a great collaboration on the study of Histone H3K56ac in *C. albicans*. Thanks to the Institut de recherche en immunologie et en cancérologie (IRIC) for hosting me during my Ph.D. studies. Thanks to the Department of Biochemistry, McGill University, for providing this PhD program and I am grateful for the travel award provided by the department. I also thank the *Candida* community for setting up the *Candida* Genome Database, an important tool for my research that I took it for granted.

Last but not the least, I would like to express my deepest gratitude to my family, mum, dad and Simon for supporting me from a distance of 7000-9000 Miles away. To my friends, Erwin Lamping, Katharina Trunk, Sophie Desmeules and Marianne Desrosiers for countless coffee times, laughter and emotional support. To Alex, for his patience, support, support and support during this last year and the writing period.

Abstract

Candida albicans is a major fungal pathogen that causes systemic bloodstream infections with high mortality rate in immune-compromised patients. Current treatment of candidiasis involves the use of azoles (the most widely used antifungal agents that target ergosterol biosynthesis) and echinocandins (the latest approved drugs that target cell wall). However, the efficacy of these drugs can be compromised by the emergence of *C. albicans* drug-resistant strains. Thus, understanding the molecular mechanisms of azole resistance as well as identifying new biological targets are important for the development of novel and effective therapeutic strategies. In this thesis, I report our research findings on the contribution of ABC transporters Cdr1p and Cdr2p to azole resistance in a clinical azole resistant strain and show that Cdr1p is a major determinant of azole resistance. Furthermore, we also discovered that phosphorylation plays a positive regulatory role on Cdr1p function and is important for Cdr1p-mediated azole resistance. In an effort to search for new antifungal targets, we explored the function of genes involved in the acetylation of histone H3 lysine 56 (H3K56) in *C. albicans*. We found that the gene encoding H3K56 deacetylase Hst3p is essential for cell growth and survival of *C. albicans*. Inhibition of Hst3p using nicotinamide, a form of vitamin B3, is fungicidal for both drug-susceptible and drug-resistant *C. albicans* as well as another important human fungal pathogen *Aspergillus fumigatus*, making it a promising target to develop a novel class of antifungal agents with broad antifungal properties. Taken together, these studies provide fundamental knowledge of molecular determinants contributing to *C. albicans* azole resistance and pathogenesis.

Résumé

Candida albicans est un pathogène fongique responsable d'infections systémiques dont le taux de mortalité est élevé chez les patients immunocompromis. À l'heure actuelle, le traitement de la candidose est rendu possible par l'utilisation de deux classes d'agents antifongiques aux modes d'actions distincts : les azoles (les plus couramment utilisés, ils ciblent la biosynthèse de l'ergostérol) et les échinocandines (nouvellement mises sur le marché, elles interfèrent avec la synthèse de la paroi fongique). Toutefois, face à l'émergence de résistances développées par certaines souches de *C. albicans* l'efficacité de ces antifongiques se trouve compromise. Il est donc capital de mieux comprendre les mécanismes moléculaires impliqués dans la résistance aux azoles, ainsi que d'identifier de nouvelles cibles biologiques pour permettre le développement d'approches thérapeutiques innovantes et efficaces. Dans ce manuscrit de thèse, je décris nos travaux portant sur la contribution relative des transporteurs ABC Cdr1p et Cdr2p à la résistance aux azoles en utilisant une souche clinique résistante de *C. albicans*, et démontre que Cdr1p contribue majoritairement à cette résistance. D'autre part, nous montrons que la phosphorylation a un effet positif sur la régulation de Cdr1p, et également que cette modification post-traductionnelle joue un rôle important dans la résistance aux azoles Cdr1p-dépendante. Dans l'optique d'identifier de nouvelles cibles antifongiques, nous avons étudié la fonction des gènes impliqués dans l'acétylation de la lysine 56 de l'histone H3 (H3K56) chez *C. albicans*. Nous avons découvert que le gène codant pour la déacétylase de H3K56, à savoir Hst3p, est essentiel pour la survie et la croissance cellulaire chez *C. albicans*. L'inhibition de Hst3p par la nicotinamide, une forme de vitamine B3, a un effet fongicide sur de multiples souches de *C. albicans,* qu'elles soient normales ou résistantes aux médicaments, ainsi que sur un autre pathogène important chez l'humain, *Aspergillus fumigatus*, faisant de cette enzyme une cible prometteuse pour le développement de nouveaux agents antifongiques à large spectre. L'ensemble des connaissances fondamentales générées au cours de mes

travaux de doctorat permettra de mieux comprendre certains déterminants moléculaires clés qui contribuent à la résistance de *C. albicans* envers les médicaments azolés, ainsi qu'à sa pathogénicité.

Table of contents

List of figures

List of tables

List of abbreviations

a.a.	amino acid(s)
ABC	ATP-binding cassette
AMB	amphotericin B
ATP	adenosine triphosphate
bp	base pair(s)
CDR	*Candida* drug resistance
CGD	*Candida* genome database
CFW	calcofluor white
CTL	control
CSF	caspofungin
DAPI	4',6-diamidino-2-phenylindole
DOXY	doxycycline
DNA	deoxyribonucleic acid
EtBr	ethidium bromide
FLC	fluconazole
FPZ	fluphenazine
gDNA	genomic DNA
H3K56	histone 3 lysine 56
H3K56ac	acetylated histone 3 lysine 56
HU	hydroxyurea
ITC	itraconazole
kb	kilobase (1000 nucleotides)
kDa	kilodalton
KTC	ketoconazole
Mb	megabases (1 million nucleotdies)
MCF	micafungin
MDR	multidrug resistance
MFS	major facilitator
MIC	minimal inhibitory concentration
MMS	methyl methane sulfonate
MS	mass spectrometry
NA	nicotinic acid
NAC	*N*-acetyl-$_{L}$-cysteine
NAM	nicotinamide
NBD	nucleotide-binding domain
NTE	N-terminal extension
ORF	open reading frame
PDR	pleiotropic drug resistance
PC / PE / PS	phosphatidylcholine, -ethanolamine, -serine
P-gp	P-glycoprotein
PI	propidium iodide
R6G	rhodamine 6G
RNA	ribonucleic acid

SDS-PAGE	sodium dodecyl sulfate-polyacrylamide gel electrophoresis
SEM	standard error of the mean
TM	transmembrane segment
TMD	transmembrane domain
VitC	vitamin C
WT	wild-type

Contribution of authors

Chapter II. Relative contributions of the *Candida albicans* ABC transporters Cdr1p and Cdr2p to clinical azole resistance

Tsao S, Rahkhoodaee F, Raymond M. Antimicrobiol Agents Chemotherapy, 53:1344-52 (2009).

ST constructed all mutant strains (cloning and sequencing plasmid constructs) and carried out Southern and Northern blotting, membrane protein extraction and Western blotting experiments. ST performed drug susceptibility assays (MIC and spot assays) with technical assistance from FR. ST prepared all figures and wrote the manuscript with MR. MR oversaw the work.

Chapter III. Identification and characterization of N-terminal phosphorylation sites in the *Candida albicans* ABC transporter Cdr1p

Tsao S, Nehme D, Ahmadzadeh E, Weber S and Raymond M. Manuscript in preparation.

ST and SW constructed the Cdr1p revertant plasmid. ST constructed all mutant strains and performed all experiments as shown in the manuscript except EA performed nile red transport assay (Figure III.5a) and DN performed ATPase assay (Figure III.5b). ST prepared all figures and wrote the manuscript with MR. MR oversaw the work.

Chapter IV. Modulation of histone H3 lysine 56 acetylation as an antifungal therapeutic strategy

Wurtele H*, Tsao S*, Lépine G, Mullick A, Tremblay J, Drogaris P, Lee EH, Thibault P, Verreault A, Raymond M. Nature Medicine, 16:774-80 (2010).

ST and HW designed and performed most experiments; specifically, ST performed experiments for Figure IV.1e, Figure IV.2f, Figure IV.3, Figure IV.4b-d, Figure IV.5 and Supplemental Figures IVS.1g, f, and IVS.4. ST carried out fungal load and cytokine analyses with JT for Figure IV.4.6c-d and Supplemental Table IVS.4. GL constructed the yeast strains used in this study. AM and MR

designed and supervised the mouse studies. PD, PT and AV designed and performed mass spectrometry experiments. EHL provided technical support. HW and ST prepared all figures and wrote the manuscript with AV and MR; HW and ST contributed equally to this work. AV and MR oversaw the work and shared senior authorship.

Presentation

This is a manuscript-based thesis consisting of five chapters. In Chapter I, I provide a brief overview of major human fungal pathogens and currently available antifungal chemotherapeutic strategies. While the use of azoles for treating *Candida* infections (candidiasis) is the most common practice, *C. albicans* can survive in the presence of azoles by developing resistance mechanisms including the overexpression of drug efflux pumps belonging to the ATP binding cassette (ABC) transporter family. My research focuses on two aspects of candidiasis chemotherapy: investigation of the molecular mechanisms involved in ABC transporter-mediated azole resistance for developing reversal strategies of azole resistance; and characterization of genes with important functions for *C. albicans* cell growth and virulence, as it could lead to the discovery of novel antifungal targets. In Chapter II, I present the relative contributions of ABC transporters Cdr1p and Cdr2p to azole resistance in a *C. albicans* clinical isolate (published in Antimicrobial Agents and Chemotherapy: PMID 19223631). In Chapter III, I show that Cdr1p is phosphorylated, and in addition, I identified specific phosphorylation sites that are important for positive regulation of Cdr1p activity as well as Cdr1p-mediated azole resistance. In Chapter IV, I present characterization of novel genes involved in histone modification (H3K56 acetylation) and provide evidence supporting a novel antifungal therapeutic strategy by harnessing H3K56 acetylation (published in Nature Medicine: PMID 20601951). Finally, in Chapter V, I discuss similarities and differences in the function and regulation of Cdr1p and Cdr2p, highlighting the challenges and potential pitfalls in developing ABC transporter inhibitors for candidiasis chemotherapy. I also present my views in supporting the finding of H3K56 acetylation modulators as a broad-spectrum antifungal therapeutic strategy.

Chapter I

Introduction

Chapter I Introduction

The Fungi Kingdom includes some of the most important organisms, both in terms of their ecological and economical roles that shape our life. Fungi provide numerous frequently used antibiotics, such as penicillin as well as food like mushrooms, bread, champagne and beer. We live in an environment intimately associated with fungi at every level, it is rather unfortunate that occasionally fungi can cause human diseases, with clinical conditions ranging from superficial skin colonization in healthy adults to a life-threatening invasive fungal infection (mycosis) among those who are immunosuppressed or hospitalized with serious underlying diseases.

A major increase in the number of fungal diseases has been documented since the mid-1900s. This trend is correlated with major medical developments, such as the widespread use of potent antimicrobial agents, corticosteroids, cytotoxic chemotherapeutic agents, rendering patients highly susceptibile to fungal infections. Clinical data has shown that high-risk groups prone to mycoses include individuals undergoing hematopoietic stem cell transplantation, solid organ transplantation, immunosuppressive therapy, antibacterial therapy and those with AIDS (Pfaller *et al.* 2010). The most commonly encountered fungal pathogens include *Candida albicans*, *Aspergillus fumigatus*, *Cryptococcus neoformans* and *Histoplasma capsulatum*; although the list of potential fungal pathogens is ever expanding.

It is not a trivial task to treat fungal infections since fungi are eukaryotes that share genetic similarity to humans. Currently, there are a few antifungal agents for treating fungal infections, however their efficacies are compromised with the frequent development of antifungal resistance. The present thesis describes the use of molecular biology and genetic approaches to understand the mechanisms

that are involved in antifungal drug resistance in *C. albicans* and the identification of fungi-specific genes that could be targeted for novel antifungal therapy.

I.1 Fungal infections by medically important fungi: an overview

There are about 400 different fungal species listed in the *Atlas of Clinical Fungi*, among them are only several dozen fungi that can cause disease in humans (G.S. de Hoog 2001). Most human fungal pathogens belong to the Ascomycota phylum, which is the largest phylum in the Kingdom of Fungi (Fig. I.1) (Fitzpatrick *et al.* 2006). This phylum was originally defined by the production of a specialized structure, a sac (ascus) which surrounds the spores formed during sexual reproduction. There are two main subphyla within the Ascomycota; the Saccharomycotina subphylum includes yeasts such as *Candida albicans*, a commensal of humans and most frequently encountered opportunistic fungal pathogen found in immune-challenged individuals (Section I.1.1). The Pezizomycotina subphylum includes filamentous fungi such as *Aspergillus fumigatus*, a conidia-producing opportunistic human pathogen that is found wide-spread in nature (soil or decaying wood) (Section I.1.2) and *Histoplasma capsulatum*, a thermally dimorphic fungus found in nature that grows as mould at 25 ^{o}C and as yeast at 37 ^{o}C in humans (Section I.1.3). One other human pathogenic fungus that can cause severe fungal meningitis in AIDS patients is *Cryptococcus neoformans.* This organism belongs to the Basidiomycota phylum, which normally grows as a yeast form but is decorated by a prominent capsule (Section I.1.4).

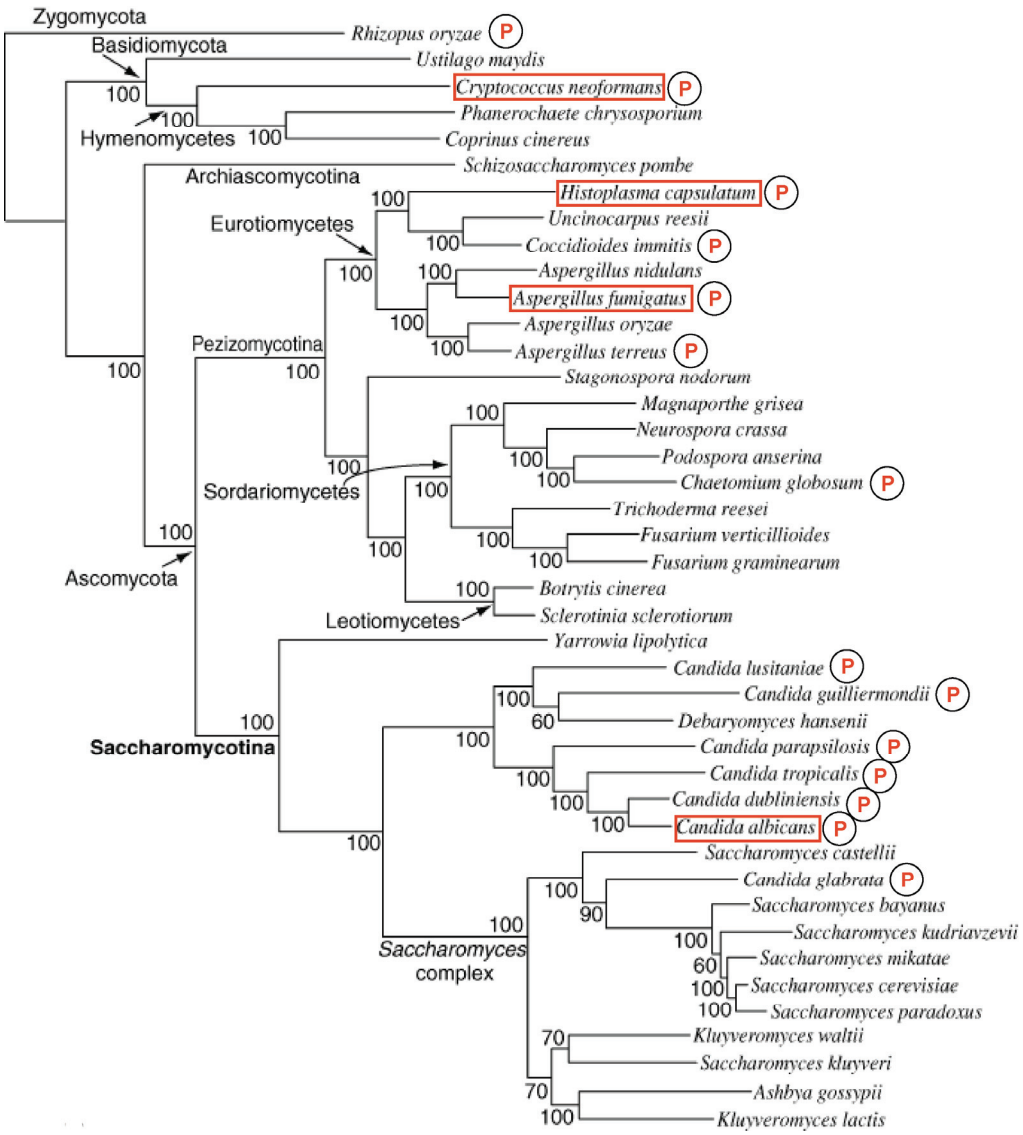

Figure I. 1 Phylogeny of Fungi

This tree is a maximum-likelihood phylogeny reconstructed using the concatenated sequences of 153 genes that are universally present in the 42 genomes shown here. Bootstrap percentages are shown for all nodes. Known human pathogens are indicated with P and important pathogens that are described in this thesis are boxed. Adapted from (Scannell *et al.* 2007).

I.1.1 *Candida albicans* and candidiasis

I.1.1.1 Morphological characteristics of *C. albicans*

C. albicans grows as smooth, white, dome-shape colonies and microscopic morphology analysis shows spherical budding yeast-like cells with an average size around 2 x 3 μm (Fig. I.2a). *C. albicans* is also known as a trimorphic fungus with the ability to switch between three morphological forms depending on the environmental stimuli. At 30 ^{o}C, *C. albicans* exists in the ovoid unicellular yeast form; in contrast, a long and narrow multicellular hyphal form of *C. albicans* is observed when growth temperature is shifted to 37 ^{o}C or when serum is added to the growth medium. In between these two extremes, this fungus can also exist as pseudohyphae where the elongated daughter cell remains attached to the mother cell, forming chains (Fig. I.3) (Sudbery *et al.* 2004). The morphogenesis of *C. albicans* is tightly coupled to the control of its cell cycle progression. Deletion of cell-cycle important genes or treatment with genotoxic chemicals often result in constitutive pseudohyphal or hyphal growth (Berman 2006). Detailed reviews of *C. albicans* morphogenesis and cell cycle regulation can be found elsewhere (Berman 2006; Whiteway *et al.* 2007).

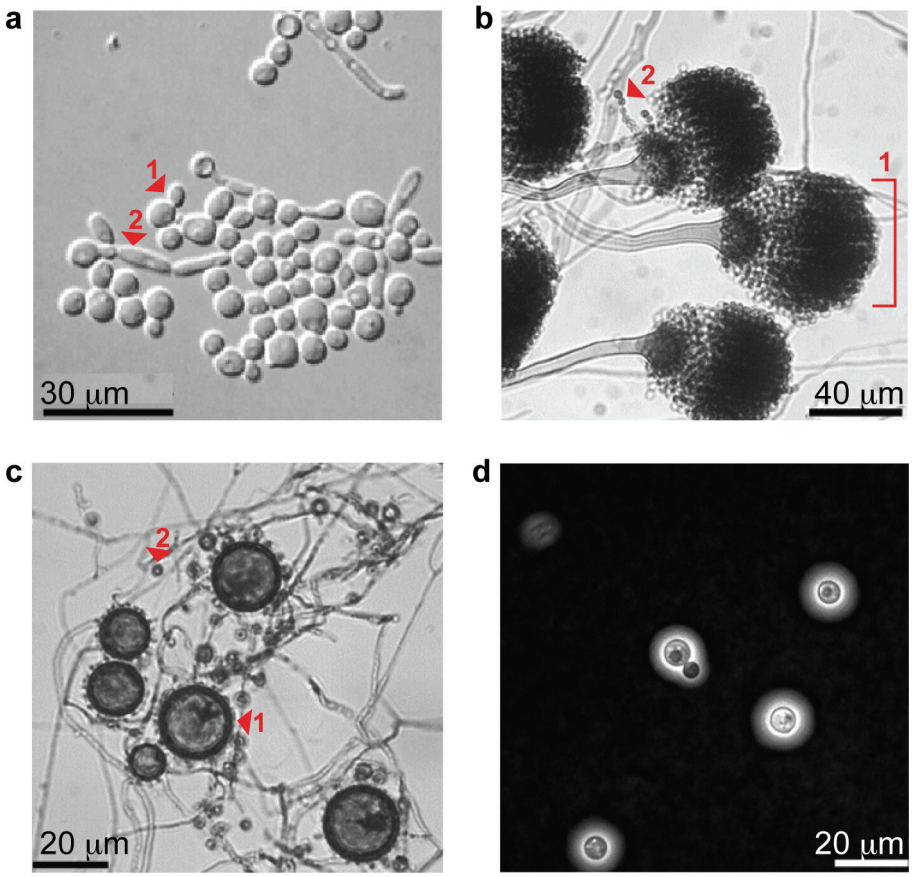

Figure I. 2 Microscopic morphology of medically important fungi

(**a**) *Candida albicans*. A yeast (arrowhead 1) and pseudohyphal (arrowhead 2) form of *C. albicans* cells. (**b**) *Aspergillus fumigatus*. Conidia head (single bracket 1) and conidia (arrowhead 2) are indicated. (**c**) *Histoplasma capsulatum*. Mycelial form of *H. capsulatum* with the characteristic large, rounded single-celled macroconidia (arrowhead 1) and small microconidia (arrowhead 2) are indicated. (**d**) *Cryptococcus neoformans*. Round budding-yeast like cells surrounded by a characteristic wide gelatinous capsule. Photos were adapted from

http://www.mycology.adelaide.edu.au/.

The ability to switch between yeast and hyphae is necessary for *C. albicans* virulence during infection, as mutant *C. albicans* strains that are constitutively yeasts (for example, transcription factor mutants *cph1Δ/cph1Δ* and *efg1Δ/efg1Δ*) or filaments (transcriptional repressor mutant *tup1Δ/tup1Δ*) are both avirulent, linking both forms to clinical pathogenesis (Braun *et al.* 2000; Lo *et al.* 1997;

Zheng *et al.* 2004). Interestingly, genes that govern cellular morphogenesis are co-regulated with genes encoding important virulence factors, adhesins and proteases [reviewed by (Kumamoto *et al.* 2005)]. The *C. albicans ALS* (agglutinin-like sequence) gene family encodes a group of glycosyl-phosphatidyl-inositol (GPI)-anchored cell surface proteins that function as adhesins. There are at least eight different *ALS* genes in the *C. albicans* genome (Braun *et al.* 2005) and *ALS3* is the most well characterized member of this family and its expression is Efg1p-dependent during hyphae formation. Recent studies have demonstrated that Als3p facilitates host cell invasion by directly interacting with the receptor cadherins on the surfaces of endothelial and epithelial cells (Phan *et al.* 2007). Other hypha-co-regulated virulence factors are the secreted aspartic proteinases (SAPs), which are hydrolytic enzymes that *C. albicans* secretes during infection to digest and destroy host cell membranes as well as surface molecules (Kumamoto *et al.* 2005; Schaller *et al.* 2005). There are at least ten different *SAP*-encoding genes; among those, the expression of *SAP4*, *SAP5* and *SAP6* is exclusively detected during hyphal morphogenesis and is also Efg1p-dependent. Furthermore, *SAP4-SAP6* have been shown to be required for host tissue damage and a mutant strain that lacks these genes showed reduced virulence in a mouse model of *Candida* infection (Felk *et al.* 2002). Taken together, the transcriptional regulatory networks of *C. albicans* coordinately control the expression of genes that are important for morphological transitions as well as genes encoding cell-adhesions and degradative enzymes for ensuring successful colonization and invasion of host tissues with enhanced virulence.

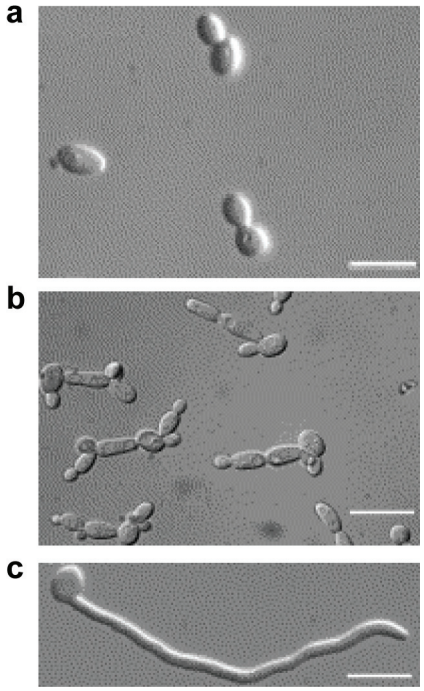

Figure I. 3 Characteristic morphologies of *C. albicans*

Microscopy pictures of (**a**) yeast; (**b**) pseudohyphal; and (**c**) hyphal morphological forms of *C. albicans*. Bar represents 10 nm. Adapted from (Sudbery *et al.* 2004).

I.1.1.2 Epidemiology of candidiasis

There are approximately more than one hundred species of *Candida*, six are well-known pathogens in humans. *C. albicans* is by far the most commonly reported species, followed by *C. glabrata*, *C. parapsilosis*, *C. tropicalis*, *C. krusei* and *C. lusitaniae* (Sims *et al.* 2005). *Candida* species are part of the commensal microbial flora of humans, mainly residing in the gastrointestinal tract and genito-urinary tracts, but also can be found in the respiratory tract, on the skin, or under the fingernails. PCR fingerprinting has been used to show that different regions of the body have different combinations of *Candida* species; in addition, the composition of *Candida* species in a single host individual could change over time and these isolates may be transmitted among family members (Kam *et al.* 2002). *Candida* species are also found in the hospital setting, on food, the floor,

surfaces of objects and on the hands of hospital personnel. In fact, nosocomial spread of *Candida* infection among patients has been traced to hand carriage (Sims *et al.* 2005).

Infections caused by *Candida* species are in general referred to as candidiasis. Candidiasis may be superficial and local or deep-seeded and disseminated via hematogenous spread to different organs in the body. Primary risk factors predisposing individuals to candidiasis include the prolonged use of antibiotics causing disruption of the balanced microflora, immune suppression, changes in the physical barriers that facilitate organism access to the bloodstream, and the duration of time a host remains immunosuppressed. *Candida* infections represent the fourth most common cause of hospital-acquired bloodstream infections in the US (Wisplinghoff *et al.* 2004).

Infectious Disease Society of America (IDSA) has recently issued guidelines based on the supporting evidence for the treatment of candidiasis (Pappas *et al.* 2009). Systemic antifungal agents shown to be effective for the treatment of candidiasis comprise four major categories: the polyenes (amphotericin B), the triazoles (fluconazole, itraconazole, voriconazole and posaconazole), the echinocandins (caspofungin and micafungin), and flucytosine (Section I.3). Historically, the most frequently used antifungal agent has been fluconazole because it is readily absorbed with high oral bioavailability and it is also the standard antifungal agent used in clinics before the diagnosis of causative fungi is confirmed (empirical therapy). However, there is an emergence of non-*albicans* species, and some of them display reduced fluconazole susceptibility. For example, *C. krusei* displays intrinsic resistance to fluconazole and *C. glabrata* also shows somewhat reduced susceptibility to this agent (Sims *et al.* 2005). Taking this trend into account, it is evident that the future treatment of candidiasis favors the use of newer antifungal agents, such as those of the echinocandin class that exhibit activity against a broad range of *Candida* species (Lewis 2009; Pappas *et al.* 2009).

I.1.2 *Aspergillus fumigatus* and aspergillosis

I.1.2.1 Morphological characteristics of *A. fumigatus*

A. fumigatus is a ubiquitous filamentous fungus that is commonly found in soil, food and air ventilation systems. *A. fumigatus* can grow at temperatures ranging between 20 to 55 ^{o}C and the colony begins as a dense white mycelium, which later assumes typical blue-green shades of color, reflecting the color of the conidia. The distinctive microscopic morphology of *A. fumigatus* is the presence of the large conidial head at the end of hypha measuring up to 400 x 50 μm and if sporulating abundantly, each conidial head can produce thousands of conidia, each measuring 2 to 5 μm in diameter (Fig. I.2b). Once the conidia are released into the atmosphere, their small size makes them buoyant and tends to keep them airborne both indoors and outdoors. Environmental surveys indicate that all humans inhale at least several hundred *A. fumigatus* conidia per day (Latge 1999). Hence, the respiratory tract is regarded as the main entrance for conidia into the human body.

The pathogenicity of *A. fumigatus* in the human host is aided by the production of several virulence factors, such as adhesins that promote interaction of conidia with host proteins, various hydrolytic enzymes and several toxic secondary metabolites with immunosuppressive properties (Karkowska-Kuleta *et al.* 2009; Tomee *et al.* 2000). Gliotoxin is the most well-studied mycotoxin and one of the most important virulence factors in *Aspergillus* pathogenesis. Gliotoxin was originally discovered as a potent antibiotic with a broad range of antimicrobial properties; it is now known to contain potent immunosuppressive properties by blocking T- and B-cell activation and subsequent immune responses. Finally, there is a considerable correlation between the amount of gliotoxin and the development of aspergillosis, as high levels of gliotoxin have been detected in infected animals and humans (Kwon-Chung *et al.* 2009; Tomee *et al.* 2000).

I.1.2.2 Epidemiology of aspergillosis

The genus *Aspergillus* contains almost two hundred species, however only a few of these organisms are potent pathogens of animals and plants. The most commonly encountered human pathogens are *A. fumigatus*, *A. flavus* and *A. niger*, with *A. fumigatus* being responsible for more than 90% of Aspergillus-related human diseases (Denning 1998). *Aspergillus* species have been implicated as a cause of fungal sinusitis, asthma, and allergic bronchopulmonary aspergillosis in immunocompetent individuals. In contrast to these relatively mild infections, *A. fumigatus* could be highly lethal in immunocompromised patients by causing invasive pulmonary infections and systemic disseminations (Latge 1999). Transplant recipients are among the most significant subgroups of immunosuppressed patients at risk for invasive aspergillosis and the mortality rate in these patients can range from 74 to 92% (Singh *et al.* 2005). These patients could contact *Aspergillus* conidia in the hospital setting, as *Aspergillus* has been cultured from ventilation systems, dust dislodged during construction and water systems (Anaissie *et al.* 2002; Patterson *et al.* 2000; Pfaller *et al.* 2010).

In the past decade, only amphotericin B and itraconazole have been effective to treat aspergillosis. In spite of their activity *in vitro*, the efficacy of these drugs *in vivo* against *A. fumigatus* remains low and, as a consequence, mortality from invasive aspergillosis remains high (Latge 1999). Recently, the IDSA has recommended the new azole derivative, voriconazole, which was demonstrated to be effective in clinical studies due to its excellent activity against most *Aspergillus* species while eliciting less toxicity to humans than amphotericin B (Pfaller *et al.* 2010; Walsh *et al.* 2008). Echinocandins also exhibit activity against *A. fumigatus in vitro*, however, chemotherapy using only echinocandins did not significantly reduce fungal burden as compared to chemotherapy with amphotericin B (Olson *et al.* 2010; Walsh *et al.* 2008).

I.1.3 *Histoplasma capsulatum* and histoplasmosis

I.1.3.1 Morphological characteristics of *H. capsulatum*

H. capsulatum exists as mycelia (mould) and releases conidia in nature, while on fungal agar between 25 to 30 ^{o}C, it forms white to brown colonies. Microscopic morphology analysis shows the presence of two types of conidia: macroconidia ranging in size between 8 to 14 μm in diameter and having a thick wall with distinctive projections on the surface, and microconidia, a small, rounded, single-cell with a smooth surface, between 2 to 4 μm in diameter which are the infectious form that can be inhaled by humans into the lungs (Fig. I.2c). Once the microconidia enter into the human body, the 37 ^{o}C body temperature induces the hyphae to yeast transition of *H. capsulatum*, the organism is converted into a smooth, moist, white and budding yeast-like morphology with a size of 3-4 x 2-3 μm.

Temperature-induced morphological change, the ability to switch from mycelial or conidia to yeast has long been held as the initial requirement for pathogenesis, as chemical treatment that blocks this transition rendered *H. capsulatum* avirulent in mice (Holbrook *et al.* 2008; Medoff *et al.* 1986). Once in the yeast form, *H. capsulatum* is phagocytosed by macrophages, in which the yeast could survive and proliferate. While inside macrophages, *H. capsulatum* secretes a large amount of calcium-binding protein (CBP) to absorb free calcium ions, delivering them back to the yeast and ensuring their survival. Therefore, secretion of CBP is an important virulence factor; it has been demonstrated that genetic deletion of *CBP1* impairs growth within macrophages and attenuates proliferation in a mouse model of pulmonary infection (Sebghati *et al.* 2000).

I.1.3.2 Epidemiology of histoplasmosis

H. capsulatum is found worldwide; however, it is endemic in the Ohio and Mississippi River Valley of the United States. Exposure to *H. capsulatum* is common for persons living within areas of endemic regions, but symptomatic

infection is uncommon, approximately only 1% of infected individuals can develop respiratory disease as pulmonary histoplasmosis (Kauffman 2007). Based on several aspects of biology, infection, and pathogenesis, *H. capsulatum* and *histoplasmosis* are fungal equivalents of the bacterium *Mycobacterium tuberculosis* and tuberculosis since both exploit the macrophage as host cell and can cause acute and persistent pulmonary and disseminated infection (Woods 2002). Patients with underlying disease or with compromised immune system can develop disseminated histoplasmosis. The estimated annual incidence of invasive histoplasmosis is around seven cases per million populations per year with 21% case-fatality ratio (Pfaller *et al.* 2010).

Treatment options for histoplasmosis include the use of amphotericin B for severe pulmonary or disseminated histoplasmosis; azoles such as itracolonazole can also be used to treat moderate to mild histoplasmosis. The commonly used azole fluconazole can be used but is not as effective as itraconazole (Kauffman 2007). Echinocandins do not have *in vitro* activity against *H. capsulatum* and are ineffective in an animal model of infection; therefore, they are not recommended for clinical use (Kohler *et al.* 2000).

I.1.4 *Cryptococcus neoformans* and cryptococcal meningitis

I.1.4.1 Morphological characteristics of *C. neoformans*

C. neoformans is a yeast with a distinctive appearance: a single spherically shaped cell of 3 to 7 μm in diameter surrounded by a polysaccharide capsule (Fig. I.2d). *C. neoformans* can be commonly isolated from pigeon or chicken droppings and it is generally accepted that this organism enters the human body via the respiratory route, as a dehydrated yeast inhaled by humans. It has been shown that a variety of factors are involved in *C. neoformans* virulence, including the ability to grow at 37 °C and production of degradative enzymes (phospholipases and ureases); however, predominant virulence factors are the production of melanin (brown to

black pigment) and capsule synthesis. Melanin production has been considered as one characteristic that differentiates pathogenic *C. neoformans* from non-pathogenic *Cryptococcus* species, as a mutant strain that is defective in melanin synthesis was more susceptible to free-radical killing, suggesting that melanin protects *C. neoformans* against oxidants produced by host effector cells. Furthermore, this strain is also less virulent in mice (Buchanan *et al.* 1998; Rhodes *et al.* 1982; Shaw *et al.* 1972; Wang *et al.* 1995). Capsule production is a unique feature of *C. neoformans* (Mitchell *et al.* 1995). Encapsulated *C. neoformans* cells are not phagocytosed or killed by neutrophils or macrophages to the same degree as acapsular mutants. Furthermore, there is also evidence showing that capsules may suppress dendritic cell response and T-cell function (Chang *et al.* 1994; Lupo *et al.* 2008).

I.1.4.2 Epidemiology of cryptococcosis

More than thirty Cryptococcal yeast species have been isolated from a variety of environmental niches, but only *C. neoformans* appears to produce disease in humans (Chayakulkeeree *et al.* 2006). *C. neoformans* is also the most common species affecting patients with AIDS and other immunocompromised conditions (Chayakulkeeree *et al.* 2006; Pfaller *et al.* 2010). Once inhaled, *C. neoformans* can hematogenously spread from lung to extrapulmonary tissues; since it has a predilection for the brain, infected persons usually contract cryptococcal meningitis. Furthermore, infection of the central nervous system is among the most common clinical manifestations, as well as the cause of death (Chang *et al.* 2004; Pfaller *et al.* 2010). Invasive cryptococcal infection is the third most common invasive mycoses after candidiasis and aspergillosis in patients who undergo transplantations (Pfaller *et al.* 2010). Treatments of cryptococcal infections usually involve the use of amphotericin B or high dosage of azoles (with fluconazole more favorable than itraconazole) in combination with 5-

flucytosine (Perfect *et al.* 2009). Surprisingly, none of the echinocandins are active against *C. neoformans* (Maligie *et al.* 2005; Pfaller *et al.* 2009).

I.1.5 Host immunity against *Candida* species

Protective immunity against fungal pathogens is achieved by the integration of innate (non-specific) and adaptive (antigen-specific) responses. The innate immunity is considered as a first-line of defense, it recognizes 'non-self', invading microorganisms and acts early after the infection. In addition, the more sophisticated adaptive mechanisms are specifically induced during infection and are required for complete elimination of the pathogen and the generation of immunological memory. Detailed review on the host immunity to fungal infections can be found elsewhere (Blanco *et al.* 2008; Medzhitov 2007; Netea *et al.* 2010; Romani 2004; van de Veerdonk *et al.* 2010). The importance of innate immunity is highlighted as it provides the first response against *Candida*; it consists of physical barriers formed by the body surfaces and mucosal epithelium of the respiratory, gastrointestinal and genito-urinary tracts. In addition, a variety of factors contributing to innate antifungal defense are present at the mucosal sites, including a microbial flora that possesses antagonistic activity against *Candida*. For example, the lactic acid bacteria could compete with *Candida* for adhesion sites and secrete substances to inhibit its growth (Morales *et al.* 2010). In addition, epithelial cells could also produce defensins with antifungal properties to inhibit the growth of fungi (Romani 2004). The innate immunity holds the pathogenic fungi under surveillance, however, if the infectious fungi breach these early lines of defense, an adaptive immune response will be activated with the generation of antigen-specific T helper (Th) (Th-1 or Th-17) effector cells that specifically target the pathogen and B cells that provide memory to prevent subsequent infection with the same microorganism. Cytokines and other mediators also play an essential role in the process and ultimately determine the type of effector response that is generated towards the pathogens as well as types

of infection. In the case of *Candida* infection at the mucosal surfaces, the Th-17 response that is characterized by the productions of IL-17 as well as IL-22, which are responsible for the recruitment of neutrophils and the production of defensins, respectively, play an important role in controlling mucosal candidiasis. On the other hand, the activation of the Th-1 response pathway is important to clear invasive candidiasis: the release of interferon-γ (IFNγ) and lymphotoxin-a (TLA) from Th-1 cells is responsible for the activation and recruitment of neutrophils and macrophages to the deep tissues (Netea *et al.* 2010; van de Veerdonk *et al.* 2010).

I.2 Molecular biology of *C. albicans* and animal models of *Candida* pathogenesis

I.2.1 Genome structure of *C. albicans*

The *C. albicans* haploid genome (a single set of chromosomes) is ~16 megabases (Mb) in size and contains about 6,000 genes over eight chromosomes (http://www.candidagenome.org/) (Braun *et al.* 2005). One noticeable feature of the *Candida* genome is the use of a non-standard genetic code: the leucine-CUG codon is translated as serine in various *Candida* species. Evolutionary studies suggested that this reassignment of the CUG codon initially evolved through a misreading mechanism. Furthermore, the fact that *Candida* species could tolerate this ambiguous coding implies that such genetic code ambiguity is probably useful for creating genetic variability and increasing the organism's potential for adaptation to new environmental niches (Moura *et al.* 2010). Another characteristic feature of the diploid *C. albicans* genome is the significant sequence divergence between chromosome homologs, thus, one single nucleotide polymorphism (SNP) was found every 330 bp in the most commonly studied wild-type strain, SC5314 (Bennett 2009). Possessing high levels of SNPs allows *C. albicans* an opportunity to rapidly generate diversity for its survival under adverse environmental conditions. There are also examples demonstrating that, in

the presence of azoles, *C. albicans* could selectively duplicate the hyperactive allele of genes encoding specific transcription factors to overcome azole stress (Section I.4.2.4).

The mating cycle in *C. albicans* is also unique. Fungal mating has been well characterized in the model yeast *Saccharomyces cerevisiae*, in which sexual reproduction and recombination is common and readily observed. The mating type locus (*MAT)* in *S. cerevisiae* exists as either one of two alleles, **a** and α, that determine the mating type of haploid cells through expression of distinct sets of transcriptional regulators: **a** type cells, which possess the *MAT* **a** allele, can mate only with α type cells, which possess the *MATα* allele, and vice versa. The product of mating is a diploid cell that is heterozygous at the *MAT* (**a**/α) locus and cannot mate. *S. cerevisiae* can then undergo meiosis under appropriate environmental conditions, thereby recreating haploid cells of **a** and α mating types. The mating type locus of *C. albicans* was found to be **a**/α diploid and therefore it was thought to be sterile. However, mutants with only one mating type (**a**/**a** or α/α) were found to mate in the laboratory but at a low frequency (Bennett *et al.* 2005). Recent findings established that *C. albicans* preserves the overall mating system as in *S. cerevisiae* but two additional requirements must occur as a prerequisite to mating. The heterozygosity at the *MTL* locus must be lost and *C. albicans* needs to convert from the white cell (normal budding yeast-like morphology) to the mating-competent opaque phase cells (opaque, flat colonies that contain oblong cells). This transition involves changes in expression of several hundred genes and the white-opaque switching is also dependent on the cell type as only **a**/**a** and α/α, but not **a**/α cells can undergo switching. Mating of these diploid strains of opposite sex produces tetraploid cells that have four copies of each chromosome (**a/a**/α/α). Instead of undergoing meiotic reduction, these cells undergo a so-called 'parasexual reduction', in which extra chromosomes will be randomly lost until they reach a near-diploid genome content. In addition, it was observed that a subset of these cells also undergo multiple gene conversion

events reminiscent of meiotic recombination, and most remain trisomic for one to several chromosomes (Bennett 2009; Bennett *et al.* 2005; Forche *et al.* 2008).

I.2.2 Genetic manipulations in *C. albicans*

A reverse genetic approach in *C. albicans* is frequently used to predict the function of a yet uncharacterized gene. The *C. albicans* gene of interest is identified and then both genomic copies in *C. albicans* are sequentially deleted to assess the function of this gene. Gene disruption in *C. albicans* utilizes homologous recombination to replace the chromosomal copy of a target gene with a linear fragment of exogenous DNA (containing a selectable marker) whose ends are identical to sequences flanking the target gene. The development and adaptation of gene disruption tools in *C. albicans* has been reviewed extensively elsewhere (Berman *et al.* 2002; De Backer *et al.* 2000). Here I briefly describe approaches that were used in my research and presented in this thesis (Chapter II, III and IV): the auxotrophic marker gene disruption system, the *SAT1*-flipper system and the GRACE (gene replacement and conditional expression) technology (Fig. I.4).

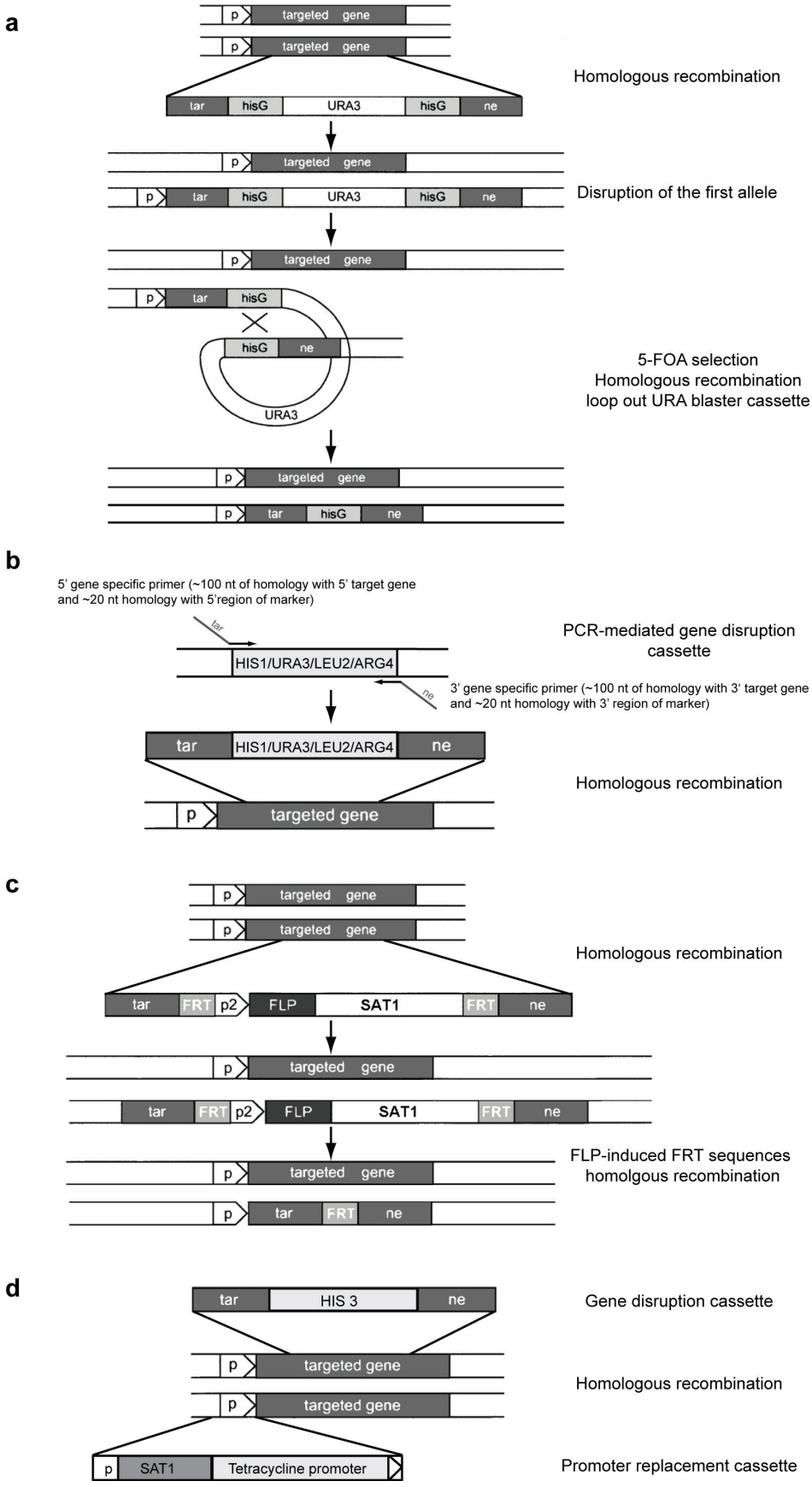
a
p
targeted gene
tar
hisG
URA3
ne
Homologous recombination
Disruption of the first allele
5-FOA selection
Homologous recombination
loop out URA blaster cassette
b
5' gene specific primer (~100 nt of homology with 5' target gene
and ~20 nt homology with 5'region of marker)
HIS1/URA3/LEU2/ARG4
PCR-mediated gene disruption
cassette
3' gene specific primer (~100 nt of homology with 3' target gene
and ~20 nt homology with 3' region of marker)
Homologous recombination
c
FRT
p2
FLP
SAT1
Homologous recombination
FLP-induced FRT sequences
homolgous recombination
d
HIS 3
Gene disruption cassette
Homologous recombination
SAT1
Tetracycline promoter
Promoter replacement cassette

Figure I. 4 Genetic tools in *C. albicans*

(**a**) The *URA*-blaster method. The recyclable *URA*-blaster cassette (*hisG-URA3-hisG*) is flanked by sequences that are homologous to upstream and downstream regions of the targeted gene. Selection for Ura^+ prototrophs is used to isolate transformants that carry the *URA*-blaster cassette after homologous recombination. Counter-selection on 5-fluoro-orotic acid (5-FOA) plates identifies isolates that have lost the *URA3* marker through recombination between the *hisG* repeats. (**b**) PCR-mediated gene disruption. PCR is used to amplify selectable markers (*HIS1*, *URA3*, *LEU2* or *ARG4*) fused by long flanking sequences (~100 nt) homologous to the upstream and downstream regions of the target gene. (**c**) The *SAT1*-Flipper strategy. The *SAT1-FLP* cassette consists of the dominant nourseothricin resistance marker *SAT1* under the control of the maltose promoter (p2) flanked by two direct repeats of the *FLP* recognition sequence *FRT*. The gene-disruption cassette is constructed by cloning the respective upstream and downstream sequences of the targeted gene on each side of the *SAT1-FLP* cassette. The FLP recombinase is activated in the presence of maltose and subsequently induces the recombination between the *FRT* repeats and allows the excision of the *SAT1-FLP* cassette. (**d**) The GRACE strategy. This strategy involves the use of the *HIS3* cassette to disrupt the first allele of the targeted gene and replacing the endogenous promoter of the second allele with the repressible tetracycline promoter. Adapted from (De Backer *et al.* 2000).

In the early 1990s, Fonzi and Irwin developed a recyclable *URA3* cassette (Ura-blaster) that was adapted for multiple sequential transformations of *C. albicans* strains that were auxotrophic for *URA3* (Fonzi *et al.* 1993). This strategy was the first and foremost genetic tool available to the *Candida* community thus most early genetic dissections of *Candida* morphologenesis and virulence pathways were performed with this strategy. However, it was shown that *URA3* expression levels influence *C. albicans* virulence in a mouse model of systemic candidiasis (Lay *et al.* 1998) as well as adhesion to human tissues (Bain *et al.* 2001). Thus, it was clearly desirable to replace *URA3* with a different selectable marker that does not influence virulence. In 2005, Noble and Johnson constructed an improved set of auxotrophic of otherwise isogenic *C. albicans* strains, providing the use of auxotrophic markers that do not influence virulence. For example, strain SN152, which is a triple auxotroph with *HIS1*, *LEU2*, and *ARG4*; this strain has also made the generation of null mutants simpler by allowing sequential transformation steps

using different selectable markers (Noble *et al.* 2005). We used this strategy in Chapter IV.

The *SAT1*-flipper system was developed by Reuss *et al.* (Reuss *et al.* 2004); this cassette contains the dominant selectable marker *SAT1*, which confers resistance to the antibacterial nourseothricin coupled with an excision system that is based on the *S. cerevisiae* 2-μm *FLP/FRT* system, allowing multiple rounds of recycling of the selectable marker (Reuss *et al.* 2004). The advantage of the *SAT1*-flipper system is that this cassette can be used with any *C. albicans* strain including clinical strains that do not have auxotrophies. In addition, the null mutant is almost genetically identical to its parental strain, apart from the excision of an target gene and the presence of a single *FRT* repeat (34 bp), thus minimizing possible interference contributed from the insertion of exogenous marker. This strategy has been used extensively in Chapters II and III.

Finally, the GRACE technology was developed and this strategy has been used to study the function of essential genes (Roemer *et al.* 2003). This strategy involves two successive manipulations in *C. albicans* strain CaSS1, which expresses a tetracycline-dependent transactivation fusion (TetR-ScGal4AD) protein (Roemer *et al.* 2003). Initially, the first allele of the gene is replaced by the auxotrophic marker *HIS3*, and then the native promoter of the second allele is replaced by the repressible tetracycline promoter. Thus, functional consequences of losing the targeted essential gene can be monitored upon tetracycline addition to the growth medium, shutting down the expression of the remaining allele of the targeted gene (Roemer *et al.* 2003). We used this strategy to study the essentiality of the *HST3* gene in Chapter IV.

I.2.3 Animal models of *Candida* pathogenesis

The study of *Candida* pathogenesis requires the investigation of *Candida* infection in animal model systems. The ideal animal model would fulfill the

following prerequisites: it would provide a close simulation of the pathophysiology of human infections, allow reproducible assessments for studying the effects of virulence factors or therapeutic agents, it would be amenable to genetic manipulations as well as genome wide expression analyses and finally, this model should be of reasonable cost and ethically acceptable. Currently there are a few different animal models that have been established for studying the pathogenicity of candidiasis. These include invertebrate models, *Drosophila melanogaster*, *Caenorhabditis elegans*, the wax moth caterpillar *Galleria mellonella* as well as the vertebrate murine models (Chamilos *et al.* 2007; Mylonakis 2008; Mylonakis *et al.* 2005). The major advantage of using the small invertebrate models (fly and roundworm) is because of their relatively simple and well-defined genetics and an innate immunity similar to that of humans; thus they offer an unparalleled opportunity to obtain a comprehensive analysis of the molecular aspects of the host immune response. On the other hand, the *G. mellonella* model system, despite the lack of complete genome sequencing, offers some unique advantages over the fly and worm models. In contrast to flies and worms, *G. mellonella* can survive at the mammalian physiological temperature of 37 °C. Furthermore, its manipulation requires much simpler laboratory equipment and resources than those used for fly and worm experiments. Indeed, *G. mellonella* is relatively large in size (approximately 300 mg and 2.5 cm in length), thus offering easy administration of exact *C. albicans* inoculum or antimicrobial substances. Recently the *G. mellonella* model has been exploited particularly for antifungal studies due to its intrinsic susceptibility to fungal infections (Mylonakis 2008).

Although invertebrate models offer a number of advantages over mammalian vertebrate models, the major disadvantage is that they lack adaptive immunity. Vertebrate models are thus indispensible systems, they are evolutionarily closer to humans, with anatomical and immunological similarity, and the host–Candida interactions are expected to be more relevant to humans. The mouse tail vein injection model is the standard animal model for assessing the host response to *C.*

albicans, the virulence of *C. albicans* mutants and the efficacy and pharmacokinetics of antifungal drugs (Ashman *et al.* 1996; Tuite *et al.* 2004). Intravenous injection of *C. albicans* inoculums leads to the establishment of an acute systemic infection involving multiple organs, including the lungs, heart, liver, kidney and spleen; high levels of fungal load can be isolated from the lungs and liver in the first few hours after *C. albicans* injection. Infected mice become progressively hypotensive, tachycardic and hypothermic and finally develop a metabolic acidosis condition and become hypoglycemic. These results indicate that the mice die of progressive septic shock and this model mirrors the clinical course of severe hematogenously disseminated candidiasis in humans (Spellberg *et al.* 2005).

The choice of mice strain is important to researchers that are interested in understanding host genetic factors involved in the disease outcome. For example, the complement pathway plays critical roles in the innate as well as adaptive mechanisms of defense against fungal infections (Frank *et al.* 1991). In particular, the importance of the complement component 5 (C5) in determining disease outcome is striking (Ashman *et al.* 2003; Kozel 1996; Lyon *et al.* 1986). A mouse strain that is C5-deficient, such as the A/J mouse, has an increased susceptibility to disseminated candidiasis that results in high levels of fungal accumulation within 24 h, providing a convenient model to rapidly and accurately measure fungal proliferation *in vivo* (Mullick *et al.* 2004). The A/J mouse model is the animal model that we used in Chapter IV. In contrast to the A/J mice, strains with a functional complement system are more resistant to fungal infections. The commonly used BALB/c or C57BL/6J mice can survive for up to two weeks following infection and ultimately die of kidney failure as a consequence of continued fungal proliferation at that site (Mullick *et al.* 2004; Spellberg *et al.* 2005).

The response of mice to systemic candidiasis can be assessed by tissue damage, fungal burden, and mortality. Kidney fungal burden estimation provides the most

quantitative measure of infection and the mortality rate correlates with the overall susceptibility to infection. Furthermore, detection of proinflammatory cytokines that are important in innate and adaptive immunity against *C. albicans*, namely tumor necrosis factor alpha (TNF-α) and interleukin-6 (IL-6), provide an additional measure of host responses to candidiasis (Tuite *et al.* 2004).

I.3 Antifungal agents and therapies

Since the late 1950s, the standard treatment for serious fungal infections has been the use of amphotericin B, an intravenous-only agent with significant nephrotoxicity. In the late 1980s and early 1990s, the introduction of imidazoles (ketoconazole) as well as triazoles (fluconazole and itraconazole) offered a safer alternative treatment option for local and systemic fungal infections. However, these agents showed inhibitory activity against a limited spectrum of fungi and the excessive use of azoles results in the development of resistance. In the past decade, there have been major advances in antifungal chemotherapy as the broader-spectrum triazoles (voriconazole and posaconazole) and echinocandin class of antifungals (caspofungin, micafungin, and anidulafungin) were introduced (Fig. I.5a). In this section, I will review the mode of actions of the major antifungal agents that are currently in clinical use as well as the proposed therapy strategy.

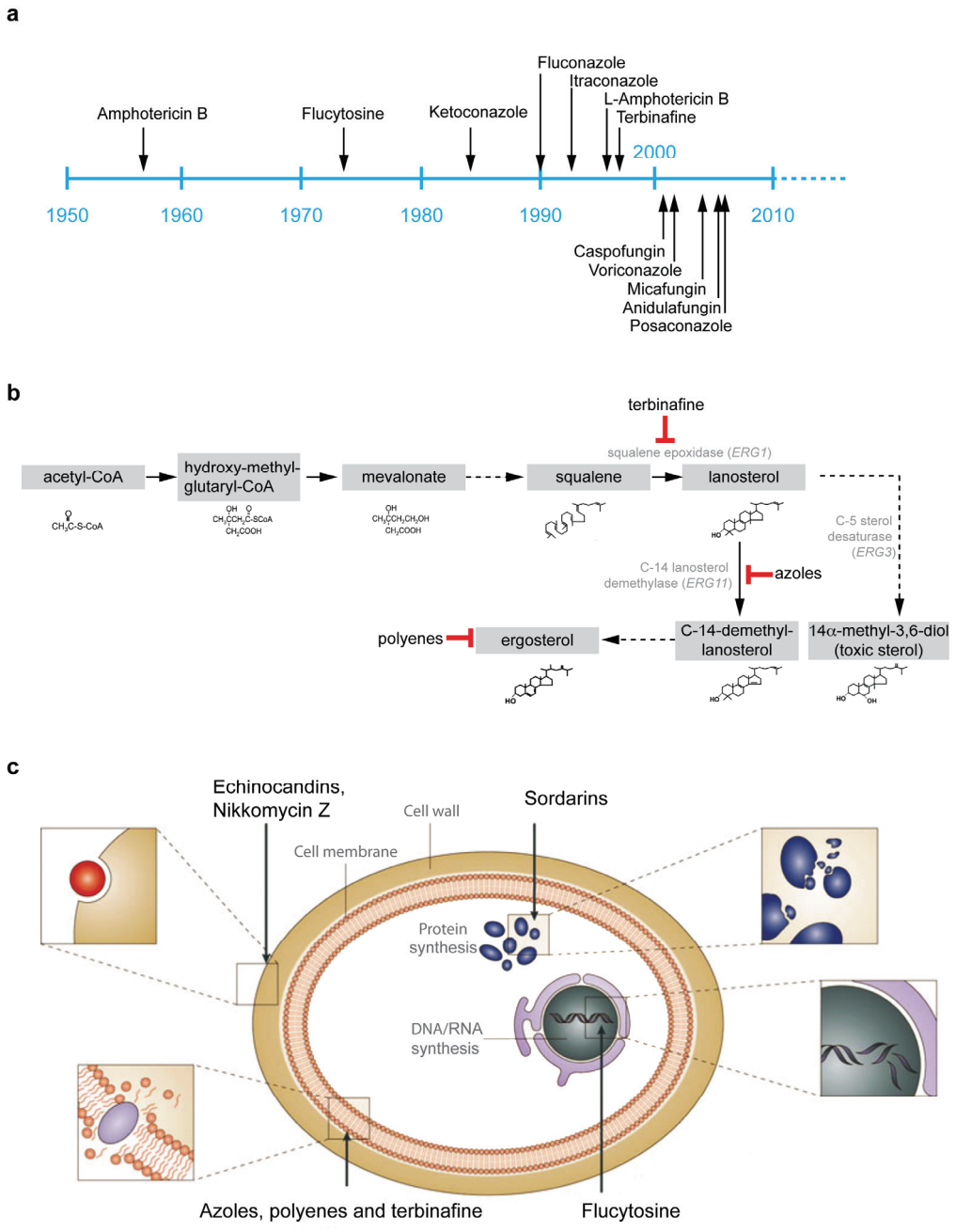

Figure I. 5 Antifungal agents: past, current and future

(**a**) Timeline of antifungal agents discovery. L-Amphotericin B, liposomal amphotericin B. (**b**) Antifungal agents targeting ergosterol biosynthetic pathway. Three antifungal agents, terbinafine, azoles and polyenes are shown. (**c**) General view of selected antifungal agents and their cellular targets. Adapted from (Akins 2005; Lupetti *et al.* 2002; Mohr *et al.* 2008; Ostrosky-Zeichner *et al.* 2010).

I.3.1 Compounds affecting fungal sterols

The fungal sterol ergosterol, equivalent to mammalian cholesterol, is an essential component of cell membranes and is required for proper membrane permeability, fluidity and the optimal function of membrane-bound enzymes such as proteins associated with nutrient transport or cell wall synthesis. The ergosterol biosynthetic pathway converts acetic acid to ergosterol, using largely the same enzymes as in the mammalian biosynthesis of cholesterol. Inhibition of the ergosterol biosynthesis pathway leads to severe consequences affecting cell growth; therefore, the ergosterol biosynthesis pathway has been the target for many antifungals (Fig. I.5b).

I.3.1.1 Polyenes

The polyene amphotericin B is the first-line antifungal agent of choice for treating invasive mycoses including aspergillosis, histoplasmosis and cryptococcosis (Pfaller *et al.* 2010). Amphotericin B is a large, poly-unsaturated organic compound (Fig. I.6); it targets the fungal cell membrane by interaction with ergosterol and forms transmembrane channels (Fig. I.5b-c). Consequently, this action leads to altered membrane permeability, allowing leakage of important cellular contents such as potassium, chloride and sodium ions, resulting in loss of membrane potential and eventually cell death (Odds *et al.* 2003; Ramos *et al.* 1996). Furthermore, there is evidence suggesting that treatment with polyenes also causes oxidative damage, which may contribute to their fungicidal activity (Liu *et al.* 2005; Sokol-Anderson *et al.* 1986). Ergosterol and cholesterol share structural similarities; although amphotericin B preferentially binds to ergosterol rather than to its mammalian counterpart, it nevertheless can bind to cholesterol at high concentrations with low affinity thus causing major side effects. Indeed, amphotericin B is often associated with renal toxicity, particularly in patients requiring long treatment. The mechanism of amphotericin B-induced nephrotoxicity is thought to be due to a direct interaction between the drug and the epithelial cell membranes, resulting in tubular dysfunction, as well as

vasoconstriction and subsequent reduction of renal blood flow (Mohr *et al.* 2008). The introduction of lipid formulations of amphotericin B, in which the drug is encapsulated in liposomes, significantly reduces the toxicity (Herbrecht *et al.* 2003).

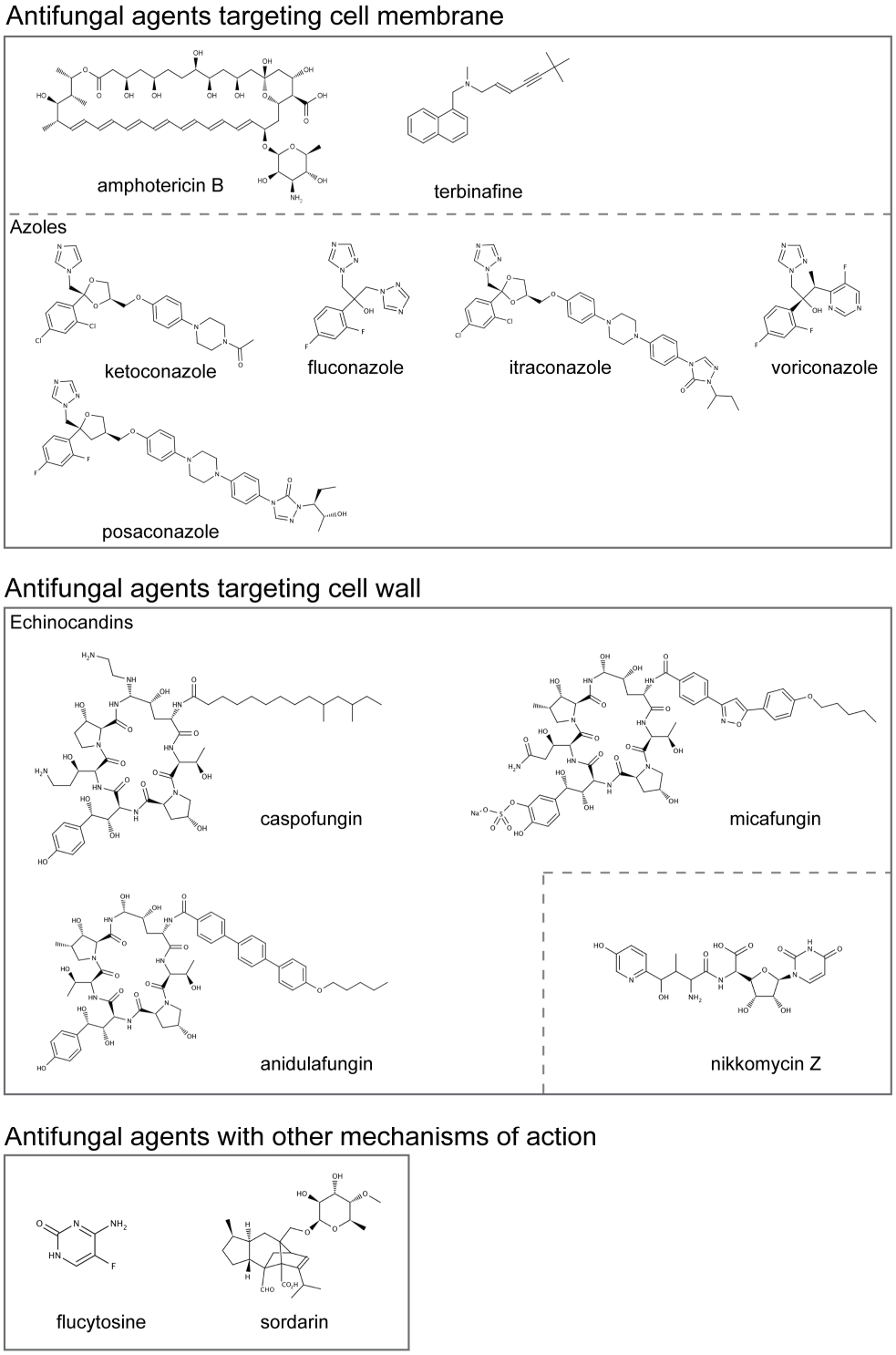

Figure I. 6 Structures of selected antifungal agents

Structures of antifungal agents described in this thesis. The structures were downloaded from the PubChem database (http://pubchem.ncbi.nlm.nih.gov/) and edited using the MarvinSketch software.

I.3.1.2 Azoles

Members of the azole family have activity against different fungi, and some are water-soluble, are available in oral formulations and lack the serious nephrotoxic side effects observed with amphotericin B. Azoles are characterized by the presence of five-membered azole rings (Fig. I.6) and are grouped into two general classes: imidazoles, which contain two nitrogens, and triazoles, which have three nitrogens in the azole ring. Similar to amphotericin B, azoles exert their antifungal action by targeting the fungal cell membrane (Fig. I.5b-c). Unlike amphotericin B, azoles inhibit cytochrome P450-dependent 14α-demethylase (encoded by *ERG11*), preventing the conversion of lanosterol to ergosterol, thus leading to ergosterol depletion as well as accumulation of 14α-methylsterols (Fig. I.5b). Depletion of ergosterol results in alteration of the plasma membrane structure, and consequently, it could affect the optimal function of some membrane proteins, rendering cells with increased vulnerability to further damage (Lupetti *et al.* 2002). In addition, early studies suggested that this methylated sterol intermediate is cytotoxic and the accumulation of this product upon azole treatment is responsible for the growth inhibition (Akins 2005; Kelly *et al.* 1995). It is important to note that azoles are considered fungistatic rather than fungicidal agents, as they inhibit the growth of fungi without causing cell death.

The imidazole ketoconazole was among the first developed azole drugs and is the only member of imidazoles that is still in clinical use. The success of ketoconazole led to the development of the triazoles, including fluconazole and itraconazole, as these newer azoles exhibit better activity against a wider spectrum of fungi and are less toxic than ketoconazole. Fluconazole is readily absorbed, with high oral bioavailability, and is probably the most commonly used agent for AIDS patients who suffer from oral candidiasis (Pappas *et al.* 2009). Fluconazole is also used in empirical treatment for suspected invasive candidiasis in immunocompromised patients or as prophylactic treatment for organ transplant patients (Pappas *et al.* 2009). However, long-term and prophylactic treatment using fluconazole has probably contributed to the recently observed shift towards

increased infections with non-albicans *Candida* species that exhibit decreased fluconazole susceptibility. Itraconazole, on the other hand, has good activity against *C. albicans* as well as an improved activity against fluconazole-resistant *C. krusei* and *C. glabrata* and is therefore often used on patients who have experienced treatment failure with fluconazole (Pappas *et al.* 2009).

Recently, the development of the second-generation triazoles voriconazole and posaconazole represents significant advances in the understanding of structure-activity relationships for antifungal azoles as these new triazoles have an enhanced specificity for fungal Erg11p targets and a slower metabolism *in vivo* (Sable *et al.* 2008). Voriconazole and posaconazole, which have been approved in the United States in 2002 and 2006, respectively, showed broader spectrum activity than fluconazole and excellent *in vitro* activity against most *Candida* species, including some fluconazole-resistant strains, and are also fungicidal against *Aspergillus fumigatus* and *Cryptococcus neoformans* (Johnson *et al.* 2008; Sable *et al.* 2008).

I.3.1.3 Allylamine terbinafine

An early step in the ergosterol biosynthesis pathway is the target for another class of antifungal agent, the allylamine terbinafine, which inhibits squalene epoxidase (encoded by *ERG1*) (Fig. I.5b-c and Fig. I.6) (Krishnan-Natesan 2009; Odds *et al.* 2003). Terbinafine exhibits good *in vitro* fungicidal activity against dermatophytic fungi (for example, *Trichophyton rubrum* and *Tinea pedis*) as well as *Candida* species. Despite its good *in vitro* activity, terbinafine is not recommended for first-line or primary therapy for life-threatening, invasive mycoses caused by *Candida* species, *A. fumigatus* or *C. neoformans*, due to its failure to achieve and maintain high therapeutic plasma concentrations in humans (Krishnan-Natesan 2009). Currently, terbinafine is used for treating dermatophytic fungal infections of the nail and skins (Krishnan-Natesan 2009).

I.3.2 Compounds affecting fungal cell walls

The fungal cell wall determines cell shape and integrity. In budding yeasts like *S. cerevisiae* and *C. albicans*, the cell wall is composed of three major groups of polysaccharides: polymers of mannose (mannan, accounting for ~40% of the cell wall dry mass), polymers of glucose (β-glucan, ~60% of the cell wall dry mass) and polymers of *N*-acetylglucosamine (chitin, ~2 % of the cell wall dry mass) (Klis *et al.* 2001; Klis *et al.* 2002). β–Glucan is the major component of the fungal cell wall and can be divided into two subtypes following the mode of glucose linkages: long chains of β-1,3-glucose units which represents about 85% of total cell wall β-glucan, and short chain β-1,6-glucose units that accounts for 15% of total β-glucan (Klis *et al.* 2002). Furthermore, it is important to note that while there are similarities in fungal cell wall compositions, there are also differences. These differences include the presence of galactomannans found in *Aspergillus fumigatus*, the presence of α-glucans in addition to β-glucans in *H. capsulatum*, and the presence of chitosan in *Cryptococcus neoformans* (Levitz 2010). Nevertheless, the cell wall structure is unique to fungi and is not shared by its mammalian hosts; it thus represents a good target for antifungal drugs (Fig. I.6).

I.3.2.1 Echinocandins

Echinocandins inhibit the synthesis of β-1,3-glucan synthase which is a large (210-kDa) heterodimeric, integral membrane protein. Treatment with echinocandins leads to the inhibition of structural glucan synthesis, resulting in cell wall destabilization, induction of osmotic as well as oxidative stresses, and ultimately cell death (Denning 2003; Kelly *et al.* 2009). In *S. cerevisiae*, genes that encode the β-1,3-glucan synthase complex are *FKS1* and *FKS2*; orthologs of *FKS1* are found in all fungi, with percentage identity varying from 53% in *C. neoformans* to 72% in *C. albicans*.

Members of the echinocandin family are large lipopeptide molecules that contain an amphiphilic cyclic hexapeptide with an *N*-linked acyl lipid side chain (Fig. I.6). The differences in composition of the side chain render members of echinocandin family with different degrees of solubility (Denning 2003). Caspofungin, micafungin and anidulafungin are echinocandins which have received approval in the United States in 2001, 2005 and 2006, respectively. These agents all exhibited excellent *in vitro* activity against *C. albicans*, with micafungin being the most active agent followed by anidulafungin and caspofungin (Cappelletty *et al.* 2007; Pfaller *et al.* 2010). Echinocandins also showed very strong activity against other *Candida* species, including intrinsically azole-resistant *C. glabrata* and *C. krusei*; however, echinocandins are less active against *C. parapsilosis* (Cappelletty *et al.* 2007). Furthermore, echinocandins have activity against *Aspergillus* species but are not active against *C. neoformans*, probably due to mechanisms other than the β-1,3-glucan synthase activity (Cappelletty *et al.* 2007; Maligie *et al.* 2005). Finally, echinocandins have good *in vitro* activity against *H. capsulatum* but showed only marginal effects in a mouse model of histoplasmosis (Cappelletty *et al.* 2007; Kohler *et al.* 2000).

I.3.2.2 Chitin synthesis inhibitor

Nikkomycin Z was first identified in the 1970s, however, its development is only initiated recently. Nikkomycin Z is a peptide nucleoside and it exerts its fungicidal activity through the competitive inhibition of chitin synthases and thereby interferes with fungal cell wall synthesis and structure (Fig. I.6) (Hector 1993). Nikkomycin Z has been shown to exhibit good activity against *Candida* species as well as *H. capsulatum*, but only limited activity against *C. neoformans* and *A. fumigatus* (Ganesan *et al.* 2004; Hector 1993). As mammalian hosts do not possess the cellular target of nikkomycin Z, it is therefore potentially fungal-specific and indeed, this is supported by data from preclinical toxicology studies; currently, nikkomycin Z is in phase I clinical trials (Ostrosky-Zeichner *et al.* 2010).

I.3.3 Other compounds with antifungal properties

I.3.3.1 Flucytosine

Flucytosine, (5-fluorocytosine, 5-FC) a fluorinated cytosine analogue (Fig. I.5c and Fig. I.6), can be rapidly converted to 5-fluorouracil within fungal cells. This compound becomes incorporated into fungal RNA in place of uridylic acid and alters the amino-acylation of tRNA, causing premature chain termination. In addition, it also inhibits DNA synthesis through its effects on thymidylate synthase. For this mechanism of action, the target cells must possess cytosine permease to internalize the flucytosine molecule, cytosine deaminase to convert it to 5-fluorouracil, and uracil phosphoribosyl transferase to convert 5-fluorouracil into a substrate for nucleic acid synthesis (Vermes *et al.* 2000). Most filamentous fungi lack these enzymes and hence the useful spectrum of flucytosine is restricted to pathogenic yeast such as *Candida* species and *C. neoformans* (Odds *et al.* 2003). The use of flucytosine as a single agent is limited because of the prevalence of intrinsically resistant strains and the frequent emergence of resistant strains during treatment, resulting from mutations in the permease, deaminase and/or phosphoribosyl transferase enzymes (Whelan 1987). However, flucytosine has been used successfully in combination with amphotericin B for treatment of cryptococcal meningitis, possibly due to the increased flucytosine penetration through amphotericin B-damaged fungal cell membranes (Perfect *et al.* 2009).

I.3.3.2 Sordarins

Sordarins are a class of semi-synthetic natural products that were discovered by screening and shown to have antifungal activity in the early 1970s. Sordarins have a unique mode of action as they selectively bind to elongation factor 2 (EF2); this enzyme catalyzes the translocation of the ribosome along mRNA during elongation of the emerging polypeptide chain. Sordarins inhibit this translocation by stabilizing the EF2/ribosome complex and inhibit protein synthesis (Fig. I.5c and Fig. I.6) (Dominguez *et al.* 1998; Odds *et al.* 2003). It

was surprising how sordarins exert substrate specificity, since EF2 is evolutionally conserved and *C. albicans* EF2 displays more than 85% amino acid sequence homology with the human homolog. Early studies suggested that EF2 is a protein with extreme conformational flexibility, as it displays subtle conformational variations depending on the binding partners (adenylic or guanylic nucleotides or ribosomes). This conformational flexibility is responsible for its biological properties and may explain how such a conserved protein can be the primary target of antifungal agents such as sordarins (Dominguez *et al.* 1998; Soe *et al.* 2007). However, the disadvantage of this conformational flexibility is that currently studied sordarins and their derivatives do not possess a broad antifungal spectrum against a wide range of pathogenic fungi: although the *in vitro* efficacy of sordarins are good against *C. albicans*, *C. glabrata*, *C. tropicalis*, *C. neoformans* and *H. capsulatum*, sordarins are relatively inactive against *C. parapsilosis*, *C. krusei* and *A. fumigatus*. (Dominguez *et al.* 1998; Graybill *et al.* 1999; Herreros *et al.* 1998). Nevertheless, the sordarin derivative FR290581, which is currently under development, has shown greatly improved antifungal activity against *Candida species* including *C. parapsilosis* (Hanadate *et al.* 2009; Ostrosky-Zeichner *et al.* 2010).

I.3.4 Combination therapy

Combination therapy, employing the use of more than one antifungal agent, is a therapeutic strategy for making pathogenic fungi susceptible to certain pre-existing drugs. There are other advantages including the potential to slow down the development of drug resistance in monotherapy as well as to provide a broader antifungal spectrum. Successful examples include the fluconazole-flucytosine combination used in treating invasive candidiasis and the amphotericin B-flucytosine combination used in treating cryptococcal meningitis [reviewed in (Johnson *et al.* 2004; Lupetti *et al.* 2003; Steinbach *et al.* 2010)]. Here I will selectively discuss agents that could potentially synergize with azoles and lead to new therapeutic strategies against *C. albicans* infections.

I.3.4.1 Combination of calcineurin inhibitors and azoles

Calcineurin is a calcium, calmodulin-dependent, serine-threonine specific protein phosphatase that is highly conserved from yeast to humans and mediates many important cellular processes (Hemenway *et al.* 1999). It has important physiological roles in *C. albicans* as calcineurin mediates tolerance to a variety of stresses, including salt, high pH and membrane stress (Cannon *et al.* 2007; Cruz *et al.* 2002; Steinbach *et al.* 2007). Most importantly, calcineurin contributes to azole tolerance in *C. albicans* and is essential for survival in the presence of azoles (Cruz *et al.* 2002). Calcineurin, on the other hand, is a common target for two clinically used immunosuppressive drugs, cyclosporin A and tacrolimus FK506. While these two compounds alone exhibit low *in vitro* antifungal properties against *C. albicans*, a potent synergistic activity has been reported when combined with fluconazole, allowing azoles to become fungicidal against *C. albicans*, *C. glabrata* and *C. krusei* (Cruz *et al.* 2002; Marchetti *et al.* 2000; Onyewu *et al.* 2003). The hypothesis that has been put forth to explain this synergistic effect assumes that cell membrane perturbations resulting from ergosterol depletion by azoles trigger a stress response pathway which would normally be counterbalanced by the signaling pathway involving activation of calcineurin (Cannon *et al.* 2007; Steinbach *et al.* 2007).

Efficacy of the combination of fluconazole and cyclosporin A was tested in a rat model of experimental *C. albicans* endocarditis (Marchetti *et al.* 2000). In this model, the combination of fluconazole and cyclosporin A was indeed more effective than either drug alone at treating both primary heart vegetative lesions and kidney lesions formed via hematogenous dissemination, suggesting that this combination therapy could be effective in an *in vivo* setting. Future research on developing non-immunosuppressive analogs of calcineurin inhibitors could have great therapeutic potential as it would augment the intrinsic antifungal activity of azoles.

In addition to directly targeting calcineurin, it has been shown that calcineurin is the substrate of the heat shock protein HSP90 and the activity of HSP90 potentiates the evolution of drug resistance by stabilizing calcineurin (Cowen *et al.* 2005). Using HSP90 inhibitors abrogates drug resistance of diverse fungal pathogens; furthermore, HSP90 inhibitors resulted in fungicidal activity of fluconazole and rescued wax moth *G. mellonella* from *C. albicans* infection. However, the lack of selectivity of current Hsp90 inhibitors causes high host toxicity in a mouse model of candidasis (Cowen *et al.* 2009). Because HSP90 is highly conserved, finding a compound to inhibit HSP90 in fungi, but not in humans, is a significant hurdle scientists must overcome in the future.

I.3.4.2 Histone deacetylase inhibitors (HDACi) with azoles

It has been recognized in recent years that chromatin remodeling controls gene expression. Histone acetylation at lysine residues results in a relaxed chromatin structure (euchromatin) and facilitates gene transcription; conversely, histone deacetylation often leads to the formation of a compacted heterochromatin structure and is linked to gene repression. Aberrant regulation of this epigenetic mechanism has been shown to cause inappropriate gene expression or repression, a key event in the pathogenesis of many forms of cancer. Histone deacetylase inhibitors (HDACi) are currently being explored as potent chemotherapeutic agents in treating haematological malignancies such as cutaneous T-cell lymphoma, myelodysplastic syndromes and diffuse B-cell lymphoma [reviewed in (Bolden *et al.* 2006)]. Interestingly, exposure of *C. albicans* to the most-studied HDACi, Trichostatin A (TSA), affected its yeast-to-hyphae morphogenesis, and as expected, resulted in compromised pathogenicity and reduced virulence (Hnisz *et al.* 2010; Simonetti *et al.* 2007). Furthermore, TSA has also been found to enhance azole activity against *C. albicans* by interfering with the transcriptional regulation of sterol biosynthesis genes. In addition, TSA abolishes the azole-mediated upregulation of *ERG1, ERG11* as well as genes

involved in azole resistance (*CDR1* and *CDR2*) (Section I.4) (Smith *et al.* 2002). These promising results encouraged researchers to conduct chemical screens for potent HDACi inhibitors that synergize with azoles against *C. albicans* (Mai *et al.* 2007; Pfaller *et al.* 2009). Most recently, a Montreal-based pharmaceutical company (MethylGene Inc.) had reported one such candidate HDACi compound, MGCD290, which shows impressive synergy with azoles against many species of *Candida* as well as *Aspergillus* (Pfaller *et al.* 2009). This inhibitor is currently in phase I clinical trials (http://www.methylgene.com/). In Chapter IV of this thesis, we characterized novel genes involved in histone modifications in *C. albicans* and suggested that targeting these gene products either alone or in combination with already existing antifungal agents could lead to the development of new therapeutic strategies.

I.4 Molecular mechanisms of antifungal resistance

Fungal disease that is refractory to treatment with antifungal drugs is defined as clinically drug-resistant. Antifungal susceptibility of clinical isolates is commonly determined by *in vitro* measurement of minimum inhibitory concentrations (MICs) of antifungal agents against clinical isolates. To ensure compatibility and to allow a direct comparison of susceptibility data from different laboratories, quantitative measurements are performed according to standardized protocols established by the US Clinical and Laboratory Standards Institute (CLSI, http://www.clsi.org/). Specifically, antifungal resistance is defined as a lack of reduction in fungal growth in the presence of an antifungal agent at concentrations higher than an established "breakpoint" MIC. For example, based on established clinical data, *C. albicans* isolates exhibiting MICs of fluconazole and itraconazole greater than 64 and 1 μg/mL, respectively, often correlates with failure in the treatment of clinical infections (Ghannoum *et al.* 1999). Cases of *C. albicans* as well as other pathogenic fungi resistant to almost all available antifungal agents have been reported. To circumvent these recurring

clinical problems, it is important to understand the molecular mechanisms of antifungal resistance. In order to decipher drug resistance mechanisms, many researchers use a "matched set" of susceptible and resistant clinical isolates (characterized by RFLP and electrophoretic karyotyping) to compare and analyze changes in gene expression in the azole-resistant strains versus otherwise isogenic azole susceptible strains by genome-wide gene expression analyses and proteomic studies (Barker *et al.* 2003; Hoehamer *et al.* 2010; Liu *et al.* 2005; Liu *et al.* 2007). Extensive and excellent reviews on this subject are available elsewhere (Anderson 2005; Cannon *et al.* 2009; Cowen 2008; Lupetti *et al.* 2003; Morschhauser 2010; Odds *et al.* 2003; Sanglard *et al.* 2002; White *et al.* 1998); here, I will discuss cellular mechanisms of the most frequently-encountered and well-documented clinical azole resistance in *C. albicans*.

I.4.1 Clinical amphotericin B resistance

Amphotericin B is a potent fungicidal agent. Although rare, resistance of clinical isolates of *Candida* species to amphotericin B has been reported. Fungal resistance to amphotericin B can be intrinsic or acquired. Intrinsic resistance to amphotericin B is common for *C. lusitaniae*, a *Candida* species that has reduced ergosterol content as compared to other amphotericin B-susceptible *Candida* strains (Young *et al.* 2003). Acquired resistance to amphotericin B in *C. albicans* is often associated with mutations resulting in alteration of the membrane lipid composition as well as reduced levels of ergosterol. Furthermore, inhibition of ergosterol biosynthesis with azoles causes subsequent phenotypic resistance to amphotericin B, consistent with the model that ergosterol is its primary binding site (Akins 2005).

I.4.2 Clinical azole resistance

Prophylactic use of azole drugs for solid-organ transplant recipients, intensive care unit patients, neutropenic patients receiving chemotherapy and stem cell

transplant recipients at risk of candidiasis, combined with the fungistatic nature of azole drugs, are responsible for the widespread clinical occurrence of azole resistance.

I.4.2.1 Alterations in *ERG11* and sterol composition

Modification of the target enzyme and/or enzymes in the same biochemical pathway is a common mechanism of acquiring resistance. Previous biochemical and molecular biology studies on sterol content analysis in azole resistant clinical *C. albicans* strains provided information concerning alterations that have occurred during the course of treatment (Asai *et al.* 1999; Loffler *et al.* 2000; White *et al.* 1998). The azole target, lanosterol demethylase (encoded by *ERG11*), has been found to contain mutations or altered expression patterns in azole-dresistant strains, causing reduced affinity or efficacy to azole drugs and minimizing the impact of the drug on the cell. In addition, a loss-of-function mutation in *ERG3*, which acts at a later step (downstream of *ERG11*) in the ergosterol biosynthesis pathway results in a decreased accumulation of the toxic sterols that would otherwise occurr when Erg11p is inhibited and can also contribute to azole resistance in *C. albicans*.

I.4.2.2 Reduced intracellular azole accumulation

Early studies using radioactively labeled azoles, such as [^{3}H]-fluconazole, demonstrated that resistant isolates often accumulate less drugs (up to 10-fold) in an energy-dependent manner, than do matched sensitive isolates, suggesting an involvement of efflux pumps (Albertson *et al.* 1996; Sanglard *et al.* 1995; Venkateswarlu *et al.* 1995). The expression of two types of membrane proteins has been implicated in the resistance of clinical isolates to azoles. Cdr1p and Cdr2p are two homologous transporters belonging to the ATP-binding cassette (ABC) superfamily that use energy from ATP hydrolysis (Section I.5) as well as Mdr1p that belongs to the major facilitator superfamily (MFS) and requires a

proton gradient force as the source of energy (Fig. I.7). Previous clinical studies revealed that the overexpression of Cdr1p and Cdr2p is more frequently encountered in azole-resistant strains than overexpression of Mdr1p; however, expression of both types of transporters is associated with high levels of fluconazole resistance (Lopez-Ribot *et al.* 1999; Sanglard *et al.* 1995).

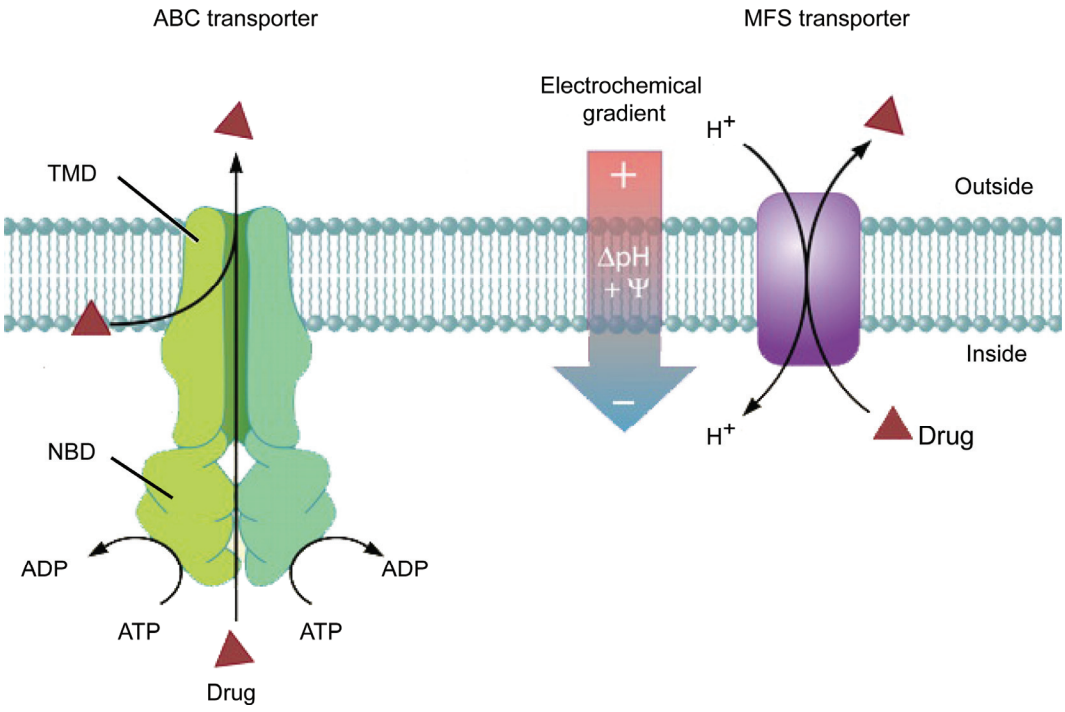

Figure I. 7 The MDR transporters

Multidrug transporter of the ATP-binding cassette (ABC) superfamily uses energy generated from ATP hydrolysis to transport drugs out of the cell from cytosol or hydrophobic drug that partition in the plasma membrane (left). Another type of transporter contributing to azole-resistant phenotype of *C. albicans* belongs to the proton-motive-force dependent transporter (MFS) superfamily (right). The transmembrane electrochemical proton gradient is generated by other H^+-translocating-ATPase present in the membrane (not shown). Adapted from (Cannon *et al.* 2009).

Initially, the ABC transporter genes *CDR1* and *CDR2* were identified using functional complementation studies in *S. cerevisiae*. Expression of either *CDR1* or *CDR2* in the *S. cerevisiae* mutant strain lacking the ABC transporter Pdr5p is

able to confer resistance to drugs like cycloheximide and azoles. Since drug resistance mediated by this type of transporters in microorganisms is an effect that has been well documented, these findings support the proposition that both Cdr1p and Cdr2p could function as drug efflux pumps (Prasad *et al.* 1995; Sanglard *et al.* 1997; Sanglard *et al.* 1995). Single deletion of the *CDR1* gene from an azole-susceptible laboratory strain resulted in an increased susceptibility to azoles; in addition, inducible overexpression of *CDR1* in another azole-susceptible laboratory strain conferred reduced azole susceptibility (Niimi *et al.* 2004b; Sanglard *et al.* 1996). Deletion of *CDR2* from an azole-susceptible strain showed no phenotype, however, deleting *CDR2* in a *cdr1*Δ/*cdr1*Δ strain further increased azole susceptibility in this strain, uncovering the contribution of Cdr2p to azole susceptibility (Sanglard *et al.* 1997). These results demonstrated that both Cdr1p and Cdr2p function as azole efflux pumps in *C. albicans.* However, the direct demonstration that Cdr1p and Cdr2p contribute to clinical azole resistance in an azole-resistant clinical isolate and their relative contributions to the overall azole resistance has not been determined, primarily due to the lack of selectable markers required for genetic manipulation (see Chapter II).

MDR1, a member of the MFS transporter family, is an integral transmembrane protein with 12 transmembrane segments. It was initially identified as a gene that conferred resistance to the antimicrotubule drug benomyl and the anticancer drug methotrexate from screening of *Candida* genomic libraries (Ben-Yaacov *et al.* 1994; Fling *et al.* 1991). Structural and functional studies of Mdr1p suggested that amino acids located in transmembrane helix 5 are critical for the drug/H+ antiport activity (Pasrija *et al.* 2007). Deletion of *MDR1* from an azole-resistant, *MDR1*-overexpressing *C. albicans* isolate resulted in reduced fluconazole resistance of the mutants. In addition, a moderate level of Mdr1p expression in an azole-susceptible *C. albicans* strain was sufficient to confer increased fluconazole resistance. Taken together, these results confirmed that *MDR1* overexpression contributes to the resistant phenotype in *C. albicans* (Hiller *et al.* 2006; Wirsching *et al.* 2000a; Wirsching *et al.* 2001). However, in contrast to the Cdr1p and Cdr2p

transporters which exhibit a wide spectrum of antifungal substrate specificity, Mdr1p confers resistance to fluconazole but not to the related azoles ketoconazole and itraconazole, which are often used in the treatment of *Candida* infections (Wirsching *et al.* 2000b).

I.4.2.3 Transcriptional regulation of azole resistance

The major determinants of azole resistance are regulated at the transcriptional level and efforts have been made to decipher the regulatory circuitries involved in clinical azole resistance (Morschhauser 2010; Shahi *et al.* 2009). Three transcription factors governing three distinct transcriptional activation pathways have been identified in clinical azole-resistant isolates. They are Upc2 (uptake control for sterols), Tac1p (transcriptional activator of *CDR* genes) and Mrr1p (multidrug resistance regulator), belonging to the fungal-specific zinc cluster (Zn_2Cys_6) transcription factor family responsible for the constitutive up-regulation of *ERG11*, *CDR1/CDR2* and *MDR1*, respectively (Coste *et al.* 2004; Morschhauser *et al.* 2007; White *et al.* 2005). Recently, an exhaustive study analyzing 29 clinical isolates identified 17 different gain-of-function (GOF) mutations in Tac1p with the most frequent substitution mutation (21%) at Asn 972 (non-conservative mutation, N972D, N972I and N972S) located within the putative activation domain (Coste *et al.* 2009). Based on the frequency of the favored selection, it is tempting to postulate that this mutation at Asn 972 confers the highest Tac1p activity and azole resistance among the different GOF Tac1p variants. However, a direct comparison of the level of azole resistance conferred by *tac1Δ/tac1Δ* strains carrying different GOF *TAC1* alleles has not been performed. Nevertheless, genome-wide expression and location analyses of four matched sets of azole-susceptible and azole-resistant clinical isolates generated a list of Tac1p targets: in addition to *CDR1* and *CDR2*, Tac1p also regulates many other genes involved in lipid metabolism, some of which also contribute to drug resistance (Liu *et al.* 2007). For example, deletion of *PDR16*, encoding a phosphatidylinositol transfer protein in *C. albicans* resulted in increased azole

susceptibility (Saidane *et al.* 2006). Currently, the contribution of other Tac1p targets in addition to Cdr1p, Cdr2p and Pdr16p to overall azole resistance has not been determined (see Discussion).

GOF mutations have also been identified for Mrr1p as well as for Upc2p, leading to increased resistance to azoles (Dunkel *et al.* 2008a; Dunkel *et al.* 2008b). The hyperactive Mrr1p coordinately up-regulates *MDR1* as well as other genes involved in oxidative stress, some of which seem to contribute to the fluconazole resistance phenotype (Morschhauser *et al.* 2007). In the case of Upc2p, the hyperactive protein could regulate *ERG11*, genes involved in the ergosterol biosynthesis pathway as well as the drug efflux genes *CDR1* and *MDR1*, underscoring its key role in the development of azole resistance (Dunkel *et al.* 2008b; Znaidi *et al.* 2008). It is currently believed that drugs (such as itraconazole and progesterone) could bind directly to the transcription factors of this family and activate gene transcription via a nuclear-receptor-like pathway, in a mechanism similar to the regulation of human multidrug resistance by the PXR (pregnane X receptor) nuclear receptor pathway (Thakur *et al.* 2008).

I.4.2.4 Alternative mechanisms contributing to overall azole resistance

C. albicans is a diploid organism and in the presence of azole stress, mutations conferring increased drug resistance could first occur in one of the two alleles of a gene (such as those encoding transcription factors or the azole target *ERG11*) and a further increase in drug resistance is observed when the second allele also acquires the same mutation. This process, referred to as "selection for loss of heterozygosity", can be achieved by mitotic recombination, gene conversion or by aberrant chromosome formation (Selmecki *et al.* 2006; 2010; Selmecki *et al.* 2008). Selmecki and Berman provided the first example of aberrant chromosome formation causing azole resistance (Selmecki *et al.* 2006). They found that when under azole stress, *C. albicans* could modify its own chromosomes by duplicating one arm of chromosome 5 and deleting the other, replacing it with the duplicated

arm. The altered chromosome is known as an isochromosome. Most importantly, this part of the duplicated isochromosome contains two genes, the transcription factor *TAC1* responsible for overexpressing *CDR1/2* as well as *ERG11*, thus providing a direct correlation between the level of azole resistance and copy numbers of these genes. Furthermore, collaborative efforts from *Candida* research laboratories using large-scale sequencing and chromosome analyses of many related clinical isolates as well as strains derived from the *in vitro* evolution of azole-resistance, document different ways that *C. albicans* adopts to overcome azole stress. These often include combinations of more than one mechanism: *TAC1* and/or *ERG11* mutations, loss of heterozygosity of *TAC1* and/or *ERG11* and aneuploidy, highlighting the genome plasticity of *C. albicans* during the course of azole-resistance acquisition (Coste *et al.* 2007; Selmecki *et al.* 2008; Selmecki *et al.* 2009). Genomic alterations and loss of heterozygosity in the *MRR1* and *UPC2* genes have also been recently documented in association with increased azole resistance (Dunkel *et al.* 2008b; Morschhauser *et al.* 2007). Finally, the detection of these described alterations in other fungal pathogens isolated directly from patients suggests that variations in chromosome organization and copy number are a common mechanism used by pathogenic fungi to rapidly generate diversity in response to stressful growth conditions, including, but not limited to, antifungal drug exposure (Marichal *et al.* 1997; Morschhauser 2010; Schubert *et al.* 2008).

Another cellular mechanism that has been observed in azole-resistant strains that could contribute to maintaining high levels of resistance against azoles is the increased stability of the *CDR1* mRNA transcript (Manoharlal *et al.* 2008). The length of the polyadenylated (polyA) tail of *CDR1* from azole-resistant isolates was approximately 1.5-times longer than that obtained from azole-susceptible strains, correlating with a longer half-life of the *CDR1* transcript in the azole-resistant strain (Manoharlal *et al.* 2008). The follow-up study showed that the gene encoding poly(A) polymerase (*PAP1*), responsible for mRNA adenylation, had lost its heterozygosity in the azole-resistant strain and therefore contributed to

hyperadenylation and subsequent increased stability of *CDR1* transcripts (Manoharlal *et al.* 2010). It is, however, presently not known if other genes that are involved in azole resistance are also under similar post-transcriptional regulation.

I.4.3 Clinical echinocandin resistance

Currently, clinical resistance against echinocandins appears to be rare, which is likely due to the fungicidal properties of echinocandins. Moreover, unlike azoles, these newly available, FDA-approved echinocandins have not yet become the antifungal agents commonly used in prophylaxic treatment of *Candida* infections (Pappas *et al.* 2009). However, cases of clinical resistance have been reported (Laverdiere *et al.* 2006; Perlin 2007). Furthermore, it is anticipated that the number of infecting strains with reduced echinocandin susceptibility will rise as patient exposure to this drugs broadens.

The mechanism associated with *C. albicans* clinical echinocandin resistance is the mutation in the echinocandin-responsive gene *FKS1* under selective pressure. Recent genetic studies have identified two "hot-spot" regions in Fks1p where mutations occur and these regions are highly conserved among the fungal *FKS* family (Park *et al.* 2005; Perlin 2007). These mutations include the non-conservative amino acid substitutions Phe641 to Pro649 ("hot-spot 1") and Arg1352 ("hot-spot 2"). Among these, the highest frequency of substitutions is found at Ser645 (S645P, S645F or S645Y) of "hot-spot 1". Additionally, *in vitro* enzymatic assays demonstrated that mutant Fks1p containing the S645P mutation is up to 1000-fold less sensitive to caspofungin, micafungin and anidulafungin, confirming that mutations in Fks1p cause echinocandin resistance (Park *et al.* 2005; Perlin 2007).

I.5 ATP-binding cassette (ABC) transporters

One of the most prominent characteristics of ABC transporters is that they share a highly conserved nucleotide binding domain, NBD, which has been demonstrated to be involved in ATP binding and hydrolysis, thereby providing energy for a large number of biological processes. Mutation or misregulation of ABC transporters has been associated with a number of human diseases and importantly, it has been implicated in the multidrug resistance phenotypes of tumor cells or responsible for antimicrobial resistance (Section I.4.2.2.).

I.5.1 The ABC superfamily

ABC transporters and ABC proteins together constitute one of the most abundant protein superfamilies (the ABC superfamily). They are involved not only in the transport of a wide variety of substances, but they are also involved in many cellular processes. Members of the ABC superfamily are ubiquitous and can be found in all species from bacteria to human. For example, about 5% of the entire *Escherichia coli* genome encodes components of the ABC superfamily (Linton *et al.* 1998); 29 ABC genes are found in the yeast *S. cerevisiae* genome (Decottignies *et al.* 1997), 26 ABC genes are found in *C. albicans* (Braun *et al.* 2005) and 50 genes are found in the human genome (Dean *et al.* 2001c). Structural and functional studies of ABC transporters established a widely accepted model that the basic functional unit for an ABC transporter requires four structural domains: two TMDs and two NBDs. These four domains, however, can be found encoded as separate polypeptides, as found in some prokaryotic transporters, or fused in one of many different configurations into multidomain polypeptides, as found in eukaryotic transporters (Fig. I.8). Eukaryotic ABC transporters are organized either as half-length transporters containing only one TMD and one NBD or as full-length transporters containing duplicated TMDs and NBDs (Hyde *et al.* 1990). Interestingly, it has been demonstrated that half-length transporters must form either homodimers or heterodimers in order to produce a functional transporter.

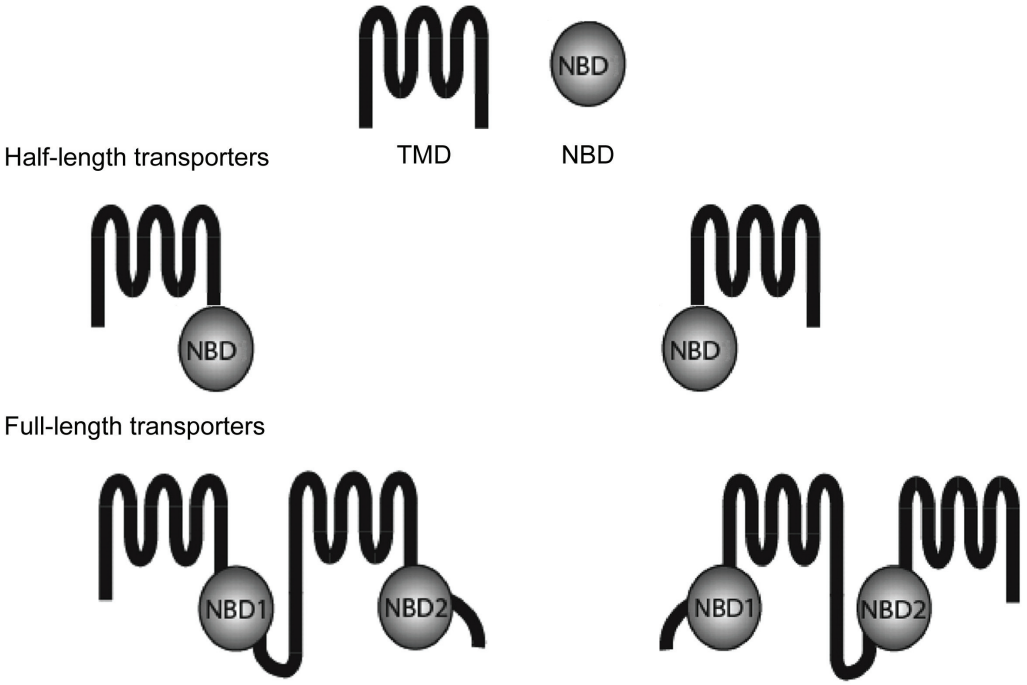

Figure I. 8 Overall architecture of the ABC superfamily

Basic 'building blocks' of ABC transporters are the cytosolic nucleotide-binding domain (NBD) and the membrane-spanning transmembrane domain (TMD) (top panel). In eukaryotes, these two domains are fused together as a half-length transporter either in a 'forward' (TMD-NBD) or a 'reversed' topology; half-length transporters homo- or hetero-dimerize to form a functional transporter (middle panel). The full-length transporter consists of two NBD and two TMD domains fused into a single polypeptide (bottom panel). Adapted and modified from (Paumi *et al.* 2009).

A classification has been established for the mammalian ABC superfamily. Human ABC transporters have been divided into seven subfamilies, designated ABCA to ABCG, based on similarity in gene structure (half- versus full-length transporters), order of the domains and sequence homology in the NBDs and TMDs [http://nutrigene.4t.com/humanabc.htm, (Dean *et al.* 2001c)]. Hence, members of each subfamily across species tend to have partially overlapping physiological and biochemical functions. Finally, orthologs from six of these

seven mammalian ABC gene subfamilies are also found in the yeast genome (Decottignies *et al.* 1997; Paumi *et al.* 2009).

I.5.2 ABCA to ABCG subfamilies

In this section, I will cover selected members of ABC transporters from ABCA, ABCB, ABCC, ABCD and ABCG subfamilies, starting with examples from mammalian transporters, transporters from the *S. cerevisiae* and *C. albicans* origins. Members of ABCE and ABCF subfamilies contain only NBD domains with no TMD domains, since they are not actually ABC transporters so they will not be discussed here. The goal is to highlight the wide spectrum of cellular processes in which these transporters participate. In addition, extensive summaries of ABC transporter subfamilies can be found in these reviews (Abele *et al.* 2004; Albrecht *et al.* 2007; Burke *et al.* 2007; Dean *et al.* 2001a; Dean *et al.* 2001c; Fletcher *et al.* 2010; Gottesman *et al.* 2001; Gottesman *et al.* 2006; Guggino *et al.* 2006; Krishnamurthy *et al.* 2006; Lamping *et al.* 2010; Paumi *et al.* 2009; Riordan 2008).

I.5.2.1 ABCA subfamily

This family contains some of the largest transporters in humans (over 2,100 amino acids with a predicted molecular weight of more than 200 kDa). A distinct feature of members of this subfamily is the presence of two large extracellular domains (ECDs) between the first and second transmembrane helices (TMHs) in each predicted TMD, organized in a TMH_1-ECD_1-TMD_1(TMH_{2-6})-NBD_1-TMH_7-ECD_2-TMD_2(TMH_{8-12})-NBD_2 fashion. The human ABCA transporter family is composed of twelve full-length transporters. Members of this subfamily have been mostly associated with lipid trafficking. The best-characterized genes are *ABCA1*, encoding a cholesterol transporter that transports excess cholesterol from peripheral tissues onto high density lipoproteins (HDL) (Bodzioch *et al.* 1999) and *ABCA4*, encoding a photospecific transporter of retinoids and is expressed

exclusively in retinal photoreceptor cells (Allikmets *et al.* 1997). Mutations in these genes are associated with human diseases; the *ABCA1* gene is responsible for Tangier's disease, which is a rare inherited disorder of defective cholesterol transport. Patients with this condition have an elevated amount of blood cholesterol and their tonsils are visibly affected, usually appearing orange or yellow and extremely enlarged (Bodzioch *et al.* 1999; Rust *et al.* 1999). Mutations in *ABCA4* have been linked to Stargardt macular degeneration and related retinal degenerative diseases that eventually lead to total vision loss (Allikmets *et al.* 1997; Koenekoop 2003).

The ABCA subfamily was previously reported to be absent in yeasts (Braun *et al.* 2005; Dean *et al.* 2001b; Decottignies *et al.* 1997; Paumi *et al.* 2009); however, a very recent phylogenetic analysis of the ABC proteins extracted from the genomes of 27 fungal species revealed an uneven distribution of *ABCA* genes among fungi. It is found in Chytridiomycota species (*Batrachochytrium dendrobatidis* and *Spizellomyces punctatus*), which are distantly related to Saccharomycotina species (*S. cerevisiae* and *C. albicans*), with the exception of *Yarrowia lipolytica* (Kovalchuk *et al.* 2010). There are two full-length and two half intact ABCA transporters found in *S. punctatus*; however, none of their functions have been characterized (Kovalchuk *et al.* 2010).

I.5.2.2 ABCB subfamily

The ABCB subfamily contains four full-length transporters (TMD_1-NBD_1-TMD_2-NBD_2) and seven half (TMD_1-NBD_1) transporters; it is the only human subfamily having both sizes of transporters (Dean *et al.* 2001a). Among members of this subfamily, ABCB1 (or MDR1/P-gp) was the first identified mammalian ABC transporter, which had been extensively studied due to its clinical importance. Overexpression of ABCB1/MDR1/P-gp confers multidrug resistance (MDR) in cancer cells and is often associated with the failure of chemotherapy (Ambudkar *et al.* 1999; Gottesman *et al.* 2006). *ABCB1* is highly expressed in hepatocytes

and capillary endothelial cells comprising the blood-brain barrier; it can also be found in the intestinal epithelium, renal tubular cells and adrenal glands (Ambudkar *et al.* 1999; Gottesman *et al.* 2002; Gottesman *et al.* 1996). Remarkably, ABCB1 has been shown to transport many structurally unrelated hydrophobic substrates including the cytotoxic agents vinblastine, doxorubicin, actinomycin as well as lipids, steroids, xenobiotics and peptides (Ambudkar *et al.* 1999). Hence, the primary function of ABCB1 is thought to protect cells by removing toxic agents as well as harmful metabolites. Substrate promiscuity is a hallmark of ABCB1 and enormous effort has been dedicated to determining the structure of this protein as this information is important for the rational design of anticancer drugs and MDR inhibitors. A 3.8-angstrom crystal structure of mouse ABCB1, which has 87% sequence identity to human has been produced. This structure reveals a large internal cavity (~6000 $Å^3$) formed by two TMD domains, which is large enough to accommodate at least two compounds simultaneously and may contain overlapping drug binding sites (Aller *et al.* 2009). This was the first full-length mammalian ABC transporter (exporter) that has been crystallized. It provided structural information that significantly advanced our knowledge of the transport mechanism in this class of transporters.

The well studied ABCB half transporters are ABCB2/TAP1 and ABCB3/TAP2, transporters associated with antigen processing (TAP). These transporters are located in the ER and Golgi and are involved in transporting and presenting proteasome-produced peptides to the major histocompatibility complex (MHC) I molecule, their functions are thus important in the adaptive immune system (Abele *et al.* 2004; Romsicki *et al.* 1999). ABCB2 and ABCB3 half transporters must heterodimerize to transport peptides as dimerization of NBDs from each transporter is required to convert energy from ATP hydrolysis to peptide transport (Janas *et al.* 2003; Lacaille *et al.* 1998). Indeed, it was demonstrated that mutations in *ABCB2* result in dramatically decreased expression of *ABCB3*, highlighting the observation that the stability of the TAP complex depends on the presence of both proteins (Lankat-Buttgereit *et al.* 2002). Mutations in *ABCB2* as

well as in *ABCB3* have also been documented in Bare Lymphocyte Syndrome. This disease is characterized by severe downregulation of MHC class I which is partly due to mutations in *ABCB2/ABCB3*. These patients suffer from frequent recurrent bacterial infections of the respiratory tract. Furthermore, the TAP complex is also a target for viruses or tumors to escape immune surveillance by employing strategies to downregulate the expression of *ABCB2/ABCB3* (Abele *et al.* 2004; Lankat-Buttgereit *et al.* 2002).

In *S. cerevisiae*, members of the ABCB family include the only full-length transporter Ste6p that is expressed at the plasma membrane and three other half transporters (Atm1p, Mdl1p and Mdl2p) that are located in the mitochondria. Ste6p was the first identified yeast ABC transporter and it has been shown to function as the pheromone transporter for **a**-factor which mediates mating (Kuchler *et al.* 1989; McGrath *et al.* 1989). *S. cerevisiae* Ste6p has been characterized extensively, partly because of its structural similarities with the mammalian multidrug transporter ABCB1; expression of mouse P-gp/MDR3 in an *S. cerevisiae ste6Δ* strain restores the ability of cells to export **a**-factor (Raymond *et al.* 1992). Recently, Ste6p has been used as a model transporter for studying the fate of membrane proteins in intracellular trafficking, membrane localization and proteolytic turnover pathways (Kolling 2002; Kolling *et al.* 1997; Krsmanovic *et al.* 2005). The half-length transporter Atm1p has been shown to be important for mitochondrial iron homeostasis by mediating free iron transport into the cytosol; *atm1Δ* cells accumulate high levels of free iron which results in increased oxidative stress within the cell (Kispal *et al.* 1997). On the other hand, functional roles for Mdl1p and Mdl2p are less clear although Mdl1p appears to be able to partially complement Atm1p deficiency and is probably involved in mitochondrial peptide transport (Burke *et al.* 2007; Young *et al.* 2001). Orthologs of yeast ABCB members are present in *C. albicans*, however, except for the full-length transporter Hst6p (homolog of STE6) which has been shown to be a functional homolog of *S. cerevisiae* Ste6p, other half transporters (*ATM1*,

ORF19.1077; *MDL1*, ORF19.2615 and *MDL2*, ORF19.13043) remain to be characterized (Braun *et al.* 2005; Raymond *et al.* 1998).

I.5.2.3 ABCC subfamily

There are twelve full-length transporters in this subfamily, representing the largest subfamily of ABC transporters in humans. Among its members, ABCC1/MRP1 was the first identified transporter and it was cloned in 1992 from the drug-selected human lung cancer cell line (Deeley *et al.* 2006; Munoz *et al.* 2007). Characterization of ABCC1/MRP1 reveals the presence of one additional TMD at the N-terminus, with the topological arrangement as TMD_0-TMD1-NBD_1-TMD_2-NBD_2. ABCC1/MRP1 transports a broader range of xenobiotics (displaying some overlapping substrate specificity with ABCB1/P-gp) as well as many glutathione (GSH)-conjugates compounds and heavy metals. ABCC1/MRP1 also transports diverse physiological substrates such as folates, GSH-, sulphate-, and glucuronide- conjugates of steroids, leukotrienes and prostaglandins. These activities of ABCC1/MRP1 are important in normal cellular processes such as export of endogenous intermediates and protection from toxic accumulation (Deeley *et al.* 2006; Munoz *et al.* 2007).

The most well known transporter of this subfamily is the cystic fibrosis transmembrane conductance regulator (ABCC7/CFTR), which is associated with the disease cystic fibrosis affecting approximately 30,000 patients in the United States and an estimated 60,000 individuals worldwide (Guggino *et al.* 2006). CFTR is the only ABC transporter known to function as an ion channel and is involved in maintaining ion and fluid homeostasis. Mutations in the *CFTR* gene are associated with abnormal Cl^- and Na^+ ion transport in several tissues including the lungs, pancreas, gastrointestinal tract, liver, sweat glands and male reproductive organs; among these sites, the function of CFTR in the lung is of major importance. The most frequently encountered CFTR mutation is the F508Δ mutation, resulting in protein misfolding and premature degradation. Significant

reduction in functional CFTR transporters in the plasma membrane of airway epithelial cells leads to the accumulation of viscous mucus in the lung airways, allowing bacterial colonization (*Pseudomonas aeruginosa*) and chronic inflammation with acute exacerbations by impaired mucociliary clearance (Cheung *et al.* 2008; Guggino *et al.* 2006; Riordan 2008; Sloane *et al.* 2010).

Another unique feature of CFTR that distinguishes it from the rest of the other family members is the presence of an additional regulatory domain, the R domain; thus, the domain organization of CFTR is TMD_1-NBD_1-R-TMD_2-NBD_2. Extensive research established that this domain plays important roles in the regulation of CFTR activity: phosphorylation by protein kinase A (PKA) at multiple sites within the R domain increases ATP binding at the NBDs and therefore stimulates transporter activity (Hegedus *et al.* 2009; Mense *et al.* 2006; Ostedgaard *et al.* 2001; Seibert *et al.* 1999; Winter *et al.* 1997). Due to the clinical importance of CFTR, ongoing research is focusing on understanding the regulatory mechanisms that modulate the activity, turnover as well as the intracellular trafficking of CFTR (Guggino *et al.* 2006). Additionally, research is also focusing on screening for small molecules to act as molecular chaperone for correcting the folding defects as well as enhancing channel activity of mutant CFTR proteins (Rosser *et al.* 2009).

In *S. cerevisiae*, the ABCC subfamily contains six full-length transporters which have a distinguishing structural feature: the presence of an additional N-terminal domain, comprising a TMD with five transmembrane segments (TMD_0) and a short cytosolic loop (L_0) (TMD_0-L_0-TMD_1-NBD_1-TMD_2-NBD_2). However, this structural topology does not apply to Yor1p (yeast oligomycin resistance 1), the only transporter in this family that does not contain TMD_0, only L_0 (Katzmann *et al.* 1995). Furthermore, Yor1p is also the only ABCC transporter that is localized at the plasma membrane. The overexpression of *YOR1* confers a pleiotropic drug resistance phenotype (PDR), protecting cells against increasing concentrations of oligomycin, rhodamine, as well as phosphatidylethanol amine (Decottignies *et al.*

1998). Finally, despite the inverted domain topology organization, Yor1p shares overlapping substrate specificities with a member of the ABCG subfamily, Pdr5p (see I.5.2.5) (Decottignies *et al.* 1998).

The Ycf1l (yeast cadium factor) is a vacuolar membrane-bound transporter that mediates vacuolar detoxification of heavy metals and glutathione-S conjugates (GS-conjugates), as well as the red pigment accumulating in *ade2Δ* mutant cells (Sharma *et al.* 2003; Szczypka *et al.* 1994). Interestingly, recent studies suggest that the activity of Ycf1p is affected by its phosphorylation status, as phosphorylation at Ser908 and Thr911 at the region connecting NBD1-TMD2 is essential for cadmium detoxification (Eraso *et al.* 2004); on the other hand, phosphorylation at Ser251 in the L_0 region of Ycf1p has a negative impact on its function (Paumi *et al.* 2008).

In *C. albicans*, there are four annotated genes belonging to the ABCC subfamily. ORF19.1783 and ORF19.6478 are mostly likely the otholog of *S. cerevisiae* Yor1p and Ycf1p, respectively; however they have not yet been functionally characterized (Braun *et al.* 2005).

I.5.2.4 ABCD subfamily

ABCD is the smallest subfamily as compared to other ABC subfamilies and contains only four half-length transporters with the TMD-NBD arrangement in human. They are exclusively localized to the peroxisomal membrane and are involved in transporting very-long-chain (24-30 carbons) fatty acids. The best characterized transporter is ABCD1/ALD, which has been implicated in X-linked adrenoleukodystrophy (ALD). ALD is a neurodegenerative disorder characterized by the accumulation of very-long-chain fatty acids in the serum, brain and adrenal cortex (Dean *et al.* 2001c; Wanders *et al.* 2007). In *S. cerevisiae*, there are only two members of the ABCD subfamily, namely, *PXA1* and *PXA2*. Early genetic and biochemical analyses showed that Pxa1p and Pxa2p

must heterodimerize to form a complete peroxisomal functional unit and mediate the uptake of activated long-chain fatty acids from the cytosol into the yeast peroxisomal matrix where they are subject to β-oxidation (Shani *et al.* 1996; Wanders *et al.* 2007). *C. albicans PXA1*/ORF19.7500 and *PXA2*/ORF19.5255 are orthologs of *S. cerevisiae PXA,* but their functions have not yet been characterized (Braun *et al.* 2005).

I.5.2.5 ABCG subfamily

Members of this subfamily in humans are all half-size transporters with a unique "reversed" domain arrangement (NBD-TMD). There are six members in this subfamily and four of them (ABCG1, ABCG2, ABCG4 and ABCG5) have been described in human (Dean *et al.* 2001a). The best characterized transporter is ABCG2 (MXR/BCRP), whose overexpression was found to confer multidrug resistance in breast cancer cells (Doyle *et al.* 1998; Krishnamurthy *et al.* 2006). ABCG2 has been shown in different biochemical assays to function as a homodimer, including experiments demonstrating that a nonfunctional ABCG2 (bearing a mutation in the NBD) can act as an effective dominant-negative inhibitor when co-transfected with wild-type ABCG2 (Ozvegy *et al.* 2001; Ozvegy *et al.* 2002). Furthermore, functional ABCG2 has been shown to transport many structurally unrelated chemotherapeutic agents, such as mitoxantrone, camptothecin and doxorubicin; interestingly, ABCG2 also shares overlapping substrate specificity with ABCB1/P-gp, including doxorubicin, topotecan, methotrexate as well as the fluorescent compounds Hoechst 33342 and rhodamine 123, highlighting the promiscuous character of this transporter (Krishnamurthy *et al.* 2006).

In contrast to the relatively small size of the mammalian ABCG subfamily, the *S. cerevisiae* ABCG subfamily is the biggest ABC subfamily and is comprised of a total of ten members. Among its members, *ADP1* encodes the only half-size transporter with unknown function, others are full-length transporters arranged in

the NBD_1-TMD_1-NBD_2-TMD_2 fashion. Notably, this type of full-length transporter is not found in mammals but rather in fungi and plants (Taglicht *et al.* 1998; Verrier *et al.* 2008). More importantly, *S. cerevisiae* Pdr5p (pleiotropic drug resistance 5) has been shown to be a functional homolog of human ABCB1/P-gp due to its ability to transport a large number of structurally unrelated compounds (cycloheximide, azoles, mycotoxins, fluorescent compounds, etc), and its ability to confer PDR (Balzi *et al.* 1994). Pdr5p is also the most abundant plasma membrane-bound ABCG transporter in *S. cerevisiae* during the logarithmic growth phase and its level decreases significantly when cells exit exponential growth, suggesting a role in cellular detoxification during active growth; however its endogenous substrate(s) remain to be identified (Mamnun *et al.* 2004).

The closest homologs of Pdr5p are Pdr10p (67% sequence identity) and Pdr15p (75% identity); however, functional analyses of these two transporters suggested that, unlike Pdr5p, Pdr10p and Pdr15p do not contribute to the PDR phenotype and only exhibit weak activity against a limited spectrum of drugs (Wolfger *et al.* 2004). Another transporter that recognizes many structurally unrelated xenobiotics and is therefore implicated in the PDR network is Snq2p. This transporter shares some but not all substrate specificities with Pdr5p, as both mediate resistance to staurosporine, fluphenazine and are involved in sterol transport (Mahe *et al.* 1996). However, only Snq2p could confer cellular resistance to the mutagen 4-nitroquinoline *N*-oxide (4NQO) (Decottignies *et al.* 1995; Servos *et al.* 1993). The closest homolog of Snq2p is Pdr12p, sharing about 60% sequence identity. Expression of *PDR12* mediates resistance to weak organic acids that are frequently used in food preservatives as well as organic acids produced in amino acid catabolism (Hazelwood *et al.* 2006; Piper *et al.* 1998). The transporters belonging to this subfamily that have been most recently characterized are Aus1p and Pdr11p; both have been implicated in sterol uptake when endogenous sterol biosynthesis is impaired during anaerobic growth. *AUS1* is also upregulated in response to azole treatment, implying that it could mediate

drug efflux or is involved in the compensatory response to the compromised plasma membrane integrity caused by azole treatment (Barker *et al.* 2003; Wilcox *et al.* 2002). Finally, despite the fact that yeast ABCG transporters have been studied extensively during the last two decades, the functions of *ADP1*, *PDR18* and *YOL075c* are still unknown.

Similar to *S. cerevisiae*, the ABCG subfamily of *C. albicans* forms the largest subfamily with seven full-length transporters and two half-sized transporters (Braun *et al.* 2005). Among the full-length transporters, Cdr1p and Cdr2p have been characterized extensively due to their important role in azole resistance (Prasad *et al.* 1995; Sanglard *et al.* 1997; Sanglard *et al.* 1995; White *et al.* 1998) (Section I.4.2.2). Cdr1p and Cdr2p display a high degree of sequence homology (84% identity, 92% similarity) and their function has been characterized mostly using the heterologus overexpression system constructed in *S. cerevisiae*. The *CDR1* and *CDR2* genes have been cloned into either episomal or integrative expression vectors and expressed in the *S. cerevisiae* mutant strains that lack several endogenous ABC transporters (Dogra *et al.* 1999; Gauthier *et al.* 2003; Nakamura *et al.* 2001; Smriti *et al.* 2002). Collectively, researchers showed that expression of either Cdr1p or Cdr2p in *S. cerevisiae* confers resistance to many structurally unrelated compounds with antifungal properties, including azoles (fluconazole, ketoconazole, itraconazole), cycloheximide and rhodamine 6G. On the other hand, despite both proteins sharing similar substrate specificities, they also exhibit distinct activities against other compounds. For example, only Cdr2p is able to confer resistance against the immunosuppressant FK506/FK520, not Cdr1p (Gauthier *et al.* 2003). Finally, both Cdr1p and Cdr2p have been proposed to function as general phospholipid translocators. Using fluorescent-tagged phospholipid analogs, both Cdr1p and Cdr2p could elicit in-to-out (flop) transbilayer movement of the phosphatidylethanolamine (PE) analog from the inner-layer to the outer-layer of the plasma membrane. This function is important for maintaining asymmetrical distribution of phospholipids in the plasma membrane and its integrity (Dogra *et al.* 1999; Smriti *et al.* 2002).

Cdr3p shares 56% sequence identity with Cdr1p. Functional characterization showed that its disruption did not affect the drug susceptibility, which is probably due to the fact that its expression is not detected in white cells (Cdr3p is an opaque-phase ABC transporter) (Balan *et al.* 1997). However, forced overexpression in white cells neither affected the drug susceptibility profiles in *C. albicans*, indicating that this transporter is not involved in drug transport (Balan *et al.* 1997). Another transporter that shares a high degree of sequence homology with Cdr1p but is not involved in drug transport is Cdr4p, with 62% sequence identity to Cdr1p. Disruption of both alleles of *CDR4* from *C. albicans* did not increase azole susceptibility, hence the biological function of *CDR4* remains to be determined (Franz *et al.* 1998). Currently, our understanding of other *C. albicans* ABCG transporters is very limited as there is no functional studies available for the annotated ABCG members *CDR5* (ORF19.918), *SNQ2* (ORF19.5759), *CDR6* (ORF19.4531) as well as two half-size transporters ORF19.3120 and *ADP1* (ORF19.459).

Finally, recent phylogenetic analyses reported that the fungal ABCG subfamily is probably the group that shows the greatest evolutionary diversity and the least conserved transporter members. For example, the number of ABCG transporters ranges from less than ten members in *C. albicans*, *C. krusei* and *C. dubliniensis* to up to twenty members in *Aspergillus* species (Kovalchuk *et al.* 2010; Lamping *et al.* 2010). This difference is probably a result of differential gene multiplication during adaptive evolution, potentially reflecting different environmental niches occupied by each species and the range of xenobiotics they encounter during growth. Nevertheless, it is currently difficult to validate this hypothesis, as our understanding about the physiological functions of these fungal transporters in general is very limited.

I.5.3 Structure of ABC transporters and mechanisms of transport

In order to understand the mechanism by which ABC transporters mediate unidirectional transport of molecules across membranes, structural data are essential. Obtaining such data has not been a trivial task due to inherent difficulties in purification and reconstitution of these membrane proteins in an active form. With enormous efforts invested for more than two decades, genetic, biochemical and structural studies have provided a wealth of information regarding our understanding of the molecular mechanism underlying ABC transport, although many questions still remain. These data have been summarized in several recent reviews (Davidson *et al.* 2004; Ernst *et al.* 2010; Higgins 2007; Hollenstein *et al.* 2007; Kerr *et al.* 2010; Linton 2007; Locher 2009; Oswald *et al.* 2006). Here, I will summarize some central findings that are important for our understanding of fungal multidrug transporters.

I.5.3.1 Important structural characteristics of ABC transporters

The NBDs of all ABC transporters, whether of prokaryotic or eukaryotic origin, share extensive amino acid sequence identity and several characteristic motifs. These motifs include the Walker A motif, which is composed of the consensus sequence GX_4GKS/T, where X represents any amino acid; this motif is responsible for binding to the phosphates of ATP or ADP. The Walker B motif contains four consecutive hydrophobic amino acids (Φ) followed by a glutamic acid, ΦΦΦΦD; this motif is important for making water-bridged contact with Mg^{2+} and is the catalytic base for ATP hydrolysis. In between the Walker A and Walker B motifs, there is the LSGGQ Signature motif that has originally been used as the 'signature' to identify ABC transporters. The LSGGQ motif also participates in ATP binding. Additionally, there is a Q-loop (glutamine or glutamic acid), which serves as the contact point between the NBD and the intracellular loops of the TMDs, playing an important role in the 'conformational cross-talk' between NBD and TMD hence coupling ATP hydrolysis to substrate

transport. Finally, there is the H-loop located downstream of the Walker B motif consisting of a highly conserved histidine residue which forms a hydrogen bond with the γ-phosphate of ATP. Structural and biochemical analyses of various ABC proteins demonstrated that the two 'L-shaped' NBDs, upon ATP binding, form a 'head-to-tail' dimer configuration as two ATP molecules are "sandwiched" at the interface of the NBD dimer, each ATP molecule is coordinately bound by the Walker A motif from one NBD and the Signature motif from the opposing NBD (Dawson *et al.* 2006; Oswald *et al.* 2006).

Most prokaryotic or eukaryotic transporters contain two NBDs equipped with identical consensus motifs as described above. However, the primary structure of most members of the yeast ABCG subfamily of ABC transporters, including *S. cerevisiae* Pdr5p, *C. albicans* Cdr1p and Cdr2p, reveals a profound asymmetry between the two NBDs (Jha *et al.* 2003a). They contain a typical Signature motif but have a degenerate Walker A and Walker B motif in their N-terminal NBD (NBD1). The highly conserved lysine of the Walker A motif ($GX_4G\underline{K}S/T$) has been replaced by a cysteine ($GX_4G\underline{C}S/T$) and the histidine of the H-loop is also missing in NBD1. Moreover, the Signature motif sequence deviates from the canonical amino acids (LNVEQ instead of LSGGQ) in the C-terminal NBD (NBD2) (Jha *et al.* 2003a). While the functional roles of these atypical motifs in these fungal transporters are not yet clear, it has been shown in several prokaryotic and eukaryotic ABC transporters that the invariant Lys residue in the Walker A motif is critical for the ATPase activity and transporter function (Davidson *et al.* 2004). Earlier experiments performed using a purified NBD1 from *C. albicans* Cdr1p showed that mutagenesis of the unique NBD1 Walker A cysteine to alanine resulted in a loss of ATP hydrolysis, suggesting a special ATP-dependent functional role for this atypical arrangement (Jha *et al.* 2004; Jha *et al.* 2003a; Jha *et al.* 2003b). However, this result is unexpected and contradicts another study in *S. cerevisiae* Pdr5p, where mutation of the corresponding cysteine to tyrosine did not affect the multidrug resistance profile (Egner *et al.* 1998). Taken together, although the functional roles of these atypical motifs of

fungal transporters are being debated, the structural and catalytic importance of these residues raises questions concerning the functional status of the deviant Walker A motif in the NBD1 of fungal ABCG transporters (see section I.5.3.2).

The transmembrane domain (TMD) typically, but not always, consists of six α-helices or transmembrane segments. Two TMDs together form a channel across the membrane, allowing passage of the substrates. These domains also contain a substrate-binding site (or sites) that contribute to transport specificity. Hence, unlike the highly conserved NBD domain, primary sequences of TMDs are much less conserved among different ABC transporters, reflecting a vast number of already identified transport substrates by different transporters. To date, there are at least two distinct substrate binding sites identified in ABCB1/P-gp (Shapiro *et al.* 1997). These are referred to as the H-site and the R-site, as binding sites for Hoechst 33342 and Rhodamine 123, respectively. In line with this, the recent crystal structure of ABCB1/P-gp revealed a large size drug-binding pocket that could accommodate at least two compounds simultaneously (Aller *et al.* 2009). These data explained, at least in part, the ability of this protein to transport a broad range of different substrates. Mapping of drug binding sites has been performed for the fungal transporter *S. cerevisiae* Pdr5p using biochemical competition assays. It suggested there are at least two, maybe three, independent binding sites in Pdr5p (Golin *et al.* 2003; Golin *et al.* 2000; Kolaczkowski *et al.* 1996). Furthermore, extensive molecular modeling suggests that the size of the substrate, despite its hydrophobicity, is an important parameter for Pdr5p substrate recognition, as it recognizes substrates that have surface volumes greater than 90 $Å^3$ and an optimal substrate size of around 200–225 $Å^3$. It is anticipated that *C. albicans* Cdr1p could have drug binding pockets similar to that of *S. cerevisiae* Pdr5p based on the overall sequence conservation. Indeed, experiments using photoaffinity compounds in drug competition assays revealed two distinct binding sites (Shukla *et al.* 2003).

In an effort to further our understanding of the structural and functional relationships of fungal transporters despite the lack of high-resolution structural data, researchers have used a random mutagenesis approach. This approach generated some potentially interesting mutants of *S. cerevisiae* Pdr5p (Egner *et al.* 1998; Tutulan-Cunita *et al.* 2005). Of particular importance was the data generated with S1360 in the hydrophilic face of the predicted transmembrane segment 11 (TMS11) of Pdr5p (Egner *et al.* 2000; Egner *et al.* 1998). A S1360F substitution resulted in altered drug transport for only a subset of substrates, such as azole derivatives and cycloheximide. On the other hand, the inhibitory effect of the immunosuppressive compound FK506 on Pdr5p-mediated antifungal resistance was greatly reduced by the S1360F mutation. The importance of TMS11 has also been demonstrated in *C. albicans* Cdr1p, where the equivalent mutation, the T1351F mutation in Cdr1p also resulted in reduced Cdr1p function (Shukla *et al.* 2004a; Shukla *et al.* 2003). Finally, these random mutagenesis studies also showed several mutants of Pdr5p with altered substrate specificity; intriguingly, these mutations are located in the nucleotide-binding domains. Taken together, these results imply that there is potential intensive cross-talk between energy consumption (NBD) and substrate selection (TMD).

I.5.3.2 Model of transport mechanism

The fundamental transport mechanism of ABC transporters appears to be conserved despite their diverse cellular functions. The "ATP-switch" model has been established based on the recent structural and biochemical data from a number of ABC transporters, including the most recently solved crystal structure of mammalian ABCB1/P-gp (Aller *et al.* 2009). The ATP-switch model describes a multistep process involving communication via conformational changes between the NBDs and TMDs (Fig. I.9). Initially at the pre-transport state, the transporter is sitting at the plasma membrane in an inward facing conformation with two separated NBD monomers and a large internal cavity formed by the TMDs facing the cytoplasm. The transport cycle is initiated upon substrate

binding to the TMDs and this induces a conformational change involved in transmitting a signal from the TMDs to the NBDs to enhance ATP binding. The NBDs subsequently undergo the first conformational change forming a 'closed' NBD dimer by binding two ATP molecules at the dimer interface. This 'switch' of NBDs from the 'open' to the 'closed' conformation induces changes in the TMDs necessary for releasing bound substrates to the extracellular space, resulting in an outward facing state of the transporter. The second conformational change at the NBDs or the reverse of this switch, from the 'closed' dimer to the 'open' dimer is facilitated by ATP hydrolysis and ADP/Pi release and resets the transporter back to the initial inward facing state, ready for the next transport cycle. The scheme described here is a general model of transport, however, the details and temporal order of nearly every sub-step is under intense debate. Extensive reviews on structural and biochemical data discussing molecular mechanisms of transport can be found elsewhere (Hollenstein *et al.* 2007; Kerr *et al.* 2010; Kos *et al.* 2009; Linton 2007).

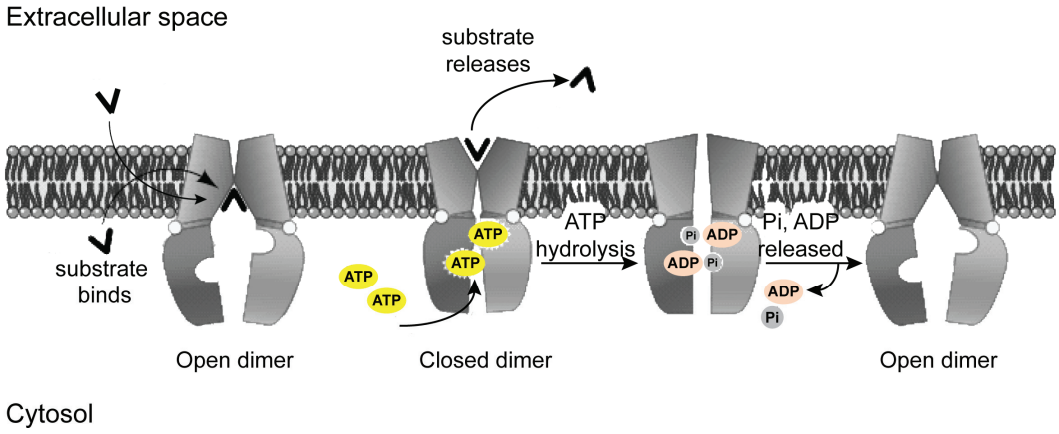

Figure I. 9 The simplified view of the mechanism of transport

Substrate binding to TMDs of the inward facing ABC transporter induces a conformational change in the NBDs and increases its affinity for ATP. NBDs dimerize and bind two ATP molecules at the interface of the dimer. The dimerization of NBDs induces conformational change in the TMDs resulting an outward facing state of the transporter, thus facilitating release of the bound substrate. ATP hydrolysis triggers dissociation of the NBD dimer and brings further conformational changes in the TMDs. Finally, phosphate and ADP release restores the transporter to the initial inward facing conformation ready for the subsequent cycle. Adapted and modified from (Linton 2007).

This ATP switch model predicts that two molecules of ATP can be equally hydrolyzed at the two binding sites constituted by the NBD dimerization, specifically, the ATP nucleotide is positioned in between the Walker A motif of one NBD and the Signature motif of the opposing NBD. In the case of fungal ABCG transporters with one typical NBD and one degenerate NBD, this situation would create only one active and one corrupted ATPase site. The active site is also called the 'NBD2 composite', consisting of the typical Walker A motif of NBD2 and the Signature motif of NBD1; and the corrupted site is the 'NBD1 composite' site, including the non-consensus residues from the Walker A motif of NBD1 and the Signature motif of NBD2. It is currently not yet understood how the ATP-switch model can be applied to this type of transporter with asymmetrical NBDs or whether there are alternative mechanisms. It is possible that ATP binding/hydrolysis cannot occur at the NBD1 composite and instead,

NBD1 could serve as a 'regulatory' platform for dimerization that is unique to fungal ABCG transporters (Wada *et al.* 2005). Although such a function may be possible in ABCG monomers, evidence from purified *S. cerevisiae* Pdr5p suggests it functions as a dimer, indicating that intermolecular interactions could also play role(s) in the regulation and function of this type of transporter (Ferreira-Pereira *et al.* 2003).

I.5.4 Regulation of ABC transporter

Regulation of many ABC transporters takes place at the level of gene expression, as is the case of *C. albicans* Cdr1p and Cdr2p (Section I.4.2.3.). However, the activity of ABC transporters, once expressed, may also be regulated. For this purpose, some transporters contain an additional regulatory domain, for example, the R domain of ABCC7/CFTR that is the target site for protein kinase A-mediated phosphorylation. Specifically, it has been demonstrated that lack of phosphorylation of the R domain prevents its NBD1-NBD2 dimerization, thus preventing the function of this transporter; this effect is reversed by phosphorylation of the R domain, implying that phosphorylation plays a positive regulatory role on CFTR activity [Section I.5.2.3. and (Dahan *et al.* 2001; Mense *et al.* 2006)]. For other transporters that do not contain a defined regulatory domain, such as the mammalian transporter ABCB1/P-gp, phosphorylated residues have been shown to cluster at the cytoplasmic loop connecting the NBD1 to TMD2 (the linker loop), however the role of phosphorylation on P-gp function is currently unclear due to some controversial results (Conseil *et al.* 2001; Germann *et al.* 1996; Glavy *et al.* 1997; Lelong-Rebel *et al.* 2005; Sachs *et al.* 1999; Zhang *et al.* 2004). Phosphorylation has been shown to play both positive and negative regulatory roles on the activity of some yeast ABC transporters; some of the best characterized examples include ABCC/Ycf1p (Eraso *et al.* 2004; Paumi *et al.* 2008) as well as ABCG/Pdr5p (Decottignies *et al.* 1999). Furthermore, the phosphorylation status could also influence the cellular

trafficking and turnover of the transporter via an ubiquitination-mediated process, as it has been demonstrated for ABCB/Ste6p (Kelm *et al.* 2004; Kolling 2002; Kolling *et al.* 1997). Regardless of these findings, our understanding of how ABC transporters are regulated by post-translational modifications is far from complete, since in many cases the participating kinases/ubiquitin ligases as well as the signaling pathways have not yet been identified. In particular, whether the activity of *C. albicans* Cdr1p and Cdr2p is also modulated by post-translational modifications is unknown (Chapter III).

Another factor that has been postulated to influence the function of ABC transporters is its surrounding membrane lipids. This is not surprising since certain phospholipids and cholesterol are defined substrates for ABC transporters (Pomorski *et al.* 2004). In line with this, cholesterol has been shown to have positive effects on the activity of ABCB1/P-gp and this transporter is also found enriched in a cholesterol-rich microdomain of the plasma membrane, called the lipid raft (Orlowski *et al.* 2006). These data suggest an intimate relationship between the lipid composition and ABC transporters. In yeast, *S. cerevisiae* Pdr5p as well as *C. albicans* Cdr1p and Cdr2p have been shown to be involved in translocating phospholipid phosphatidylethanolamine (PE) across the lipid transbilayer; their activity is also affected by the phospholipid composition of the plasma membrane (Decottignies *et al.* 1998; Smriti *et al.* 2002; Smriti *et al.* 1999). Interestingly, previous studies suggested that the membrane lipid composition is slightly different between *S. cerevisiae* and *C. albicans*. The percentage of PE of the total membrane phospholipids is approximately two-fold higher in *S. cerevisiae* than that in *C. albicans* (Loffler *et al.* 2000; van den Hazel *et al.* 1999), although it is currently not known if this variation contributes to any physiological functions. However, the functional characterization of *C. albicans* Cdr1p and Cdr2p to date have been mostly done by heterologous expression in *S. cerevisiae*. Taking into account the difference in the plasma membrane lipid composition between the two yeasts, the functional characterization of Cdr1p and Cdr2p would be best studied in *C. albicans* (Chapter II and III).

I.6 Rationale and objectives

The fungal pathogen *Candida albicans* is the fourth most common cause of hospital-acquired infections and systemic candidiasis is associated with a high mortality rate. Current treatment of candidiasis involves the use of azoles, the most widely used antifungal agents that target ergosterol biosynthesis. However, the efficacy of azoles is compromised by the frequent emergence of *C. albicans* azole-resistant strains. Furthermore, clinical management of fungal infections is facing challenges from an ever-increasing spectrum of fungal diseases caused not only by *C. albicans*, but by some intrinsically azole-resistant *Candida* species, as well as other fungal pathogens.

My Ph.D. research studies focused on two different aspects of *C. albicans* infection chemotherapy. The first objective was to obtain a better understanding of the molecular mechanisms responsible for ABC transporter-mediated azole resistance. I propose that the knowledge gained here could help us to find ways to reverse transporter-mediated azole resistance in the long term (Chapters II and III). My second objective, as the need for better antifungal drugs remains, I propose to identify and to study important functional genes in *C. albicans* that show evolutionary conservation among other pathogenic fungi but are not found in human. The products of these genes could represent interesting biological targets for the development of new antifungal agents with novel mechanisms and broad spectrum of antifungal activities (Chapter IV).

Chapter II

Relative contributions of the *Candida albicans* ABC transporters Cdr1p and Cdr2p to clinical azole resistance

Chapter II Relative contributions of the *Candida albicans* ABC transporters Cdr1p and Cdr2p to clinical azole resistance

It has been documented that overexpression of the ABC transporters Cdr1p and Cdr2p is linked to a decreased intracellular accumulation of azole drugs and a reduced azole-susceptibility of *C. albicans* cells. However, the direct demonstration that Cdr1p and Cdr2p contribute to azole resistance in clinical azole resistant strain is lacking, as is our knowledge of the relative contribution of each transporter to clinical azole resistance. Hence, we investigated the relative importance of these two transporters for the observed azole resistance in a clinical isolate.

Relative Contributions of the *Candida albicans* ABC Transporters Cdr1p and Cdr2p to Clinical Azole Resistance

Running Title: Cdr1p- and Cdr2p-mediated clinical azole resistance

Sarah Tsao[1,2], Fariba Rahkhoodaee[1] and Martine Raymond[1,2,3*]

[1]Institute for Research in Immunology and Cancer, Université de Montréal, Montreal, QC, Canada H3T 1J4; [2]Department of Biochemistry, McGill University, Montreal, QC, Canada H3G 1Y6; [3]Département de Biochimie, Université de Montréal, Montreal, QC, Canada H3C 3J7.

*Corresponding author:
Martine Raymond, Institute for Research in Immunology and Cancer, Université de Montréal, P.O. Box 6128, Station Centre-Ville, Montreal, Quebec, Canada H3C 3J7. Phone: (514) 343-6746. Fax: (514) 343-6843. E-mail: martine.raymond@umontreal.ca.

II.1 Abstract

Candida albicans frequently develops resistance to treatment with azole drugs due to the acquisition of gain-of-function mutations in the transcription factor Tac1p. Tac1p hyperactivation in azole-resistant isolates results in the constitutive overexpression of several genes, including *CDR1* and *CDR2* which encode two homologous transporters of the ATP-binding cassette family. Functional studies of Cdr1p and Cdr2p have been carried out so far by heterologous expression in the budding yeast *Saccharomyces cerevisiae* and by gene deletion or overexpression in azole-sensitive *C. abicans* strains in which *CDR1* expression is low and *CDR2* expression is undetectable. Thus, the direct demonstration that *CDR1* and *CDR2* overexpression causes azole resistance in clinical strains is still lacking, as is our knowledge of the relative contribution of each transporter to clinical azole resistance. In the present study, we used the *SAT1* flipper system to delete the *CDR1* and *CDR2* genes from clinical isolate 5674. This strain is resistant to several azole derivatives due to a strong hyperactive mutation in Tac1p and expresses high levels of Cdr1p and Cdr2p. We found that deleting *CDR1* had a major effect, reducing resistance to fluconazole (FLC), ketoconazole (KTC) and itraconazole (ITC) by 6-, 4-, and 8-fold, respectively. Deleting *CDR2* had a much weaker effect, reducing FLC or KTC resistance by 1.5-fold, and had no effect on ITC resistance. These results demonstrate that Cdr1p is a major determinant of azole resistance in strain 5674 and potentially in other clinical strains overexpressing Cdr1p and Cdr2p, while Cdr2p plays a more minor role.

II.2 Introduction

Candida albicans is one of the leading causes of fungal infections affecting immunocompromised individuals. *Candida* infections range from chronic superficial infections of the skin and mucosal surfaces to invasive, life-threatening systemic infections (Mathews *et al.* 2002; Sims *et al.* 2005). Many antifungal drugs used to treat *Candida* infections target the biosynthesis of ergosterol, the major sterol in the fungal cell membranes (Odds *et al.* 2003). Polyenes, such as amphotericin B (AMB), directly bind to ergosterol and form pores in the cell membrane, resulting in low selectivity and high toxicity (Odds *et al.* 2003). Azoles, a class of well-tolerated antifungal drugs that includes fluconazole (FLC), ketoconazole (KTC), itraconazole (ITC), and new-generation derivatives such as voriconazole and posaconazole, target the enzyme lanosterol 14α-demethylase (Erg11p), which is involved in ergosterol biosynthesis, blocking the production of ergosterol and causing the accumulation of toxic intermediate sterol species (Odds *et al.* 2003). As a consequence, the fluidity and permeability of the fungal cell membrane are changed and the activity of membrane-bound proteins, such as enzymes involved in cell wall synthesis, is altered (Odds *et al.* 2003).

However, the fungistatic rather than fungicidal action of azole drugs leads to the frequent emergence of azole-resistant (A^R) *C. albicans* strains (Akins 2005; White *et al.* 1998). One mechanism of azole resistance consists of increased levels of *ERG11* RNA, resulting in an increased production of the Erg11p enzyme, or point mutations in the *ERG11* gene, producing an enzyme with a reduced binding affinity for azole drugs (Akins 2005; White *et al.* 1998). Also, several A^R clinical isolates overexpress the *CDR1* and *CDR2* genes, which encode two homologous transporters of the ATP-binding cassette (ABC) family, and/or the *MDR1* gene, which encodes a major facilitator (Akins 2005; White *et al.* 1998). A number of A^R strains overexpress *CDR1* and *CDR2* but not *MDR1,* whereas other strains overexpress only *MDR1* (Sanglard *et al.* 1995), suggesting the involvement of two distinct transcriptional pathways. Also, some A^R strains overexpress the three

genes, probably due to the accumulation of independent mutations in the two pathways, leading to high levels of resistance in response to stepwise drug selection (White *et al.* 1998). The overexpression of transporter genes in A^R isolates suggested that a reduced accumulation of azoles in the cell was responsible for the observed azole resistance phenotype (Akins 2005; White *et al.* 1998). By using a dominant selectable marker, it was shown that deleting *MDR1* in A^R clinical isolates overexpressing this gene reduced the resistance of the cells to FLC, providing a direct demonstration that *MDR1* is involved in clinical FLC resistance (Wirsching *et al.* 2000a). However, the direct contribution of *CDR1* and *CDR2* to clinical azole resistance remained to be determined.

Recent progress has been made in deciphering the regulatory circuitry that governs the regulation of *CDR1*, *CDR2*, *MDR1,* and *ERG11* in *C. albicans* clinical strains. It was shown that the upregulation of the *CDR1* and *CDR2* genes in A^R isolates is due to gain-of-function mutations in the zinc cluster transcription factor Tac1p (Coste *et al.* 2006; Coste *et al.* 2004). Most of these mutations consist of C-terminal amino acid substitutions or small in-frame deletions (Coste *et al.* 2007; Coste *et al.* 2006). Tac1p was also shown to activate the transcription of *CDR1* and *CDR2* upon cell treatment with different compounds such as fluphenazine (FPZ) and steroids (estrogen, progesterone) (Coste *et al.* 2004) but the mechanisms by which these compounds trigger Tac1p activity are still unknown. Similarly, gain-of-function mutations in two other zinc cluster transcription factors, Mrr1p and Upc2p, have recently been shown to be responsible for the constitutive upregulation of Mdr1p and Erg11p, respectively, in clinical A^R isolates (Dunkel *et al.* 2008a; Morschhauser *et al.* 2007). These data confirmed the involvement of different transcriptional pathways in the upregulation of the *CDR1*/*CDR2*, *MDR1*, and *ERG11* genes in A^R isolates.

The Cdr1p and Cdr2p transporters show 84% amino acid sequence identity and are close homologs of *Saccharomyces cerevisiae* Pdr5p, a major effector of cell tolerance to xenobiotic compounds in budding yeast (Balzi *et al.* 1994; Prasad *et*

al. 1995; Sanglard *et al.* 1997). These transporters are formed by two similar halves, each with an N-terminal hydrophilic domain that contains an ATP-binding motif followed by a C-terminal hydrophobic domain with six predicted transmembrane segments that presumably contain the drug binding sites, a structure characteristic of the pleiotropic drug resistance subfamily of ABC transporters found in fungi and plants (Taglicht *et al.* 1998; Verrier *et al.* 2008). Because of the advanced genetics of *S. cerevisiae*, most studies of Cdr1p and Cdr2p have been carried out with heterologous expression systems in *S. cerevisiae,* where Cdr1p and Cdr2p were expressed under the control of a strong promoter, leading to very high levels of azole resistance (~100-fold) (Gauthier *et al.* 2003; Saini *et al.* 2006). It was shown that the two transporters localize at the plasma membrane (Schuetzer-Muehlbauer *et al.* 2003; Shukla *et al.* 2003), bind rhodamine 6G (R6G) (Gauthier *et al.* 2003), export their substrates in an energy-dependent manner, and possess ATPase and phospholipid translocase activities (Lamping *et al.* 2007; Smriti *et al.* 2002). Expression systems in *S. cerevisiae* have also proved useful for structure-function studies of the transmembrane and ATP-binding domains of Cdr1p (Jha *et al.* 2004; Rai *et al.* 2005; Saini *et al.* 2006).

However, there is evidence supporting the importance of studying these transporters in a potentially more relevant host, namely, *C. albicans* A^R cells. First, the function of ABC transporters is influenced by their lipid environment (Romsicki *et al.* 1999; Smriti *et al.* 1999) and, since *S. cerevisiae* and *C. albicans* have different plasma membrane lipid compositions (Loffler *et al.* 2000; van den Hazel *et al.* 1999), the function of Cdr1p and Cdr2p could be altered in *S. cerevisiae*. Also, the *S. cerevisiae* strains used for these studies carry deletions in (up to seven) genes which encode endogenous ABC transporters (Gauthier *et al.* 2003; Lamping *et al.* 2007). Since these ABC transporters can function as sterol transporters or phospholipid flippases (Decottignies *et al.* 1998; Raychaudhuri *et al.* 2006), the deletion of these genes may affect the plasma membrane composition of the recipient yeast and thus Cdr1p and Cdr2p function. On the

other hand, Cdr1p and Cdr2p function has been studied by gene deletion, by using the URA-blaster system, in *C. abicans* azole-sensitive (A^S) strains, in which *CDR1* expression is low and *CDR2* expression is undetectable (Sanglard *et al.* 1997). Deletion of *CDR1* resulted in increased azole susceptibility, whereas deletion of *CDR2* did not render the cells more susceptible to azoles, due to the lack of *CDR2* expression in these cells (Sanglard *et al.* 1997). Interestingly, the *cdr1Δ/cdr1Δ cdr2Δ/cdr2Δ* double mutant was found to be more susceptible to azole drugs and other toxic compounds than the *cdr1Δ/cdr1Δ* single mutant (Sanglard *et al.* 1997). Another study showed that the inducible expression of *CDR1* in an A^S strain carrying a homozygous deletion of the gene resulted in resistance to several antifungal agents, including azole drugs (Niimi *et al.* 2004b). Also, genome-wide expression and location analyses of the Tac1p regulon have shown that, in A^R strains, *CDR1* and *CDR2* are coregulated with many other genes, some of them predicted to be involved in membrane protein trafficking and lipid metabolism and potentially modulating Cdr1p and Cdr2p function (Liu *et al.* 2007). Taken together, these observations emphasized the need for directly studying Cdr1p and Cdr2p in A^R *C. albicans* clinical isolates. In the present study, we addressed this question by deleting the two genes, individually and in combination, from a well-characterized A^R clinical isolate in which the Tac1p pathway is activated (Saidane *et al.* 2006; Znaidi *et al.* 2007).

II.3 Materials and methods

Strains and growth media.

The *C. albicans* strains used in this study are listed in Table II.1; for details of their construction, see the supplemental material. Strains were routinely grown at 30˚C in YPD medium containing 1% yeast extract (EMD Biosciences, Darmstadt, Germany), 2% Bacto peptone (BD Biosciences, Sparks, MD), and 2% glucose (Sigma, St. Louis, MO). For solid medium, 2% agar (Difco, BD) was added.

Table II. 1 *C. albicans* strains used in this study

Strain	Genotype or phenotype	Parent	Reference
Clinical isolates			
SC5314	A^s		(Gillum et al., 1984)
5457	A^s		(Saidane et al., 2006)
5674	A^r (*CDR1 CDR2* overexpression)	5457	(Saidane et al., 2006)
SZY31	*tac1*Δ::*FRT*/*tac1*Δ::*FRT*	5674	(Znaidi et al., 2007)
5674 *cdr2* mutant derivatives			
STY1	*cdr2A*Δ::*SAT1-FLP*/*CDR2B*	5674	This study
STY2	*CDR2A*/*cdr2B*Δ::*SAT1-FLP*	5674	This study
STY3	*cdr2A*Δ::*FRT*/*CDR2B*	STY1	This study
STY4	*CDR2A*/*cdr2B*Δ::*FRT*	STY2	This study
STY5	*cdr2A*Δ::*FRT*/*cdr2B*Δ::*SAT1-FLP*	STY3	This study
STY6	*cdr2A*Δ::*SAT1-FLP*/*cdr2B*Δ::*FRT*	STY4	This study
STY7	*cdr2A*Δ::*FRT*/*cdr2B*Δ::*FRT*	STY5	This study
STY8	*cdr2A*Δ::*FRT*/*cdr2B*Δ::*FRT*	STY6	This study
5674 *cdr1* mutant derivatives			
STY13	*cdr1A*Δ::*SAT1-FLP*[a]/*CDR1B*	5674	This study
STY14	*cdr1A*Δ::*SAT1-FLP*[a]/*CDR1B*	5674	This study
STY37	*CDR1A*/*cdr1B*Δ::*SAT1-FLP*[b]	5674	This study
STY38	*CDR1A*/*cdr1B*Δ::*SAT1-FLP*[b]	5674	This study
STY15	*cdr1A*Δ::*FRT*/*CDR1B*	STY13	This study
STY16	*cdr1A*Δ::*FRT*/*CDR1B*	STY14	This study
STY41	*CDR1A*/*cdr1B*Δ::*FRT*	STY37	This study
STY42	*CDR1A*/*cdr1B*Δ::*FRT*	STY38	This study
STY17	*cdr1A*Δ::*FRT*/*cdr1B*Δ::*SAT1-FLP*[b]	STY15	This study
STY18	*cdr1A*Δ::*FRT*/*cdr1B*Δ::*SAT1-FLP*[b]	STY16	This study
STY19	*cdr1A*Δ::*FRT*/*cdr1B*Δ::*FRT*	STY17	This study
STY20	*cdr1A*Δ::*FRT*/*cdr1B*Δ::*FRT*	STY18	This study
5674 *cdr1*, *cdr2* mutant derivatives			
STY25	*cdr2A*Δ::*FRT*/*cdr2B*Δ::*FRT cdr1A*Δ::*SAT1-FLP*[a]/*CDR1B*	STY7	This study
STY26	*cdr2A*Δ::*FRT*/*cdr2B*Δ::*FRT cdr1A*Δ::*SAT1-FLP*[a]/*CDR1B*	STY7	This study
STY27	*cdr2A*Δ::*FRT*/*cdr2B*Δ::*FRT cdr1A*Δ::*FRT*/*CDR1B*	STY25	This study
STY28	*cdr2A*Δ::*FRT*/*cdr2B*Δ::*FRT cdr1A*Δ::*FRT*/*CDR1B*	STY26	This study
STY29	*cdr2A*Δ::*FRT*/*cdr2B*Δ::*FRT cdr1A*Δ::*FRT*/*cdr1B*Δ::*SAT1-FLP*[b]	STY27	This study
STY30	*cdr2A*Δ::*FRT*/*cdr2B*Δ::*FRT cdr1A*Δ::*FRT*/*cdr1B*Δ::*SAT1-FLP*[b]	STY28	This study
STY31	*cdr2A*Δ::*FRT*/*cdr2B*Δ::*FRT cdr1A*Δ::*FRT*/*cdr1B*Δ::*FRT*	STY29	This study
STY32	*cdr2A*Δ::*FRT*/*cdr2B*Δ::*FRT cdr1A*Δ::*FRT*/*cdr1B*Δ::*FRT*	STY30	This study
STY45	*CDR2A-SAT1-FLP*/*cdr2B*Δ::*FRT cdr1A*Δ::*FRT*/*cdr1B*Δ::*FRT*	STY31	This study
STY47	*CDR2A-FRT*/*cdr2B*Δ::*FRT cdr1A*Δ::*FRT*/*cdr1B*Δ::*FRT*	STY45	This study

[a] Disruption cassette derived from pCDR1koA.
[b] Disruption cassette derived from pCDR1koB.

Reagents and antifungal compounds.

Molecular biology reagents and restriction enzymes were purchased from Invitrogen (Carlsbad, CA) or from New England Biolabs (Ipswich, MA). Hot-Start KOD^{+} DNA polymerase (Novagen, La Jolla, CA) was used for the amplification and cloning of PCR products. DNA primers were purchased from Integrated DNA Technologies (San Diego, CA). PCR and plasmid DNA fragments were purified using DNA purification kits from Qiagen (Mississauga, ON, Canada). Acid-washed glass beads (425 to 600 nm) used for genomic DNA, and total protein extracts were purchased from Sigma. All chemical and antifungal compounds were purchased from Sigma unless otherwise stated.

RNA preparation and Northern blotting.

Cell growth, total RNA extraction by the hot phenol method, and Northern blot hybridizations were carried out as described previously (Saidane *et al.* 2006). The *CDR1* and *CDR2* probes used in this experiment were also described previously (Saidane *et al.* 2006). The resulting blots were exposed to a Fujifilm Imagine Plate screen and analyzed with the MultiGauge software (version 2.3; Fujifilm).

Membrane protein preparation and Western blotting.

Total membrane extracts from *C. albicans* cells were prepared as follows. Overnight cultures were diluted into 100 ml of fresh YPD medium to an optical density at 600nm (OD_{600}) of 0.1. Logarithmically growing cells (OD_{600} of 1.0) were harvested, washed once with ice-cold distilled H_2O, and resuspended in 5 ml extraction buffer (10 mM Tris-HCl [pH 7.5]; 400 mM NaCl; 10% glycerol; 1 mM sodium orthovanadate; 50 mM sodium fluoride; 50 mM sodium β-glycerophosphate; 10 mM β-mercaptoethanol; 1 μM MG132 and protease inhibitors; 1 mM phenyl-methyl-sulfonyl-fluoride; leupeptin, pepstatin, and aprotinin at 5 μg/ml each). Cell suspensions were then frozen in liquid nitrogen and stored at -80˚C. Frozen cell pellets were disrupted with a the Freezer Mill (SPEX CetriPrep, Metuchen, NJ) with four cycles of successive grinding and

cooling periods, each cycle consists of 2 min of grinding at an impact frequency of 14 times/s followed by a 2-min cooling interval. Total protein extracts were cleared by centrifugation at 1,000 x *g* for 5 min at 4˚C. Total membrane extracts were harvested by centrifuging the total protein extracts at 260,000 x *g* for 45 min at 4˚C. Protein concentrations were determined with the micro-BCA protein assay kit from Pierce (Rockford, IL), and total protein extracts (20 μg) were separated by sodium dodecyl sulfate-polyacrylamide gel electrophoresis (7.5% acrylamide, 37.5:1 acrylamide/bisacrylamide ratio). The gels were either stained with Coomassie or transferred to a nitrocellulose membrane with a Trans Blot SD Semi-Dry transfer apparatus (Bio-Rad). The membrane was stained with Ponceau reagent (0.1 % Ponceau S in 5 % acetic acid) prior to immunodetection. Immunodetection of Cdr1p and Cdr2p was performed with anti-Cdrp (1:1,000 dilution), anti-Cdr2p (1:4,000 dilution) (Gauthier *et al.* 2003) or anti-Cdr1p (1: 4,000 dilution) (de *et al.* 2002) polyclonal antibodies and an ECL chemoluminescence kit (SuperSignal chemiluminscent substrate; Pierce).

Drug susceptibility testing.

Liquid microtiter plate assays were performed as described previously (Znaidi *et al.* 2007). The drug concentrations tested were 0.2, 0.4, 1.5, 3.1, 6.2, 12.5, 25, 50, 100, 150, and 200 μg/ml for FLC; 0.001, 0.002, 0.005, 0.009, 0.019, 0.038, 0.075, 0.15, 0.2, 0.3, 0.4, 0.6 and, 1.2 μg/ml for KTC; 0.0004, 0.0008, 0.0016, 0.0031, 0.0063, 0.0125, 0.025, 0.05, 0.1, 0.2, and 0.4 μg/ml for ITC; 0.8, 1.6, 3.1, 6.3, 12.5, 19, 25, 38, 50, 75, and 100 μg/ml for FPZ; 0.032, 0.063, 0.125, 0.25, 1, 2, 4, 8, and 16 μg/ml for R6G; and 0.032, 0.063, 0.125, 0.25, 0.5, 1, 2, 4, 8, 16, and 32 μg/ml for AMB. Stock solutions of FLC, FPZ, and R6G were prepared in water at concentrations of 5, 10, and 128 mg/ml, respectively; stock solutions of KTC, ITC, and AMB were prepared in dimethyl sulfoxide at concentrations of 3, 1, and 10 mg/ml, respectively. Cell growth was measured spectrophotometrically by determining the OD_{620} after 48 h of incubation at 30˚C in YPD. The MICs for 50% of the strains tested (MIC_{50}s) were determined as the first concentration of drug capable of reducing growth by 50% compared to that of control cells grown

in the absence of the drug. The data are presented as the mean of three independent experiments performed in duplicate. Spot assays were performed as described previously (Saidane *et al.* 2006). Cells grown overnight were resuspended in YPD to an OD_{600} of 0.1. Tenfold serial dilutions of each strain were spotted onto YPD plates containing the drugs tested.

II.4 Results

Deletion of the *CDR1* and *CDR2* genes in the *C. albicans* A^R clinical isolate 5674.

To determine the contribution of *CDR1* and *CDR2* to clinical azole resistance, we used the *SAT1* flipper strategy, which allows the dominant selection of transformants with the *SAT1* gene, which confers nourseothricin resistance (Reuss *et al.* 2004), to delete the *CDR1* and *CDR2* genes, independently or in combination, from the A^R clinical isolate 5674. This strain and A^S strain 5457 were isolated from the same patient and shown by DNA fingerprinting analysis to be highly related (Saidane *et al.* 2006). Compared to strain 5457, strain 5674 is resistant to several azole derivatives and overexpresses the *CDR1* and *CDR2* RNAs at high levels due to a strong gain-of-function mutation in the transcription factor Tac1p (N972D) (Saidane *et al.* 2006; Znaidi *et al.* 2007). Tac1p appears to be the key determinant of azole resistance in strain 5674, since deletion of the *TAC1* gene in that strain causes a complete loss of azole resistance, the resulting *tac1*Δ/*tac1*Δ mutant being as susceptible to azole drugs as strain 5457 (Znaidi *et al.* 2007). This proposition is also supported by the demonstration that strain 5674 does not overexpress the *MDR1* or *ERG11* genes (Saidane *et al.* 2006), suggesting that no other transcriptional pathways are activated in this strain besides the Tac1p pathway, and does not carry mutations in *ERG11* (K. S. Barker and P. D. Rogers, personnal communication). Finally, strain 5674, as well as other A^R strains carrying an activated Tac1p protein, overexpress many genes that encode proteins with predicted functions in lipid metabolism, phospholipid translocation, and protein trafficking which could possibly modulate Cdr1p and Cdr2p activity (Liu *et al.* 2007). Therefore, the use of strain 5674 to delete *CDR1* and *CDR2* allows the analysis of Cdr1p and Cdr2p function in a clinically relevant, well-characterized host.

We constructed a *CDR2* deletion cassette, consisting of the *SAT1-FLP* marker flanked by approximately 1 kb of *CDR2* upstream and downstream sequences

amplified from strain SC5314 (see Fig. II.S1a in the supplemental material). The correct integration of the deletion cassette at the *CDR2* locus was verified by Southern blotting (see Fig. II.S1c in the supplemental material). Two independent heterozygous mutants with the expected integration profile were chosen to delete the second allele, yielding two independent homozygous *cdr2*Δ/*cdr2*Δ mutants, STY7 and STY8 (see Fig. II.S1c in the supplemental material). Deletion of the *CDR1* gene from strain 5674 was performed essentially as described for *CDR2*, with the exception that two different *CDR1* deletion constructs were used to delete the two alleles, generating the two independent homozygous *cdr1*Δ/*cdr1*Δ mutants STY19 and STY20 (see Fig. II.S2 in the supplemental material). *CDR1* was also deleted from strain STY7, producing two mutant strains lacking both transporter genes, STY31 and STY32 (*cdr1*Δ/*cdr1*Δ *cdr2*Δ/*cdr2*Δ) (see Fig. II.S2 in the supplemental material). Finally, we constructed strain STY47, in which one allele of *CDR2* was re-integrated at its original locus in strain STY31 (see Fig II.S3 in the supplemental material).

Cdr1p and Cdr2p expression in strains 5457 and 5674 and strain 5674 mutant derivatives.

We analyzed the expression of the *CDR1* and *CDR2* genes in strains SC5314, 5457, and 5674 and different 5674 mutant derivatives by Northern and Western blotting.

For the Northern blot analysis, total RNA was prepared and the mRNA levels of *CDR1* and *CDR2* were detected using gene-specific probes derived from the first 340 and 294 bp of the *CDR1* or *CDR2* open reading frame, respectively, a region where the level of sequence homology between the two genes is low (Saidane *et al.* 2006). Low levels of *CDR1* transcript were detected in A^S strains SC5314 and 5457, and high levels in A^R strain 5674 (Fig II.1a, top, lanes 1 to 3), whereas *CDR2* transcripts were detected only in the A^R strain (Fig. II.1a, middle, lanes 1 to 3). As previously reported, deleting the *TAC1* gene in strain 5674 (SZY31) decreased *CDR1* and *CDR2* expression to levels similar to those detected in the

A^S strains (Fig. II.1a, lane 4) (Znaidi *et al.* 2007). In strain STY7 (*cdr2*Δ/*cdr2*Δ), we detected a signal for *CDR1* but not for *CDR2*, confirming the deletion of *CDR2* in that strain (Fig. II.1a, lane 5). Similarly, the absence of a signal for *CDR1* in strain STY19 (*cdr1*Δ/*cdr1*Δ) was consistent with the deletion of *CDR1* in that strain (Fig. II.1a, lane 6). Furthermore, we did not detect any signal for *CDR1* and *CDR2* in strain STY31 (*cdr1*Δ/*cdr1*Δ *cdr2*Δ/*cdr*Δ), in line with the deletion of the two genes in that strain (Fig. II.1a, lane 7). The *CDR1* and *CDR2* RNA levels detected in strain STY7 and STY19, respectively, were comparable to those detected for each gene in strain 5674, indicating that the expression of one gene remained unaffected by the deletion of the other one, ruling out the presence of a potential compensatory overexpression effect. Finally, detection of a full-length *CDR2* transcript confirmed the expression of *CDR2* in the *CDR2*-complemented strain STY47 (Fig. II.1a, lane 8).

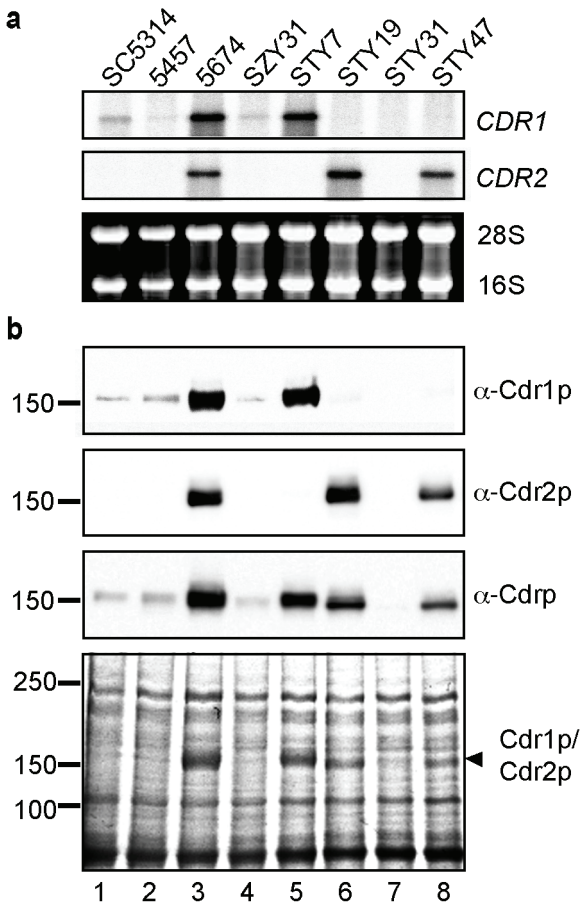

Figure II. 1 Expression of *CDR1* and *CDR2* in strains SC5314, 5457 and 5674 and in 5674 mutant derivatives

(**a**) Northen blot analysis. Total RNA extracts were prepared from the strains indicated at the top and analyzed by Northern blotting with gene-specific probes for *CDR1* (top) or *CDR2* (middle). rRNAs are shown as loading controls (bottom). (**b**) Western blot analysis. For the immunodetection of Cdr1p and Cdr2p, total membrane protein extracts were prepared from the strains and analyzed by Western blotting with the anti-Cdr1p, anti-Cdr2p and anti-Cdrp antibodies. A Coomassie-stained gel of the protein extracts is shown at the bottom, with the positions of the molecular mass standards and predicted positions of Cdr1p and Cdr2p indicated on the left and right, respectively. The values on the left are molecular sizes in kilodaltons.

Immunodetection of Cdr1p and Cdr2p was performed with three different polyclonal antibodies, two antibodies specific for Cdr1p or Cdr2p that were raised against the NH_2-terminal domain of the Cdr1p (anti-Cdr1p) or Cdr2p (anti-Cdr2p) protein, respectively, and one antibody that was raised against a short peptide

sequence perfectly conserved between the two proteins and that recognizes both transporters (anti-Cdrp) (de *et al.* 2002; Gauthier *et al.* 2003). By using the anti-Cdr1p antibody, we found that the pattern of Cdr1p expression was consistent with the one observed by Northern blotting, namely, low levels in strains SC5314, 5457, and SZY31 and high levels in strain 5674 (Fig. II.1b, lanes 1 to 4). The Cdr1p levels in strain STY7 were similar to those in strain 5674, confirming that Cdr1p expression was unaffected by the deletion of *CDR2* (Fig. II.1b, lanes 3 and 5). Finally, Cdr1p was undetectable in strains STY19, STY31 and STY47, consistent with the deletion of the *CDR1* gene in these strains (Fig. II.1b, lanes 6 to 8). Western blotting with the anti-Cdr2p antibody also showed that Cdr2p expression in these strains was consistent with the Northern blot results. Cdr2p levels were similar in strains 5674 and STY19, indicating that Cdr2p expression remained unchanged by the deletion of *CDR1* (Fig. II.1b, lanes 3 and 6). Cdr2p expression was lower in strain STY47 than in strains 5674 or STY19, consistent with the presence of only one allele of *CDR2* in STY47 versus two alleles in 5674 and STY19 (Fig. II.1b, lane 8). Finally, Western blotting with the generic anti-Cdrp antibody confirmed the results obtained with the anti-Cdr1p and anti-Cdr2p specific antibodies. The absence of a signal in strain STY31 demonstrate that the anti-Cdrp antibody, which was previously characterized using *S. cerevisiae* strains expressing Cdr1p or Cdr2p (Gauthier *et al.* 2003), does not recognize any other proteins in *C. albicans* besides Cdr1p and Cdr2p and is therefore specific for these two transporters. The results obtained with the generic antibody also showed that Cdr2p appears to be expressed at slightly (approximately twofold) lower levels than Cdr1p, an observation corroborated by sodium dodecyl sulfate-polyacrylamide gel electrophoresis and Coomassie staining (Fig. II.1b, compare lanes 5 and 6). In addition, the Western blot assay with the generic antibody and the Coomassie gel showed that Cdr2p migrates slightly faster than Cdr1p (Fig. II.1b, compare lanes 5 and 6). Since the two transporters have very similar predicted lengths (1,501 residues for Cdr1p and 1,499 for Cdr2p), this difference in migration may potentially reflect distinct posttranslational modifications.

Susceptibilities of the *cdr* mutants to azole drugs and other antifungal agents. We used MIC assays to determine the functional consequences of deleting *CDR1* and/or *CDR2* on the azole resistant phenotype of strain 5674 (Fig. II.2). All of the experiments were performed using two independently generated mutant strains per knock-out construction (Table II.1) and yielded similar results; thus, only one set of strains is shown in Fig. II.2 for clarity. As expected, strain 5674 was more resistant to the three azoles tested than strain 5457, whereas deleting *TAC1* from strain 5674 (SZY31) decreased the resistance of the cells to levels similar to those observed in strain 5457 (Fig. II.2a, b, and c). Deleting *CDR1* from strain 5674 had a major effect, reducing resistance to FLC, KTC, and ITC by 6-, 4-, and 8-fold, respectively, while deleting *CDR2* had a smaller effect (1.5-, 1.5-, and 1.0-fold) (Fig. II.2a, b, and c; Table II.2). These results demonstrate that Cdr1p is the major determinant of azole resistance in strain 5674 while Cdr2p plays a more minor role, even when normalized for the slightly lower abundance of Cdr2p than Cdr1p (Fig. II.1b). Interestingly, the deletion of both genes had a drastic effect and caused a reduction of the resistance to FLC, KTC, and ITC by 375-, 300-, and 500-fold, respectively, highlighting a strong synergism between the two transporters (Table II.2). Reintroducing one allele of *CDR2* under the control of its own promoter at its original locus in strain STY31 (yielding strain STY47) partially restored FLC resistance, causing a 16-fold increase in FLC MIC_{50}s (6.3 μg/ml for strain STY47 versus 0.4 μg/ml for strain STY31; Fig. II.3). This experiment confirmed that the strong azole hypersusceptibility of strain STY31 was due to the simultaneous inactivation of the Cdr1p and Cdr2p functions (Fig. II.3). The level of FLC resistance of strain STY47 was lower than that of strain STY19, consistent with the lower levels of Cdr2p expression in that strain versus STY19 (Fig. II.1).

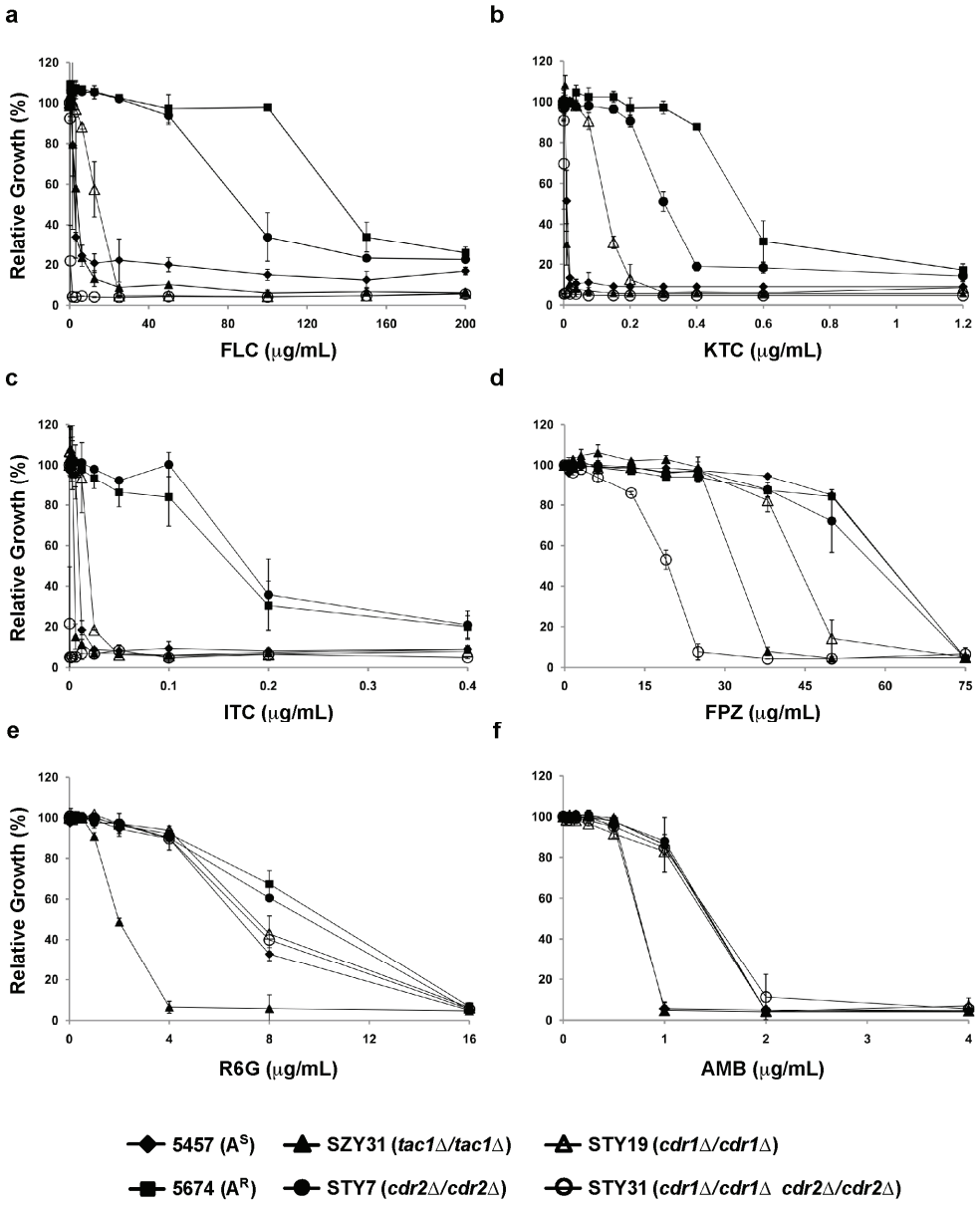

Figure II. 2 Drug resistance profiles of the testing strains

Profiles of resistance of strains 5457 and 5674 and strain 5674-derived *tac1* and *cdr* mutants to azole drugs and different compounds with antifungal activity, as determined by microtiter plate liquid assays. (**a**) FLC resistance. Cells were incubated for 48 h at 30˚C in liquid YPD medium with the indicated concentrations of FLC. The data are presented as the relative growth of cells in FLC-containing medium as compared to the growth of the same strain in FLC-free medium, which was set at 100%. The data are the mean of three independent experiments performed in duplicate. (**b**) KTC resistance. (**c**) ITC resistance. (**d**) FPZ resistance. (**e**) R6G resistance. (**f**) AMB resistance. For panels B to F, the experiments were performed as described for panel **a**.

Table II. 2 Drug susceptibilities of the starins used in this study

Strain	MIC_{50} (μg/ml)[a]					
	FLC	KTC	ITC	FPZ	R6G	AMB
5457 (A^s)	3.1	0.018	0.0125	75	8	1
5674 (A^r)	150	0.6	0.2	75	16	2
SZY31 (*tac1*Δ/*tac1*Δ)	6.2	0.009	0.0063	38	2	1
STY7 (*cdr2*Δ/*cdr2*Δ)	100	0.4	0.2	75	16	2
STY19 (*cdr1*Δ/*cdr1*Δ)	25	0.15	0.025	50	8	2
STY31 (*cdr1*Δ/*cdr1*Δ *cdr2*Δ/*cdr2*Δ)	0.4	0.002	0.0004	25	8	2

[a] Values presented are MIC_{50}s after 48 h of incubation (derived from Fig. 2).

We also tested FPZ, a calmodulin inhibitor with antifungal properties previously shown to be a substrate of Cdr1p and Cdr2p and a strong inducer of Tac1p activity (Coste *et al.* 2004; Sanglard *et al.* 1997; Znaidi *et al.* 2007). We found that strain 5674 was not more resistant to FPZ than strain 5457 (Fig. II.2d and Table II.2), possibly because this compound can directly induce Tac1p function. In line with this, we found that strain SZY31 (*tac1*Δ/*tac1*Δ) was twofold more susceptible to FPZ than was strain 5674. Deleting *CDR1* or *CDR2* from strain 5674 had only marginal or no effect on the resistance of the cells to FPZ (1.5- and 1-fold, respectively). When comparing strain STY7 (*cdr2*Δ/*cdr2*Δ; Cdr1p-expressing strain) and STY19 (*cdr1*Δ/*cdr1*Δ; Cdr2p-expressing strain) to strain STY31 (*cdr1*Δ/*cdr1*Δ *cdr2*Δ/*cdr2*Δ; no Cdr1p and Cdr2p), we found that the presence of *CDR1* or *CDR2* contributed to three- and twofold increased FPZ resistance, respectively. Finally, the decrease of FPZ susceptibility was about 1.5-fold between strains 5674 and STY19 (due to the deletion of *CDR1*) and 2-fold between strains STY19 and STY31 (due to the deletion of *CDR2*). Based upon these small differences, it can be concluded that Cdr1p and Cdr2p display similarly low activities towards FPZ. These results also suggest that FPZ is a poorer substrate for Cdr1p and Cdr2p than azole drugs and/or that it possesses a narrower window of antifungal activity.

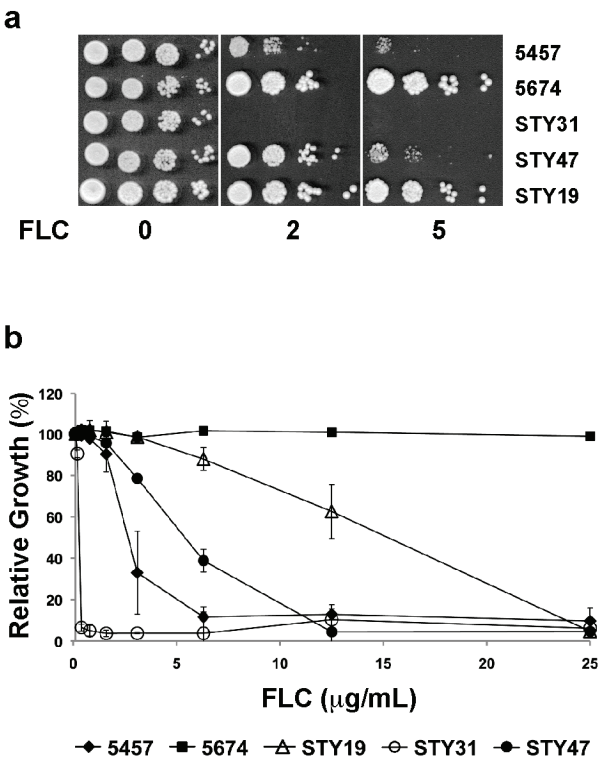

Figure II. 3 Phenotypic analysis of the *CDR2* revertant.

The FLC susceptibilities of strains 5457, 5674, STY19, STY31, and STY47 were analyzed by spot (**a**) and MIC (**b**) assays as described in the legends of Fig. II.2 and Fig. II.4

We similarly investigated R6G, a fluorescent substrate of many ABC transporters that has been used to study the functions of Cdr1p and Cdr2p in *S. cerevisiae* (Gauthier *et al.* 2003; Lamping *et al.* 2007; Saini *et al.* 2006) and in *C. albicans* (Maebashi *et al.* 2001; Maesaki *et al.* 1999). Our results showed that strain 5674 was only twofold more resistant to R6G than was strain 5457 (Fig. II.2e and Table II.2). Deleting *CDR1* from strain 5674 reduced the resistance of the cells to R6G by twofold, to levels similar to those observed in strain 5457, while deletion of *CDR2* clearly had no effect. These results suggest that R6G is not a good substrate to study Cdr1p and Cdr2p in A^R *C. albicans* cells. Interestingly, we found that the *tac1*Δ/*tac1*Δ mutant is

eight-fold more susceptible than strain 5674, indicating that Tac1p possesses another, as-yet-unidentified target affecting cell susceptibility to R6G.

Finally, we also tested AMB, which targets ergosterol. We found that all the strains had the same profile, with the exception of 5457 and the *tac1*Δ/*tac1*Δ mutant, which were slightly hyper-susceptible (Fig. II.2f and Table II.2). These results demonstrate that Tac1p plays a minor role in regulating cell tolerance to AMB but through a target other than Cdr1p and Cdr2p.

To assess the phenotypic consequences of deleting the *CDR* genes by an independent method, the strains were also analyzed by spot assay (Fig. II.4). The results obtained with this method were consistent with those obtained by the MIC assays, confirming the results described above and indicating that the observed phenotypes are similar on solid and liquid media.

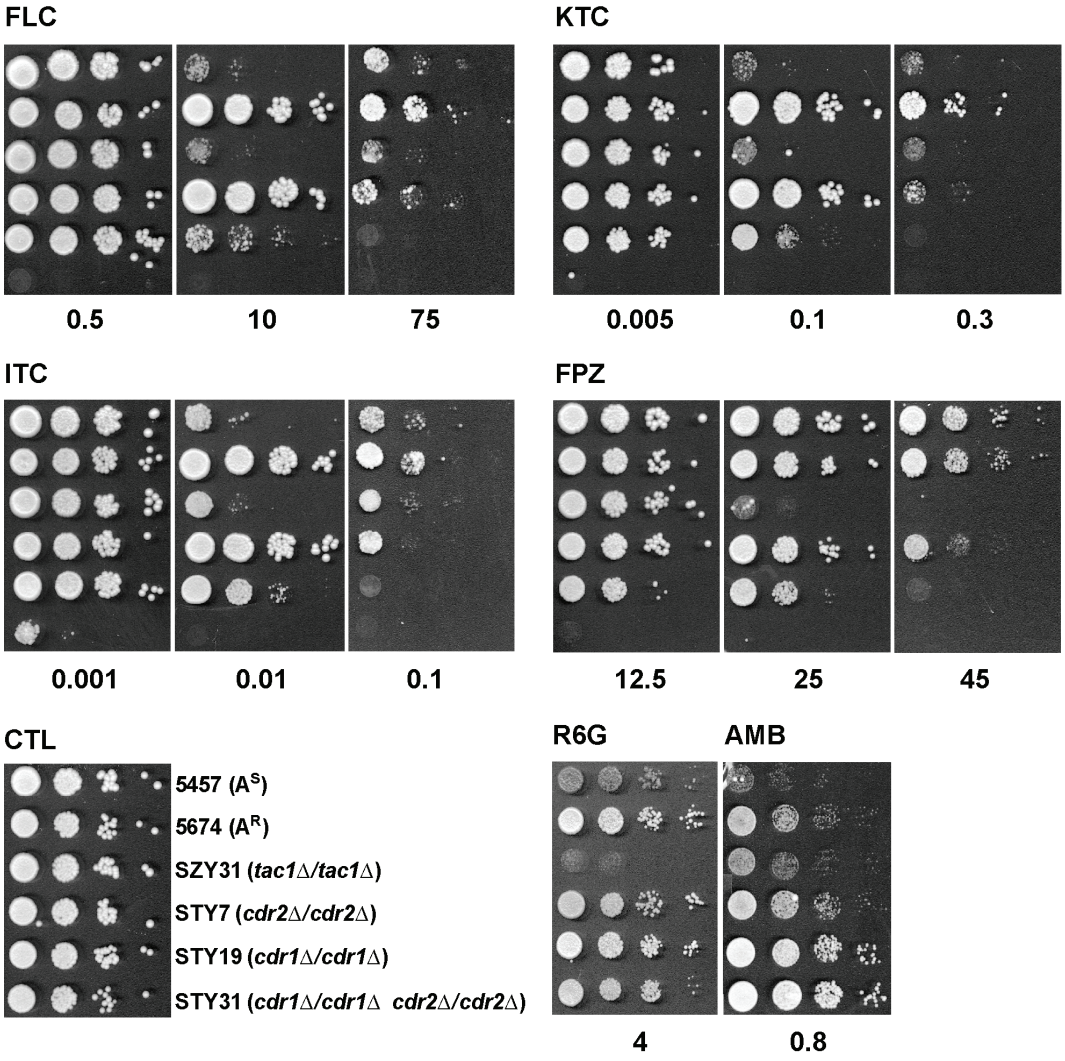

Figure II. 4 Spot assays of the testing strains

Profiles of resistance of strains 5457 and 5674 and strain 5674-derived *tac1* and *cdr* mutants to azole drugs and different compounds with antifungal activity, as determined by spot assays. Serial 10-fold dilutions of cells, starting at OD_{600} of 0.1, were spotted on YPD plates containing FLC, KTC, ITC, FPZ, R6G, or AMB at the indicated concentrations (micrograms per milliliter) or no drug (CTL). The plates were incubated for 48 h at 30˚C.

II.5 Discussion

Deletion of the *CDR1* and *CDR2* genes in the A^R clinical isolate 5674 with the *SAT1* flipper system, coupled to the characterization of the resulting mutants by quantitative MIC assays, allowed us to directly determine the relative contributions of the Cdr1p and Cdr2p transporters to clinical azole resistance. We show that deleting *CDR1* reduced resistance levels by 4- to 8-folds, depending on the different azoles tested (FLC, KTC, and ITC), while deleting *CDR2* only slightly affected the FLC and KTC resistance (by 1.5-fold) and did not affect ITC resistance. Thus, Cdr1p plays a major role in FLC, KTC, and ITC resistance whereas Cdr2p plays a minor role. It is possible that removing Cdr1p or Cdr2p affects azole resistance directly, by diminishing active azole export, and/or indirectly, by altering the activity of other proteins able to modulate azole intracellular accumulation (including Cdr1p or Cdr2p) or the phospholipid composition of the membrane. Assuming that transporter-mediated resistance to an antifungal compound reflects the ability of the transporter to export this compound, as previously proposed (Ernst *et al.* 2008; Lamping *et al.* 2007; Sanglard *et al.* 1996), our data could be interpreted as meaning that Cdr1p is a better transporter of azoles than is Cdr2p, although it cannot be ruled out that the effect of *CDR2* deletion might be masked by Cdr1p activity or by other, as-yet-unknown, compensatory mechanisms.

Our results show that deleting *CDR2* in the *cdr1*Δ*/cdr1*Δ mutant has a much stronger effect than deleting the gene from strain 5674. Since Cdr1p and Cdr2p have some substrates in common, this could potentially be due to a masking effect of the activity of Cdr2p by Cdr1p, as previously proposed in a similar study of ABC transporters in *S. cerevisiae* (Decottignies *et al.* 1998). In that study, deleting *S. cerevisiae PDR5* from a wild-type strain did not affect oligomycin susceptibility whereas deleting *PDR5* from a *yor1*Δ strain (carrying a deletion of the *YOR1* gene, which encodes another ABC transporter) led to a pronounced oligomycin sensitivity, stronger than that observed in the *yor1*Δ strain

(Decottignies *et al.* 1998). Similarly, in the case of *S. cerevisiae PDR16* and *PDR17*, which encode two homologous phospholipid transfer proteins, deleting *PDR16* from a wild-type strain resulted in increased susceptibility of the cells to KTC and miconazole by 10- and 20-fold, respectively, and deleting *PDR17* had no effect, whereas deleting both genes in the same strain led to a 40- and 80-fold increased susceptibility (van den Hazel *et al.* 1999). In the present study, however, the double deletion of *CDR1* and *CDR2* was performed in an already resistant strain. We found that deleting both genes not only abolished azole resistance but further reduced it to levels lower than those observed in the A^S strain 5457 and the *tac1*Δ*/tac1*Δ mutant (Fig. II.2a to c). This could be potentially due, at least in part, to the Tac1p-independent low level of Cdr1p expression in these strains (Fig. II.1), which has been eliminated in strain STY31 as a result of the *CDR1* deletion. In fact, the deletion of both genes had a striking effect as it reduced azole resistance by 300- to 500-fold (by comparison to 4- to 8-fold for *cdr1*Δ*/cdr1*Δ and 1.0- to 1.5-fold for *cdr2*Δ*/cdr2*Δ), uncovering a strong synergism between the two transporters. Synergism between transporters has previously been reported for bacterial multidrug resistance pumps (Lomovskaya 2002) and also members of P-type ATPase and ABC transporter family involved in regulating the phospholipid composition of the membrane of erythrocytes in mammals (Daleke 2008). Cdr1p and Cdr2p have been shown to function as phospholipid floppases, being able to translocate fluorescent phospholipids across the membrane lipid bilayer in an ATP-dependent fashion (Shukla *et al.* 2007; Smriti *et al.* 2002), and it is possible that the abrogation of Cdr1p and Cdr2p activity may cause a major alteration of the asymmetrical distribution of phospholipids in the cell membrane which would exacerbate cell response to drugs. Since it was not observed with AMB (Fig. II.2f and Fig. II.4), which directly targets ergosterol, this synergism appears to be specific for azoles and possibly involves the accumulation in the already perturbed plasma membrane of toxic ergosterol intermediates as a result of Erg11p inhibition.

R6G is a heterocyclic, lipophilic, and cationic fluorescent compound that is a substrate for many ABC transporters. Because of its antifungal properties and the ease of its detection, R6G has been used extensively to study yeast ABC transporters for their ability to confer R6G resistance and transport, these two parameters being closely correlated (Ernst *et al.* 2008; Lamping *et al.* 2007). In particular, it was shown that expression of Pdr5p, Cdr1p, and Cdr2p in *S. cerevisiae* confers high levels of R6G resistance and efflux [(Ernst *et al.* 2008; Lamping *et al.* 2007; Saini *et al.* 2006), our unpublished observation]. In one of these studies, R6G resistance was quantified by MIC assay and shown to be more than a 1,000-fold greater than that of the negative control strain (Saini *et al.* 2006). Based on these findings, it was expected that deletion of the *CDR1* and *CDR2* genes from strain 5674 would affect cell susceptibility to R6G. Instead, we found that *CDR1* and *CDR2* deletion only marginally reduced R6G resistance in strain 5674 (Fig. II.2e). A similar situation has been observed in other A^R strains, TIMM3165 and GU5, in which elevated levels of *CDR1* and *CDR2* RNAs were accompanied by a 128-fold increase of resistance to FLC but only by a 4-fold increase in resistance to R6G, compared to A^S strains (Banerjee *et al.* 2007; Maebashi *et al.* 2001). Interestingly, we found that deletion of *TAC1* from strain 5674 significantly decreased the resistance of the cells to R6G (by eight-fold), uncovering the existence of another, as-yet-unidentified, Tac1p target that modulates R6G resistance. Our recent analysis of the Tac1p regulon identified a gene, orf19.4531, whose protein product may have this function. This gene encodes a putative ABC transporter of the pleiotropic drug resistance subfamily homologous to Cdr1p and Cdr2p (Liu *et al.* 2007). orf19.4531 was found to be upregulated together with *CDR1* and *CDR2* in a *TAC1*-dependent manner in four independent A^R clinical strains, including strain 5674 (Liu *et al.* 2007). Alternatively, the decreased resistance of the cells to R6G may be due to another Tac1p target or to a combination of other Tac1p targets, since many of these genes are predicted to regulate the lipid or phospholipid composition of the plasma membrane in *C. albicans*. We are currently investigating the role of these genes in azole and R6G resistance by deleting them in strains 5674 and STY31.

This approach may allow us to identify new genes that affect drug resistance either directly or indirectly by regulating Cdr1p or Cdr2p function.

II.6 Acknowledgements

We thank Sadri Znaidi for critical reading of the manuscript, Sébastien Lemieux for advice, Joachim Morschhäuser for the gift of pSFS2A, Dominique Sanglard for providing the anti-Cdr1p antibody, the Institute for Research in Immunology and Cancer Genomic Platform for DNA sequencing, and the *Candida* Genome Database for sequence information.

This work was supported by a research grant to M.R. from the Canadian Institutes of Health Research (MT-15679). The Institute for Research in Immunology and Cancer is supported by the Canadian Center of Excellence in Commercialization and Research, the Canadian Foundation for Innovation, and the Fonds de Recherche en Santé du Québec.

II.7 Supplemental material

Relative contribution of the *Candida albicans* ABC transporters Cdr1p and Cdr2p to clinical azole resistance: Construction of the mutant strains used in this study.

Sarah Tsao[1,2], Fariba Rahkhoodaee[1] and Martine Raymond[1,2,3*]

II.8 Supplemental materials and methods

Plasmid construction.

Plasmid pSFS2A containing the *SAT1-FLP* cassette (Reuss *et al.* 2004) was used to construct the *CDR1*- and *CDR2*-deletion plasmids. The *SAT1-FLP* cassette consists of the dominant nourseothricin resistance marker *SAT1* under the control of the maltose promoter flanked by two direct repeats of the *FLP* recognition sequence *FRT* (Reuss *et al.* 2004). The *CDR1* and *CDR2* deletion plasmids were created by cloning their respective upstream and downstream sequences on each side of the *SAT1-FLP* cassette in pSFS2A. All plasmids and primer combinations used in this study are listed in Table IIS.1. The *CDR2* deletion plasmid (pCDR2ko) was constructed by first cloning the PCR-amplified gDNA fragment $CDR2_{down}$ (positions +4024 to +5045 of the *CDR2* gene relative to the ATG translation start codon) from *C. albicans* SC5314 into the *Xho*I-*Apa*I sites of plasmid pSFS2A, yielding plasmid pCDR2down. Next, the PCR-amplified DNA fragment $CDR2_{up}$ (-1000 to -1) was cloned into the *Sac*II-*Not*I sites of pCDR2down to yield plasmid pCDR2ko (Fig. IIS.1a). For *CDR1*, two separate deletion plasmids were similarly constructed: pCDR1koA consisting of the *SAT1-FLP* cassette flanked by $CDR1_{down}$ (+4460 to +5492) and $CDR1_{up}$ (-1000 to +23) and pCDR1koB containing $CDR1_{down}$ (+3971 to +4506) and $CDR1_{up}$ (+1 to +524) sequences (Fig. IIS.2a). A *CDR2* complementing plasmid (pCDR2REV; Table IIS.1) was generated by replacing $CDR2_{up}$ DNA fragment from the pCDR2ko with a PCR-amplified fragment from strain SC5314 that contains the entire *CDR2* gene (-1000 to +5299) (Fig. IIS.3a). *Escherichia coli* DH10B cells were used for all DNA cloning procedures and maintenance of plasmid constructs. *E. coli* cells were grown in Luria-Bertani (LB) medium to which chloramphenicol (34 μg/mL) was added as required.

Strain construction.

All sequential gene deletions were performed in the *C. albicans* A^R clinical isolate 5674 (Saidane *et al.* 2006), using the gene deletion plasmids described above and

listed in Table IIS.1. The *CDR2* or *CDR1* deletion cassettes were released from the plasmid constructs by *Apa*I digestion (1-5 µg) and were used to transform strain 5674. *C. albicans* transformations were performed using the standard lithium acetate protocol with minor modifications as described elsewhere (Znaidi *et al.* 2007) or by electroporation (Reuss *et al.* 2004), using the GenePulserII system (Bio-Rad) and 0.2 cm gap cuvettes (electric pulse of 1.8 kV, 25 µF and 200 Ω). Transformed *C. albicans* cells were harvested by centrifugation, washed once with 1 mL YPD (for heat shock treated cells) or 1 mL of sorbitol 1M (for electroporated cells), resuspended in 2 mL of YPD medium and incubated for 4 hours at 30˚C with shaking. Nourseothricin-resistant (Nou^R) transformants were selected on YPD agar plates supplemented with 200 µg/mL nourseothricin (Werner Bioagents, Jena, Germany) after growth at 30˚C for 24 hours. Nou^R transformants containing the correctly integrated cassette were identified by Southern blot analysis. At least two independent Nou^R transformants were chosen to loop-out the *SAT1* resistance marker: they were grown overnight at 30˚C in YNB liquid medium (0.67% yeast nitrogen base without amino acids from Difco, BD, supplemented with 2% maltose from BioShop, Burlington, Canada) and 100-200 cells were spread on YPD plates and incubated for 2 days at 30˚C. Nourseothricin sensitive (Nou^S) transformants with the correctly looped-out cassette were identified by Southern blot analysis. Two Nou^S strains were used for the deletion of the second allele, producing at the end two independent Nou^S homozygous mutants per gene to be deleted. Plasmid pCDR2ko was used to sequentially delete both alleles of *CDR2*. In the case of *CDR1*, we used plasmid CDR1koA to delete the *CDR1A* allele and plasmid CDR1koB to delete the *CDR1B* allele. Plasmid pCDR2Rev was used to reintroduce a wild-type *CDR2* allele into the *cdr2*Δ*/cdr2*Δ strain.

Genomic DNA isolation and Southern blotting.

For the isolation of *C. albicans* gDNA, the phenol/chloroform/isoamylalcohol and glass beads disruption method was used (Hoffman *et al.* 1987). Southern blot hybridizations were carried out as described previously (Saidane *et al.* 2006).

Genomic DNA samples (1 μg) were digested to completion with the appropriate restriction enzyme, separated by gel electrophoresis on a 1% agarose gel and transferred to a nylon membrane (Hybond-N; Amersham Pharmacia Biotech). The DNA probes used in this study were generated by PCR-amplification (Table IIS.1, Fig. IIS.1b, Fig. IIS.2b and Fig. IIS.3b). ^{32}P-labelled DNA probes were generated by random priming (Feinberg *et al.* 1984). The blots were washed under high stringency conditions as described previously (Saidane *et al.* 2006). The resulting blots were exposed to a FUJI FILM Imagine Plate screen and analyzed using the MultiGauge software (version 2.3 FUJI FILM).

II.9 Supplemental results

Deletion of *CDR2* in the *C. albicans* A^R 5674 clinical isolate.

A *CDR2* deletion cassette was constructed, consisting of the *SAT1-FLP* marker flanked by *CDR2* upstream (-1000 to -1) and downstream (+4024 to +5045) sequences amplified from strain SC5314 (Fig. IIS.1a). The cassette was released by digestion with *Apa*I and used to transform strain 5674. Nou^R transformants were analysed by Southern blotting, using *Pst*I-digested genomic DNA and a *CDR2* upstream probe (Fig. IIS.1b, probe 1). All transformants had the correct integration profile in which one of the two *CDR2* alleles was replaced by the *SAT1-FLP* cassette, as judged from the appearance of a 3.7-kb fragment (Fig. IIS.1b, middle panel and data not shown). Two independent heterozygous mutants (one with allele A deleted and one with allele B deleted) were grown in the presence of maltose to allow for FLP-mediated excision of the *SAT1-FLP* cassette and the resulting strains were similarly analyzed by Southern blotting (Fig. IIS.1c, top panel). As predicted from the *C. albicans* genome sequence (www.candidagenome.org), the *CDR2* upstream probe detected a single fragment of 5.5 kb in strain SC5314, corresponding to the two wild-type alleles of *CDR2* (Fig. IIS.1c, top panel, lane 1). In the clinical strains 5457 and 5674, the probe detected two fragments of 5.5 kb and 14.9 kb corresponding to the two *CDR2* alleles designated *CDR2A* and *CDR2B*, respectively (Fig. IIS.1c, top panel, lanes 2 and 3) and consistent with the loss of a *Pst*I site in allele *CDR2B* in these strains as compared to strain SC5314 (Fig. IIS.1b). The two independent heterozygous *CDR2*/*cdr2*Δ mutants STY3 and STY4 displayed the expected restriction profile, each carrying one *CDR2* wild-type allele (*CDR2B* in STY3, as deduced from the 14.9-kb band, and *CDR2A* in STY4, as deduced from the 5.5-kb band) as well as one common *cdr2-FRT* allele (10.9 kb) (Fig. IIS.1c, top panel, lanes 4 and 5). A second round of transformation of strains STY3 and STY4 with the *CDR2* deletion construct followed by looping out of the *SAT1-FLP* cassette generated two independent homozygous *cdr2*Δ/*cdr2*Δ mutants, STY7 and STY8. Both strains were found to carry only one band corresponding to the *cdr2A/B-FRT*

alleles (Fig. IIS.1c, top panel, lanes 6 and 7), consistent with the complete deletion of *CDR2* in these strains. Southern blot analysis of the strains using the *CDR2* ORF internal probe confirmed that *CDR2* was deleted in strains STY7 and STY8 (Fig. IIS.1c, bottom panel, lanes 6 and 7).

Deletion of *CDR1* in strains 5674 and STY7 (*cdr2*Δ/*cdr2*Δ).

Deletion of the *CDR1* gene in strain 5674 was performed essentially as described above for *CDR2*, with the exception that two different *CDR1* deletion constructs were used to delete the two alleles. *CDR1* was also deleted in strain STY7 (*cdr2*Δ/*cdr2*Δ) to obtain a double deletion mutant lacking both transporters (*cdr1*Δ/*cdr1*Δ *cdr2*Δ/*cdr2*Δ). We first constructed the *CDR1* deletion cassette pCDR1koA consisting of the *SAT1-FLP* cassette flanked by *CDR1* upstream (-1000 to +23) and downstream (+4460 to +5492) sequences (Fig. IIS.2a). This cassette was used to transform strains 5674 and STY7. Southern blot analysis identified transformants displaying an integration profile consistent with the *CDR1A* allele being replaced by the *SAT1-FLP* cassette, as judged from the appearance of a 16.7-kb band, using the *CDR1* upstream probe 1 and *Kpn*I as restriction enzyme (Fig. IIS.2b, middle panel, and data not shown). Two independent transformants for each parental strain (5674 and STY7) were submitted to excision of the *SAT1-FLP* cassette and the resulting strains were similarly analyzed by Southern blotting (Fig. IIS.2c, top panel). The *CDR1* probe 1 detected a single fragment of 5.5 kb in strain SC5314, corresponding to the two wild-type alleles of *CDR1* (Fig. IIS.2c, top panel, lane 1). In contrast, *CDR1* alleles in strain 5457 or 5674 displayed different *Kpn*I restriction site polymorphisms; each allele could be distinguished as a 6.5-kb and an 8.5-kb fragments in strain 5457 or as a 6.5-kb (allele *CDR1B*) and 5.9-kb (allele *CDR1A*) fragments in strain 5674 (Fig. IIS.2c, top panel, lanes 2 and 3). The two heterozygote mutants derived from strain 5674 (STY15, STY16) and those derived from strain STY7 (STY27, STY28) had the correct restriction profile, each carrying a 6.5-kb band corresponding to the wild-type *CDR1B* allele and a

12.5-kb band corresponding to the *cdr1A::FRT* allele (Fig. IIS.2c, top panel, lanes 4, 5, 10 and 11).

Since deletion of the *CDR1B* allele with plasmid pCDR1koA was unsuccessful, we constructed a second deletion cassette, pCDR1koB (Fig. IIS.2a), containing the $CDR1_{up}$ (+1 to +524) and $CDR1_{down}$ (+3971 to +4506) sequences designed to promote recombination within the *CDR1* ORF whose sequence is less divergent between the two alleles than the non-coding regions. This cassette was used to delete the *CDR1B* allele in strain 5674 to produce heterozygote mutants containing only allele *CDR1A*, generating two independent transformants with the *CDR1B* allele being replaced by the *SAT1-FLP* cassette. This integration was verified by the appearance of a 4.1-kb *Eco*RI-fragment, using the *CDR1* probe 3 that contains the *CDR1* ORF sequences from +1 to +524 (Fig. IIS.2b, middle panel and data not shown). The resulting post-excision heterozygote mutants (STY41, STY42) were analyzed with the *CDR1* probe 1 and were found to carry the 5.9-kb fragment diagnostic of the wild-type *CDR1A* allele and a 14.1-kb fragment corresponding to the *cdr1B-FRT* allele (Fig. IIS.2c, top panel, lanes 6 and 7). Plasmid pCDR1koB was also used to delete the *CDR1B* allele in strains STY15, STY16, STY27 and STY28, thereby generating two independent homozygous *cdr1*Δ/*cdr1*Δ mutants (STY19, STY20) and two independent homozygous *cdr1*Δ/*cdr1*Δ *cdr2*Δ/*cdr2*Δ mutants (STY31, STY32) (Table II.1). These four post-excision mutants had the correct restriction profile, giving rise to fragments of 12.5 kb and 14.1 kb corresponding to the *cdr1A-FRT* and *cdr1B-FRT* alleles, respectively (Fig. IIS.2c, top panel, lanes 8, 9, 12 and 13). The complete deletion of *CDR1* in these strains was independently confirmed by the absence of signal using a *CDR1* internal probe (Fig. IIS.2c, bottom panel, lanes 8, 9, 12 and 13).

Reintroduction of *CDR2* in strain STY31 (*cdr1*Δ*/cdr1*Δ *cdr2*Δ*/cdr2*Δ).

A *CDR2*-complementing cassette was constructed, consisting of *CDR2* upstream sequences (-1000 to -1), the entire *CDR2* open reading frame (+1 to +5299), the

SAT1-FLP cassette and the *CDR2* downstream sequences (+4024 to +5045) (Fig. IIS.3a). The cassette was released by digestion with *Apa*I and used to transform strain STY31. Southern blot analysis using the *CDR2* upstream probe 1 identified transformants displaying an integration profile consistent with one *cdr2*Δ-*FRT* allele being replaced by the *CDR2A* allele, restoring the *Pst*I site and allowing the detection of a 5.5 kb fragment (Fig. IIS.3b, middle panel and data not shown). Several transformants were analyzed and showed identical restriction patterns (data not shown), thus only one representative was used for the excision of the *SAT1-FLP* cassette (STY45, Table II.1). This yielded strain STY47 which was analyzed by Southern blotting (Fig. IIS.3c). The predicted 5.5-kb and 10.9-kb fragments were detected using the *CDR2* upstream probe 1 in STY47 and confirmed the presence of one remaining *cdr2*Δ-*FRT* allele and one reintroduced *CDR2A* allele at the *CDR2* locus (Fig. IIS.3b, bottom panel and Fig. IIS.3c, lane 4).

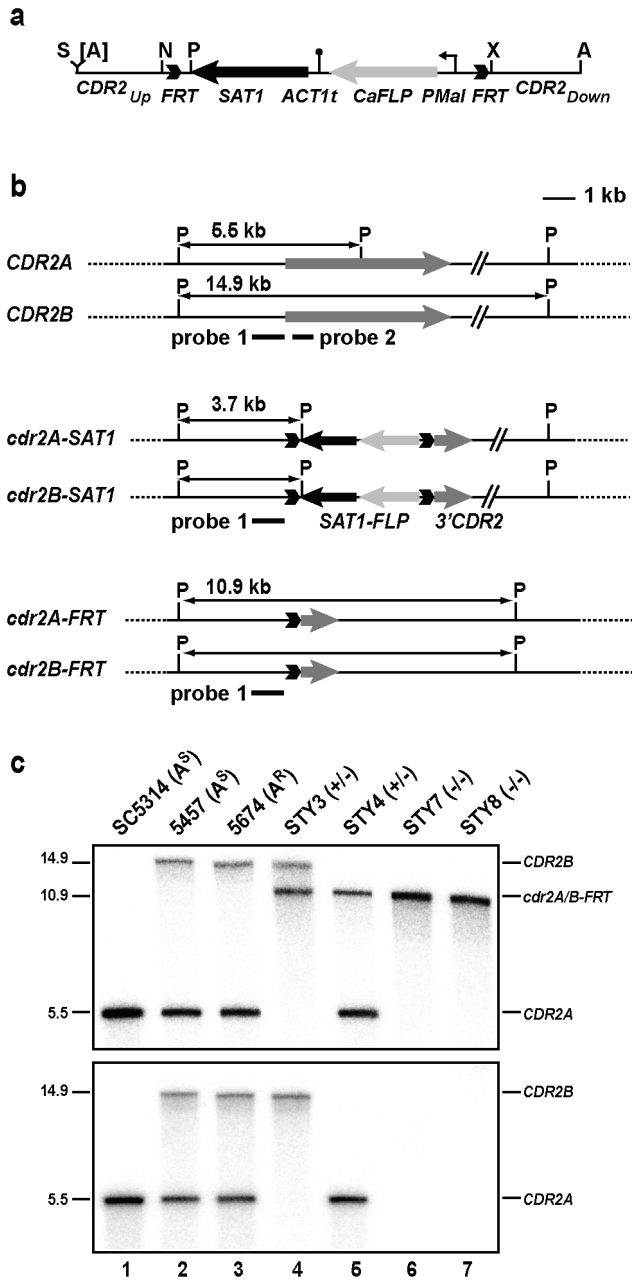

Figure II S. 1 Sequential deletion of the *CDR2* alleles in strain 5674

(**a**) Schematic representation of plasmid pCDR2ko containing the *CDR2*-deletion cassette. The cassette consists of, from left to right: $CDR2_{up}$, *CDR2* upstream region (positions -1000 to -1, with respect to the ATG initiation codon); *FRT*, FLP recombination target; *SAT1*, nourseothricin resistance marker; *ACT1t*, transcription termination sequence of the *C. albicans ACT1* gene; *CaFLP*, *C. albicans*-adapted *FLP* gene; *PMal*, maltose promoter and $CDR2_{down}$, *CDR2* downstream region (+4024 to +5045). Abbreviations for restriction sites are: S, *Sac*II; A, *Apa*I; N, *Not*I; P, *Pst*I; X, *Xho*I. The *Apa*I site shown in brackets was introduced by PCR. (**b**) *Pst*I

restriction maps of the *CDR2* locus. Top, wild-type *CDR2* alleles of strain 5674 (*CDR2A*, *CDR2B*) showing *Pst*I restriction site polymorphism. Middle, *cdr2::SAT1-FLP* integrated alleles. Bottom, *cdr2::FRT* alleles (*cdr2A-FRT*, *cdr2B-FRT*; post-excision of the *SAT1-FLP* element). The size of the *Pst*I fragments detected by the *CDR2* probes (thick lines) in Southern blot experiments is indicated. (**c**) Southern blot analysis of *Pst*I-digested gDNA from wild-type strains and 5674 mutant derivatives. The membranes were probed with the *CDR2* probe 1 (upstream probe; top panel) or the *CDR2* probe 2 (internal probe; bottom panel). The strains tested are indicated above the figure. The size and identity of each band are indicated at the left and the right of the blot, respectively.

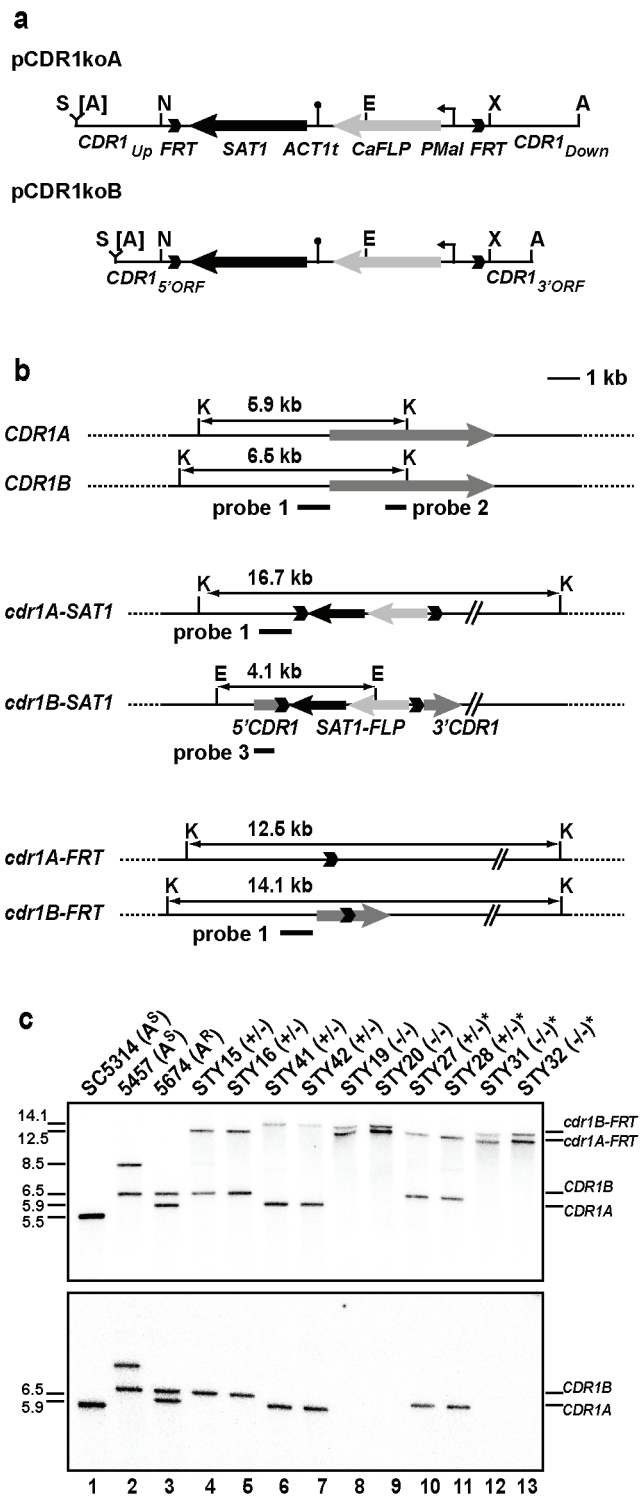

Figure II S. 2 Sequential deletion of the *CDR1* alleles in strain 5674 and STY7 (*cdr2*Δ/*cdr2*Δ)

(**a**) Schematic representation of plasmids pCDR1koA (top) and pCDR1koB (below) containing two independent *CDR1* deletion cassettes. pCDR1koA (from left to right): $CDR1_{up}$, *CDR1*

upstream region (–1000 to +23, with respect to the ATG codon); *SAT1-FLP* sequences and $CDR1_{down}$, *CDR1* downstream region (+4460 to +5492). pCDR1koB: $CDR1_{5'ORF}$, 5'-*CDR1* ORF sequences (+1 to +525), *SAT1-FLP* sequences and $CDR1_{3'ORF}$, 3'-*CDR1* ORF sequences (+3971 to +4506). Abbreviations for restriction sites are: S, *Sac*II; A, *Apa*I; N, *Not*I; E, *EcoR*I; X, *Xho*I. The *Apa*I site shown in brackets was introduced by PCR. (**b**) Restriction map of the *CDR1* locus. Top, wild-type *CDR1* alleles of strain 5674 (*CDR1A*, *CDR1B*) showing *Kpn*I restriction site polymorphism. Middle, *Kpn*I restriction map of the *cdr1A*::*SAT1-FLP* integrated allele and *EcoR*I restriction map of the *cdr1B::SAT1-FLP* integrated allele. Bottom, *cdr1::FRT* disrupted alleles (*cdr1A-FRT*, *cdr1B-FRT*; post-excision of the *SAT1-FLP* element). The size of the *Kpn*I or *EcoR*I fragments detected by the *CDR1* probes (thick line) in the Southern blot experiments is indicated. (**c**) Southern blot analysis of *Kpn*I-digested gDNA from wild-type and *cdr1*Δ mutant strains in the 5674 and STY7 (*) background. The membranes were probed with the *CDR1* probe 1 (upstream probe; top panel) or the *CDR1* probe 2 (internal probe; bottom panel). The strains tested are indicated above the figure. The size and identity of each band are indicated at the left and the right of the blot, respectively.

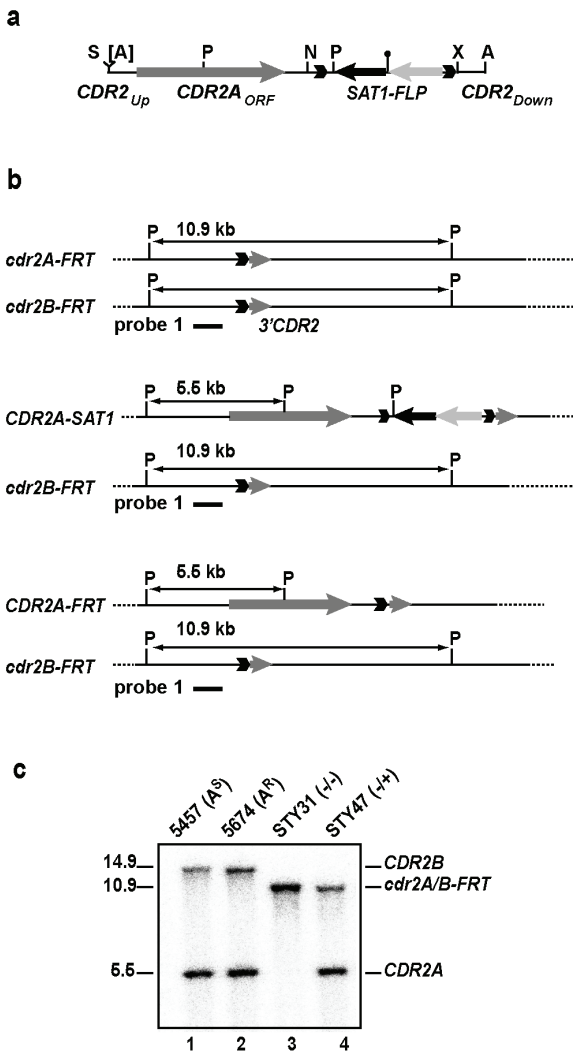

Figure II S. 3 Reintroduction of *CDR2* in strain STY31

(**a**) Schematic representation of plasmid pCDR2Rev containing the *CDR2*-reintegration cassette. The cassette consists of, from left to right: $CDR2_{up}$, *CDR2* upstream region (-1000 to -1); the entire *ORF* of the *CDR2A* allele (+1 to +5299); *SAT1-FLP* sequences; and $CDR2_{down}$, *CDR2* downstream region (+4024 to +5045). Abbreviations are the same as in Fig. IIS.1. (**b**) *Pst*I restriction maps of the *CDR2* locus. Top: the two *cdr2*Δ*-FRT* alleles of strain STY31 (*cdr2A-FRT*, *cdr2B-FRT*). Middle: Integration of the *CDR2* cassette at the *cdr2A-FRT* locus (*CDR2A-SAT1*). Bottom: the *CDR2A-SAT1* allele after loop-out (*CDR2A-FRT*). The size of the *Pst*I fragments detected by the *CDR2* probe 1 (thick lines) for the Southern blot experiments is indicated. (**c**) Southern blot analysis of *Pst*I-digested gDNA from wild-type strains and 5674 mutant derivatives indicated above the figure. The size and identity of each band are indicated at the left and the right of the blot, respectively.

Table II S. 1 Primers used in this study

Plasmid or probe	Primer	Sequence (5' – 3')[a]	Restriction site(s) or Location
Plasmid			Restriction site(s)
pCDR2ko	MR1227	TCCCCGCGGGCCCGATACTGACAATAACAAATCAACTG	*Sac*II, *Apa*I
	MR1228	AAGGAAAAAAGCGGCCGCATGTTTTTATTGTATGTGTTAATTAG	*Not*I
pCDR2down	MR1300	GCGCTCGAGGATAATGCTGCTAATTTGGCTACAAC	*Xho*I
	MR1301	GCGGGGCCCGATCAAATTTATTAAATTGATCACG	*Apa*I
pCDR1koA	MR1302	TCCCCGCGGGCCCCTTGTCATCGAATATACATC	*Sac*II, *Apa*I
	MR1303	AAGGAAAAAAGCGGCCGCGACGACATCTTAGAATCTGACAT	*Not*I
pCDR1downA	MR1304	GCGCTCGAGAGCTAGAGTTCCAAAGGGTAAC	*Xho*I
	MR1305	GCGGGGCCCCAATCATGGTAATACCCCTT	*Apa*I
pCDR1koB	MR1632	TCCCCGCGGGCCCATGTCAGATTCTAAGATGTCGTCGC	*Sac*II, *Apa*I
	MR1633	AAGGAAGCGGCCGCGGCATCCATTGATTTCAAAATATC	*Not*I
pCDR1downB	MR1627	GCGCTCGAGCATTTTATGTTTACACAGCAACCATGGG	*Xho*I
	MR1626	GCGGGGCCCTTATTTCTTATTTTTTTTCTCTCTGTTACCC	*Apa*I
pCDR2Rev	MR1227	TCCCCGCGGGCCCGATACTGACAATAACAAATCAACTG	*Sac*II, *Apa*I
	MR1386	AAGGAAAAAAGCGGCCGCGATTGTCGTTCTTTAGTAAATCTGGC	*Not*I
Probe			Location[b]
CDR2-Probe 1	MR1227	TCCCCGCGGGCCCGATACTGACAATAACAAATCAACTG	-1000 to -975
	MR1228	AAGGAAAAAAGCGGCCGCATGTTTTTATTGTATGTGTTAATTAG	-26 to -1
CDR2-Probe 2	MR1783	TACTGCAAACACGTCTTTGTCGCAACAGCT	+6 to +35
	MR1784	GTCTGGTTTCTTCAATTTATTGATTG	+455 to +480
CDR1-Probe 1	MR1302	TCCCCGCGGGCCCCTTGTCATCGAATATACATC	-1000 to -980
	MR1303	AAGGAAAAAAGCGGCCGCGACGACATCTTAGAATCTGACAT	+1 to +23
CDR1-Probe 2	MR1781	TATATTTTCCGTTTTCGGTCAACTT	+1545 to +1569
	MR1782	ACCAGCCAAATAATTGGTACCACTA	+2232 to +2256
CDR1-Probe 3	MR1632	TCCCCGCGGGCCCATGTCAGATTCTAAGATGTCGTCGC	+1 to +25
	MR1633	AAGGAAGCGGCCGCGGCATCCATTGATTTCAAAATATC	+502 to +525

[a] Restriction sites introduced for cloning purposes are underlined.
[b] All nucleotide positions are numbered with respect to ATG set at +1.

Chapter III

Identification and characterization of N-terminal phosphorylation sites in the *Candida albicans* ABC transporter Cdr1p

Chapter III

Identification and characterization of N-terminal phosphorylation sites in the *Candida albicans* ABC transporter Cdr1p

During the course of my study, I observed that both Cdr1p and Cdr2p could be detected as multiple bands in Western blots when allowed for extended protein separation on SDS-PAGE. This observation led us to investigate whether these transporters could be post-translationally modified. More specifically, we investigated whether the function of Cdr1p is modulated by phosphorylation since it has been shown as the major determinant of the azole resistance phenotype of *C. albicans*.

Identification and characterization of N-terminal phosphorylation sites in the *Candida albicans* ABC transporter Cdr1p

Running Title: Cdr1p phosphorylation

Sarah Tsao[1,2], Dominic Nehme[1], Elaheh Ahmadzadeh[1], Sandra Weber[1] and Martine Raymond[1,2,3*]

[1]Institute for Research in Immunology and Cancer, Université de Montréal, Montreal, QC, Canada H3T 1J4; [2]Department of Biochemistry, McGill University, Montreal, QC, Canada H3G 1Y6; [3]Département de Biochimie, Université de Montréal, Montreal, QC, Canada H3C 3J7.

*Corresponding author:
Martine Raymond, Institute for Research in Immunology and Cancer, Université de Montréal, P.O. Box 6128, Station Centre-Ville, Montreal, Quebec, Canada H3C 3J7. Phone: (514) 343-6746. Fax: (514) 343-6843. E-mail: martine.raymond@umontreal.ca.

III.1 Abstract

Overexpression of ATP-binding cassette (ABC) transporters in the pathogenic microorganisms is a frequent cause of the emergence of drug-resistant strains. The human fungal pathogen *Candida albicans* is involved in a wide range of infections and azoles have been used commonly to treat these infections. However, failure of *C. albicans* azole chemotherapy has been documented and it is often associated with the emergence of azole-resistant strains. *C. albicans* Cdr1p is an ABC transporter that plays a major role in ABC transporter-mediated azole resistance. In order to investigate possible regulatory mechanism(s) involved in the modulation of Cdr1p function, we examined whether Cdr1p is a phosphoprotein and whether phosphorylation modulates Cdr1p-mediated azole resistance. Using Western blotting and mass spectrometry analyses, we found that Cdr1p is phosphorylated in *C. albicans*. Interestingly, the identified phosphorylation sites are located at two places of the protein, the N-terminal extension (NTE) region (Thr^{49}/Thr^{51}/Ser^{54}) and the linker region (Ser^{849}) of Cdr1p. Mutations of all three NTE phosphorylation sites to alanines resulted in a reduced azole resistance while mutation of Ser849 had no effect. Furthermore, negatively charged glutamate mutations of all three NTE sites mimicked phosphorylation and allowed wild-type azole resistance. Finally, we used biochemical assays to demonstrate that phosphorylation is important for Cdr1p ATPase activity and transport function.

III.2 Introduction

Transporters of the ATP-binding cassette (ABC) superfamily are found in all living organisms, from microorganisms to human. Most ABC transporters are expressed at membranes of cell surfaces or organelles and are involved in transporting various substrates, such as metabolic products, lipids, and drugs across membrane barriers (Dean *et al.* 2001a). Membrane transporters that contain at least one nucleotide binding domain (NBD) and one transmembrane domain (TMD) are described as 'half transporters' and require dimerization to form a functional transporter. 'Full transporters', on the other hand, are comprised of two NBDs and two TMDs with all necessary functional units. The NBD of ABC transporters contains highly conserved sequence motifs participating in nucleotide binding and hydrolysis, thereby providing energy to translocate substrates across membranes through the channel formed by the TMDs. The arrangement of the NBDs and TMDs within the transporter polypeptide varies according to the type of ABC transporter. The TMD-NBD (in half transporter) or TMD_1-NBD_1-TMD_2-NBD_2 (in full transporter) is the typical domain arrangement found for many ABC transporters, including human TAP1/2 involved in antigen peptide transport, multidrug transporter P-glycoprotein and the cystic fibrosis transmembrane conductance regulator CFTR. Nevertheless, transporters with the 'reversed' topological arrangement as NBD-TMD are also found in human, an example of this type of transporter is the half-length multidrug transporter ABCG2 (or breast cancer resistance protein, BCRP) (Dean *et al.* 2001c).

In yeast, there is a unique subfamily of ABC transporters (PDR/CDR/ABCG subfamily) containing the full-length transporters with NBD_1-TMD_1-NBD_2-TMD_2 topological arrangement that are not found in humans (Paumi *et al.* 2009). The best-characterized member of this subfamily is *Saccharomyces cerevisiae* Pdr5p as it is involved in exporting a wide spectrum of xenobiotics out of the cell and contributes to a pleiotropic drug resistance (PDR) phenotype. In addition, it has

been demonstrated to transport phospholipids as well as structurally unrelated chemical compounds with surface volume of at least 90 $Å^3$ (Decottignies *et al.* 1998; Golin *et al.* 2003). Interestingly, the full transporter Pdr5p appears as a 'duplicated' mammalian half transporter ABCG2 and it shares overlapping substrate specificity with ABCG2 for the anticancer drug doxorubicin and the fluorescent compound rhodamine (Decottignies *et al.* 1998; Huang *et al.* 2007). Unlike mammalian ABCG2, although dimerization is not a functional prerequisite for Pdr5p, biochemical and genetic studies suggested a close intermolecular interactions or a dimeric organization of Pdr5p (Ferreira-Pereira *et al.* 2003; Subba Rao *et al.* 2002). Finally, transcriptional regulation of Pdr5p is controlled by the transcription factors Pdr1p/Pdr3p. Gain-of-function mutations in these transcription factors lead to constitutive transcriptional activation of *PDR5* (Moye-Rowley 2003). Most interestingly, a recent study showed that substrates of Pdr5p, for example azoles, could directly activate its transcription by binding to Pdr1/3p, leading to Pdr5p-mediated azole resistance (Thakur *et al.* 2008).

Homologs of Pdr5p and a similar PDR network are also found in the pathogenic fungus *Candida albicans* (Lamping *et al.* 2010; Morschhauser 2010). *C. albicans* is one of the leading causes of fungal infections affecting immunocompromised individuals and is the fourth most common cause of nosocomial bloodstream infections (Wisplinghoff *et al.* 2004). Antifungal therapy with azoles is a widely adopted treatment option; however, its efficacy is often compromised by the emergence of azole-resistant clinical strains (Akins 2005). An important mechanism of clinical azole resistance in *C. albicans* is the selection of gain-of-function mutations in the Tac1p transcription factor, leading to the constitutive overexpression of *CDR1* and *CDR2* genes (Coste *et al.* 2004). Cdr1p and Cdr2p are two homologous ABC transporters sharing 84% sequence identity and 92% sequence similarity (Gauthier *et al.* 2003). Furthermore, both transporters have been demonstrated to be structural and functional homologs of *S. cerevisiae* Pdr5p (Prasad *et al.* 1995; Sanglard *et al.* 1995).

Using biochemical or genetic experimental approaches, we and others have shown that both Cdr1p and Cdr2p are directly responsible for the azole-resistant phenotype of *C. albicans*, with Cdr1p playing a more important role than Cdr2p (Holmes *et al.* 2008; Tsao *et al.* 2009). As the importance of Cdr1p in drug resistance becomes evident, it is of interest to have a better understanding of how the expression and function of Cdr1p is regulated. Recent studies suggested a role of poly(A) polymerase (*PAP1*)-dependent mechanism involved in post-transcriptional regulation of *CDR1* by enhancing its mRNA stability in azole-resistant isolates (Manoharlal *et al.* 2008; Manoharlal *et al.* 2010). Currently, it is not clear if other cellular mechanisms, such as post-translational modifications (PTMs) could also play a role in regulating Cdr1p stability (or activity) thereby contributing to azole resistance phenotype.

Phosphorylation has been shown to play regulatory roles in mammalian as well as yeast ABC transporters across subfamilies. Phosphorylation of mammalian ABCG2 by a serine/threonine kinase Pim1 was suggested to be required for its dimerization as well as the optimal transport activity (Xie *et al.* 2008). Phosphorylation at the cytosolic linker region connecting NBD_1 to TMD_2 of the full transporter *S. cerevisiae* Ste6p (TMD_1-NBD_1-TMD_2-NBD_2) has been well documented and the role of this phosphorylation is thought to direct ubiquitination for transporter turnover (Kelm *et al.* 2004; Kolling 2002). Other examples include recent studies in *S. cerevisiae* Ycf1p (TMD_0-TMD_1-NBD_1-TMD_2-NBD_2) showing that, phosphorylation could play either a positive or a negative regulatory roles of the transporter activity, as the activity of Ycf1p is enhanced by phosphorylation at residues located within the linker region connecting NBD_1-TMD_2 (Eraso *et al.* 2004) or by dephosphorylation at the residue located near the N-terminus of Ycf1p (within the cytosolic loop connecting TMD_0-TMD_1) (Paumi *et al.* 2009). Finally, homologous transporters that display the same domain configurations of *C. albicans* Cdr1p, both *S. cerevisiae* Pdr5p and *C. glabrata* Cdr1p are also subjected to phosphorylation (Decottignies *et al.* 1999; Wada *et al.* 2002; Wada *et al.* 2005). Phosphorylation of *S. cerevisiae* Pdr5p is important for

its protein stability; deletion of genes encoding casein kinase I abolished Pdr5p phosphorylation and caused vacuolar degradation of Pdr5p (Decottignies *et al.* 1999). In the case of *C. glabrata* Cdr1p, the Akt-dependent phosphorylation of Cdr1p was demonstrated by using the antibody that recognizes phosphorylated Akt substrate peptides. Mutation of the putative Akt phosphorylation residues locating near the NBD_1 of *C. glabrata* Cdr1p reduced its ATPase activity, suggesting that phosphorylation plays a direct role in modulating transporter function (Wada *et al.* 2005).

In the present study, we used biochemical and proteomics methods to investigate whether *C. albicans* Cdr1p is subjected to phosphorylation and whether phosphorylation plays a role in regulation of Cdr1p function, more specifically, Cdr1p-mediated azole resistance.

III.3 Experimental procedures

Strains and growth media

The *C. albicans* strains used in this study are listed in Table III.1. Strains were routinely grown at 30 ˚C in YPD medium containing 1% yeast extract (BD Biosciences, Sparks, MD), 2% Bacto peptone (BD) and 2% glucose (Sigma, St. Louis, MO). For solid media, 2% agar (Difco, BD) was added. Nourseothricin-resistant (Nou^R) transformants were selected on YPD agar plates supplemented with 200 μg/mL nourseothricin (Werner Bioagents, Jena, Germany). Loss of the nourseothricin resistance marker *SAT1* was induced by growing Nou^R strains overnight at 30 ˚C in YNB liquid medium (0.67% yeast nitrogen base without amino acids from Difco, BD, supplemented with 2% maltose from BioShop, Burlington, Canada). One to two hundred cells were spread on YPD plates and grown for 2 days at 30 ˚C. *Escherichia coli* DH10B cells were used for all DNA cloning procedures and maintenance of plasmid constructs. *E. coli* cells were grown in Luria-Bertani (LB) medium to which chloramphenicol (34 μg/mL) was added as required. DNA primers were purchased from Integrated DNA Technologies (San Diego, CA). Acid-washed glass beads (425-600 nm), all chemical and antifungal compounds were purchased from Sigma unless otherwise stated.

Table III. 1 *C. albicans* strains used in this study

Strain	Genotype	Parent	Reference
5674	*tac1*^{N972D} *CDR1/CDR1 CDR2/CDR2* (Azole-resistant: *CDR1*, *CDR2* overexpression)		(Saidane *et al.*, 2006) (Znaidi *et al.*, 2007)
STY31	*cdr1AΔ::FRT/cdr1BΔ::FRT/cdr2AΔ::FRT/cdr2BΔ::FRT*	5674	(Tsao *et al.*, 2009)
STY31+*CDR1*	*CDR1-SAT1/cdr1BΔ::FRT/cdr2AΔ::FRT/cdr2BΔ::FRT*	STY31	This study
STY31+*cdr1*^{3A}	*cdr1T49A/T51A/S54A-SAT1/cdr1BΔ::FRT/cdr2AΔ::FRT/cdr2BΔ::FRT*	STY31	This study
STY31+*cdr1*^{S849A}	*cdr1S849A-SAT1/cdr1BΔ::FRT/cdr2AΔ::FRT/cdr2BΔ::FRT*	STY31	This study
STY31+*cdr1*^{T49A}	*cdr1T49A-SAT1/cdr1BΔ::FRT/cdr2AΔ::FRT/cdr2BΔ::FRT*	STY31	This study
STY31+*cdr1*^{T51A}	*cdr1T51A-SAT1/cdr1BΔ::FRT/cdr2AΔ::FRT/cdr2BΔ::FRT*	STY31	This study
STY31+*cdr1*^{S54A}	*cdr1S54A-SAT1/cdr1BΔ::FRT/cdr2AΔ::FRT/cdr2BΔ::FRT*	STY31	This study
STY31+*cdr1*$^{T49A/T51A}$	*cdr1T49A/T51A-SAT1/cdr1BΔ::FRT/cdr2AΔ::FRT/cdr2BΔ::FRT*	STY31	This study
STY31+*cdr1*$^{T51A/S54A}$	*cdr1T51A/S54A-SAT1/cdr1BΔ::FRT/cdr2AΔ::FRT/cdr2BΔ::FRT*	STY31	This study
STY31+*cdr1*$^{T49A/S54A}$	*cdr1T49A/S54A-SAT1/cdr1BΔ::FRT/cdr2AΔ::FRT/cdr2BΔ::FRT*	STY31	This study
STY31+*cdr1*^{3E}	*cdr1T49E/T51E/S54E-SAT1/cdr1BΔ::FRT/cdr2AΔ::FRT/cdr2BΔ::FRT*	STY31	This study

Construction of plasmids and *C. albicans* strains used in this study

A smaller version of the plasmid pSFS2A (pSFS2A^{short}) containing the truncated *SAT1-FLP* cassette (Reuss *et al.* 2004) was constructed by removing a 1.4-kb *Bam*HI-*Hind*III fragment containing part of the *FLP* sequences from pSFS2A. This pSFS2A^{short} plasmid was used in order to facilitate the cloning of the entire *CDR1* gene, yielding the *CDR1*-complementing plasmid (pCDR1REV). Precisely, this plasmid was constructed as follows: first, DNA fragment of *CDR1*$_{down}$ (positions +4826 to +5492 of the *CDR1* gene relative to the ATG translation start codon) were PCR-amplified from *C. albicans* SC5314 genomic DNA (Hot-Start KOD^{+} DNA polymerase; Novagen, La Jolla, CA) using primers MR1305 and MR1836 (see Table III.2 for primer sequences) and subsequently cloned between the *Xho*I-*Apa*I sites of plasmid pSFS2A^{short}, generating plasmid pSF^{short}CDR1down. Next, primers MR1512 and MR1835 were used to amplify the *CDR1* gene containing the promoter, ORF and terminator (-472 to +4826 relative to the ATG) and cloned between the *Sac*II-*Not*I sites of pSF^{short}CDR1down to yield plasmid pCDR1REV. MR1512 also introduced an *Apa*I site at the 5'-end of the fragment to allow the release of the cassette for *C.*

albicans transformation (see below). Specific phosphorylation mutations of the *CDR1* ORF in plasmid pCDR1REV were created by site-directed mutagenesis (Stratagene). Mutations were confirmed by sequencing.

Table III. 2 Primers used in this study

Constructs	Primer	Sequence (5' – 3')[a]
Plasmid		
pCDR1REV	MR1305	GCGGGGCCCCAATCATGGTAATACCCCTT
	MR1836	GATCCGAAGTTCCTATTCTCTAGAAAGTATAGGAACTTCCTCGAGAAAGAACAAACTCCTCGCCCCCCGC
	MR1512	ATGCACCGCGGGCCCACCGTTGTAGTTGAGACGGATATC
	MR1835	TCTAGAGAATAGGAACTTCAGATCCACTAGTTCTAGAGCGGCCGCGACAGATGAGAAACACTTTTTCCCA
Site-directed mutagenesis primers[b]		
CDR1T49A	MR2408	GAAAACATTCAGAATTTAGCCAGAGCTTTCACTCATGATTCTTTCAAAG
CDR1T51A	MR2329	TTCAGAATTTAGCCAGAACTTTCGCTCATGATTCTTTCAAAGATGAC
CDR1S54A	MR2409	CCAGAACTTTCACTCATGATGCTTTCAAAGATGACTCGTCA
CDR1T49A/T51A	MR2099	CATTCAGAATTTAGCCAGAGCTTTCGCTCATGATTCTTTCAAAGATGACTCGTCAGC
CDR1T51A/S54A	MR2095	CATTCAGAATTTAGCCAGAACTTTCGCTCATGATGCTTTCAAAGATGACTCGTCAGC
CDR1T49A/S54A	MR2097	CATTCAGAATTTAGCCAGAGCTTTCACTCATGATGCTTTCAAAGATGACTCGTCAGC
CDR1T49A/T51A/S54A	MR2023	CATTCAGAATTTAGCCAGAGCTTTCGCTCATGATGCTTTCAAAGATGACTCGTCAGC
CDR1T49E/T51E/S54E	MR2330	GCCCATACAAGTGAAAACATTCAGAATTTAGCCAGAGAATTCGAACATGATGAATTCAAAGATGACTCG TCAGCAGGTTTATTGAAATAC
CDR1S849A	MR1071	GGGTAGTACTGGAGCTGTTGATTTCCC

[a] Restriction sites introduced for cloning purposes are underlined. [b] Mutated bases are underlined.

C. albicans strains expressing the WT or Cdr1p phosphomutant variants were constructed by reintroducing one copy of the *CDR1* WT or *cdr1* mutant allele at the native chromosomal locus (*CDR1-A* allele locus) in strain STY31 (*cdr1*Δ/*cdr1*Δ *cdr2*Δ/*cdr2*Δ) (Tsao *et al.* 2009). To facilitate integration by homologous recombination, the WT *CDR1* or *cdr1* phosphomutant transformation cassettes were released from the respective plasmids by *Apa*I digestion (1-5 μg) and were used to transform strain STY31. *C. albicans* transformation was performed by electroporation as described previously (Tsao *et al.* 2009). Nou^R transformants containing the correctly integrated cassette were identified by Southern blot analysis. At least two independent strains per construct were generated and analyzed.

Membrane protein preparation and Western blotting

Total membrane extracts from *C. albicans* azole-resistant strain 5674 or 5674-derived mutant strains used in this study were prepared from 100 mL cultures of Logarithmic growing cells (OD_{600} of 1.0) using the Freezer Mill (SPEX CetriPrep, Metuchen, NJ) as described previously (Tsao *et al.* 2009). Protein concentrations were determined using the micro-BCA protein assay kit from Pierce (Rockford, IL) and total membrane extracts (25 μg) were separated by SDS-PAGE (6% acrylamide, 37.5:1 acrylamide:bis-acrylamide) or Low-bis SDS-PAGE (6% acrylamide, 37.5:0.25 acrylamide:bis-acrylamide). The gels were either stained with Coomassie Blue or transferred to a nitrocellulose membrane with a Trans Blot SD Semi-Dry transfer apparatus (Bio-Rad). The membrane was stained with Ponceau reagent (0.1 % Ponceau S in 5 % acetic acid) prior to immunodetection. Immunodetection of Cdr1p and Cdr2p was performed with polyclonal antibodies anti-Cdrp (1:1,000 dilution), anti-Cdr2p (1:4,000 dilution) (Gauthier *et al.* 2003) and anti-Cdr1p (de *et al.* 2002) using an ECL chemoluminescence kit (SuperSignal chemiluminscent substrate, Pierce). Dephosphorylation reactions of Cdr1p were performed by incubating membrane extracts (25 μg) with 200 U λ-phosphatase (NEB, Ontario, CA) with or without phosphatase inhibitors (2 mM imidazole, 1.2 mM sodium molybdate, 1 mM sodium orthovanadate and 4 mM sodium tartrate dehydrate) and incubated at 37 ^{o}C for 30 min.

Mass spectrometry

Total membranes extracts from *C. albicans* azole-resistant strain 5674 and STY7 were separated by 6% SDS-PAGE, stained with colloidal coomassie (10% ammonium sulfate, 0.1% coomassie G250, 3% ortho-phosphoric acid and 20% ethanol) and the gel band corresponding to Cdr1p was excised and digested with trypsin. The tryptic peptides were analyzed by nanoLC-MS using an Eksigent system (Dublin, CA) interfaced to an LTQ-Orbitrap mass spectrometer (Thermo Fisher Scientific, Waltham, MA) via a nanoelectrospray ionization source. LC separations were performed using custom-made C_{18} columns. Sample injection volume was 5 μL, and tryptic digests were first loaded on the pre-column at a flow rate of 4 μL/min and subsequently eluted onto the analytical column using a

gradient from 10% to 60% aqueous acetonitrile (0.2% formic acid) over 56 min with a flow rate of 0.6 μL/min. Data-dependent acquisition mode was enabled and each Orbitrap survey scan (Resolution: 60,000) was followed by three MS/MS scan with dynamic exclusion for a duration of 30 sec on the LTQ linear ion trap mass spectrometer. Multiply charged ions with intensity values above 10,000 counts were selected for MS/MS sequencing. The normalized collision energy was set to 25%. Each sample was analyzed with at least three replicates. Mass calibration used an internal lock mass (protonated $(Si(CH_3)_2O))_6$; *m/z* 445.12057) and provided mass accuracy within 5 ppm for all nanoLC-MS experiments. Raw MS/MS spectra acquired from replicate LC-MS/MS analyzes (n=3) were combined into a single file using Mascot Distiller (version 2.1.1.0, Matrix Science) to reduce spectral redundancy and to correctly identify precursor m/z from survey scans. Interested peptides were confirmed by back blasting against the Candida genome database (http://www.candidagenome.org/). Assignment of phosphorylation sites were validated through manual inspection of relevant MS/MS spectra.

Drug susceptibility testing

Liquid microtiter plate assays were performed as described previously (Tsao *et al.* 2009). The drug concentrations tested were 0.1, 0.2, 0.4, 0.8, 1.5, 3.1, 6.2, 12.5, 25, 50 and 100 μg/mL for fluconazole (FLC); 0.025, 0.04, 0.05, 0.08, 0.1, 0.15, 0.2, 0.3, 0.4, 0.6, and 0.8 μg/mL for ketoconazole (KTC). Stock solutions of FLC were prepared in water at concentrations of 5 mg/mL; stock solutions of KTC were in DMSO at a concentration of 3 mg/mL. Cell growth was measured spectrophotometrically at an OD_{620} after 48 hours of incubation at 30˚C in YPD. The MIC_{50} values were determined as the first concentration of drug sufficient to reduce growth by 50% as compared to control cells grown in the absence of drug. The data presented are the mean of three independent experiments performed in duplicate. Spot assays were also performed as previously described (Saidane *et al.* 2006). Briefly, overnight grown cells were resuspended in YPD to an OD_{600}

of 0.1. Tenfold serial dilutions of each strain were spotted onto YPD plates containing the tested drugs.

Indirect immunofluorescence

C. albicans strains that express WT or phosphomutant Cdr1p were grown to early logarithmic phase (OD_{600} of 0.5) and approximately 1 OD_{600} unit of cells were fixed in the fixation solution (0.1 M KPO_4, pH 6.4, 3.7% formaldehyde) for 1 h at room temperature. Cells were then washed extensively with 0.1 M KPO4, pH 6.4 and resuspended in 225 µL freshly prepared spheroplasting solution [1 M K_2HPO_4, 37 mM citric acid, 1.2 M sorbitol, 20 µL glusulase (DuPont, Boston, MA), 2 µL of 10 mg/mL zymolase 100T (MP biomedicals, Solon, OH)] and incubated at 30 ^oC for 30 min. The Cdrp-generic antibody was used at a 1:250 dilution and the secondary antibody Alexa Fluor® 488-labeled goat anti-rabbit IgG was used at a 1:500 dilution (Molecular Probes, Eugene, OR). Epifluorescence microscopy was performed with a Zeiss Axio-Imager Z1 microscope. Image analysis was carried out with the Zeiss AxioVision 4.8 software.

Nile Red accumulation assay

C. albicans strains that express WT or phosphormutant Cdr1p were grown to early logarithmic phase (OD_{600} of 0.5). Cells were harvested by centrifugation and washed twice with PBS. The cell pellet was then resuspended in 1.5 ml PBS and incubated for 1 h at 30 °C in a shaking incubator. After the incubation, Nile Red (Sigma cat #72485) was added to cells at a final concentration of 6 µM from a 10 mM stock in DMSO and incubated for 30 min at 30 °C. Following this incubation, 200 µl of the cell suspension were transferred to a single well in a black 96-well plate (Perkin Elmer cat#6005329) and the fluorescence intensity was read in a FlexStation II microplate reader (Molecular devices) using an excitation wavelength of 553 nm and an emission wavelength of 636 nm. One reading was taken every 9 sec for the duration of the experiment. After 5 min, glucose was added to cells in each well to a final concentration of 0.8% to allow

energy-dependent efflux and the fluorescence reading was taken every 9 sec, for a further 25 minutes. We used the fluorescence values obtained at 10 min after addition of glucose in order to report the intracellular accumulation of Nile Red. After this time point and until the end of the experiment, no further changes in the Nile Red accumulation were detected in all tested strains.

Colorimetric ATPase activity assay

Cdr1p ATPase activity in purified total membrane extracts was measured as oligomycin-sensitive ATPase activity based on a previous publication (Shukla *et al.* 2003). The assay was performed according to (Nakamura *et al.* 2001) with modifications. Briefly, to each well of a 96-well plate, 80 µl of Assay Medium Cocktail (75 mM MES-Tris pH 7.5, 75 mM KNO_3, 0.3 mM ammonium molybdate and 10 mM sodium azide) were added. To the wells used to determine the standard curve for released phosphate (Pi), 15 µl of the appropriate concentration of KH_2PO_4 in water was added so that there were 100, 70, 50, 30, 20, 10 or 0 nmoles of Pi in each well (for example, 10 µl of 10mM KH_2PO_4 and 5 µl of H_2O was added to a well containing 80 µl of Assay Medium Cocktail to obtain 100 nmoles of Pi in this well). Separately, magnesium ATP was prepared by mixing 28.8 mM ATP with 1 M $MgCl_2$ and neutralizing immediately with NaOH until the pH reached 7.0. The volume of ATP solution required for the assay (25 µl per well for a final concentration of 6 mM) and the assay medium cocktail previously dispensed in the 96-well plate were pre-incubated at 30 °C for 30 min immediately prior to the assay. Following this pre-incubation period, oligomycin (Sigma cat # O-4876 at a final concentration of 20 µM from a 1 mM stock in DMSO) was dispensed in the proper wells and the protein membranes (10 µg in a volume of 15 µl) were then dispensed to start the reaction. Each sample was assayed in triplicate with and without oligomycin. The plate was incubated at 30 °C for 30 min. Following this reaction period, 130 µl of development reagent (1.2% ammonium molybdate in 6 M H_2SO_4, 80 mM sodium ascorbate and 1% SDS) was added and the blue color was allowed to develop for 10 min. The plate was then read in a microplate reader at 750 nm. Every time an assay was

conducted, a standard curve was derived allowing the number of nmoles of Pi released by the ATPase activity to be calculated from the OD_{750} obtained. Using this standard curve, the ATPase activity was reported as the average activity without oligomycin from which the average activity in the presence of this inhibitor was subtracted.

***In silico* analysis**

Prediction of Cdr1p phosphorylation sites was performed with NetPhos 2.0 (http://www.cbs.dtu.dk/services/NetPhos/) and kinase predictions were made with NetPhosK 1.0 (http://www.cbs.dtu.dk/services/NetPhosK/). Sequence alignment was performed using JalView (Waterhouse *et al.* 2009).

III.4 Results

Investigation of Cdr1p phosphorylation

In a previous study, as well as ours, *C. albicans* Cdr1p appears to migrate as a doublet band in Western blots (Coste *et al.* 2006) (Fig. III.1a, top panel, lane 1), suggesting that Cdr1p is subjected to post-translational modification. To test whether Cdr1p is a phosphoprotein, we performed dephosphorylation assays of total membranes containing high levels of Cdr1p and Cdr2p extracted from the azole-resistant strain 5674 (Saidane *et al.* 2006; Tsao *et al.* 2009; Znaidi *et al.* 2007) (Fig. III.1a, upper panel). Treatment with λ-phosphatase slightly increased the mobility of Cdr1p as detected using the specific anti-Cdr1p antibody that recognizes the NH_2-terminal domain of Cdr1p (de *et al.* 2002; Tsao *et al.* 2009) (Fig. III.1a, upper panel, compare lanes 1 and 2). The fact that this mobility shift was inhibited by the addition of phosphatase inhibitors in the reaction (lane 3) strongly suggests that Cdr1p is a phosphoprotein. Due to the overlapping structure and function of Cdr1p and Cdr2p, and because some antibodies cross-reacted between Cdr1p and Cdr2p, the presence of Cdr2p in strain 5674 could obscure biochemical and functional studies of Cdr1p. For these reasons, we performed all the subsequent studies in strains lacking Cdr2p (Tsao *et al.* 2009). In strain STY7, a *cdr2*Δ/*cdr2*Δ strain that is otherwise isogenic with strain 5674, a similar migration pattern of Cdr1p was also detected using the anti-Cdr1p antibody as well as by another antibody, a generic anti-Cdrp that recognizes the NBD_2 of Cdr1p (Fig. III.1a, lower panel).

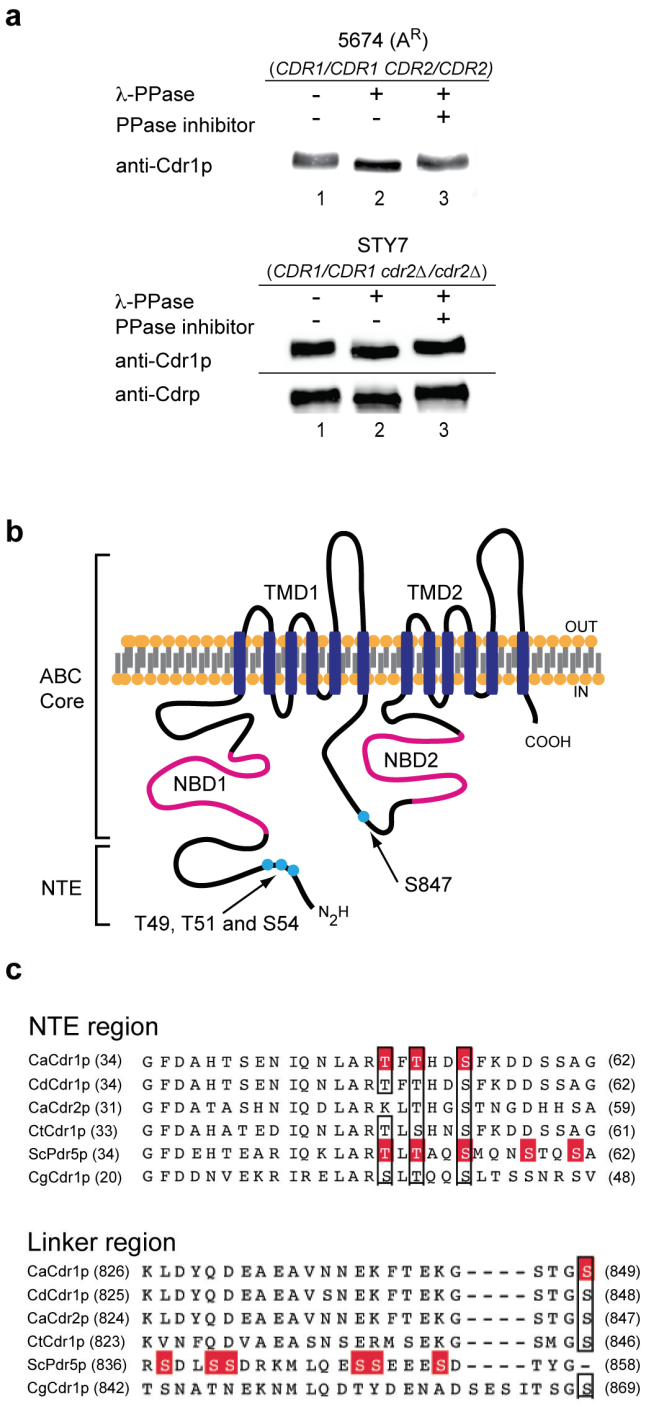

Figure III. 1 Phosphorylation of Cdr1p

(**a**) Dephosphorylation assays. Total membrane lysates extracted from the azole-resistant (A^R) clinical strain 5674 (upper panel) and STY7 (lower panel) were treated or not with λ-phosphatase in the presence or absence of phosphatase inhibitors and separated by SDS-PAGE. Migration patterns of Cdr1p were detected using either the specific anti-Cdr1p or the generic anti-Cdrp

antibodies. (**b**), Schematic representation of Cdr1p consists of an N-terminal extension (NTE) and an ABC "core" region containing two nucleotide binding domains (NBD) and two transmembrane domains (TMD) organized in the NBD_1-TMD_1-NBD_2-TMD_2 topology. Cdr1p phosphorylation at Thr^{49}, Thr^{51} and Ser^{54} within the NTE as well as at Ser^{847} within the linker region connecting TMD_1-NBD_2 was identified by mass spectrometry. (**c**) Sequence comparison of the Cdr1p NTE and linker regions with other closely-related ABC transporters. The protein sequences of *C. albicans* Cdr1p (CaCdr1p), *C. dubliniensis* Cdr1p (CdCdr1p), *C. albicans* Cdr2p (CaCdr2p), *C. tropicalis* Cdr1p (CtCdr1p), *S. cerevisiae* Pdr5p (ScPdr5p) and *C. glabrata* Cdr1p (CgCdr1p) were aligned using JalView. Shading indicates mass spectrometry-identified phosphorylated residues for CaCdr1p and ScPdr5p; conserved residues are boxed.

We used mass spectrometry to identify the phosphorylation sites in Cdr1p. Mass spectrometry analyses of Cdr1p were performed in strain STY7 to avoid possible sequence misassignment that could come from contaminations of Cdr2p peptides. We separated membrane lysate of STY7 on SDS-PAGE, excised and trypsin-digested the gel band corresponding to Cdr1p and submitted it to the liquid chromatography tandem mass spectrometry (LC-MS/MS) analyses. We obtained ~62% sequence coverage of Cdr1p cytosolic segments (excluding the hydrophobic TMD and extracellular loops) and identified four phosphorylation sites, Thr^{49}, Thr^{51}, Ser^{54} and Ser^{847}. While Thr^{49}, Thr^{51} and Ser^{54} are located at the NH_2-terminal extension (NTE) region of Cdr1p, Ser^{847} is situated in the linker region connecting the N-terminal TMD_1 to the C-terminal NBD_2 (Fig. III.1b). Importantly, sequence alignment of *C. albicans* Cdr1p with other closely related homologs revealed a conservation of phosphorylatable residues (serines or threonines) at the corresponding NTE phosphorylation sites (Fig. III.1c, upper panel). Remarkably, phosphorylation of these three conserved residues in *S. cerevisiae* Pdr5p was also detected in recently published large-scale phosphoproteomic studies (Chi *et al.* 2007; Li *et al.* 2007; Smolka *et al.* 2007; Stark *et al.* 2010) (Fig. III.1c). In contrast to the highly conserved NTE phosphorylation sites, the linker phosphorylation region is less well conserved. All the phosphorylated serines identified in *S. cerevisiae* Pdr5p are absent in transporters of the *Candida* origin whereas the phosphorylated serine of Cdr1p

(CaCdr1p Ser^{849}) is conserved among these *Candida* origin transporters (Fig. III.1c, lower panel). Taken together, these results imply that phosphorylation at the NTE region could be a general feature for members of the yeast PDR/CDR/ABCG transporter subfamily.

Characterization of Cdr1p phosphorylation

In order to study the function of these identified phosphorylation sites, we constructed a plasmid carrying the *CDR1* gene next to the dominant selectable marker *SAT1* (Fig. III.2a). The cloned *CDR1* can be used to transform 5674-derived *cdr1Δ/cdr1Δ cdr2Δ/cdr2Δ* strain STY31 (Tsao *et al.* 2009). The expression of *CDR1* in the resulting strain is under the control of its own promoter and driven by the hyperactive transcription factor Tac1p. We used MIC assays to determine the functional expression of WT *CDR1* in this system (Fig. III.2b). Reintroducing one allele of *CDR1* in STY31 resulted in an increased resistance to KTC (MIC_{50} of 0.3 μg/mL for strain STY31+*CDR1* as compared to MIC_{50} <0.025 MIC μg/mL for strain STY31). In addition, a gene dosage effect was also observed as the strain STY31+*CDR1* displayed an approximately 50% of KTC resistance compared to that of strain STY7, which carries two functional alleles of *CDR1* (*CDR1/CDR1 cdr2Δ/cdr2Δ*; MIC_{50} of 0.6 μg/mL). Taken together, these results confirmed the functional expression of *CDR1* in strain STY31 and this strategy was used for the construction of *C. albicans* strains expressing Cdr1p phosphomutants.

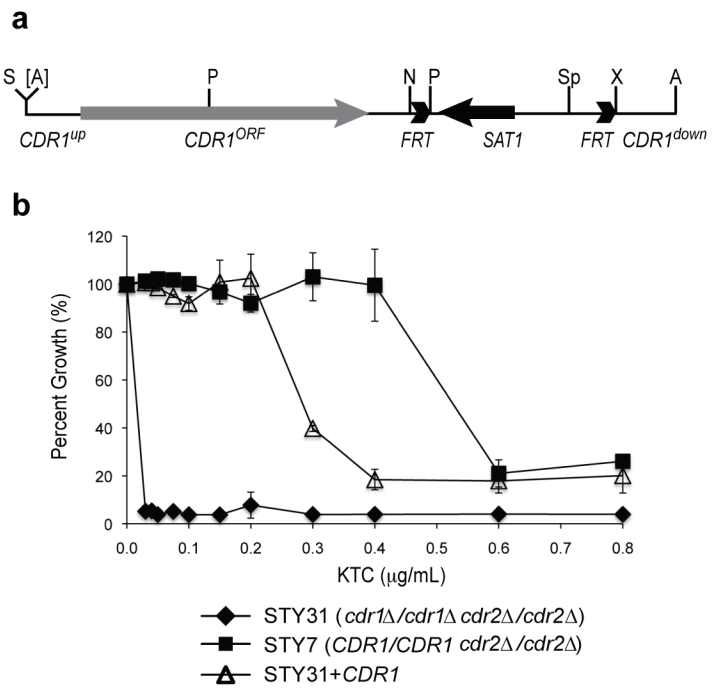

Figure III. 2 Expression of *CDR1* in strain STY31 (*tac1^{N972D} cdr1Δ/cdr1Δ cdr2Δ/cdr2Δ*)

(**a**) Schematic representation of plasmid pCDR1Rev containing the *CDR1*-reintegration cassette. The cassette consists of, from left to right: $CDR1_{up}$, *CDR1* upstream region; the entire *ORF* of the *CDR1* allele; *FRT*, FLP recombination target; *SAT1*, nourseothricin resistance marker; *ACT1t*, transcription termination sequence of the *C. albicans ACT1* gene and $CDR1_{down}$, *CDR1* downstream region. Abbreviations for restriction sites are: S, *Sac*II; A, *Apa*I; N, *Not*I; Sp, *Spe*I; P, *Pst*I; X, *Xho*I. The *Apa*I site shown in brackets was introduced by PCR. (**b**) Azole resistance profiles of 5674 (*tac1^{N972D}CDR1/CDR1 CDR2/CDR2*)-derived strains STY7 (*tac1^{N972D} CDR1/CDR1 cdr2Δ/cdr2Δ*; closed square) and STY31 (*tac1^{N972D} cdr1Δ/cdr1Δ cdr2Δ/cdr2Δ*; closed diamond) as well as strain STY31+*CDR1* (*tac1^{N972D} cdr1Δ/cdr1Δ cdr2Δ/cdr2Δ* + *CDR1*; open triangle), in which one allele of WT *CDR1* was reintroduced at the endogenous locus. Cells were incubated for 48 h at 30 °C in liquid YPD medium with the indicated concentrations of ketoconazole (KTC). The data are presented as the relative growth of cells in KTC-containing medium compared to the growth of the same strain in KTC-free medium, which was set at 100%. The data are the mean of three independent experiments performed in duplicate. Two independently generated *CDR1*-reverting strains were tested and yielded similar results; thus only one representative strain (STY31+*CDR1*) is shown here.

We constructed two mutant variants of Cdr1p; one was a triple alanine mutant (*cdr1*^{3A}), in which all three NTE phosphorylated residues (Thr^{49}, Thr^{51} and Ser^{54}) were changed to alanines; the other one was the linker mutant containing the S849A mutation. The migration patterns and expression levels of these Cdr1p mutants were analyzed by Western blotting using the generic anti-Cdrp antibody (Fig. III.3a). This antibody recognizes a peptide outside the targeting mutagenesis region, therefore, the affinity of this antibody to the testing Cdr1p mutants is likely not to be affected. Immunodetection of the *cdr1*^{3A} mutant revealed increased gel mobility when compared to that of the WT Cdr1p or to the *cdr1*^{S849A} mutant (Fig. III.3a); importantly, the *cdr1*^{3A} mutant exhibited a migration pattern that is similar to the dephosphorylated form of Cdr1p (Fig. III.1a). To test whether these triple alanine mutations had largely abolished the phosphorylation of Cdr1p and caused increased gel mobility, we tested the *cdr1*^{3A} mutant in the dephosphorylation assay. We found that the mobility shift of *cdr1*^{3A} band was no longer detectable in the presence of λ-phosphatase (Fig. III.3b). These data strongly suggests that Thr^{49}, Thr^{51} and Ser^{54} constitute major phosphorylation sites of Cdr1p.

We examined whether phosphorylation of Cdr1p at NTE is important for the plasma membrane localization using an indirect immunofluorescence microscopy (Fig. III.3c). In strain expressing the WT Cdr1p, a fluorescence signal was detected at the cell periphery indicating plasma membrane localization. In strain expressing the *cdr1*^{3A} mutant, a similar fluorescence signal as of that observed in the WT strain was also detected, suggesting that the triple alanine mutation does not affect the localization of Cdr1p. Next, we asked whether phosphorylation at NTE is important for Cdr1p function by testing the ability of strains expressing WT or phosphomutant Cdr1p to grow in the presence of azole drugs (Fig. III.3d). Interestingly, the strain expressing the *cdr1*^{3A} mutant showed a significantly reduced resistance to both azole drugs as compared to that of the strain expressing the WT Cdr1p (e.g. FLC MIC_{50} of 0.4 μg/mL for strain STY31, 3.1 μg/mL for the *cdr1*^{3A} mutant and 50 μg/mL for the WT Cdr1p), indicating that phosphorylation

at NTE is important for Cdr1p-mediated azole resistance. In contrast, the strain expressing the *cdr1*^{S849A} mutant conferred azole resistance that is indistinguishable to the WT strain, suggesting that mutation of S849A has no effect on Cdr1p function. We also carried out drug resistance assays on solid media plates containing azole drugs and obtained similar results (Fig. III.3e). Taken all together, these results demonstrate that the NTE mutant (*cdr1*^{3A}) is properly localized yet exhibits an impaired azole transport activity.

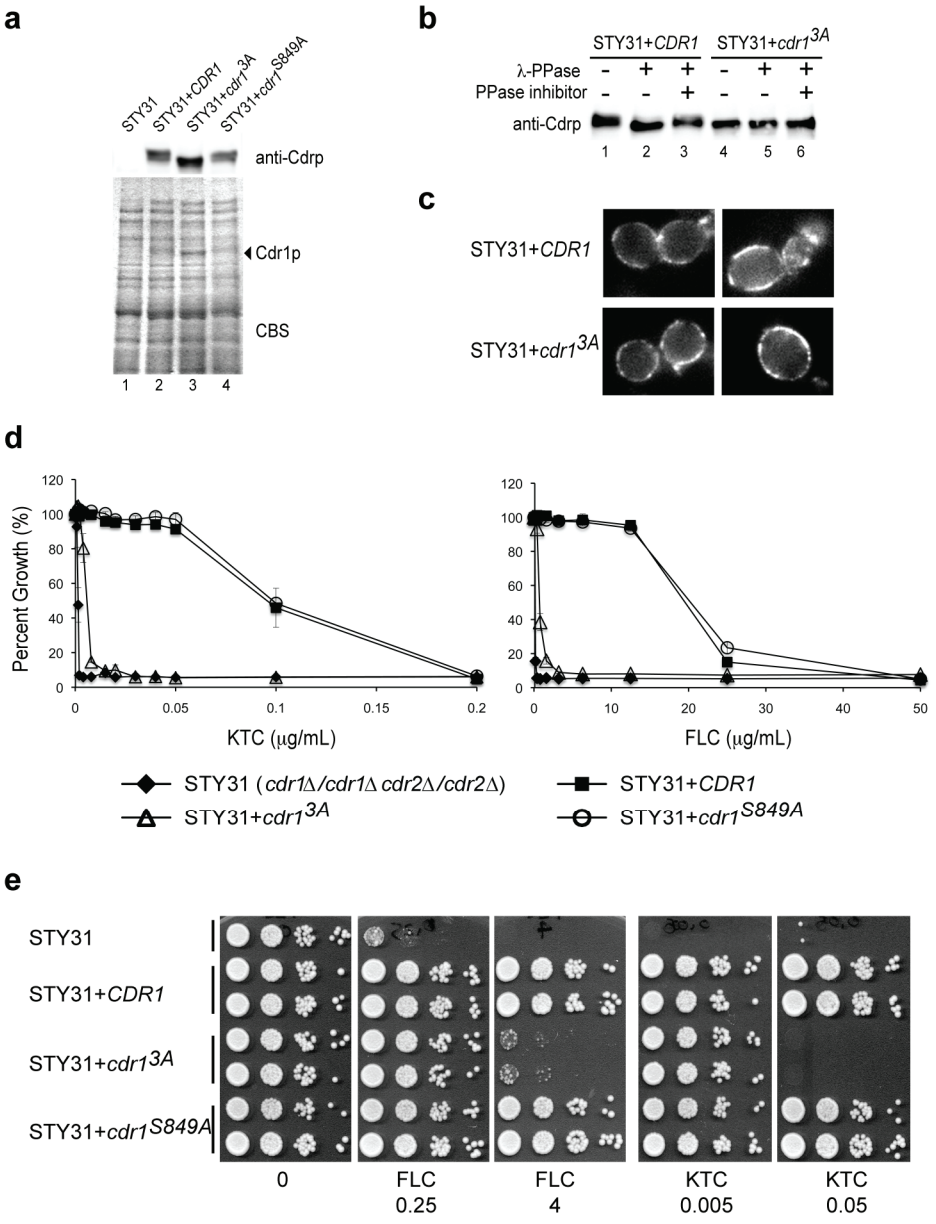

Figure III. 3 Characterization of Cdr1p phosphomutants

(**a**) Expression profiles of Cdr1p WT and phosphomutants. Total membranes extracted from STY31 and STY31-derived strains expressing Cdr1p WT, Cdr1p NTE phosphorylation mutant (*cdr1*^{3A}, T49A/T51A/S54A) and the linker mutant (*cdr1*^{S849A}) were separated by SDS-PAGE and analyzed by Western blotting with generic anti-Cdrp antibody. A Coomassie-stained gel of the protein extracts is shown at the bottom (CBS); arrow indicates the predicted position of Cdr1p. (**b**) Dephosphorylation assay. Total membrane lysates extracted from strains STY31+*CDR1* and STY31+*cdr1*^{3A} were treated or not with λ-phosphatase in the presence or absence of phosphatase inhibitors and separated by SDS-PAGE. Migration patterns of WT and the *cdr1*^{3A} mutant Cdr1p

were detected using the generic anti-Cdrp antibody. (**c**) Localization of WT and the *cdr1*^{3A} mutant Cdr1p was detected using the generic anti-Cdrp antibody and visualized by using a fluorescent secondary antibody with an epifluorescence microscope. (**d**) Azole resistance profiles of strains as described in the panel (**a**) were analyzed by MIC assay. MIC assay was performed as described in the legend to Fig. III.2b. KTC, ketoconazole; FLC, fluconazole. (**e**) Spot assay. Azole resistance profiles of strains STY31 and two independent strains of STY31 expressing Cdr1p WT, Cdr1p phosphorylation mutants (*cdr1*^{3A} or *cdr1*^{S849A}) were determined by spot assays. Serial 10-fold dilutions of cells, starting at an OD_{600} of 0.1, were spotted onto YPD plates containing FLC or KTC at the indicated concentrations (micrograms per milliliter) or no drug. The plates were incubated for 48 h at 30°C.

To test whether the presence of negatively charged residues (as provided by phosphorylation) on the NTE region is critical for Cdr1p function, we constructed a strain carrying the triple glutamate mutations of Cdr1p (*cdr1*^{3E}; where Thr^{49}, Thr^{51} and Ser^{54} were simultaneously mutated to glutamate). Western blotting analyses showed that the migration pattern and the signal intensity of *cdr1*^{3E} were detected at levels comparable to that of the WT (Fig. III.4a, compare lanes 2 and 10). Notably, it was also evident that *cdr1*^{3A} was expressed at a higher level and accompanied by a faster gel mobility, contrasting to that of the WT and the *cdr1*^{3E} mutant (Fig. III.4a, compare lanes 2, 9 and 10) (see below). Finally, the functionality of the *cdr1*^{3E} mutant was similarly tested in MIC assay. This mutant exhibited high levels of resistance to FLC comparable to that of the WT Cdr1p (Fig. III.4b). In summary, judging from the Western blotting and MIC analyses, the phosphomimetic mutant exhibited a WT-like phenotype that is distinct from the *cdr1*^{3A} mutant. These data strongly supports the proposition that negatively charged residues, as conferred by phosphorylation at the NTE of Cdr1p, is important for its stability and function.

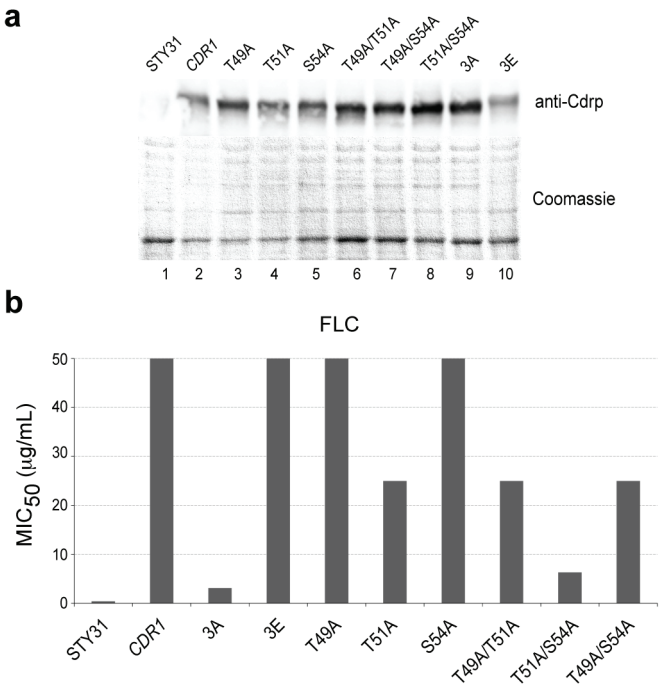

Figure III. 4 Characterization of Cdr1p NTE phosphomutants

(**a**) Expression profiles of Cdr1p NTE phosphomutants. Total membranes extracted from strains expressing single, double and triple phosphorylation mutations of Cdr1p were separated by SDS-PAGE and analyzed by Western blotting with the anti-generic antibody. (**b**) Azole resistance profiles of these strains were analyzed by MIC assay as described in legends to III.2**b** and III.3**d**. The plotted graph of cell growth versus azole concentrations are not shown for clarity; concentrations of FLC that were able to inhibit growth by 50% compared to that of control cells grown in the absence of the drug (MIC_{50}) are shown.

Characterization of Cdr1p NTE phosphorylation

Since the *cdr1*^{3A} mutant exhibited major functional defects, we asked whether all three sites are required for this phenotype by determining the individual contribution of each residue to the overall phosphorylation status and function of Cdr1. We replaced Thr^{49}, Thr^{51} and Ser^{51} with alanine, individually and in combination. Western blotting analysis showed that the signal intensity detected for each mutant was somewhat varied. Variations in signal intensities implied that all the single- and double-NTE mutants exhibited different levels of expression, ranging between a 'low-level expression' as observed for the WT and

the *cdr1*^{3E}, to a 'high-level expression' as observed for the *cdr1*^{3A} (Fig. III.4a, lanes 2 to 10). These data suggest that the phosphorylation status affects Cdr1p levels. We also analyzed the functionality of these mutants using MIC assays (Fig. III.4b). We found that single alanine mutations at Thr^{49} and Ser^{54} showed no effect, while the T51A mutation showed a 2-fold reduction in azole resistance, suggesting that phosphorylation at Thr^{51} plays a predominant role on Cdr1p function. The double T49A/T51A mutant was not more susceptible than the single T51A mutant, suggesting that phosphorylation at T49 plays a neglectable or a very minor role. Mutation of S54A in addition to T51A further reduced FLC resistance by about 4-fold, demonstrating that phosphorylation at these two sites has a synergistic effect on Cdr1p function. Furthermore, despite the fact that the T51A/S54A double mutation already showed a strong reduction in Cdr1p-mediated azole resistance, this strain was still slightly more resistant than the *cdr1*^{3A} mutant, possibly uncovering a contribution of phosphorylation at Thr^{49} or at another site that is yet to be identified. Finally, while single mutation of either T49A or S54A showed no effect, combination of T49A and S54A showed a 2-fold reduction in activity, confirming that phosphorylation at these two sites has a functional impact. Taken together, phosphorylation of Cdr1p at all three residues Thr^{49}/Thr^{51}/Ser^{54} is required for its optimal function, with phosphorylation at Thr^{51} playing a predominant role.

NTE phosphorylation plays important role for Cdr1p activity

We employed an independent method to measure the transport activity of Cdr1p using the fluorescent lipophilic dye Nile Red. Nile Red has been documented to be strongly fluorescent only in a highly hydrophobic environment such as membrane bilayers and in addition, previous studies showed that it is a good substrate for some bacterial and yeast ABC transporters (Bohnert *et al.* 2010; Ivnitski-Steele *et al.* 2009). Furthermore, Nile Red can be quickly extruded from pre-loaded cells in *S. cerevisiae* strain expressing WT *C. albicans* Cdr1p, resulting in reduced intracellular accumulation of this compound (Ivnitski-Steele *et al.* 2009). In our hands, *C. albicans* strain STY31 accumulated ~10-fold more

Nile Red than strain expressing WT Cdr1p, consistent with the proposition that Cdr1p actively effluxes Nile Red out of the cell (Fig. III.5a). Strain expressing the *cdr1*^{3A} mutant accumulated high levels of fluorescence comparable to that of STY31, suggesting alanine mutations at the NTE region impaired the function of Cdr1p. Strain expressing *cdr1*^{3E}, on the other hand, accumulated very little Nile Red comparable to that of strain expressing the WT Cdr1p, indicating the phosphomimetic mutation conserved its function. These results are largely in agreement with the azole resistance profile as reported above. Interestingly, the *cdr1*^{3A} mutant showed a complete abolished transporter function for Nile Red but not for azoles suggesting mutations at these residues affected the substrate specificity or the ATPase activity of this transporter. However, these results could also suggest that the Nile Red transport assay is less sensitive than the azole resistance assay for discriminating between different mutants.

We performed ATPase assay to determine whether the observed phenotype of the *cdr1*^{3A} mutant (reduced azole resistance and increased Nile Red accumulation) correlated with a diminished Cdr1p ATPase activity. The ATPase assay was performed using membrane fractions extracted from *C. albicans* strain STY31 and STY31-derived strains expressing either WT or mutant Cdr1p (Fig. III.5b). In this assay, Cdr1p-specific ATPase activity of the isolated membrane fraction was measured as an oligomycin-sensitive release of inorganic phosphate. Oligomycin is a compound that does not affect the ATPase activity of the Pma1p (a major proton pump that is also present in this membrane fraction) and that was shown to be a specific inhibitor of Pdr5p and Cdr1p (Decottignies *et al.* 1994; Nakamura *et al.* 2001; Shukla *et al.* 2003). The ATPase activity detected in strain STY31 represents the basal level activity contributed by ATPases other than Cdr1p and Cdr2p whereas the increased ATPase activity detected in the STY31+CDR1 strain corresponds to the specific activity contributed by Cdr1p. The *cdr1*^{3A} mutant showed a strongly reduced ATPase activity, consistent with our proposition that non-phosphorylated mutations at the NTE region significantly impaired the Cdr1p ATPase activity and transporter function. Surprisingly, the *cdr1*^{3E} mutant also

showed a decreased ATPase activity indicating that the constitutive phosphorylation of Cdr1p as mimicked by glutamate mutations affected the ATPase function of Cdr1p. These results further suggested that the regulation of Cdr1p phosphorylation is important for its optimal ATPase activity. Finally, as the *cdr1*^{3E} mutant exhibited a WT-like transporter function in transporting azoles and Nile Red despite the compromised ATPase activity, implying that a minimal ATPase activity was sufficient to confer full transporter function.

Taken together, we have used three independent assays to characterize the function of Cdr1p phosphomutants and obtained generally consistent results indicating that phosphorylation of Cdr1p NTE residues positively regulate its function.

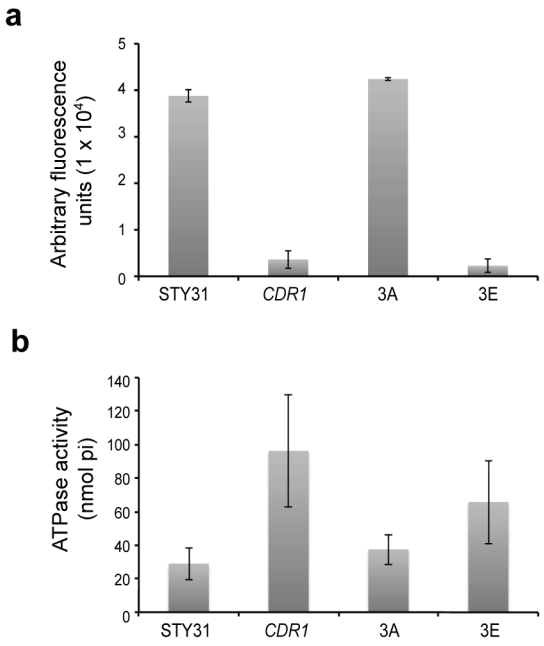

Figure III. 5 Functional characterizations of Cdr1p NTE phosphomutants by Nile red transport assay and *in vitro* ATPase assay

(**a**) Nile Red transport assay. The transport activity of Cdr1p WT or mutants was measured as its ability to export the fluorescent compound Nile Red. Nile Red accumulated in each strain was measured after glucose addition to the cell for initiating transport. Fluorescence values presented here were taken after 10 min of addition of glucose. (**b**) *In vitro* ATPase activity of Cdr1p WT or

mutants was measured as the oligomycin-sensitive release of inorganic phosphate. The data presented here are an average value from three independent experiments.

III.5 Discussion

Yeast ABC transporters of the ABCG subfamily appeared to be regulated by phosphorylation. Previous studies have shown that the level of phosphorylation could directly influence the stability and activity of *S. cerevisiae* Pdr5p and *C. glabrata* Cdr1p, respectively (Decottignies *et al.* 1999; Wada *et al.* 2005). Despite these findings, our current knowledge towards to phosphorylation-dependent regulation of yeast ABCG transporters is far from complete and only a few kinases involved in ABC transporter phosphorylation have been characterized. In the present study, we provide evidence that *C. albicans* Cdr1p is phosphorylated (Fig. III.1a). Furthermore, using the LC-MS/MS analyses, we have obtained 62% sequence coverage of Cdr1p cytosolic region and identified four phosphorylation sites (Thr^{49}, Thr^{51}, Ser^{54} and Ser^{849}) (Fig. III.1b). Interestingly, we noticed that the predicted phosphorylation sites in *S. cerevisiae* Pdr5p [Ser^{420} (Decottignies *et al.* 1999)] and *C. glabrata* Cdr1p [Ser^{307} and Ser^{484} (Wada *et al.* 2005)] are conserved at equivalent positions in Cdr1p. However these residues were not phosphorylated based on our mass spectrometry analyses; yet, peptides containing these residues were recovered (data not shown).

During the course of our study, new phosphorylation sites of *S. cerevisiae* Pdr5p with not-yet associated functions have been reported in independent large-scale mass spectrometry studies (Chi *et al.* 2007; Li *et al.* 2007; Smolka *et al.* 2007) and these data is now being compiled in the PhosphoGrid database (http://www.phosphogrid.org/) (Stark *et al.* 2010). Despite the fact that the total sequence coverage of Pdr5p is unknown, mass spectrometry identified eleven phosphorylation sites (Fig. III.1c). Interestingly, similar to our findings for *C. albicans* Cdr1p, phosphorylated residues in *S. cerevisiae* Pdr5p are also clustered at two locations, the NTE and the linker regions. The three identified phosphorylated residues at the Pdr5p NTE region are conserved in *C. albicans* Cdr1p and these sites (Thr^{49}, Thr^{51}, Ser^{54}) were also found to be phosphorylated in the present study.

The functional importance of phosphorylation occurring at the NTE region is highlighted by our mutagenesis studies. We showed that the *cdr1*^{3A} mutant exhibited faster gel mobility similar to that of the dephosphorylated Cdr1p and also that this mutation resulted in an impaired Cdr1p function (Figs. III.3 and III.5). Furthermore, the finding that Cdr1p function can be mimicked by negatively charged amino acids, as demonstrated by the *cdr1*^{3E} mutant (Figs. III.4 and III.5), corroborates our proposition that phosphorylation at the NTE region of Cdr1p is required for its function. On the other hand, the S849A mutation did not affect Cdr1p activity, suggesting that phosphorylation of the linker region plays a minor, or if any, functional role (Fig. III.3d-e). Although it is possible that additional phosphorylation sites of the Cdr1p linker region were not identified in the present study.

Our result showed that the phosphorylation status of Cdr1p affected the amount of Cdr1p expressed at the plasma membrane, since the *cdr1*^{3A} mutant was consistently expressed at higher levels than the Cdr1p WT and the *cdr1*^{3E} mutant (Figs. III.3a and III.4a). This finding suggests that phosphorylation could affect the protein stability and turnover. The link between phosphorylation and protein stability has already been reported for *S. cerevisiae* Pdr5p (Decottignies *et al.* 1999). Phosphorylation of Pdr5p is abolished in a casein kinase deletion mutant and the stability of Pdr5p in this mutant is reduced in a vacuolar protease Pep4p-dependent manner. Dephosphorylated Pdr5p is probably mislocalized and followed by vacuolar degradation. These results suggest that phosphorylation could act as a signal for plasma membrane trafficking of Pdr5p. In our case, we showed that a stronger signal was detected for the phosphorylation-deficient Cdr1p (*cdr1*^{3A} mutant) compared to the WT Cdr1p in Western blots, a result that supports the hypothesis that phosphorylation could be involved in a negative regulation of Cdr1p stability. Further studies, including pulse-chase experiments to determine the WT and phosphomutant Cdr1p protein half-life and turnover; examination of the ubiquitination status of Cdr1p (which could serve as a signal

for degradation) will aid to our understanding of the role of phosphorylation in control of Cdr1p protein fate.

We demonstrated that phosphorylation at the NTE region of Cdr1p is involved in the modulation of its transport function and of its optimal ATPase activity. Interestingly, we noticed that the presence of NTE region is a unique feature that is conserved within members of the yeast ABCG subfamily. Due to the lack of structural information, secondary structure of the NTE region as well as its relative position to the ABC core domain are completely unknown. Nevertheless, we noticed that the NTE region contains many Ser/Thr as well as charged residues, suggesting that it might be involved in the intra- or intermolecular interactions of transporters. Indeed, early genetic interaction and electron microscopy studies of *S. cerevisiae* Pdr5p suggested a homodimeric organization of Pdr5p and this interaction is possibly established via the first cytosolic loops as demonstrated by a yeast-two-hybrid study (CL1, which contains the entire NTE and NBD1) (Ferreira-Pereira *et al.* 2003; Subba Rao *et al.* 2002). Since the NTE region of Pdr5p contains a cluster of phosphorylation sites, it is therefore tempting to speculate that phosphorylation of the Pdr5p NTE region could promote homodimerization of two Pdr5p transporters. In line with this, we also expect that this model could be directly applied to *C. albicans* Cdr1p given the similarity between these two transporters.

On the other hand, although it has not been widely considered, a recent study using the newly optimized yeast membrane two-hybrid technology highlights the involvement of cytosolic modulators for regulating ABC transporter activity (Paumi *et al.* 2007). *S. cerevisiae* ABCC subfamily member Ycf1p has been used as the 'bait' protein in this study and among a few identified interacting partners, Tus1p, a guanine nucleotide exchange factor, has been shown to stimulate the activity of Ycf1p by 2 fold (Paumi *et al.* 2007). Although similar studies have not yet been performed for yeast ABCG transporters; we can speculate that the NTE region could serve as an interaction site with protein partners in order to modulate

the function of these transporters, and that phosphorylation of NTE could be important for regulating such interactions.

What is the kinase(s) responsible for Cdr1p phosphorylation? Our single site mutational analyses showed that while individual mutations had no effect, combination mutations of both Thr^{49} and Ser^{54} of Cdr1p conferred a reduced azole-resistance phenotype similar to that of the single site mutation of Thr^{51} and all three sites mutation resulted in a significantly reduced azole-resistance (Figs. III.3d-e and III.4b). These data suggested that Thr^{51} is the dominant phosphorylation site and that phosphorylations at Thr^{49} and Ser^{54} contribute to the phosphorylation at Thr^{51} by creating an acidic environment surrounding Thr^{51}, that could be important for specific kinase recognition and the overall phosphorylation at these sites. Analyzing the surrounding residues of Thr^{51}, we find Arg at the P-3 position (Fig. III.1c), suggesting that Thr^{51} could be a substrate for a 'basophilic-type' kinase (describing kinases that preferentially phosphorylate substrates having basic residues in close proximity to the phosphorylation site), such as protein kinase C (PKC). However, a recent informative large-scale peptide-based screening for determination of kinase consensus phosphorylation site motifs in *S. cerevisiae* suggested other kinases that strongly select for Arg at P-3 as well as Leu at P-5 position, a pattern that is also present in Cdr1p sequence (Fig. III.1c). Deduced from this published data, kinase candidates for Cdr1p could include the calmodulin-dependent protein kinases (CMK1 or CMK2) as well as a putative kinase RTK1 (YDL025C) (Mok *et al.* 2010). Whether functional homologs of these *S. cerevisiae* kinases exist in *C. albicans* and whether they are responsible for phosphorylating Cdr1p require further experimental investigations.

The synergistic effect of Thr^{51} and Ser^{54} could suggest that phosphorylation at Thr^{51} is a prerequisite for the phosphorylation at Ser^{54}. If this is the case, the phosphorylation at Thr^{51} may allow phosphorylation at Ser^{54} by an 'acidophilic-type' kinase (describing kinases that preferentially phosphorylate substrates

having acidic residues in close proximity to the phosphorylation site), such as casein kinase I (CKI). CKI is very selective for acidic amino acids or phosphorylated residues at positions between P-3 to P-5; therefore, phosphorylation of Ser^{54} by CKI could be dependent on the primary phosphorylations at Thr^{51} (P-3) and Thr^{49} (P-5) positions. In line with this, the fact that mutation at Thr^{49} showed phenotype only when Ser^{54} was mutated, led us to speculate that phosphorylation at Thr^{49} may be involved for enhancing CKI recognition. Taken together, it is tempting to speculate that at least two different kinases are involved in sequential phosphorylations of Cdr1p at the NTE region, a basophilic kinase that phosphorylates Thr^{51} that, in turn, primes the region for the secondary phosphorylation by CKI.

We have additional lines of evidence suggesting that CKI could be involved in Cdr1p phosphorylation. In general, spatial proximity is a key factor that influences substrate selection by a protein kinase (Ptacek *et al.* 2005). Indeed, yeast CKI is a palmitoylated plasma membrane-bound kinase, located at the same subcellular compartment as Cdr1p and it has been shown to be involved in the phosphorylation of several membrane proteins in *S. cerevisiae*, including uracil permease Fur4p (Marchal *et al.* 2000) and glucose transporters Rgt2p (Moriya *et al.* 2004). Most importantly, CKI has been demonstrated to be involved in Pdr5p phosphorylation (Decottignies *et al.* 1999). Therefore, it will be important to investigate whether *C. albicans* CKI is also involved in Cdr1p phosphorylation at the NTE region.

In summary, we examined whether phosphorylation regulates Cdr1p function by site-directed mutagenesis in *C. albicans* followed by various functional analyses. Our results showed that NTE phosphorylation is important for Cdr1p function and work is ongoing to test whether CKI is involved in the NTE phosphorylation of Cdr1p and therefore contributed to Cdr1p-mediated azole resistance.

III.6 Acknowledgements

The authors would like to thank Joachim Morschhäuser for the gift of pSFS2A, the IRIC Genomic Platform for DNA sequencing and the IRIC Proteomic Platform for mass spectrometry analysis. This work was supported by a research grant to M.R. from the Canadian Institutes of Health Research (MT-15679). IRIC is supported by the Canadian Center of Excellence in Commercialization and Research, the Canadian Foundation for Innovation, and the Fonds de Recherche en Santé du Québec.

Chapter IV

Modulation of histone H3 lysine 56 acetylation as an antifungal therapeutic strategy

Chapter IV Modulation of histone H3 lysine 56 acetylation as an antifungal therapeutic strategy

Studies from our lab, as well as others, demonstrated the presence of several distinct transcriptional pathways controlling expression of multiple azole resistance effectors in addition to Cdr1p and Cdr2p. Thus, targeting Cdr1p and Cdr2p by pharmacological inhibitors is likely to offer limited therapeutic success while the need for better antifungal drugs remains of high priority. An alternative approach would be to identify and characterize new genes that are essential for *C. albicans* pathogenicity to serve as novel antifungal targets. Acetylation of histone H3 lysine 56 (H3K56) has been recently identified to be a particularly important post-translational modification for fungal growth in *S. cerevisiae*. Therefore we investigated whether H3K56 acetylation could also be found in *C. albicans* and its modulation could allow for new antifungal therapeutic avenues.

Modulation of histone H3 lysine 56 acetylation as an antifungal therapeutic strategy

Hugo Wurtele[1,&], Sarah Tsao[1,&], Guylaine Lépine[1], Alaka Mullick[2,3], Jessy Tremblay[2,3], Paul Drogaris[1], Eun-Hye Lee[1], Pierre Thibault[1,4], Alain Verreault[1,5*], Martine Raymond[1,6*]

[1]Institute for Research in Immunology and Cancer, Université de Montréal, Montreal, Canada, [2]Biotechnology Research Institute, National Research Council of Canada, Montreal, Canada, [3]Département de Microbiologie et Immunologie, [4]Département de Chimie, [5]Département de Pathologie et Biologie Cellulaire, [6]Département de Biochimie, Université de Montréal, Montreal, Canada

[&]These authors contributed equally to this work

*Corresponding authors: Institute for Research in Immunology and Cancer, Université de Montréal, P.O. Box 6128, Succursale Centre-Ville, Montreal, Qc, Canada H3C 3J7 alain.verreault@umontreal.ca; martine.raymond@umontreal.ca

H3 K56 acetylation and *C. albicans* virulence

IV.1 Abstract

Candida albicans **is a major fungal pathogen that causes serious systemic and mucosal infections in immunocompromised individuals. In yeast, histone H3 Lys56 acetylation (H3K56ac) is an abundant modification regulated by enzymes that have fungal-specific properties, making them appealing targets for antifungal therapy. Here, we demonstrate that H3K56ac in *C. albicans* is regulated by the *RTT109* and *HST3* genes, which respectively encode the H3K56 acetyltransferase (Rtt109p) and deacetylase (Hst3p). We show that reduced levels of H3K56ac sensitize *C. albicans* to genotoxic and antifungal agents. Inhibition of Hst3p activity by conditional gene repression or nicotinamide treatment results in a loss of cell viability associated with abnormal filamentous growth, histone degradation, and gross aberrations in DNA staining. We show that genetic or pharmacological alterations in H3K56ac levels reduce virulence in a mouse model of *C. albicans* infection. Our results demonstrate that modulation of H3K56ac is a unique strategy for treatment of *C. albicans* and, possibly, other fungal infections.**

H3K56ac is an abundant post-translational modification found in newly synthesized H3 molecules deposited throughout the genome during DNA replication (Celic *et al.* 2006; Masumoto *et al.* 2005). Originally discovered in yeast (Hyland *et al.* 2005; Masumoto *et al.* 2005; Ozdemir *et al.* 2005; Xu *et al.* 2005; Zhou *et al.* 2006), H3K56ac also exists in human cells (Das *et al.* 2009; Tjeertes *et al.* 2009; Xie *et al.* 2009; Yuan *et al.* 2009). In *Saccharomyces cerevisiae*, H3K56ac peaks when new histones are synthesized during S-phase (Masumoto *et al.* 2005) and is mediated by the histone acetyltransferase Rtt109p (Driscoll *et al.* 2007; Han *et al.* 2007; Tsubota *et al.* 2007). H3K56ac is removed genome-wide by the histone deacetylases Hst3p and Hst4p during the G2 and M phases (Celic *et al.* 2006; Maas *et al.* 2006). Tightly regulated H3K56ac plays a key part in the DNA damage response, as mutants that cannot acetylate or

deacetylate Lys56 are extremely sensitive to genotoxic agents (Celic *et al.* 2006; Han *et al.* 2007; Maas *et al.* 2006; Masumoto *et al.* 2005; Thaminy *et al.* 2007).

C. albicans is a major human fungal pathogen in terms of both its clinical importance and its use as an experimental model for fungal pathogenesis (Berman *et al.* 2002; Cowen *et al.* 2002). It is one of the leading causes of infections affecting immunodeficient individuals, including HIV-infected individuals and patients undergoing cancer therapy. *C. albicans* is the fourth most common cause of nosocomial bloodstream infections in the US and is associated with high mortality rates (Pfaller *et al.* 2007; Sims *et al.* 2005; Wisplinghoff *et al.* 2004). Treatment of candidiasis involves the use of azole or echinocandin drugs that respectively target ergosterol and cell wall biosynthesis, respectively, but their efficacy can be compromised by the emergence of drug-resistant strains (Akins 2005; Perlin 2007). As the fungal enzymes that regulate H3K56ac have diverged considerably from their human counterparts (Frye 2000; Wang *et al.* 2008), we sought to determine whether these enzymes could be potential targets for treatment of *C. albicans* infections.

IV.2 Results

H3K56ac modulates fungicidal agent sensitivity in *C. albicans*

We first verified the presence of H3K56ac in *C. albicans.* Immunoblots of total lysates from SC5314 and SN152 strains probed with an antibody against H3K56ac (Celic *et al.* 2006; Masumoto *et al.* 2005) revealed a band of the expected molecular weight (~15 kDa) (Fig. IV.1a). We also isolated histones from *C. albicans* cells and analyzed them by mass spectrometry. The product ion spectrum of a doubly protonated precursor peptide (*m/z* 638.99^{2+}) shows a *y*-type fragment ion series that confirms acetylation of Lys56 on the basis of the 42-Da mass shift between the *y7* and *y8* fragment ions (Fig. IV.1b). We also estimated the stoichiometry of H3K56ac by derivatization of nonmodified lysine e-amino groups with deuterated acetic anhydride prior to trypsin digestion (Celic *et al.*

2006; Masumoto *et al.* 2005). In different asynchronously growing cultures, the Lys56-acetylated peptide was present in 20 to 27% of H3 molecules (Fig. IV.1c,d). Thus, H3K56ac is an abundant modification in *C. albicans*. This is in stark contrast to the low stoichiometry of H3K56ac (1%) in human cells (Das *et al.* 2009; Xie *et al.* 2009).

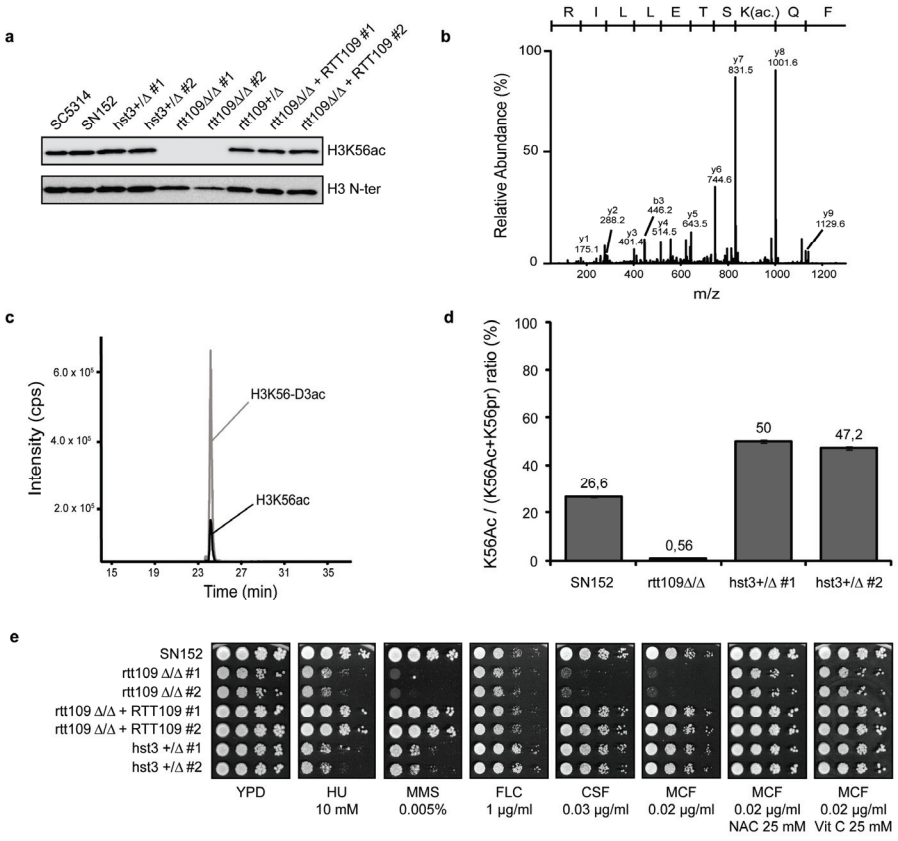

Figure IV. 1 H3K56 acetylation modulates genotoxic and fungicidal agent sensitivity in *C. albicans*

(**a**) Immunoblot of H3K56ac and total H3 in whole-cell lysates from exponentially growing populations of each strain. (**b**) Fragmentation spectrum of precursor ion *m/z* 638.9^{2+} showing the presence of H3K56ac. (**c**) Extracted ion chromatograms for *m/z* 638.9^{2+} (H3K56ac) and its deuterated analog *m/z* 640.4^{2+} (H3K56-D3Ac). (**d**) Stoichiometry of H3K56ac determined by mass spectrometry for histones purified from exponentially growing cells. ε-NH2 of Lys56 is modified with either an acetyl (ac) or a deuterated acetyl (pr) group. (**e**) Colony formation assays (tenfold serial dilutions of each strain). YPD, control; HU, hydroxyurea; MMS, methyl methane sulfonate; FLC, fluconazole; CSF, caspofungin; MCF, micafungin; NAC, N-acetyl-$_L$-cysteine; VitC, vitamin C.

The *RTT109* gene encodes an acetyltransferase responsible for H3K56ac (Driscoll *et al.* 2007; Han *et al.* 2007; Tsubota *et al.* 2007); its ortholog in *C. albicans* is orf19.7491 (*RTT109*). Deletion of both alleles of *RTT109* in strain SN152 led to nearly complete disappearance of H3K56ac on the basis of immunoblots and mass spectrometry (Fig. IV.1a,d, and Supplementary Table IV.1). Deacetylation of H3K56 requires the sirtuins Hst3p and Hst4p in *S. cerevisiae.* Deletion of both genes results in DNA damage sensitivity and thermosensitivity, but the double mutant remains viable (Celic *et al.* 2006; Maas *et al.* 2006; Thaminy *et al.* 2007). We only found one gene in *C. albicans* (orf19.1934; *HST3*) encoding a potential ortholog of *S. cerevisiae HST3* and *HST4*. We generated a heterozygous deletion mutant for *HST3* in SN152, but were unable to obtain an *hst3*Δ/ *hst3*Δ (*hst3*Δ/Δ hereafter) homozygous mutant, suggesting that the *C. albicans HST3* gene is essential. Although immunoblots of whole-cell extracts from *hst3*Δ/*HST3* (*HST3*+/Δ hereafter) cells failed to detect an increase in H3K56ac (Fig. IV.1a), the stoichiometry of H3K56ac monitored by quantitative mass spectrometry was twofold higher than in wild-type cells (Fig. IV.1d, and Supplementary Table IV.1).

We studied the survival of *C. albicans rtt109* and *hst3* mutants treated with genotoxic and antifungal agents. Deletion of both alleles of *RTT109* conferred sensitivity to hydroxyurea and methyl methane sulfonate (Fig. IV.1e). *HST3*+/Δ heterozygous mutants were also sensitive to these agents (Fig. IV.1e). We also tested the susceptibility of these mutants to two families of antifungal agents: azoles (fluconazole) and echinocandins (caspofungin, micafungin). We found that *rtt109*Δ/*rtt109*Δ (*rtt109*Δ/Δ hereafter) and *HST3*+/Δ cells were no more susceptible to fluconazole than wild-type cells, but the *rtt109*Δ/Δ strain was very sensitive to both echinocandins (Fig. IV.1e). Because echinocandins induce oxidative stress (Kelly *et al.* 2009), we tested whether the echinocandin sensitivity of *rtt109*Δ/Δ mutants could be suppressed by antioxidants. The antioxidants N-acetyl-$_L$-cysteine and vitamin C restored viability of *rtt109*Δ/Δ mutant cells

exposed to micafungin (Fig. IV.1e). These results show that genetic perturbation of H3K56ac sensitizes *C. albicans* to genotoxic and antifungal drugs.

H3K56 deacetylation by Hst3p is essential in *C. albicans*

Since we were unable to obtain a homozygous *hst3*Δ/Δ mutant, we generated strains in the CaSS1 background (Roemer *et al.* 2003) in which we deleted one copy of the *HST3* gene and placed the other copy under the control of a promoter that can be repressed with doxycycline (*hst3*Δ/pTET-HST3, Supplementary Methods and Supplementary Fig. IV.2c–e). Addition of doxycycline to *hst3*Δ/*pTET-HST3* cells resulted in a strong decrease in *HST3* mRNA levels and a concomitant increase in H3K56ac (Fig. IV.2a,b). To confirm this result, we isolated histones either before or after doxycycline addition and determined the stoichiometry of modification by mass spectrometry. We found that the fraction of H3 molecules that were Lys56-acetylated increased from 48% to 87% when we treated the *hst3*Δ/*pTET-HST3* strain with doxycycline for 7.5 h (Fig. IV.2c, and Supplementary Table IV.1). The degree of acetylation of other lysine residues in the N-terminal tail of H3 did not increase upon *HST3* repression with doxycycline (Supplementary Table IV.1). To obtain equal amounts of histone H3 for immunoblotting, we needed to load increasing amounts of total proteins as a function of time after doxycycline addition (Fig. IV.2b). Immunoblots of whole-cell lysates from equal numbers of cells confirmed that the levels of both H3 and H4 declined over time following doxycycline addition to *hst3*Δ/*pTET-HST3* cells (Fig. IV.2b). This time-dependent loss of H3 and H4 suggests that *HST3* repression leads to pronounced changes in chromatin structure.

Repression of *HST3* expression with doxycycline severely impaired the growth of *hst3*Δ/*pTET-HST3* cells (Fig. IV.2d). To determine whether repression of *HST3* was fungistatic or fungicidal, we performed colony formation assays after transient doxycycline exposure. We grew tenfold serial dilutions of *hst3*Δ/*pTET-HST3* and control cells in liquid cultures in the presence or absence of doxycycline for 24 h and then transferred the cells to solid medium lacking

doxycycline. We found that the number of colony-forming units in *hst3*Δ/*pTET-HST3* cultures was much lower after a 24 h exposure to doxycycline (Fig. IV.2e) compared to control cells, suggesting that transient *HST3* repression led to cell death. To confirm this, we used propidium iodide staining of nucleic acids as a measure of cell death; live cells are not permeable to propidium ions (Deere *et al.* 1998). Almost all *hst3*Δ/*pTET-HST3* cells killed with heat (65 °C for 30 min) or treated for 24 h with doxycycline stained with propidium iodide (Fig. IV.2f). We also observed that *HST3* repression with doxycycline triggered anomalous filamentous growth (Fig. IV.2f). It was possible that filamentous growth in itself could increase propidium iodide staining, irrespective of cell viability. To rule out this possibility, we grew *hst3*Δ/*pTET-HST3* cells in the absence of doxycycline but under conditions that induce a switch to filamentous growth. We found that the resulting filaments were negative from propidium iodide staining (Fig. IV.2f). These results demonstrate that, unlike in *S. cerevisiae* and *Schizosaccharomyces pombe*, repression of *HST3* in *C. albicans* leads to a loss of cell viability.

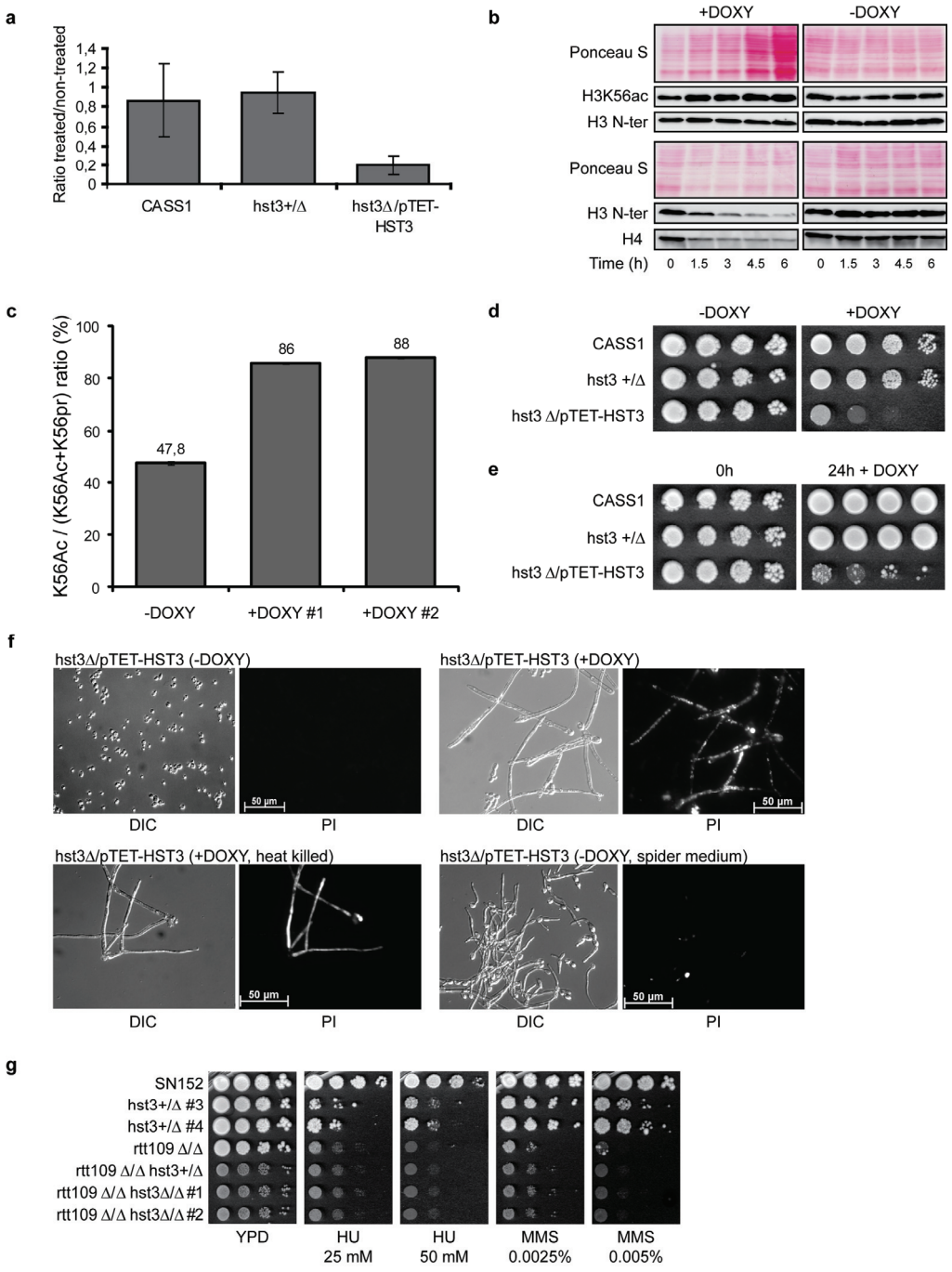

Figure IV. 2 ***HST3*** **controls H3K56 deacetylation and is required for cell viability in** ***C. albicans***

(**a**) Repression of *HST3* mRNA by doxycycline treatment, as measured by quantitative RT-PCR. Results are the mean of three experiments ± s.e.m. (**b**) Immunoblots of lysates from *hst3*Δ/*pTET-HST3* cells treated with doxycycline (+Doxy, 40 µg ml^{-1}) or left untreated (–Doxy). Equal amounts of histone H3 (top) or of total proteins (bottom) were loaded for each time point. (**c**) Stoichiometry of H3K56ac determined by mass spectrometry using histones purified from

*hst3*Δ/*pTET-HST3* cells grown in the absence or presence of doxycycline (duplicates). (**d**) Growth of *hst3*Δ/*pTET-HST3* cells on plates containing doxycycline (50 μg ml^{-1}) or control plates. CASS1, wild-type strain. (**e**) Growth of *hst3*Δ/*pTET-HST3* cells transiently exposed to doxycycline (50 μg ml^{-1}) for 24 h and plated on YPD lacking doxycycline. (**f**) Lethality of *hst3*Δ/*pTET-HST3* cells caused by doxycycline treatment (20 μg ml^{-1} for 24 h), as assayed by fluorescence microsopy after propidium iodide staining. Control cells were either heat-killed or triggered to undergo filamention (spider medium). DIC, Differential interference contrast. PI, Propidium iodide. (**g**) Susceptibility to genotoxic agents of WT (SN152), single (*rtt109*Δ/Δ, *hst3*+/Δ) and double (*rtt109*Δ/Δ *hst3*+/Δ, *rtt109*Δ/Δ *hst3*Δ/Δ) mutants (tenfold serial dilutions), as determined by colony formation assays.

We hypothesized that the high levels of H3K56ac induced by repression of *HST3* were causing cell death. This model predicts that deletion of the *RTT109* acetyltransferase gene should rescue the lethality of the *hst3*Δ/Δ mutant. Consistent with this, we were able to delete both alleles of the *HST3* gene in the *rtt109*Δ/Δ genetic background (Fig. IV.2g, and Supplementary Fig. IV.2f-h). The *rtt109*Δ/Δ *hst3*+/Δ and *rtt109*Δ/Δ *hst3*Δ/Δ mutants are not more susceptible to genotoxic agents than the *rtt109*Δ/Δ strain, although they grow more slowly than either *rtt109*Δ/Δ or *hst3*+/Δ mutants (Fig. IV.2g and Supplementary Fig. IV.2h). These results demonstrate that the lethality of *hst3*Δ/Δ mutants depends upon the *RTT109* gene. Therefore, we conclude that H3 Lys56 hyperacetylation is toxic to *C. albicans* cells and that H3K56ac is a major physiological substrate of *C. albicans* Hst3p.

Under conditions that normally maintain the yeast form of *C. albicans*, *HST3* repression with doxycyline triggered a transition to filamentous growth (Fig. IV. 3a). True hyphae typically lack constrictions at sites of septation and have narrow (~2 μm) parallel cell walls along their entire length (Sudbery *et al.* 2004). In contrast, pseudohyphae have visible constrictions at sites of septation (Sudbery *et al.* 2004). To determine whether *HST3* repression produced true hyphae, we stained *hst3*Δ/*pTET-HST3* cells grown in doxycycline-containing medium with DAPI and calcofluor white to visualize DNA, cell walls and septa. Cells initially

appeared to divide normally, as we observed many budded cells after 3 h of doxycycline treatment (Fig. IV. 3b). After 6 h, we observed pseudohyphae-like cells with septal junctions (Fig. IV.3b). Notably, at later time points (9 and 24 h), most cells appeared as abnormal 'V-shaped' filaments (Fig. IV.3b). In contrast to *HST3* repression, *hst3*Δ/*pTET-HST3* cells in spider medium lacking doxycycline (conditions that preserve *HST3* expression) produced hyphae with parallel-sided, narrow germ tubes and no clear septal junctions (Fig. IV.3a). These features are clearly different from the morphological changes observed after repression of *HST3* (Fig. IV.3b). After 9 h and 24 h of doxycycline treatment, *hst3*Δ/*pTET-HST3* cells showed diffuse or absent DAPI staining (Fig. IV.3b), suggesting that *HST3* repression resulted in DNA fragmentation and degradation. This is consistent with the presence of high levels of spontaneous DNA damage previously reported in *S. cerevisiae hst3*Δ *hst4*Δ mutants (Celic *et al.* 2006). These results indicate that inappropriately high levels of H3K56ac lead to DNA fragmentation, histone H3 and H4 degradation and an anomalous morphological transition that culminate in cell death. Remarkably, all these events occured when the stoichiometry of H3K56ac increased from about 48% to 87% after *HST3* gene repression (Fig. IV.2c and Supplementary Table IV.1). Some of these pronounced phenotypes were not reported in *S. cerevisiae* and *S. pombe* cells that lack H3K56 deacetylases (Celic *et al.* 2006; Haldar *et al.* 2008; Maas *et al.* 2006; Thaminy *et al.* 2007; Xhemalce *et al.* 2007). In addition, we observed that a fraction of *rtt109*Δ/Δ cells (about 10%) spontaneously formed pseudohyphae with abnormal nuclear DNA staining (Supplementary Fig. IV.1g), indicating that tightly regulated levels of H3K56ac are crucial for proper chromatin structure and morphogenesis in *C. albicans*.

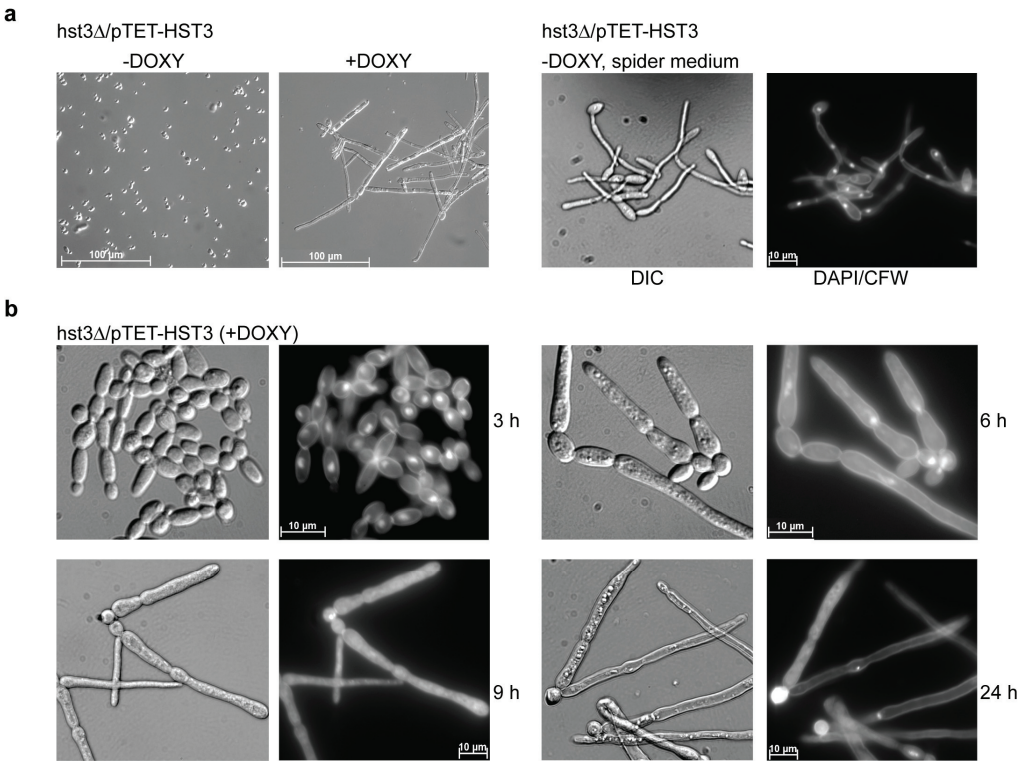

Figure IV. 3 ***HST3*** **repression triggers abnormal changes in cell morphology and DNA staining**

(**a**) Left, differential interference contrast (DIC) images of *hst3Δ/pTET-HST3* cells grown in YPD medium at 30 °C in the absence or presence of doxycycline (20 μg ml^{-1} for 24 h). Right, cells grown in spider medium at 37 °C (hyphae-inducing conditions), stained with DAPI and calcofluor white (CFW) to mark DNA and cell walls, respectively, and visualized by epifluorescence microscopy. (**b**) DIC and epifluorescence images showing the morphology, DNA, septa and cell walls of *hst3Δ/pTET-HST3* cells monitored at various times after doxycycline addition.

Hst3p inhibition with nicotinamide is cytotoxic to *C. albicans*

Hst3p is a member of a family of NAD^+-dependent histone deacetylases known as sirtuins (Supplementary Fig. IV.3). These enzymes are inhibited by nicotinamide, a product of the NAD^+-dependent deacetylation reaction. We reasoned that nicotinamide treatment of *C. albicans* cells should phenocopy *HST3* repression. Addition of nicotinamide to wild-type cells caused an increase in H3K56ac (Fig. IV.4a) and led to robust growth inhibition (Fig. IV.4b,c). Furthermore, growth

inhibition was not observed with nicotinic acid, which does not inhibit Hst3p[1], and was *RTT109*-dependent (Fig. IV.4b,c). This suggests that nicotinamide exerts its effect through inhibition of H3K56 deacetylation. Finally, incubation of wild-type cells for 24 h with nicotinamide triggered the formation of V-shaped filaments with abnormal DNA staining (Fig. IV.4d), similar to those observed in doxycycline-treated *hst3*Δ/*pTET-HST3* cells (Fig. IV.3b).

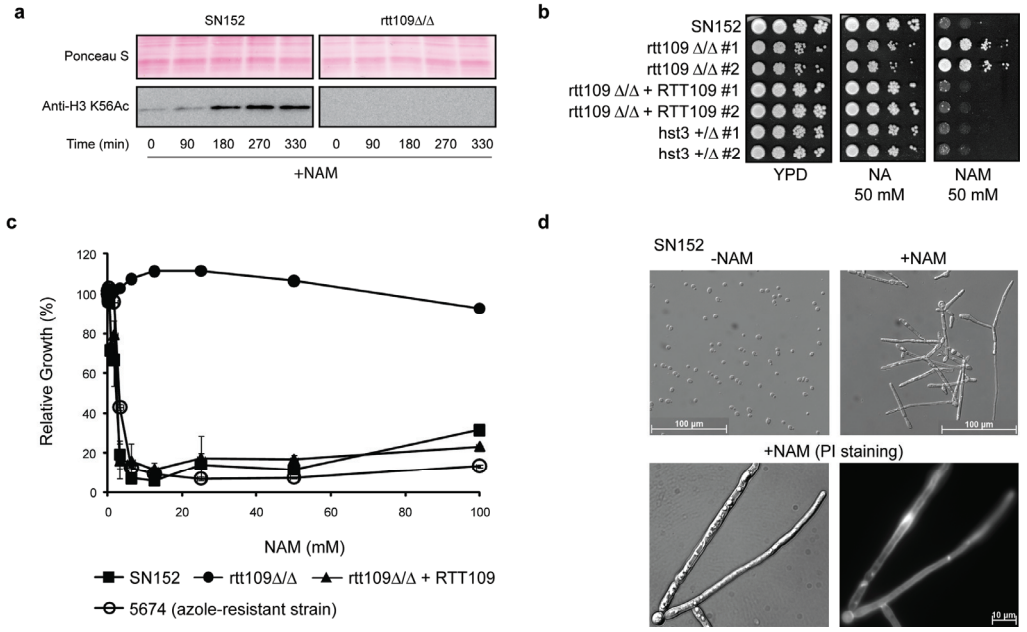

Figure IV. 4 *HST3* repression and nicotinamide are cytotoxic to *C. albicans* strains that express *RTT109*

(**a**) Immunoblots of H3K56ac in wild-type (SN152) and *rtt109*Δ/Δ cells treated with 100 mM nicotinamide (+NAM). (**b**) Colony formation assays performed in the absence (YPD) or presence of either nicotinic acid (NA) or nicotinamide (NAM). (**c**) The growth of each strain (monitored by OD_{620} in a microtiter plate assay) at a given NAM concentration, as plotted as a percentage of its growth in the absence of NAM. (**d**) The effect of NAM on wild-type SN152 cells (50 mM NAM at 30 °C for 24 h), as monitored by DIC and fluorescence microscopy to detect either DNA (DAPI) or cells walls and septa (CFW).

These results prompted us to determine whether other clinically relevant isolates of *C. albicans* and fungal species are susceptible to growth inhibition by

nicotinamide. Several azole- and echinocandin-resistant clinical isolates of *C. albicans* were as sensitive to nicotinamide as a wild-type strain (Figs. IV.4c and IV.5a and Supplementary Fig. IV.4). We also found that other pathogenic *Candida* species were susceptible to nicotinamide. We observed robust growth inhibition of *C. krusei* at 25 mM nicotinamide, whereas growth of *C. tropicalis, C. glabrata* and *C. parapsilosis* was inhibited at higher nicotinamide concentrations (Fig. IV.5b). Nicotinamide also strongly inhibited the growth of *Aspergillus fumigatus* and *Aspergillus nidulans*, which are pathogenic to humans and plants, respectively (Fig. IV.5c). These results demonstrate that nicotinamide has broad antifungal properties.

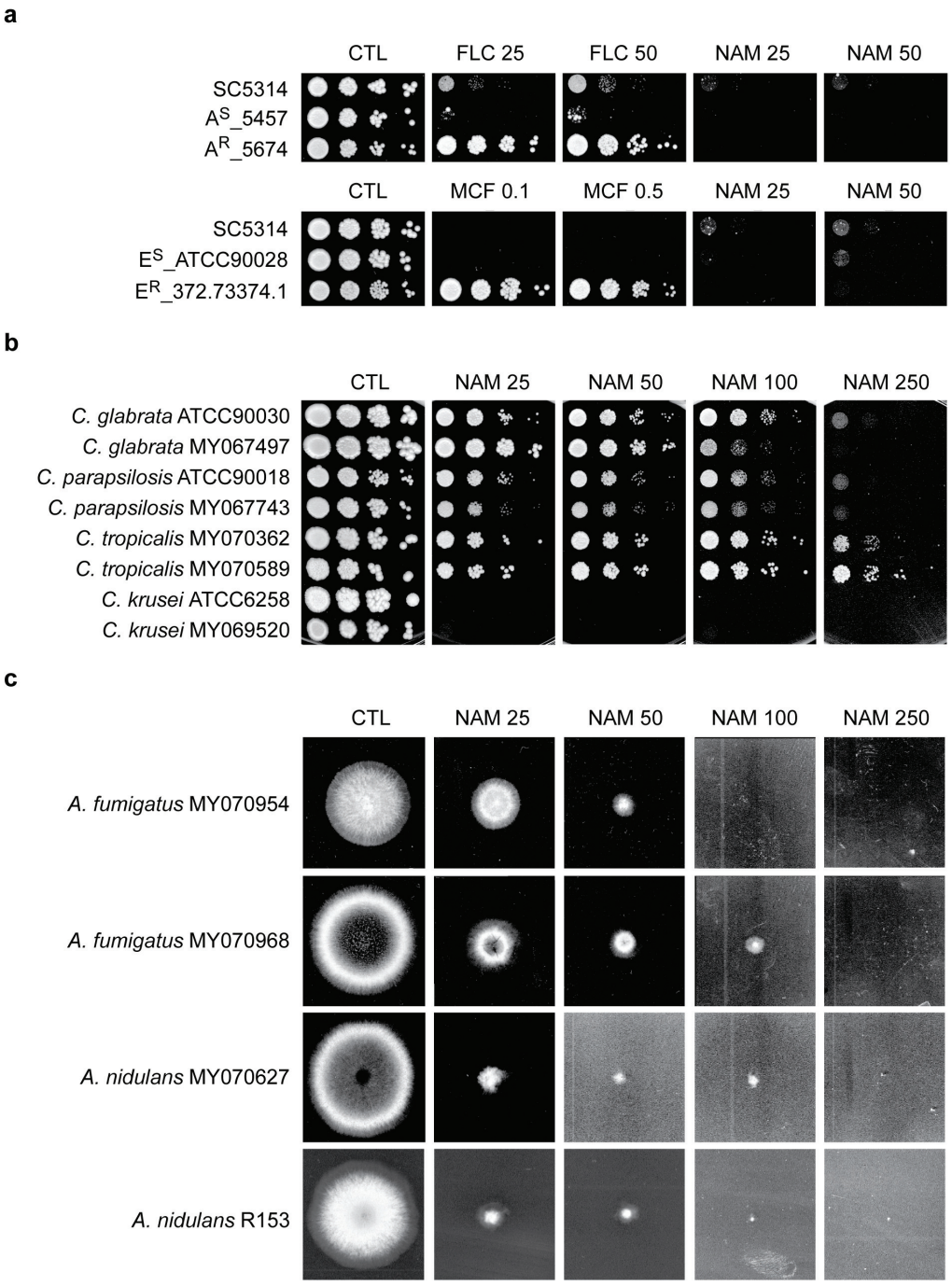

Figure IV. 5 Nicotinamide inhibits growth of several clinically important pathogenic fungi

(**a**) Growth of azole-susceptible (A^S) and azole-resistant (A^R) strains (top) as well as echinocandin-susceptible (E^S) and echinocandin-resistant (E^R) strains (bottom), as tested in colony formation assays. Plates contained fluconazole (FLC; μg ml^{-1}), micafungin (MCF; μg ml^{-1}) or nicotinamide (NAM; mM). Ctl, control plates without NAM or antifugal agent. (**b**) Growth of two independent

strains per *Candida* species on YPD medium containing NAM (mM). (**c**) Growth of two independent *A. fumigatus* or *A. nidulans* strains on complete medium containing NAM (mM).

Modulation of H3K56ac reduces *C. albicans* virulence in mice

We investigated the effect of H3K56ac modulation on *C. albicans* virulence using A/J mice, which are very sensitive to *C. albicans* infection (Mullick *et al.* 2004; Mullick *et al.* 2006). This phenotype results, at least in part, from a deficiency in the C5 component of the complement system (Tuite *et al.* 2005). A/J mice accumulate high fungal loads within 24 h, providing a convenient model to rapidly and accurately measure fungal proliferation *in vivo* (Mullick *et al.* 2006). We first investigated the effect of *HST3* repression on *C. albicans* virulence. A/J mice were injected with wild-type (SC5314 or KTY3) or *hst3*Δ/*pTET-HST3* cells and tetracycline was included in the drinking water of the mice to repress *HST3*. The kidney fungal loads of mice injected with *hst3*Δ/*pTET-HST3* cells were markedly lower than those of mice injected with wild-type strains (Fig. IV.6a). In addition, clinical symptoms typical of a *C. albicans* infection were not visible in mice injected with *hst3*Δ/*pTET-HST3* cells (data not shown). We next determined whether nicotinamide treatment would mimic the effect of *HST3* repression *in vivo.* We gave mice nicotinamide 30 min before and 8 h after infection with *C. albicans*. Nicotinamide greatly lowered kidney fungal loads and clearly alleviated clinical signs of disease progression in mice injected with wild-type cells (Fig. IV.6b). In contrast, nicotinamide failed to protect mice injected with *rtt109*Δ/Δ cells, both in terms of fungal load and in terms of symptoms of candidiasis (Fig. IV.6b). As expected, introduction of a wild-type *RTT109* gene into *rtt109*Δ/Δ cells re-established sensitivity to nicotinamide (Fig. IV.6b). Nicotinamide has been reported to have complex immunomodulatory effects in mammals (Maiese *et al.* 2009). However, under our experimental conditions, nicotinamide had no obvious side effects, as judged by the absence of various inflammation markers (Supplementary Table IV.4) and by careful monitoring of the mice. Furthermore, the fact that the antifungal effect of nicotinamide requires *RTT109*-dependent

H3K56ac firmly establishes that nicotinamide exerts its therapeutic effect through inhibition of Hst3p-mediated H3K56 deacetylation, rather than by enhancing the host immune response. These results indicate that genetic or pharmacological inhibition of Hst3p leads to a loss of virulence in mice.

We also investigated the effect of the *RTT109* deletion on virulence. We injected A/J mice intravenously with wild-type, *rtt109*Δ/Δ or *rtt109*Δ/Δ+*RTT109* revertant cells. At the time of killing (24 h post-infection), only mice injected with wild-type and revertant cells displayed clinical manifestations of advanced candidiasis (data not shown). This prompted us to investigate the effect of *RTT109* deletion on other parameters of *C. albicans* virulence. A/J mice suffer from cardiac dysfunction and accumulate high fungal loads in kidneys and the heart (Mullick *et al.* 2006). We found reduced fungal loads in the heart and kidneys of mice infected with *rtt109*Δ/Δ as compared with wild-type or revertant cells (Fig. IV.6c**)**. We also observed that, compared with wild-type and revertant strains, the *rtt109*Δ/Δ mutant elicited a weaker inflammatory response in A/J mice, as evidenced by significantly lower amounts of interleukin-6, a key pro-inflammatory cytokine, and keratinocyte-derived chemokine, which is crucial for granulocyte recruitment (Fig. IV.6d). These results show that loss of Rtt109p reduces the virulence of *C. albicans* in A/J mice.

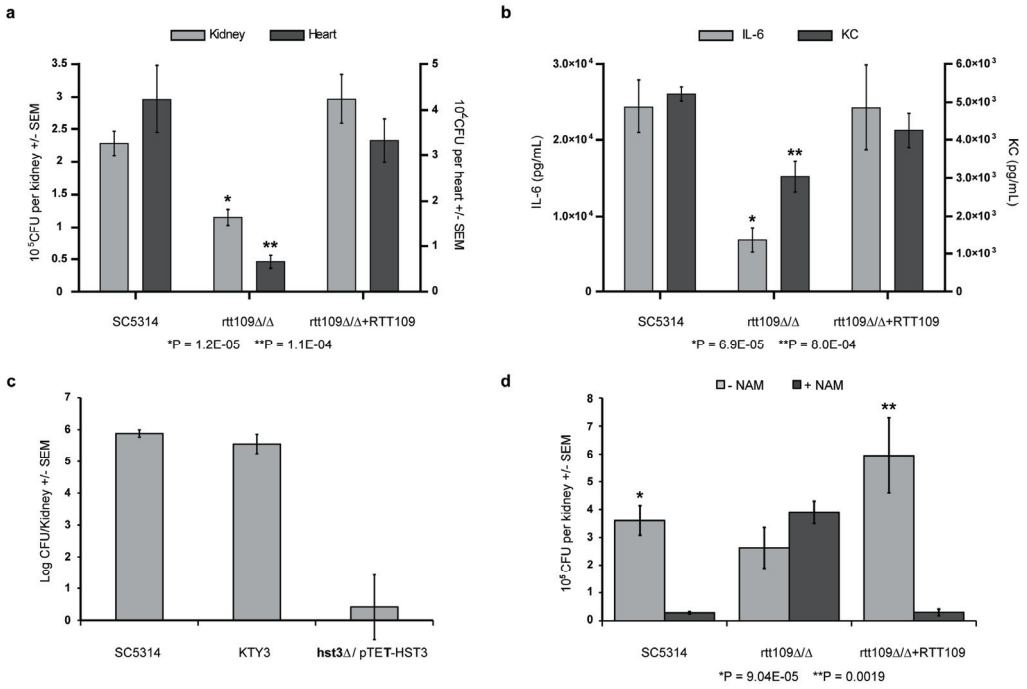

Figure IV. 6 Modulation of H3K56ac levels reduces virulence in a mouse model of *C. albicans* infection

(**a**) Kidney fungal loads (CFU, colony forming units) of A/J mice injected with 5×10^4 cells of each strain. Mice were given tetracycline in their drinking water to repress the *pTET-HST3* allele. SC5314 and KTY3 are two distinct wild-type strains. (**b**) Kidney fungal loads of A/J mice injected with 3×10^5 cells of each strain. Mice were injected with nicotinamide 30 min before and 8 h after *C. albicans* infection. *P* values for two-tailed Student's *t*-test are indicated for comparison of fungal loads in NAM-treated and untreated mice. (**c**) Kidney and heart fungal loads of A/J mice injected with 3×10^5 cells of each strain. *P* values for two-tailed Student's *t*-test are indicated for comparison of fungal loads in mice injected with *rtt109*Δ/Δ versus SC5314 WT cells. (**d**) Cytokine levels in the blood of the mice described in **c**. *P* values for two-tailed Student's *t*-test are indicated for comparison of cytokine levels in mice injected with *rtt109*Δ/Δ versus SC5314 WT cells. IL-6, Interleukin-6. KC, keratinocyte-derived chemokine.

IV.3 Discussion

Two major classes of chemicals are commonly used to treat candidiasis: azoles and echinocandins. However, the emergence of strains that are resistant to these agents requires the development of novel approaches of clinical intervention. In this report, we have identified two enzymes as attractive novel therapeutic targets to treat *C. albicans* infections and possibly those caused by other pathogenic fungi. These enzymes, Rtt109p and Hst3/Hst4p, respectively acetylate and deacetylate histone H3K56 in *C. albicans*, *S. cerevisiae* and *S. pombe* (Celic *et al.* 2006; Driscoll *et al.* 2007; Haldar *et al.* 2008; Han *et al.* 2007; Maas *et al.* 2006; Thaminy *et al.* 2007; Tsubota *et al.* 2007; Xhemalce *et al.* 2007), and potential orthologs exist in several other pathogenic fungi. In *C. albicans*, disruption of the *RTT109* gene conferred acute sensitivity to two distinct echinocandin family members, and this sensitivity was suppressed by antioxidants. Given that *RTT109* mutations render *C. albicans* and other yeasts sensitive to genotoxic agents that impede DNA replication (Driscoll *et al.* 2007; Haldar *et al.* 2008; Han *et al.* 2007; Tsubota *et al.* 2007; Xhemalce *et al.* 2007), it seems likely that the marked echinocandin sensitivity of *rtt109* mutants arises from oxidative damage to DNA (Dizdaroglu 2005). Deletion of *RTT109* also leads to pseudohyphae formation and reduces the growth rate of *C. albicans* in rich medium. Concordant with this, we found that *rtt109*Δ/Δ mutants are less virulent than wild-type *C. albicans* cells in the A/J mouse model. Given these results, Rtt109p inhibitors would be expected to enhance the cytotoxicity of echinocandins and reduce the virulence of *C. albicans*. CREB-binding protein (CBP) and p300 acetylate H3K56 and other substrates in human cells (Das *et al.* 2009; Wang *et al.* 2008). Despite similarities in their polypeptide backbones suggesting an ancestral relationship, the catalytic cores, catalytic mechanisms, and substrate specificity of yeast Rtt109p and human p300/CBP are vastly different (Wang *et al.* 2008). Therefore, it is likely that chemical library screens could identify specific inhibitors of Rtt109p that do not affect human p300/CBP.

We found that repression of the *C. albicans HST3* gene is lethal even in the absence of antifungal agent. In A/J mice, Hst3p inhibition by gene repression or nicotinamide treatment considerably reduced *C. albicans* proliferation and clinical manifestation of candidiasis. Nicotinamide is a vitamin that serves as a precursor of NAD^+. It is well tolerated and used systemically to treat pellagra and skin lesions (Bogan *et al.* 2008; Niren 2006). Despite its beneficial effects, complex immunomodulatory effects of nicotinamide have been reported in mammalian cells (Maiese *et al.* 2009). This suggested that the ability of nicotinamide to curtail *C. albicans* infection might be due to an enhanced immune response of the host. However, three lines of evidence firmly establish that the main therapeutic effect of nicotinamide is exerted through inhibition of Hst3p, thus blocking H3K56 deacetylation. First, nicotinamide is not cytotoxic to *C. albicans* cells lacking Rtt109p and H3K56ac. Second, the antifungal property of nicotinamide in A/J mice depends on the presence of the *RTT109* gene. Third, as judged by the absence of various inflammation markers, short-term nicotinamide treatment has no obvious immunomodulatory effects under our experimental conditions.

There are sound biochemical arguments to suspect that selective inhibitors of Hst3p may not have major side effects in humans. Despite the fact that sirtuin-1 (SIRT1) and SIRT2 have been implicated in H3K56 deacetylation in human cells (Das *et al.* 2009; Yuan *et al.* 2009), there are sequence motifs conserved among fungal Hst3p family members that are absent from human sirtuins (Frye 2000). For instance, differences occur in the peptide binding channel of sirtuins (Cosgrove *et al.* 2006). Unlike human SIRT1 and SIRT2 (Blander *et al.* 2005; Garske *et al.* 2006; Saunders *et al.* 2007), Hst3p seems to be highly substrate-specific. In *S. cerevisiae* (Celic *et al.* 2006) or *C. albicans* (Supplementary Table IV.1), acetylation of several sites in the N-terminal tails of H3 or H4 does not increase in the absence of Hst3/Hst4p. Hence, it is conceivable that small molecules that specifically block the deacetylase activity of fungal Hst3p orthologs, without affecting human sirtuins, might be identified. Indeed, small

molecules that inhibit even closely related sirtuins with high selectivity have been identified by screening chemical libraries (Hirao *et al.* 2003).

We determined the sensitivity to nicotinamide of a broad spectrum of fungal species. All the *C. albicans* clinical isolates tested, including azole- and echinocandin-resistant strains, were very sensitive to nicotinamide. This is clinically important because, among the numerous species that cause candidiasis, *C. albicans* is responsible for the majority of cases (Pfaller *et al.* 2010) and frequently develops resistance to azoles and echinocandins (Akins 2005; Perlin 2007). The non-*albicans Candida* strains that we tested displayed various degrees of sensitivity. The strong sensitivity of *C. krusei* to nicotinamide is of particular interest, because *C. krusei* is intrinsically resistant to many antifungal drugs (Pappas *et al.* 2009). We also found that two different *Aspergillus* species, *A. fumigatus* and *A. nidulans*, were very sensitive to nicotinamide. This is noteworthy because *A. fumigatus* causes the second most common invasive mycoses in humans, after candidiasis (Dagenais *et al.* 2009). Our data thus support the notion that nicotinamide or future fungal-specific sirtuin inhibitors may prove useful to treat various fungal infections and provide a solid physiological and molecular basis for the development of novel antifungal agents that inhibit the enzymes that regulate H3K56ac. Although further *in vivo* studies will be necessary to assess the true therapeutic potential of nicotinamide and related chemicals, our results constitute a proof of principle that this strategy represents a useful therapeutic avenue.

IV.4 Acknowledgements

We are grateful to T. Roemer (Merck Research Laboratory) for providing strain CaSS1 and plasmids pHIS3 and pSAT-Tet, G. St-Germain (Laboratoire de santé publique du Québec) for strains MY067497, MY067743, MY070362, MY070589, MY069520, MY070954, MY070968 and MY070627, C. Restieri and M. Laverdière (Hôpital Maisonneuve-Rosemont) for strain 372.73374.1, C. Bachewich (Concordia University) for strain R153 and T. Edlind (Drexel University College of Medicine) for strain 20464. We are indebted to T. Roemer and M. Whiteway for critical reading of the manuscript. We thank F. Malenfant, J. Leroy, M. Mercier and P. Liscourt for excellent assistance in mouse handling. We are also grateful for the availability of the *Candida* Genome Database. This work was supported by research grants from the Canadian Institutes of Health Research to M.R. (CTP-79843, III-94587), A.M. (CTP-79843) and A.V. (CTP-79392) and from the National Science and Engineering Research Council of Canada to P.T. (STGP-322143-05). This is National Research Council of Canada publication number 52756. The Institute for Research in Immunology and Cancer is supported by funds from the Canadian Center of Excellence in Commercialization and Research, the Canadian Foundation for Innovation, and the Fonds de la Recherche en Santé du Québec.

IV.5 Author contributions

H.W. and S.T. designed and performed most experiments; G.L. constructed the yeast strains used in this study; J.T. and S.T. performed the fungal load and cytokine analyses; A.M. and M.R. designed and supervised the animal studies; P.D., P.T. and A.V. designed and performed mass spectrometry experiments; E.H.L. provided technical support; all authors participated in manuscript preparation; M.R. and A.V. supervised the study.

IV.6 Competing financial interests

The authors declare no competing financial interests.

IV.7 Methods

Strain construction. Detailed methodologies for genetic manipulations, Southern blot and northern blot analyses are presented in the Supplementary Methods. The *C. albicans* strains constructed in this study are listed in Supplementary Table IV.2, and the primers used for their construction are shown Supplementary Table IV.3. The molecular characterization of the mutant strains is described in detail in the Supplementary Results.

Immunoblots. We prepared whole-cell extracts for SDS-PAGE by an alkaline method (Kushnirov 2000) or a glass bead method (Xhemalce *et al.* 2007). Antibodies against H3K56ac (AV105), the H3 N-terminal domain (AV71/72) and recombinant *S. cerevisiae* histone H4 (AV 94) have been previously described (Gunjan *et al.* 2003; Masumoto *et al.* 2005; Xhemalce *et al.* 2007).

Identification of H3 K56 acetylation by mass spectrometry. We isolated histones from *C. albicans* as previously described for *S. cerevisiae* (Poveda *et al.* 2004). Acid-extracted histones were further purified by reverse phase HPLC (Drogaris *et al.* 2008). Nano liquid chromatography-tandem mass spectrometry analyses of H3 tryptic peptides with multiple reaction monitoring (MRM) were performed on an AB/MDS Analytical Technologies 4000 Q-Trap mass spectrometer equipped with a Nanospray II interface. We injected samples in triplicate, using multiple reaction monitoring for relative quantification.

RT-PCR. We extracted total RNA from 2×10^7 cells by the hot phenol method (Schmitt *et al.* 1990). One microgram of total RNA was reverse-transcribed to

cDNA with the SuperscriptIII reverse transcriptase enzyme (Invitrogen). Quantitative PCR was performed in triplicate with a SYBR green master mix containing Jumpstart Taq DNA polymerase (Sigma) and SYBR green nucleic acid stain (Invitrogen). We performed quantitative PCR on a Step One qPCR instrument (Applied Biosystems). Results were normalized to the *ACT1* gene signal. The Supplementary Methods contain primer sequences.

Drug susceptibility assays. We performed spot and liquid microtiter plate assays as described previously (Tsao *et al.* 2009). We monitored cell growth after 48 h of incubation at 30 °C, unless otherwise specified. We purchased genotoxic and antifungal drugs from Sigma unless otherwise stated. Caspofungin was a gift from Merck Frosst Canada and micafungin was purchased from Astellas Pharma Canada.

Microscopy. We performed DIC and epifluorescence microscopy with a Zeiss Axio-Imager Z1 microscope. Image analysis was carried out with the Zeiss AxioVision 4.8 software. DAPI staining of DNA, CFW staining of cell walls and septa and propidium iodide staining of dead cells were performed as previously described (Trunk *et al.* 2009).

***In vivo* disseminated candidiasis model.** Eight to twelve week old A/J mice were purchased from The Jackson Laboratories. Housing and all experimental procedures were approved by the Biotechnology Research Institute Animal Care Committee, which operates under the guidelines of the Canadian Council of Animal Care. To turn off the expression of the *HST3* gene (Fig. IV.6a), 5% sucrose and 2 mg ml^{-1} tetracycline were added to the drinking water of the mice 3d before infection with *C. albicans*. Inoculums of the *C. albicans* strains were grown overnight in YPD medium. Mice were injected via the tail vein with 3×10^5 blastospores, except for the conditional repression of *HST3* with tetracycline (Fig. IV.6a), where a lower dose was used (5×10^4 blastospores) to allow time for tetracycline to act. Mice were closely monitored for clinical symptoms of

candidiasis such as lethargy, hunched back and ruffled fur. Mice showing extreme lethargy were deemed moribund and were killed by exsanguination. This was typically performed at 24 h and 48 h post-injection for 3×10^5 and 5×10^4 *C. albicans* blastospores, respectively. For determination of fungal load, kidneys and hearts were homogenized in PBS and appropriate dilutions were plated on Sabouraud broth-agar plates. For the *in vivo* nicotinamide treatments (Fig. IV.6b), mice (six per treatment) were injected intraperitoneally with PBS containing nicotinamide (500 mg per kg body weight) 30 min prior to the *C. albicans* infection, as it takes 20-30 min for the nicotinamide concentration to peak in the blood stream (Horsman 1997). A second dose of nicotinamide was injected 8 h after *C. albicans* infection to maintain high nicotinamide concentrations in circulation.

Cytokine analysis. We collected mouse blood in 1.1 ml Z-gel microtubes (Sarstedt), and samples were processed as recommended by the manufacturer. To determine the levels of cytokines in circulation, we analyzed sera (12.5 μl) using the BD CBA Flex sets (BD BioSciences) according to the manufacturer's instructions. Fluorescence levels were recorded using the BD LSRII and data analysis was carried out using the FCAP Array software (BD BioSciences).

Statistical analysis. Statistical comparisons used two-tailed Student's *t*-test (kidney and heart fungal load estimations and cytokines analyses). Error bars are expressed as the s.e.m.

Additional methods. Detailed methodology is described in the **Supplementary Methods**.

IV.8 Supplementary information

Modulation of Histone H3 Lysine 56 Acetylation
as a Novel Antifungal Therapeutic Strategy

Hugo Wurtele, Sarah Tsao, Guylaine Lépine, Alaka Mullick,
Jessy Tremblay, Paul Drogaris, Eun-Hye Lee, Pierre Thibault,
Alain Verreault, Martine Raymond

IV.9 Supplementary methods

Strains and culture conditions

The *C. albicans* strains used in this study are listed in Supplementary Table IV.2 and Supplementary Fig. IV.4a. *C. albicans* cells were grown routinely at 30 ^{o}C in YPD (1% yeast extract, 2% Bacto Peptone and 2% glucose) or SD medium (0.67% Difco nitrogen base, 2% glucose and a mixture of amino acids), including 2% agar for solid media. We used spider medium to induce hyphae formation (1% Difco nutrient broth, 2% glucose and 0.2% K_2HPO_4). For *Tet* promoter repression, an overnight YPD culture was diluted into fresh YPD medium containing 20-50 μg ml^{-1} of doxycycline (Sigma) at an optical density at 600 nm (OD_{600}) of 0.005 and grown for 24 h unless otherwise indicated (Trunk *et al.* 2009). *Escherichia coli* DH10B cells were used for DNA cloning procedures. *E. coli* cells were grown in Luria-Bertani (LB) medium to which chloramphenicol (34 μg ml^{-1}) was added when required. The *C. glabrata*, *C. parapsilosis*, *C. tropicalis*, and *C. krusei* strains (Fig. IV.5b and Supplementary Fig. IV.4a) were grown as described above for *C. albicans*. The *Aspergillus* strains (Fig. IV.5c and Supplementary Fig. IV.4a) were grown on complete medium (CM) plates (0.1% yeast extract, 0.2% Bacto Peptone, 1% glucose, 0.15% casamino acids, 0.6% $NaNO_3$, 0.05% KCl, 0.05% $MgSO_4 \cdot 7H_2O$, 1% Vitamin stock solution (http://www.fgsc.net/), pH 6.8 and 2% agar).

Deletion of the *RTT109* or *HST3* genes in *C. albicans* strain SN152

The *RTT109*- or *HST3*-deletion strains were constructed using a PCR-based deletion approach (Wilson *et al.* 1999) (see Supplementary Table IV.3 for the list of primers). The deletion cassettes were constructed to carry the *HIS1* or *ARG4* markers flanked by 120-bp sequences from the upstream and downstream regions of the targeted gene (*RTT109* or *HST3*). The *HIS1*-containing amplicon was used to transform *C. albicans* strain SN152 using the standard lithium acetate protocol with minor modifications as previously described (Trunk *et al.* 2009). To disrupt the second *RTT109* allele, two independently selected His^{+} transformants carrying

a properly deleted allele, as determined by Southern blotting, were transformed with the *ARG4*-containing amplicon to generate two independent gene deletion strains.

Construction of *RTT109* revertants

Plasmid pSFS2A containing the *SAT1-FLP* cassette was used to construct the *RTT109* revertant (Reuss *et al.* 2004; Tsao *et al.* 2009). A PCR-amplified SN152 DNA fragment located downstream of *RTT109* (+1,204 to +1,740) was cloned into the *Xho*I-*Apa*I sites of plasmid pSFS2A, creating pRTT109$_{down}$. Next, a PCR-amplified fragment containing the *RTT109* open reading frame (ORF, +1 to +1,080 from ATG) as well as its upstream (-800 to -1 bp upstream of the ATG) and downstream (+1,081 to +1,740 from the ATG) regions was cloned into the *Sac*II-*Not*I sites of plasmid pRTT109$_{down}$, resulting in pRTT109$_{rev}$. The 7.3-kb *Apa*I-*Apa*I *RTT109-SAT1* fragment derived from pRTT109$_{rev}$ (Supplementary Fig. IV.1b) was used to transform the *rtt109*Δ/Δ#1 strain. Selection of the integrants was performed on YPD supplemented with 200 mg ml^{-1} of nourseothricin (Werner BioAgents, Jena, Germany).

Construction of a conditional *hst3* mutant

Conditional mutants of the *HST3* gene were constructed in the *C. albicans* CaSS1 strain (Supplementary Table IV.2 and Supplementary Fig. IV.2c-e) which expresses a tetracycline-dependent transactivation fusion protein (TetR-ScGal4AD) (GRACE technology) as described previously (Roemer *et al.* 2003; Trunk *et al.* 2009). His^{+} heterozygote mutants for *HST3* were constructed using a PCR-generated deletion cassette containing a *HIS3* selectable marker flanked by *HST3* upstream (positions -1 to -120 upstream of the ATG) and downstream (+1,465 to +1,584 downstream of the ATG) sequences. The resulting amplicon was transformed into *C. albicans* strain CaSS1 (Roemer *et al.* 2003) which was then plated on medium without histidine and incubated at 30 °C for 2 days. His^{+} clones were screened by colony PCR and analyzed by Southern blotting. The endogenous promoter (from -3 to -250 bp upstream of the ATG) of the remaining

HST3 allele was replaced in the *HST3/hst3*Δ heterozygote with a repressible tetracycline promoter (Roemer *et al.* 2003). The PCR-generated *Tet* promoter cassette containing the *SAT1* dominant selectable marker flanked by sequences homologous to *HST3* (-251 to -370 upstream of the ATG and -4 usptream of the ATG to +116 downstream of the ATG) was amplified from the template plasmid pSAT-Tet (Roemer *et al.* 2003; Trunk *et al.* 2009). The amplicon was transformed as described above into the *HST3/hst3*Δ heterozygote. The resulting integrants were selected on YPD medium supplemented with 200 μg ml^{-1} of nourseothricin (Werner BioAgents, Jena, Germany) and tested by colony PCR and Southern blotting. To repress the *Tet* promoter of the *HST3*D*/pTET-HST3* strain, an overnight culture in YPD was diluted into fresh YPD medium containing 20 μg ml^{-1} of doxycycline (Sigma) (Roemer *et al.* 2003; Trunk *et al.* 2009) at an initial OD_{600} of 0.005 and the cells were grown overnight.

Deletion of the *HST3* gene in the *C. albicans rtt109*Δ/Δ#1 strain

The *rtt109*Δ/Δ *hst3*Δ/Δ strains were also constructed using a PCR-based deletion approach (Wilson *et al.* 1999) (see Supplementary Table IV.3 for the list of primers and Supplementary Fig. IV.2f-h). The deletion cassettes were constructed to carry the *LEU2* marker amplified from plasmid pSN40 (Noble *et al.* 2005) or the *SAT1* marker from pSFS2A (Reuss *et al.* 2004). Both cassettes contained 120-bp sequences from the upstream and downstream regions of *HST3*. The *LEU2*-containing amplicon was used to transform *C. albicans* strain *rtt109*Δ/Δ#1 by electroporation as previously described (Tsao *et al.* 2009). A selected Leu^+ heterozygote shown by colony PCR to have the correct *rtt109*Δ/Δ *HST3*+/Δ genotype was electrotransformed with the *SAT1* cassette. The resulting transformants were selected on YPD medium supplemented with 200 μg ml^{-1} of nourseothricin (Werner BioAgents, Jena, Germany) and tested by colony PCR. Clones carrying the correctly disrupted alleles with *LEU2* and *SAT1* were then grown overnight in YP medium supplemented with 2% maltose to loop out the *SAT1* cassette, leaving only the *FRT* sequence. As controls, the *C. albicans* strain SN152 was also transformed as described above by electroporation with the *LEU2*

cassette or the *SAT1* cassette followed by a loop-out. The resulting double *rtt109*Δ/Δ *hst3*Δ/Δ strains and the SN152 derivatives used for their construction were tested by Southern analysis.

Southern and Northern blots

C. albicans genomic DNA (gDNA) was purified using the glass-bead method(Hoffman *et al.* 1987). Total RNA was extracted using the hot phenol method (Schmitt *et al.* 1990). Southern and Northern blots were performed as previously described (Saidane *et al.* 2006). Probes for Southern and Northern analyses were generated by PCR amplification (Supplementary Table IV.3).

Immunoblots

Whole-cell yeast extracts were prepared for SDS–polyacrylamide gel electrophoresis using an alkaline method (Kushnirov 2000) or a glass bead method (Xhemalce *et al.* 2007). Briefly, cells in exponential phase were harvested and resuspended in 100 µl of TE buffer (50 mM Tris-HCl pH 7.5 and 1.5 mM EDTA) containing protease inhibitors (1 mM phenylmethylsulfonyl fluoride and 5 µg ml^{-1} each of leupeptin, pepstatin and aprotinin). Cells were disrupted by vortexing in the presence of glass beads (5 cycles of 1 min vortex followed by 1 min cooling on ice). Total protein extracts were harvested by centrifugation. Antibodies against H3K56ac (AV105), the H3 N-terminal domain (AV71/72) and recombinant *S. cerevisiae* histone H4 (AV 94) have been previously described (Gunjan *et al.* 2003; Masumoto *et al.* 2005; Xhemalce *et al.* 2007).

RT-PCR

Total RNA was extracted from 2×10^7 cells using the hot phenol method (Schmitt *et al.* 1990). One microgram of total RNA was reverse-transcribed to cDNA using the SuperscriptIII reverse transcriptase enzyme and random primers (Invitrogen) according to the manufacturer's protocol. Quantitative PCR was performed on 1/20 of the cDNA preparation in triplicate using a SYBR green

master mix containing Jumpstart Taq DNA polymerase (Sigma) and SYBR green nucleic acid stain (Invitrogen). Quantitative PCR was performed on a Step One qPCR instrument (Applied Biosystems Inc.). Results were normalized to the *ACT1* gene signal. See Supplementary Table IV.3 for primer sequences.

Identification of H3 K56 acetylation by mass spectrometry

Histones were isolated from *C. albicans* as previously described for *S. cerevisiae* (Poveda *et al.* 2004). Acid-extracted histones were further purified by reverse phase HPLC (Drogaris *et al.* 2008). Fractions containing histone H3 were pooled, evaporated in a Speed-Vac and resuspended in 0.1 M ammonium bicarbonate. After derivatization with deuterated acetic anhydride, tryptic digests were loaded onto a 4 mm length, 360 µm i.d. trap column and separated using a 10 cm length, 150 µm i.d. analytical column packed in-house with 3 µm C_{18} particles (Jupiter 300 Å, Phenomenex, Torrance, CA) (Drogaris *et al.* 2008). The mobile phases consisted of 0.2% formic acid in water (solvent A) and 0.2% formic acid in acetonitrile (solvent B). The pump flow rate was set to 0.6 ml min^{-1} and peptide elution was achieved using a linear gradient of 5 to 40% B for the first 65 min followed by a rapid increase to 80% B for the next 3 min. Nano LC-MS/MS analyses of H3 tryptic peptides using multiple reaction monitoring (MRM) were performed on an AB/MDS Analytical Technologies 4000 Q-Trap mass spectrometer (Thornhill, ON, Canada) equipped with a Nanospray II interface. MRM transition pairs were monitored to detect the *in vivo* K56-acetylated tryptic peptide (*m/z* 638.9 → 831.5, 638.9 → 1001.6) and the peptides K56-acetylated *in vitro* with deuterated acetic anhydride (*m/z* 640.3 → 831.5 and 640.3 → 1004.6) or propionic anhydride (*m/z* 645.9 → 831.5 and 645.9 → 1015.6). Peptide sequences were confirmed by the MIDAS strategy with MRM triggering an enhanced product ion (EPI) scan in data dependant mode. Samples were injected in triplicate using MRM only for relative quantitation. A 10-ms dwell time was applied to each unique histone peptide ion MRM transition; tryptic peptides were eluted from the HPLC column using the conditions specified above.

Accurate determination of the stoichiometry of H3 acetylation at specific lysine residues

250 µl of protein A-Sepharose beads (GE healthcare) were incubated with 300 µg of affinity-purified antibody against the N-terminal domain of yeast H3 (AV71/72) for 1 h at 4 ºC in 10 mM Tris-HCl pH 8.0. The antibody beads were then washed three times with the same buffer. *C. albicans* cells (1 ml cell pellet) were resuspended in 1 ml of lysis buffer (100 mM Tris-HCl pH 8.0, 200 mM NaCl, 1X EDTA-free complete protease inhibitor cocktail (Roche), 100 mM sodium butyrate, 10 µM trichostatin A, 100 mM nicotinamide, 1 mM dithiothreitol) and lysed using a 6850 Freezer Mill (SPEX certiprep). The cell lysates were then incubated in the presence of 200 µg ml^{-1} of ethidium bromide for 30 min on ice to force histone dissociation from DNA. After two brief (5-10 seconds) pulses of sonication, the cell lysates were centrifuged at 13,000 rpm and 4 ºC for 15 min in a tabletop centrifuge (Heraeus Multifuge 3S-R). The supernatant was mixed with 50 µl of H3 antibody beads and incubated overnight at 4 ºC. The beads were washed five times in wash buffer (100 mM Tris-HCl pH 8.0, 100 mM NaCl), resuspended in 1X SDS-PAGE sample buffer and boiled for 5 min to elute bound proteins. Protein samples were resolved in an SDS-15% polyacrylamide gel (29:1 acrylamide:N,N`-methylene bisacrylamide molar ratio), which was stained with Bio-Safe Coomassie G-250 stain (Bio-Rad) and destained overnight in water. The band corresponding to *C. albicans* H3 was then cut from the gel for mass spectrometry (MS).

We found that *in vitro* acetylation with deuterated acetic anhydride (see above) or propionylation of non-modified H3K56 did not appreciably influence the stoichiometry of H3K56 acetylation determined experimentally. Therefore, the *in vivo* stoichiometry of H3K56 acetylation can be determined accurately with both methods. Gels bands were destained using deionized (DI) water, 50:50 DI water: acetonitrile (I), and pure I. The bands were washed and resuspended in a 0.1 M ammonium bicarbonate (Ambic) solution (pH 8.0). A propionic anhydride reagent (2:1 PA:water) was added to the bands in a 1:1 volume ratio and

incubated for 1 h at room temperature with shaking. The buffer and derivatization mixture was replaced with fresh reagents to perform a second propionylation reaction for 1 h. After removing excess reagent, the bands were washed with a 0.1 M Ambic solution, and evaporated to dryness in a Speed-vac. Rehydration with 0.1 M Ambic was followed by the addition of 1 μg of trypsin and overnight protein digestion. The digest supernatant was placed in a separate Eppendorf tube. Peptides were extracted twice with a 50:50 DI water:I solution containing 5 % TFA (v:v:v). The bands were incubated for 15 min at room temperature with shaking. The two solutions for peptide extraction were recovered, combined with the original tryptic digest supernatant, and evaporated to dryness in a Speed-Vac. Peptides were dissolved in the initial mobile phase (95:5 DI water:I, 0.2% formic acid (v:v:v) prior to injection onto the, 4000 Q-Trap mass spectrometer.

Precursor – product ion pairs corresponding to the following MRM transitions were monitored (Ac, acetylation; Pr, propionylation of e-amino group):
A) H3 peptide 54-FQK(Ac)STELLIR-63: *m/z* 638.9 → 1001.6
B) H3 peptide 54-FQK(Pr)STELLIR-63: *m/z* 645.9 → 1015.6
C) H3 peptide 18-K(Ac)QLASK(Pr)AAR-26: *m/z* 535.8 → 772.5
D) H3 peptide 18-K(Pr)QLASK(Ac)AAR-26: *m/z* 535.8 → 758.5
E) H3 peptide 18-K(Ac)QLASK(Ac)AAR-26: *m/z* 528.8 → 758.5
F) H3 peptide 18-K(Pr)QLASK(Pr)AAR-26: *m/z* 542.8 → 772.5
H) H3 peptide YK(Pr)PGTVALR, a non-modified peptide used for normalization of H3 quantities in each gel band and for fluctuations in the MS response: *m/z* 530.8 → 713.4

First, the abundance for each peptide MRM transition (A to F) was normalized to the ion abundance of the non-modified peptide transition (H). These normalized values (An to Fn) were then used to calculate the stoichiometry of acetylation at each lysine residue as follows.

$$\%H3K56ac = 100 \times An / (An + Bn)$$

$$\%H3K18ac = 100 \times (Cn + En) / (Cn + Dn + En + Fn)$$

$$\%H3K23ac = 100 \times (Dn + En) / (Cn + Dn + En + Fn)$$

Drug susceptibility assays

Spot assays were performed as described previously (Tsao *et al.* 2009). Cells were grown overnight in YPD at 30 ºC and diluted to an OD_{600} of 0.1. Ten-fold serial dilutions of each strain were spotted onto drug-containing YPD plates. For the *Aspergillus* plate assay (Fig. IV.5c), cells were thawed from -80 °C glycerol stocks onto CM plates and grown for 3-4 days at 30 °C. Spores were then transferred with a toothpick onto NAM-containing CM plates and incubated at 30 °C for 3 days. Genotoxic and antifungal drugs were purchased from Sigma unless otherwise stated. Caspofungin (CSF) was a gift from Merck Frosst Canada and micafungin (MCF) was purchased from Astellas Pharma Canada. Liquid microtiter plate assays were performed as described previously (Tsao *et al.* 2009). Sensitivity to nicotinamide in liquid YPD cultures was measured by monitoring cell growth spectrophotometrically at an OD_{620} after 48 h of incubation at 30 ˚C.

Morphological observations

Microscopy was performed by differential interference contrast (DIC) and epifluorescence microscopy with a Zeiss Axio-Imager Z1 microscope. Image analysis was carried out with the Zeiss AxioVision 4.8 software. DAPI staining of DNA, calcofluor white (CFW) staining of cell walls and septa, and propidium iodide staining of dead cells were performed as previously described (Trunk *et al.* 2009).

In vivo disseminated candidiasis model

Eight to twelve week old A/J mice were purchased from The Jackson Laboratories (Bar Harbor, ME). Housing and all experimental procedures were approved by the Biotechnology Research Institute Animal Care Committee, which operates under the guidelines of the Canadian Council of Animal Care. For the *HST3* virulence study (Fig. IV.6a), wild-type strains SC5314, KTY3 and the mutant *hst3*Δ/*pTET-HST3* were used. To turn off the expression of the *HST3* gene (Fig.

IV.6a), 5% sucrose and 2 mg ml^{-1} tetracycline were added to the drinking water of the mice three days prior to infection with *C. albicans*. Mice (6 per *C. albicans* strain) were injected with 200 µl of PBS containing 5×10^4 blastospores via the tail vein. When infected with this number of wild-type *C. albicans* cells, A/J mice become moribund approximately 48 h post-infection (Tuite *et al.* 2005), thus allowing ample time for tetracycline to act. Mice were closely monitored and the kidney fungal loads were determined as described above. For the *in vivo* nicotinamide treatments (Fig. IV.6b), mice (6 per treatment) were injected intra-peritoneally with 500 µl of PBS containing nicotinamide (500 mg kg^{-1}), 30 min prior to the *C. albicans* infection, since it takes 20-30 min for the nicotinamide concentration to peak in the blood stream (Horsman 1997). In addition, given that the half-life of nicotinamide *in vivo* is approximately 2 h (Horsman 1997), a second dose of nicotinamide was injected 8 h after *C. albicans* infection in order to maintain high nicotinamide concentrations in circulation. 3×10^5 rather than 5×10^4 blastospores were injected in an effort to shorten the period during which nicotinamide levels had to be maintained *in vivo*. At this higher dose, A/J mice are moribund within 24 h (Mullick *et al.* 2004). Fungal load was determined as described above.

For the *RTT109* virulence study (Fig. IV.6c-d), inoculums of strains SC5314, *rtt109*Δ/Δ and revertant *rtt109*Δ/Δ+*RTT109* were grown overnight in YPD medium and the blastospores were washed twice and resuspended in phosphate buffered saline (PBS). Mice (6 per *C. albicans* strain) were injected with 200 µl of PBS containing 3×10^5 blastospores via the tail vein. Mice were closely monitored for clinical signs such as lethargy, hunched back and ruffled fur. Mice exhibiting extreme lethargy were deemed moribund and were euthanized. For determination of fungal load, kidneys and hearts were homogenized in 5 ml PBS and 50 µl of an appropriate dilution was plated on Sabouraud broth-agar plates containing 0.35 mg L^{-1} chloramphenicol (Fig. IV.6a-c). Blood of sacrificed mice was also collected for cytokines analysis (Fig. IV.6d).

To determine whether nicotinamide administration could activate elements of the innate immune system directly, levels of six cytokines/chemokines were tested in the serum of A/J mice that had received nicotinamide treatment. For the sake of consistency with the experiment described in Fig. IV.6b, two nicotinamide injections were given, 9 h apart in a 24 h period. Nicotinamide was administered for either 1 or 3 days and cytokine levels were measured at indicated times post nicotinamide injection. Control mice received PBS injections.

Multiple sequence alignments

The *C. albicans* Hst3p sequences were used to search the Broad Institute Fungal Database (http://www.broadinstitute.org/) and the alignments were compiled with Probcons (http://probcons.stanford.edu/) (Supplementary Fig. IV.3). Residues conserved across all the fungal proteins were colored either in red (identical or highly related) or brown (related). Amino acid residues with highly related side chains were grouped as follows: aliphatic (G, A, V, I, L, M), aromatic (H, F, W, Y), nucleophilic non-charged (C, S, T), acidic (D, E), basic (H, K, R), and amides (N, Q). Histidine was grouped with both aromatic and positively charged residues. Although proline is hydrophobic, it was not considered equivalent to any other residue owing to its heterocyclic side chain that incorporates the main chain amino group. In some cases, this has led us to avoid coloring conserved hydrophobic residues when at least one of the fungal proteins had a proline at that position. Aliphatic and aromatic residues were considered related by their hydrophobic nature and therefore colored in brown. Residues with nucleophilic non-charged, acidic, and amide side chains were also regarded as related.

IV.10 Supplementary results

Deletion of *RTT109* in *C. albicans* SN152 and construction of revertants

RTT109 deletion cassettes containing the *HIS1* or *ARG4* markers flanked by *RTT109* upstream and downstream sequences were obtained by PCR amplification. The *HIS1* cassette was first used to transform SN152 and two

independently selected His^+ transformants were characterized by Southern blotting (Supplementary Fig. IV.1a and IV.1d). The expected 615-bp band corresponding to the wild-type *RTT109* allele and 1,377-bp band corresponding to the *rtt109*Δ*::HIS1* allele were observed. These strains were used to delete the second allele of *RTT109,* using the *ARG4* cassette. Selected His^+Arg^+ transformants were analyzed by Southern blotting with the *RTT109* probe 1 (Supplementary Fig. IV.1a, IV.1d and Supplementary Table IV.3). The 1,816-bp and 1,377-bp bands consistent with the replacement of the *RTT109* alleles by the *ARG4* and the *HIS1* cassettes were detected for the two independent *rtt109*Δ/Δ mutants. A wild-type *RTT109* allele was reintroduced at its original locus in strain *rtt109*Δ/Δ*#1*, using the *SAT1-FRT* cassette as previously described (Supplementary Fig. IV.1b-c) (Reuss *et al.* 2004; Tsao *et al.* 2009). The loss of the 1,816-bp band and the appearance of the wild-type 615-bp band confirmed the successful reintegration of the *RTT109* gene at its locus (Supplementary Fig. IV.1d). A 1.8-kb transcript was detected by the *RTT109* ORF probe 2 in all the strains tested, except for the *rtt109*Δ/Δ strains (Supplementary Fig. IV.1e).

We noticed that the gene neighboring *RTT109* is *SWC4* (orf19.7492), which encodes a subunit of the NuA4 histone acetyltransferase complex. These two genes share a common intergenic region, but are expressed in opposite orientations. To verify that the phenotypes of the *rtt109*Δ/Δ mutants were not due to modulation of *SWC4* expression, a Northern blot was performed with total RNA isolated from strains SN152, *rtt109*+/Δ #1, *rtt109*Δ/Δ #1 and *rtt109*Δ/Δ +*RTT109*#1. The blot was probed with an *SWC4* ORF fragment (Supplementary Fig. IV.1f). *SWC4* transcripts levels were similar in the four strains tested. Therefore, the *rtt109*Δ/Δ mutant phenotypes do not result from changes in *SWC4* gene expression.

Loss of *RTT109* affects morphogenesis

Under yeast growth conditions (YPD medium at 30 ^oC), overnight liquid cultures of the wild-type strain SN152 consisted only of yeast cells. While deleting one

allele of *RTT109* did not result in any obvious phenotype (data not shown), deletion of both *RTT109* alleles affected cell morphology. A mixture of yeast, pseudohyphae and pseudohyphae-like filaments were observed in cultures of *rtt109*Δ/Δ mutants. In addition, anucleated and multinucleated cells were observed in a fraction of the pseudohyphal cells that spontaneously formed in the *rtt109*Δ/Δ mutants (Supplementary Fig. IV.1g). Interestingly, similar morphology defects have been observed previously in *C. albicans* mutants for dynein (*CaDYN1*) and dynactin (*CaNIP100*), two proteins involved in regulating nuclear migration and positioning (Finley *et al.* 2008).

Construction of *HST3* mutants in *C. albicans*

Deletion of *HST3* in strain SN152 was attempted, as described above for *RTT109*. We replaced one allele of the *HST3* with the *HIS1* cassette and the resulting *hst3*+/Δ heterozygous mutants were characterized by Southern blotting (Supplementary Fig. IV.2a-b). In strain SN152, two bands of 786 and 1,027 bp were detected using the *HST3* probe 1, due to an *Spe*I polymorphism in the promoter region of the two *HST3* alleles. Loss of the 786-bp band and appearance of a 6,813-bp band in both heterozygote strains confirmed proper deletion of the $HST3_{1934}$ allele. However, we were unable to construct the *hst3*Δ/Δ strain despite many attempts, suggesting that *HST3* is an essential gene.

Construction of a conditional *hst3* mutant strain

Since we were unable to generate an *hst3*Δ/Δ mutant, we constructed a conditional *HST3* mutant, using the GRACE (Gene Replacement and Conditional Expression) technology (Roemer *et al.* 2003; Trunk *et al.* 2009). One allele of *HST3* (orf19.1934) was deleted and the endogenous promoter of the remaining *HST3* allele (orf19.9490) was replaced with a repressible tetracycline promoter in strain CaSS1 which expresses a chimeric tetracycline transactivator. We analyzed the resulting strains by Southern blotting (Supplementary Fig. IV.2c-d). The genomic DNA of strains CaSS1, *hst3*+/Δ and *hst3*Δ*/pTET-HST3* was isolated, digested with *Spe*I and *Cla*I and analyzed with the *HST3* probe 1. The presence of two

bands of 786 bp and 1,027 bp in CaSS1 (Supplementary Fig. IV.2d) confirmed that this strain contains the same *Spe*I polymorphism that was detected in SN152 (Supplementary Fig. IV.2b). The disappearance of the 786-bp band and the appearance of a doublet around 1,000 bp in strain *hst3*+/Δ demonstrated the insertion of the *HIS3* cassette within the *HST3* (orf19.1934) allele. The doublet consists of a 995-bp *Cla*I-*Spe*I product derived from the $hst3_{1934}$Δ*::HIS3* allele and the 1,027-bp fragment corresponding to the remaining *HST3* (orf19.9490) allele. The 2,643-bp band corresponding to the replacement of the orf19.9490 promoter with the repressible tetracycline promoter and the 995-bp band confirmed the correct integration in the *HST3* mutant strain *hst3*Δ*/pTET-HST3*. Strains *hst3*+/Δ, *hst3*Δ*/pTET-HST3* as well as the control strain CaSS1 were analyzed by Northern blotting after growth for 24 h in the absence or the presence of doxycycline (DOXY), a tetracycline derivative (Supplementary Fig. IV.2e). In the absence of doxycycline, we detected a stronger signal for the *HST3* transcript in strain *hst3*Δ*/pTET-HST3* as compared to the signals derived from strains CaSS1 and *hst3*+/Δ (Supplementary Fig. IV.2e), suggesting that the tetracycline-repressible promoter confers stronger expression in the absence of doxycycline than the endogenous *HST3* promoter. Growth of the *hst3*Δ*/pTET-HST3* strain in the presence of 20 mg ml^{-1} of doxycycline decreased the expression of *HST3* mRNA to levels lower than those detected in strains CaSS1 and *hst3*+/Δ (Supplementary Fig. IV.2e). These results were confirmed by RT-PCR analysis, using RNA from strains grown in 50 µg ml^{-1} of doxycycline (Fig. IV.2a).

Deletion of the *HST3* gene in the *rtt109*Δ/Δ mutant

The *LEU2* and *SAT1* cassettes flanked by *HST3* upstream and downstream sequences were obtained by PCR amplification. The *LEU2* cassette was first used to transform *C. albicans* strain *rtt109*Δ/Δ#1. One Leu^+ transformant, *rtt109*Δ/Δ *HST3*+/Δ, was characterized by Southern blotting (Supplementary Fig. IV.2f-g). The expected 3,961-bp band corresponding to the wild-type *HST3* allele and 1,411-bp band corresponding to the *hst3*Δ*::LEU2* allele were observed. This strain was used to delete the second *HST3* allele with the *SAT1* cassette. Two

selected Leu$^+$ Nou$^+$ transformants, *rtt109*Δ/Δ *hst3*Δ/Δ#A and *rtt109*Δ/Δ *hst3*Δ/Δ#B, were grown in the presence of maltose to induce expression of the flippase and trigger genomic excision of the *SAT1* cassette, leaving only the *FRT* sequence. Two independent Leu$^+$ Nou$^-$ strains, *rtt109*Δ/Δ *hst3*Δ/Δ#1 and #2, were analyzed by Southern blotting with the *HST3* probe 1 (Supplementary Fig. IV.2g, Supplementary Table IV.3). For all the *rtt109*Δ/Δ *hst3*Δ/Δ mutants analyzed, the detection of a 1,411-bp and 1,331-bp doublet was consistent with the replacement of the *HST3* alleles by the *LEU2* and the excised *SAT1* cassettes. Appearance of a 1,411-bp band in addition to the 3,961-bp fragment in HST3+/Δ#3 and HST3+/Δ#4 corroborated the replacement of one *HST3* allele by the *LEU2* cassette. The observation of two bands of 3,961- and 1,331-bp, for *HST3*+/Δ#5 and *HST3*+/Δ#6 confirmed the presence of the *FRT* sequence in addition to the wild-type *HST3* allele in these strains. Finally, only the *HST3* loci, corresponding to a band of 3,961-bp, were observed in SN152 and *rtt109*Δ/Δ#1 cells. Proper deletion of both *RTT109* and *HST3* was further confirmed by Southern analysis of the *rtt109*Δ/Δ *hst3*Δ/Δ mutants using both ORFs as probes (data not shown). Even following overexposure of the blots, no signal could be detected in the double mutant strains. On YPD plates, the *rtt109*Δ/Δ *hst3*Δ/Δ and *rtt109*Δ/Δ *hst3*+/Δ mutants exhibited slower growth as compared to the *rtt109*Δ/Δ and *hst3*+/Δ mutants (Supplementary Fig. IV.2h and Fig. IV.2g). Nevertheless, the viability of the *rtt109*Δ/Δ *hst3*Δ/Δ mutant confirms that the lethality of the *hst3*Δ/Δ mutant is due to H3 K56 hyperacetylation.

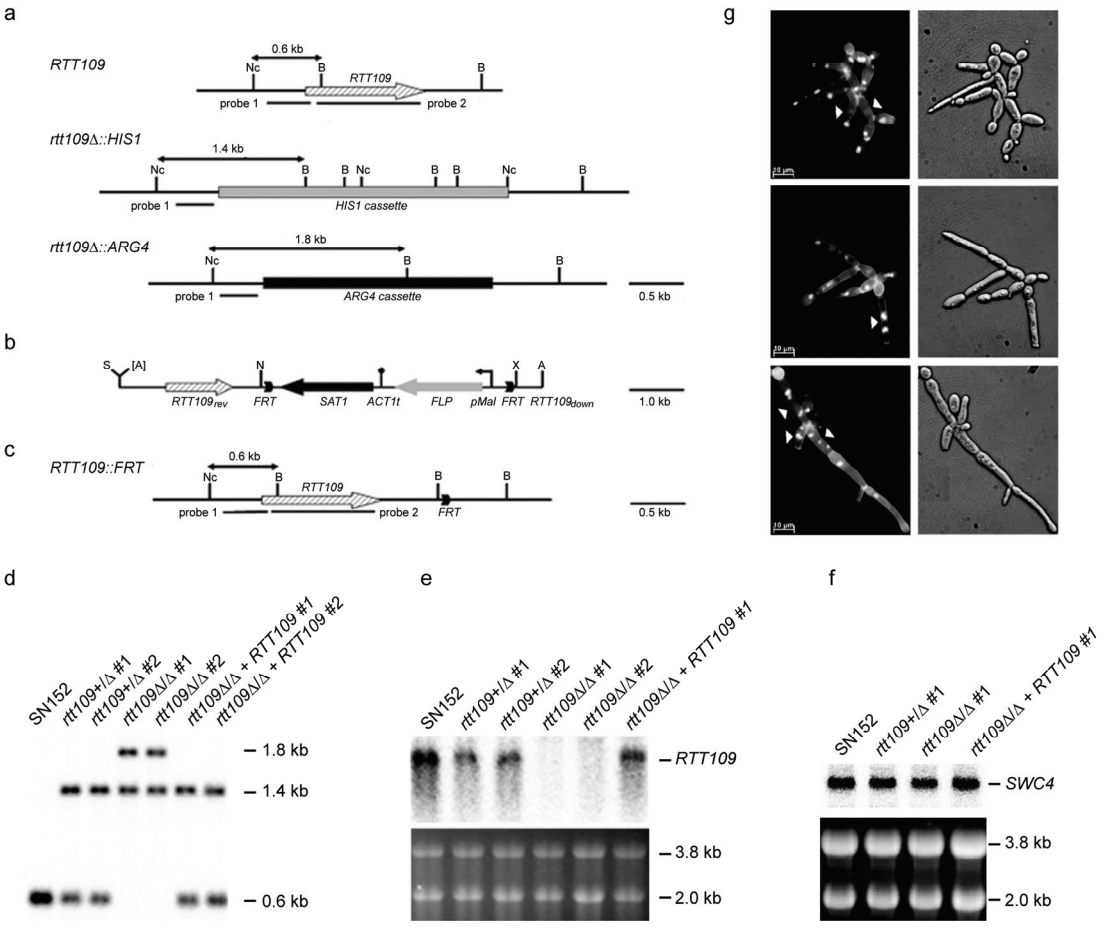

Figure IV S. 1 Characterization of *rtt109* mutants

(**a**) *Nco*I-*Bgl*II restriction maps of the *RTT109* locus and the *rtt109*Δ alleles disrupted with either *HIS1* or *ARG4* cassettes. *RTT109* probe 1 was used for Southern blot analysis. Probe 2, which detects *RTT109* ORF, was used for Northern blot analysis. (**b**) Schematic representation of the *RTT109-SAT1* complementation cassette. The cassette consists of, from left to right: $RTT109_{rev}$ including the upstream *RTT109* sequence, the entire *RTT109* ORF and the *RTT109* downstream sequences; *FRT*, FLP recombination target sites; *SAT1*, nourseothricin resistance marker; *ACT1t*, transcription termination sequence; *FLP*, flip-recombinase gene; *pMal*, maltose promoter and $RTT109_{down}$, *RTT109* downstream sequences. Restriction sites are: B, *Bgl*II; Nc, *Nco*I; S, *Sac*II; A, *Apa*I; N, *Not*I; X, *Xho*I; [A], *Apa*I site was introduced by PCR. (**c**) *Nco*I-*Bgl*II restriction map of the *RTT109* revertant allele. (**d**) Southern blot analysis of *Nco*I-*Bgl*II digested gDNA. (**e**) Northern blot analysis and corresponding denaturing RNA gel. (**f**) Testing the expression of the *SWC4* gene in *rtt109* mutants by Northern blot analysis. (**g**) Microscopy analysis of *rtt109*Δ/Δ cells with DAPI and calcofluor white staining; multinucleated or anucleated cells are indicated by arrowheads.

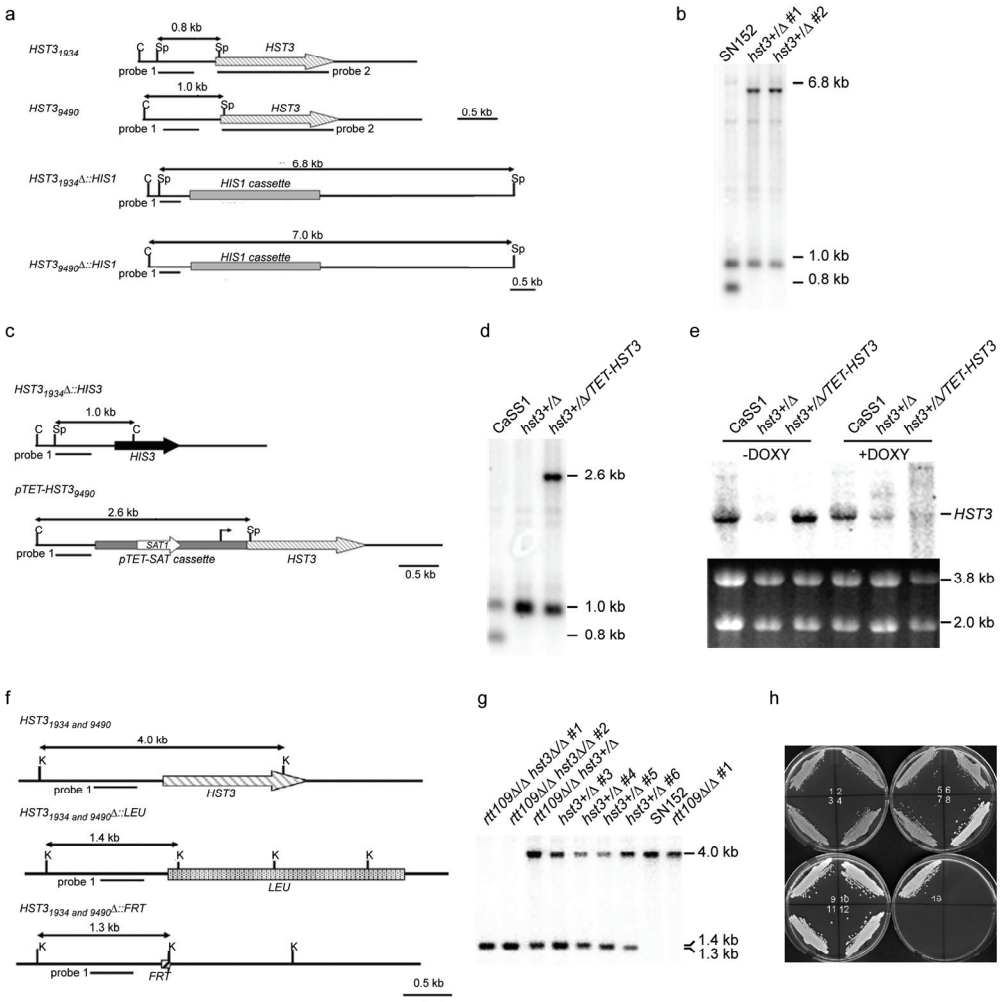

Figure IV S. 2 Characterization of *hst3* mutants

(**a**) *Cla*I-*Spe*I restriction maps of the two *HST3* alleles (orf19.1934 and orf19.9490) and the corresponding *hst3*Δ::*HIS1* loci. The *HST3* probe 1 was used for Southern blot analysis. Probe 2, which detects the *HST3* ORF, was used for Northern blot analysis. (**b**) Southern blot analysis of *Cla*I-*Spe*I-digested gDNA. (**c**) *Cla*I-*Spe*I restriction maps of *hst3*Δ::*HIS3* (orf19.1934) locus (top panel) and the promoter of *HST3* (orf19.9490) after replacement by the *pTET-SAT1* cassette (bottom panel). (**d**) Southern blot analysis of *Cla*I-*Spe*I-digested gDNA. (**e**) Northern blot analysis of conditional *hst3* mutants using probe 2. DOXY (doxycycline, 20 μg ml^{-1}). (**f**) Construction of *rtt109*Δ/Δ *hst3*Δ/Δ double mutants. *Kpn*I restriction maps of the *HST3* loci (top panel), the *hst3*Δ::*LEU2* loci (middle panel) and the *hst3*Δ::*FRT* loci (bottom panel). (**g**) Southern blot analysis of *Kpn*I-digested genomic DNA. (**h**) Growth of *rtt109*Δ/Δ *hst3*Δ/Δ mutants. Strains tested are: 1, *rtt109*Δ/Δ *hst3*Δ/Δ#1; 2, *rtt109*Δ/Δ *hst3*Δ/Δ#2; 3, *rtt109*Δ/Δ *hst3*Δ/Δ#3; 4, *rtt109*Δ/Δ *hst3*Δ/Δ#4; 5, *rtt109*Δ/Δ *hst3*Δ/Δ#5; 6, *rtt109*Δ/Δ *hst3*Δ/Δ#6; 7, *rtt109*Δ/Δ *HST3*+/Δ; 8, *HST3*+/Δ #3; 9, *HST3*+/Δ #4; 10, *HST3*+/Δ #5; 11, *HST3*+/Δ #6; 12, SN152 and 13, *rtt109*Δ/Δ#1.

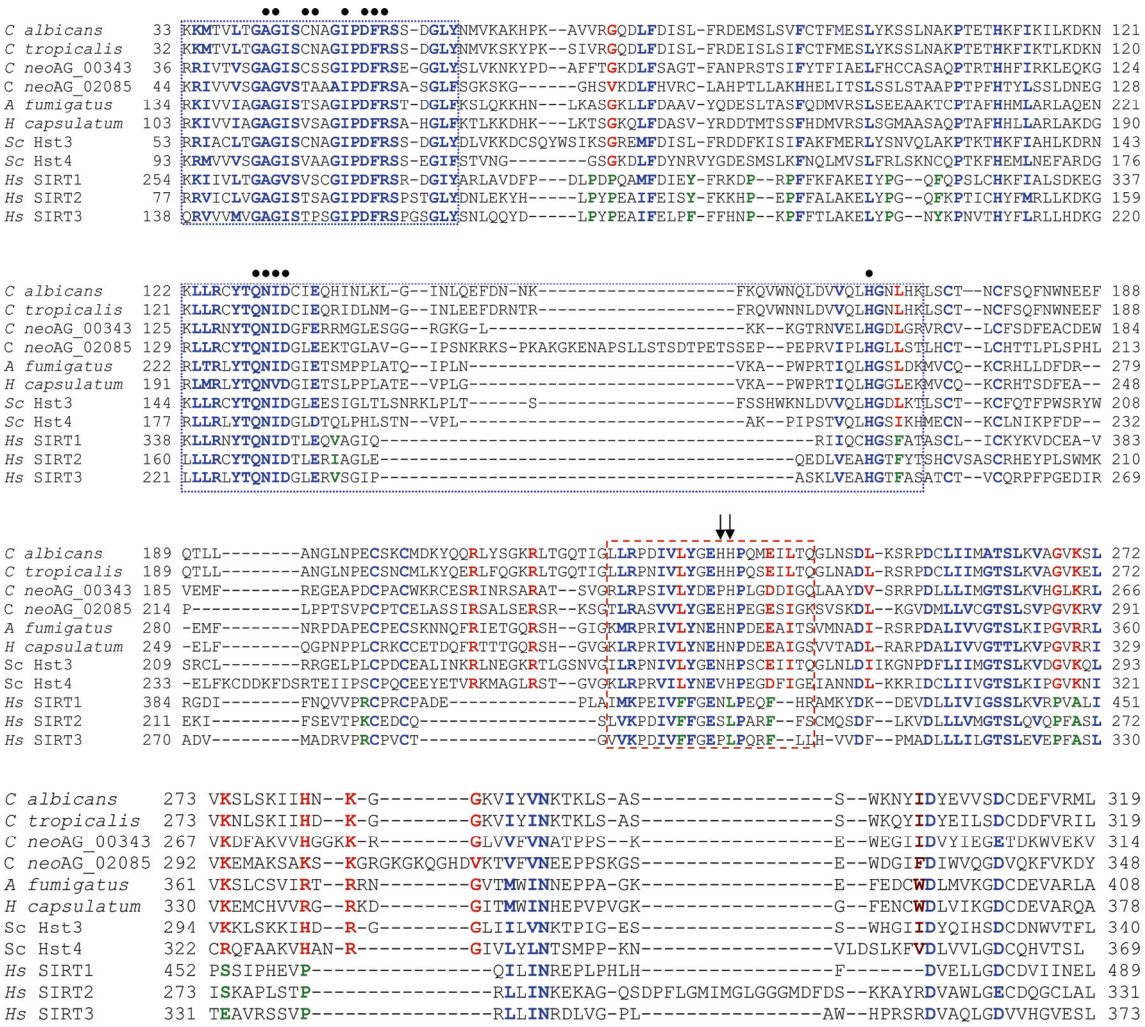

Figure IV S. 3 Sequence alignment of Class Ic sirtuins

Class Ic sirtuins homologous to Hst3p exist in different pathogenic fungi and contain potentially important sequence motifs that are different from human sirtuins. Only one putative Hst3p homologue was found in *C. tropicalis* (RT05386), *A. fumigatus* (1G1054) and *H. capsulatum* (EG02181). As is the case in *S. cerevisiae*, which possesses two related proteins (Hst3p, YOR025W and Hst4p, YDR191W), two potential Hst3p orthologs also exist in *C. neoformans*, (CneoHst3p, AG00343 and CneoHst4p, AG02085). The alignment is restricted to the catalytic cores and the human sirtuins (class Ia and Ib) that are most closely related to Hst3p are included for comparison (SIRT1: *NM_012238*; SIRT2: *NM_012237*; SIRT3: *NM_012239*). Residues colored in blue are common to all class I sirtuins. Residues colored in red and brown are conserved among Hst3p family members, but different in human sirtuins. In contrast, residues in green are conserved among human class I sirtuins, but are different in fungal Hst3p homologs. The red box includes residues that bind acetylated peptides in other sirtuins (Cosgrove *et al.* 2006) and most likely plays a similar role in Hst3p homologues. The side chains of the residues highlighted

with arrows have been implicated in peptide substrate selection (Cosgrove *et al.* 2006). The blue boxes bracket conserved regions that contain residues which directly interact with NAD^+ (black dots)(Avalos *et al.* 2005; Avalos *et al.* 2004).

a

Species	Strain name	Reference or source
Candida albicans	5457	[9]
	5674	[9]
	GU5	[27]
	6692	[9]
	1906 (A2.1)	[28]
	2307 (A3.1)	[28]
	ATCC90028	[29]
	372.73374.1	[29]
	ATCC66027	[30]
	20464	[30]
Candida glabrata	ATCC90030	ATCC[a]
	MY067497	LSPQ[b]
Candida parapsilosis	ATCC90018	ATCC
	MY067743	LSPQ
Candida tropicalis	MY070362	LSPQ
	MY070589	LSPQ
Candida krusei	ATCC6258	ATCC
	MY069520	LSPQ
Aspergillus fumigatus	MY070954	LSPQ
	MY070968	LSPQ
Aspergillus nidulans	MY070627	LSPQ
	R153	C.F. Roberts

[a] American Type Cell Culture
[b] Laboratoire de Santé Publique du Québec

b

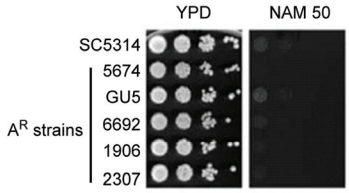

c

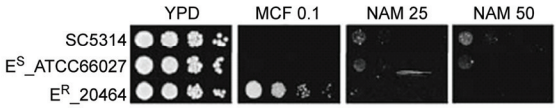

Figure IV S. 4 Activity of nicotinamide against different pathogenic fungi

(**a**) Strain list of *Candida* species and *Aspergillus* species used in this study. (**b**) Nicotinamide spot assay of a collection of azole-resistant (A^R) strains. (**c**) Nicotinamide spot assay of echinocandin-susceptible (E^S) and echinocandin-resistant (E^R) strains. NAM, nicotinamide (mM), MCF, micafungin (mg ml^{-1}).

Table IV S. 1 Stoichiometry of acetylation of H3 N-terminal tail lysine residues determined by nano-LC MS/MS and MRM

$%&() !	*+), (%-) !	-./012"!	-.341 2"56!	-."612"!
7 (8, 9%; <!=$>3/"?!	1 $@[3]!	"0A0!B!CA6!	"A"!B!CAC/!	3CAC!B!CA!!
!'"#$%&()*+,-./0123!	1 $@[3]!	CA0!B!CACE	6A33!B!CACE!	3CAF!B!CA6!
&'()*+,-./0123[6]!	1 $@[3]!	/CAC!B!CA0!	6A#F!B!CAC"!	3"AC!B!CAC/!
&'()*+,-./0123[6]!	1 $@[3]!	#EA!B!CA!	"A04!B!CAC/!	FAE!B!CA3!
+")+,-./0123!	1 $@!=EA!I!)+!,+J:?[3]!	#EA4!B!CA!	0A6!B!CAC/!	"CA!B!CA3!
+")+,-./0123!	1 $@!=EA!I!,+J:?[3]!	40AC!B!CA!	"A6E!B!CAC4!	FA!B!CAF!
+")+,-./0123!	1 $@!=EA!I!,+J:?[3]!	44AC!B!CA3!	"A#3!B!CACF!	3CA0!B!CA3!

[1] ASY = Asynchronously growing cells in exponential phase; doxy=doxycycline (40 mg ml^{-1}).

[2] %Ac of a given lysine residue was calculated as described in the Supplementary Materials and Methods section. The average values ± standard error of the mean were calculated from triplicate injections of the same tryptic digest.

[3] Independent replicates of the same strain.

Table IV S. 2 List of *C. albicans* strains used in this study

Strain Name	Parent	Genotype	Source or reference
SC5314		Wild type	(Gillum et al., 1984)
SN152	RM1000#2	*arg4Δ/arg4Δ leu2Δ/leu2Δ his1Δ/his1Δ URA3/ura3Δ::λimm434 IRO1/iro1Δ::λimm434*	(Noble and Johnson, 2005)
CaSS1	CAI4	*his3::hisG/his3::hisG leu2::tet*R-GAL4AD-*URA3/LEU2*	(Roemer et al., 2003)
KTY3	CaSS1	*his3::hisG::HIS3/his3::hisG leu2::tet*R-GAL4AD-*URA3/LEU2*	(Trunk et al., 2009)
rtt109+/Δ #1	SN152	*arg4Δ/arg4Δ leu2Δ/leu2Δ his1Δ/ his1Δ URA3/ura3Δ::λimm434 IRO1/iro1Δ::λimm434 RTT109/ rtt109Δ::HIS1*	This study
rtt109+/Δ #2	SN152	*arg4Δ/arg4Δ leu2Δ/leu2Δ his1Δ/ his1Δ URA3/ura3Δ::λimm434 IRO1/iro1Δ::λimm434 RTT109/ rtt109Δ::HIS1*	This study
*rtt109*Δ/Δ#1	*rtt109*+/Δ #1	*arg4Δ/arg4Δ leu2Δ/leu2Δ his1Δ/his1Δ URA3/ura3Δ::λimm434 IRO1/iro1Δ::λimm434 rtt109Δ::ARG4/rtt109Δ::HIS1*	This study
*rtt109*Δ/Δ#2	*rtt109*+/Δ #2	*arg4Δ/arg4Δ leu2Δ/leu2Δ his1Δ/his1Δ URA3/ura3Δ::λimm434 IRO1/iro1Δ::λimm434 rtt109Δ::ARG4/rtt109Δ::HIS1*	This study
*rtt109*Δ/Δ+*RTT109*#1	*rtt109*Δ/Δ#1	*arg4Δ/arg4Δ leu2Δ/leu2Δ his1Δ/ his1Δ URA3/ura3Δ::λimm434 IRO1/iro1Δ::λimm434 RTT109-FRT/rtt109Δ::HIS1*	This study
*rtt109*Δ/Δ+*RTT109*#2	*rtt109*Δ/Δ#1	*arg4Δ/arg4Δ leu2Δ/leu2Δ his1Δ/ his1Δ URA3/ura3Δ::λimm434 IRO1/iro1Δ::λimm434 RTT109-FRT/rtt109Δ::HIS1*	This study
HST3+/Δ #1	SN152	*arg4Δ/arg4Δ leu2Δ/leu2Δ his1Δ/ his1Δ URA3/ura3Δ::λimm434 IRO1/iro1Δ::λimm434 HST3/hst3Δ::HIS1*	This study
HST3+/Δ #2	SN152	*arg4Δ/arg4Δ leu2Δ/leu2Δ his1Δ/ his1Δ URA3/ura3Δ::λimm434 IRO1/iro1Δ::λimm434 HST3/hst3Δ::HIS1*	This study
HST3+/Δ #3	SN152	*arg4Δ/arg4Δ leu2Δ/leu2Δ his1Δ/ his1Δ URA3/ura3Δ::λimm434 IRO1/iro1Δ::λimm434 HST3/hst3Δ::FRT*	This study
HST3+/Δ #4	SN152	*arg4Δ/arg4 leu2Δ/leu2Δ Δ his1Δ/ his1Δ URA3/ura3Δ::λimm434 IRO1/iro1Δ::λimm434 HST3/hst3Δ::LEU2*	This study
*rtt109*Δ/Δ *HST3*+/Δ	*rtt109*Δ/Δ #1	*arg4Δ/arg4Δ leu2Δ/leu2Δ his1Δ/his1Δ URA3/ura3Δ::λimm434 IRO1/iro1Δ::λimm434 rtt109Δ::ARG4/rtt109Δ::HIS1 HST3/hst3Δ::LEU2*	This study
*rtt109*Δ/Δ *hst3*Δ/Δ#1	*rtt109*Δ/Δ *HST3*+/Δ	*arg4Δ/arg4Δ leu2Δ/leu2Δ his1Δ/his1Δ URA3/ura3Δ::λimm434 IRO1/iro1Δ::λimm434 rtt109Δ::ARG4/rtt109Δ::HIS1 hst3Δ::FRT/hst3Δ::LEU2*	This study
*rtt109*Δ/Δ *hst3*Δ/Δ#2	*rtt109*Δ/Δ *HST3*+/Δ	*arg4Δ/arg4Δ leu2Δ/leu2Δ his1Δ/his1Δ URA3/ura3Δ::λimm434 IRO1/iro1Δ::λimm434 rtt109Δ::ARG4/rtt109Δ::HIS1 hst3Δ::FRT/hst3Δ::LEU2*	This study
HST3+/Δ	CaSS1	*his3::hisG/his3::hisG leu2::tet*R-GAL4AD-*URA3/LEU2 HST3/hst3Δ::HIS3*	This study
*HST3*Δ/*pTET-HST3*	*HST3*+/Δ	*his3::hisG/his3::hisG leu2::tet*R-GAL4AD-*URA3/LEU2* pTet-*HST3/hst3Δ::HIS3*	This study

Table IV S. 3 List of primers used in this study

PCR-product or plasmid	Primer	Sequence (5'-3')
Gene deletion in SN152		
RTT109$_{short}$	MR1801	GATTCTTAAAATCGCGTCCTTTCATACTTTCCAATCGGTCCAAGTGAATTACTGGATTACTGTGGAATTGTGAGCGGATA[1]
	MR1803	CCCAGGTTTTAATCGAACTGGCCCCAATGCAATTACGTATCGTGTGAGGTTATCGTCGATGTTTTCCCAGTCACGACGTT[1]
RTT109$_{long}$	MR1802	TGTTGGGAATCGATTGAGGCAGAAAAAATTTCAAGCATATTGAGAATAACTAGAAGTGTTGATTCTTAAAATCGCGTCCT[2]
	MR1804	ACATCTATACTCTAATCACAATATATGATAAAATAATGACAGAGGTCAAGACCAATCGGTCCCAGGTTTTAATCGAACTG[2]
HST3$_{short}$	MR1808	ATTTGACAAGATTATCAGTACTGTCAAGAAAACTCACTATAAAACAACTACTTTTAGACGTGTGGAATTGTGAGCGGATA[1]
	MR1810	TCATTGCAATTGATTCATTAATATTACATAATGTTTACATAATTTCCAACTCTGAAACCAGTTTTCCCAGTCACGACGTT[1]
HST3$_{long}$	MR1809	AAATACAACCATCGCCAGTCTAGTTGAACAATACATAGGACATATAAAGTCCATACACCCATTTGACAAGATTATCAGTA[2]
	MR1811	TCAACAAAAGTATCTTCTACAGGTTATAATTGGTATATATGTGTGTGTCATAACATTCAGTCATTGCAATTGATTCATTA[2]
HST3$_{short\ SAT1}$	MR2344	TTTGACAAGATTATCAGTACTGTCAAGAAAACTCACTATAAAACAACTACTTTTAGACGGAGCTCCACCGCGGTGGCGGCCGCT[3]
	MR2345	TCATTGCAATTGATTCATTAATATTACATAATGTTTACATAATTTCCAACTCTGAAACCAGGTACCGGGCCCCCCCTCGAGGAA[3]
Gene reintroduction		
pRTT109$_{rev}$	MR1945	TCCCCGCGGGCCCTGATCTGGTTCTGTGGATTTTGTTGTG[4]
	MR1946	AAGGAAGCGGCCGCCTACCACAGTTGAACCACTACTACTAG[4]
pRTT109$_{down}$	MR1947	GCGCTCGAGCTGTATGTATGATTGTTGGAGGGTGAC[4]
	MR1948	GCGGGGCCCCTACCACAGTTGAACCACTACTACTAG[4]
GRACE strains construction		
HST3 HIS3$_{short}$	MR1970	TTTGACAAGATTATCAGTACTGTCAAGAAAACTCACTATAAAACAACTACTTTTAGACGGATCTTTCTGTGACTCAATTC[5]
	MR1972	TCATTGCAATTGATTCATTAATATTACATAATGTTTACATAATTTCCAACTCTGAAACCAATGGATTTTAGTCAGTAAC[5]
HST3 HIS3$_{long}$	MR1971	AAATACAACCATCGCCAGTCTAGTTGAACAATACATAGGACATATAAAGTCCATACACCCATTTGACAAGATTATCAGTA[2]
	MR1973	TCAACAAAAGTATCTTCTACAGGTTATAATTGGTATATATGTGTGTGTCATAACATTCAGTCATTGCAATTGATTCATTA[2]
HST3 P$_{short}$	MR1974	TAGAGTATTATACCAAGTATCTTTTGCACATATTCCTCATAGTCAATTACGTAAAAAAAGAGCGTCAAAACTAGAG[6]
	MR1976	GAGGTGTCAGCTGGCATACTAGTGCCTGAATTGTCAAGTAAGTCAATCAGTATCATCGTCTTAATTTAGTGTGTGTATTTG[6]
HST3 P$_{long}$	MR1975	TGTTTTTTACTTGTTCAGTATTCTAATAATCATTACCTACACATTTTCATCCAATAGCTTTAGAGTATTATACCAAGTAT[2]
	MR1977	GTAAGAACAGTCATTTTCTTACTTTTAGATATAAATTTGATCACCTCATGTAGCTTTATCGAGGTGTCAGCTGGCATACT[2]
Probes		
RTT109 probe 1	MR2008	GTTTATAGGTGGTGTATTTGGACCTAC
	MR2009	TCCCAATTGTAGATTTGGGGATATGTATCG
RTT109 probe 2	MR2127	ATCACCGATACATATCCCCAAATCTAC
	MR2128	ATTGTCACAGTTGAAACCAGATCATCG
HST3 probe 1	MR2017	TCATTTTTACTATGGCTTTGGTGTTG
	MR2018	TGAGGAATATGTGCAAAAGATACTTG
HST3 probe 2	MR2058	GATACTGATTGACTTACTTGACAATTC
	MR2129	TCAAATAGCACTTTAGCCACAGGTTCATC
SWC4 probe	MR2056	ATGTCAGCAAATGATATTCTTGATG
	MR2057	CATCGTCCTTGATCTGGTTCTGTGG
RT-PCR		
ACT1	Act1_CA_F	TCCAGAAGCTTTGTTCAGACCAGC
	Act1_CA_R	TGCATACGTTCAGCAATACCTGGG
HST3	Hst3_CA_F	AAAGAAGAGCCAATTCCCACACCG
	Hst3_CA_R	TTGGCACTGATTTCATCAGGCAGC

[1] Each primer contains 60 bp complementary to the *RTT109* or the *HST3* locus and 20 bp complementary to pGEM-HIS1 or pRS-Arg4 SpeI
(plasmid sequences are underlined).

[2] Each primer contains a 20-bp region complementary to the 5'-end of the first set of primers (underlined) and an extended 60-bp region of the
RTT109 or *HST3* locus.

[3] Each primer contains 60 bp complementary to the *HST3* locus and 24-25 bp complementary to the *SAT1* flipper cassette present on the plasmid pSFS2A (plasmid sequences are underlined).

[4] Each primer contains a region complementary to the *RTT109* locus. Restriction site(s) (underlined or bolded) were added for cloning of the
amplicon into pSFS2A and for recovery of the *RTT109* integration cassette used to transform the rtt109Δ/Δ strain.

[5] Each primer contains a region complementary to the *HST3* locus and a region complementary to pHIS3 (plasmid sequence is underlined).

[6] Each primer contains a region complementary to the *HST3* locus and a region complementary to pTET (plasmid sequence is underlined).

Table IV S. 4 Quantification of proinflammatory cytokines in mice treated with NAM

	Experimental conditions[a]		Cytokines (pg mL^{-1})					
Mouse groups	Total # injections	Mice euthanized at	IL-6	MCP-1	KC	TNF-α	IL-10	IFN-γ
0 NAM-24 h	0	24 h	6.6 ± 0.8	21.7 ± 6.1	14.3 ±0.8	12.7 ± 0.8	7.3 ± 2.2	5.1 ± 1.1
2 NAM-24 h	2	24 h	8.7 ± 1.3	26.7 ± 9.4	16.5 ± 2.8	11.0 ±1.6	6.5 ± 2.8	6.0 ± 2.3
2 NAM-72 h#1	2	72 h	1.7 ± 1.1	N.D[c]	10.0 ± 0.9	10.0 ± 0.6	N.D[c]	N.D[c]
2 NAM-72 h#2[b]	6	72 h	3.8 ± 1.2	N.D[c]	11.0 ± 0.6	8.7 ± 0.9	N.D[c]	1.8 ± 1.2
2 NAM-120 h	2	120 h	8.0 ± 0.2	44.7 ± 10.5	14.2 ± 0.6	13.6 ± 0.5	13.3 ± 1.1	7.3 ± 0.3
0 NAM-120 h	0	120 h	7.7 ± 0.2	34.3 ± 1.7	15.7 ± 0.6	13.8 ± 0.8	14.2 ± 0.5	7.7 ± 0.2

[a] Mice were injected with NAM (500 mg kg^{-1} per injection) twice a day and were euthanized at the indicated time after the first injection.

[b] Two injections daily were performed for three consecutive days.

[c.] N.D. = not detected.

Chapter V

General discussion

Chapter V General discussion

V.1 *C. albicans* Cdr1p and Cdr2p

Overexpression of the ABC transporters Cdr1p and Cdr2p is a common mechanism leading to clinical azole-resistance in *C. albicans* strains. These two highly homologous transporters (sharing 84% amino acid identity) confer comparable levels of azole resistance when individually expressed in *S. cerevisiae* [(Gauthier *et al.* 2003; Lamping *et al.* 2007), Chapter I.5.2.5]. However, in the azole-resistant clinical *C. albicans* strains, inhibition of Cdr1p using either gene-deletion strategy or pharmacological inhibitors resulted in a significant reduction of azole resistance, indicating that the role of Cdr1p in clinical azole resistance is more important than that of Cdr2p (Chapter II; (Holmes *et al.* 2008; Tsao *et al.* 2009)). This result could be at least partly explained by the fact that Cdr2p is expressed at lower levels than Cdr1p in these clinical strains (Chapter II; (Holmes *et al.* 2008; Tsao *et al.* 2009)), suggesting that these two transporters could be subjected to differential posttranslational regulations (Chapter III and see below).

Substrate specificities of Cdr1p and Cdr2p

Substrate specificities of Cdr1p and Cdr2p have been documented and summarized in Table V.1. Most of these studies were performed by individually expressing *CDR1* or *CDR2* in hypersusceptible *S. cerevisiae* mutant strains lacking endogenous ABC transporters or by deletion of *CDR1* and/or *CDR2* from *C. albicans* strains (including the azole-susceptible as well as azole-resistant strains; Chapter I.5.2.5 and Chapter II). In most cases, substrates identified from *S. cerevisiae* studies can cause growth inhibition in *C. albicans* strains lacking *CDR1* and/or *CDR2* (Table V.1). One exception is rhodamine 6G, a fluorescent compound that is often used for studying transporter functions because of its antifungal properties and its ease of detection. Our results showed that deletion of *CDR1/CDR2* genes in *C. albicans* (azole-resistant strain 5674) resulted in a marginal reduction in rhodamine 6G resistance, demonstrating that it is not a good

substrate for studying Cdr1p and Cdr2p functions in *C. albicans* (Chapter II). Interestingly, deletion of the gene encoding the Tac1p transcription factor from strain 5674 conferred a significantly reduced rhodamine 6G resistance, suggesting the presence of Tac1p-regulated factor(s) (other than Cdr1p/Cdr2p) could influence rhodamine 6G resistance in *C. albicans* (see section V.2). Taken together, these results demonstrated that, although *S. cerevisiae* heterologous expression systems have been useful for studying functions of Cdr1p/Cdr2p, it is still important to validate the functions of these transporters in *C. albicans* when possible. Nevertheless, the *S. cerevisiae* expressing system has been useful for distinguishing substrate differences between these two transporters, as *S. cerevisiae* strain expressing Cdr2p but not Cdr1p could confer resistance against FK520, Enniatin and Diamide (Table V.1).

Table V. 1 Substrate specificities of Cdr1p and Cdr2p

	Gene expression in *S. cerevisiae*		Gene deletion in *C. albicans*	
	CDR1	*CDR2*	*CDR1*	*CDR2*
Ketoconazole	R	R	S	S
Fluconazole	R	R	S	S
Itraconazole	R	R	S	S
Cycloheximide	R	R	S	S
Rhodamine 6G	R	R	R	R
Fluphenazine	R	R	S	S
FK520	HS	R	N.D.	N.D.
Enniatin	S	R	N.D.	N.D.
Nile Red	R	R	N.D.	N.D.
Diamide	S	R	N.D.	N.D.

R: Resistant
S: Susceptible
HS: Hyper-susceptible
N.D.: not determined
(Gauthier *et al.* 2003; Ivnitski-Steele *et al.* 2009; Lamping *et al.* 2007; Sanglard *et al.* 1997; Tsao *et al.* 2009)

Phosphorylation of Cdr1p and Cdr2p

We showed that Cdr1p is constitutively phosphorylated *in vivo* at the evolutionally conserved serine/threonine residues of its N-terminus region.

Alanine mutagenesis of these residues significantly affected the transporter activity of Cdr1p, suggesting that phosphorylation plays an important role in the modulation of its functions (Chapter III). During the course of this study, we also observed that Cdr2p is a phosphoprotein (unpublished data, Fig. V.1a). In addition, mass spectrometry analyses identified two phosphorylated residues, Thr52 and Ser847, located in the N-terminus and the linker region, respectively (highlighted in Fig. V.1b). Interestingly, while Cdr1p contains a NTE phosphorylation motif, LAR-pT/S-Φ-pT/S-x-x-pS-x (where p represents phosphorylation, Φ represents any hydrophobic amino acid and x represents any amino acids), Cdr2p contains LAR-K-Φ-T-x-x-S-pT (amino acid variation is underlined; Fig. V.1b). These findings suggest that Cdr2p and Cdr1p may not be regulated by phosphorylation in the same way. To test this hypothesis, I constructed Cdr2p phosphomutants and tested the ability of these mutants to grow in the presence of azoles (Fig. V.1c). Mutating the identified phosphorylated residues to alanine, (T52A alone or in combination with Ser847) did not affect the function of Cdr2p. I also constructed another Cdr2p double mutant, T48A/S51A; these residues are conserved with Cdr1p phosphorylation sites (Thr51 and Ser54) but were not identified to be phosphorylated residues in our mass spectrometry analyses. Unlike in Cdr1p, where the double mutation of T51A/S54A had significantly impaired the Cdr1p function, mutation of the corresponding residues in Cdr2p (T48A/S51A) showed a little effect (Chapter III and Fig. V.1c). These results demonstrated that NTE phosphorylation of Cdr2p is likely to play a minor role in regulating Cdr2p function. However, it is also possible that Cdr2p can function with phosphorylation of either sites (Thr52 or Thr48/Ser51), therefore a triple mutation of T48A/S51A/T52A of Cdr2p followed by azole-resistance assays will be the next step to study the function of NTE phosphorylation of Cdr2p. Furthermore, the migration pattern and abundance of Cdr2p phosphomutants will also be examined by Western blotting analyses as described for Cdr1p in Chapter III.

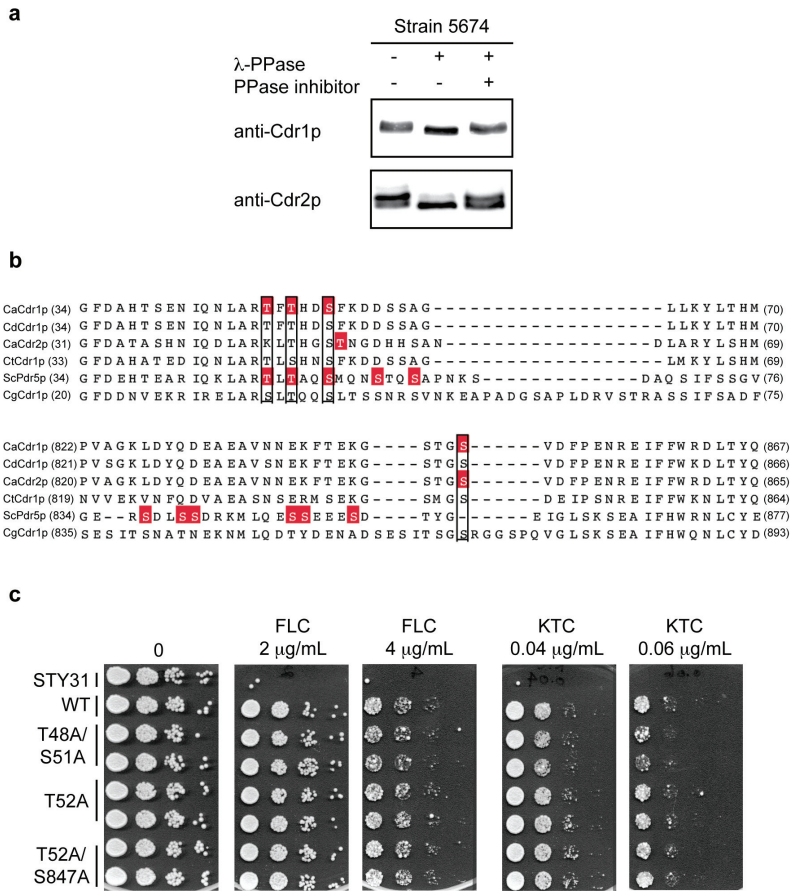

Figure V. 1 Phosphorylation analyses of *C. albicans* Cdr2p

(**a**) Dephosphorylation assays. Total membrane extracts from strain 5674 overexpressing Cdr1p and Cdr2p were treated with λ-phosphatase and separated on SDS-PAGE. Western blot analysis using the specific anti-Cdr1p and anti-Cdr2p antibodies detected shifts in the migration of Cdr1p and Cdr2p after λ-phosphatase treatment, suggesting that both proteins are phosphorylated. (**b**) Sequence comparison of the Cdr2p NTE and linker regions with other ABC transporters. The protein sequences of *C. albicans* Cdr1p (CaCdr1p), *C. dubliniensis* Cdr1p (CdCdr1p), *C. albicans* Cdr2p (CaCdr2p), *C. tropicalis* Cdr1p (CtCdr1p), *S. cerevisiae* Pdr5p (ScPdr5p) and *C. glabrata* Cdr1p (CgCdr1p) were aligned using JalView. Shading indicates mass spectrometry-identified phosphorylated residues; conserved residues are boxed. (**c**) Drug resistance profiles of Cdr2p phosphorylation mutants were analyzed in the spot assay.

Our findings in Chapter III established a link between protein abundance and the phosphorylation status of Cdr1p. While it has been shown that *CDR1* and *CDR2* are up-regulated in the transcription factor Tac1p-depenent manner (both genes

contain important consensus promoter elements, and their promoters are exchangeable for the Tac1p-dependent transcriptions (Coste *et al.* 2009)); it has been observed that the abundance of Cdr2p is less than that of Cdr1p in the membranes of many clinical azole-resistant strains (as shown by Western blotting, Chapter II; (Holmes *et al.* 2008; Tsao *et al.* 2009)). Although I cannot exclude the possibility that other unknown transcriptional or not-yet characterized post-transcriptional mechanisms are involved and contributed to differential regulations of Cdr1p/Cdr2p expressions; it is tempting to speculate that post-translational modifications, such as phosphorylation, could be involved in modulating the abundance of these transporters. Specifically, phosphorylation could be a signal for ubiquitination-dependent turnover, since this has been shown for the yeast transporter Ste6p (Kelm *et al.* 2004). It will be interesting to investigate whether phosphorylation could affect the stability of wild-type or phosphomutants of Cdr1p and Cdr2p in pulse-chase experiments for documenting their turnover rates. Western blotting analyses could be used to examine whether these transporters are subjected to ubiquitination and mass spectrometry could also be used to identify ubiquitination sites. Phosphorylation could also affect membrane trafficking, as demonstrated for *S. cerevisiae* Pdr5p (Decottignies *et al.* 1999). It would be interesting to investigate the localization of wild-type and phosphomutants of Cdr1p and Cdr2p in normal growth conditions (YPD, 30 ^{o}C; as used in my studies presented in this thesis) as well as under stress conditions (in the presence of azoles or different Cdr1p/Cdr2p substrates). Subcellular fractionations followed by Western blotting analyses could be used to determine whether phosphorylation affects the plasma membrane localization of Cdr1p and Cdr2p.

Proposed physiological roles of Cdr1p and Cdr2p

Cdr1p and Cdr2p share similar topological arrangements and enzymatic mechanisms; they also function as phospholipid floppases that are important in maintaining plasma membrane integrity (Chapter I.5.2.5). Recent studies showed that Cdr1p is preferentially localized within ergosterol/sphingolipid-enriched

microdomains of plasma membrane named lipid rafts (Pasrija *et al.* 2008). During my study, I also noticed that Cdr2p is enriched in the detergent-resistant membrane (DRM) fractions, suggesting Cdr2p is also a lipid raft-associated protein (unpublished observation). Additional experiments will be required to determine whether both Cdr1p and Cdr2p are localized in the same lipid raft fraction (see below); this experiment could be performed in an azole-resistant strain background when both transporters are expressed (i.e. strain 5674).

In yeast, lipid rafts have been implicated in a wide range of cellular processes, including signaling, protein sorting, endocytosis, cell polarity and morphogenesis (Alvarez *et al.* 2007). Sucrose gradient fractionation of membrane extracts allows the separation of different lipid raft fractions and these fractions can be distinguished by using Western blot analysis with antibodies against several well-known lipid raft associated proteins. Known yeast lipid raft markers include proton ATPase Pma1p; GPI-anchored proteins, such as Eap1p, Dfg5p and Phr1p that are known to be involved in epithelial adhesion, virulence, and proper hyphal growth (Insenser *et al.* 2006; Martin *et al.* 2004). Expression of *CDR1* transcripts from a wild-type *C. albicans* strain has been shown to be up-regulated during the hyphal formation (Dogra *et al.* 1999). Since lipid rafts are localized at the tip of the hyphal growth and could contribute to the hyphal morphogenesis (Martin *et al.* 2004), it is tempting to speculate that Cdr1p and Cdr2p maybe involved in transporting specific lipids, or lipophilic molecules, that are important for *C. albicans* morphogenesis.

Finally, characterization of the lipid raft fractions where Cdr1p and Cdr2p are associated using mass spectrometry-based proteomic profiling could lead to the identification of proteins that are co-localized within the same lipid raft fractions. These data could provide a list of potential interacting proteins with Cdr1p and Cdr2p, giving hints to signaling pathways involving Cdr1p and Cdr2p and perhaps uncovering yet unidentified physiological roles of these ABC transporters.

V.2 The Tac1p regulon: membrane lipid homeostasis and azole resistance

Changes in azole susceptibility have been linked to changes in the membrane lipid composition (Chapter I.4.2). Exposure of *C. albicans* to azoles results in depletion of ergosterol in the plasma membrane and compromises plasma membrane integrity; surviving cells thus select for mutations to mitigate these harmful effects and permit continued growth. The transcription factor Tac1p plays a central role in the azole response pathway by controlling the overexpression of Cdr1p and Cdr2p, as well as by regulating the expression of other genes involved in lipid metabolism in azole resistant *C. albicans* strains (Liu *et al.* 2007).

Pdr16p

One of the Tac1p target genes, *PDR16*, encodes a putative phosphatidylinositol transfer protein which has been shown to contribute to the overall azole resistance; *PDR16* disruption reduces, and overexpression increases, azole resistance in *C. albicans* by approximately two-fold (Saidane *et al.* 2006). *S. cerevisiae* Pdr16p localizes to lipid particles and microsomes, which are involved in the vesicular transport that control the levels of phospholipids at the plasma membrane. The loss of Pdr16p function could alter plasma membrane lipid composition and as a consequence, directly or indirectly affect the functions of relevant membrane proteins such as ABC transporters (van den Hazel *et al.* 1999). Interestingly, a recent study showed that the *S. cerevisiae pdr16*Δ strain lost the ability to evolve resistance to fluconazole over 108 generations of asexual reproduction in the presence of increasing concentrations of fluconazole, showing that Pdr16p is necessary for the appearance and/or maintenance of the azole-resistant phenotype (Anderson *et al.* 2009). Taken together, it is tempting to speculate that Pdr16p maybe responsible for facilitating the proper trafficking and/or localization of membrane proteins important for azole resistance development, namely, Cdr1p/Cdr2p and Erg proteins at the plasma membrane (Griac 2007; Saito *et al.* 2007). This also suggests that genes that are co-regulated

with Cdr1p and Cdr2p are important for cellular survival in the presence of azoles. We hypothesize that other co-regulated genes with possible lipid translocation/metabolism functions could also contribute to the overall azole resistance. Among the list of Tac1p-dependent, Cdr1p/Cdr2p-coregulated genes, we are particularly interested in investigating whether another ABC transporter, encoded by *ORF19.4531* and a putative phospholipid floppase, encoded by *RTA3*, could contribute to the azole resistant phenotype (see below).

Other ABC transporters

In *S. cerevisiae*, there are other ABC transporters besides Pdr5p that contribute to the pleiotropic drug resistance phenotype, such as Yor1p and Snq2p. Genes encoding transporter proteins that are similar to *S. cerevisiae* Yor1p or Snq2p are found in *C. albicans*, however these genes have not been characterized yet. It remains to be tested whether these putative transporters could also protect *C. albicans* against azoles. The lack of attention to these transporters from the *Candida* research community may stem from the fact that their expression in clinical strains is rarely correlated with the clinical azole resistance phenotype (Liu *et al.* 2007). In contrast, another putative ABC transporter encoded by *ORF19.4531* attracted our interest as its expression is correlated with elevated azole resistance and regulated by Tac1p. We named it Cdr6p as it exhibits a domain organization that is similar to Cdr1p/Cdr2p (Liu *et al.* 2007) (Fig. V.2a). Interestingly, inspection of its amino acid sequences revealed that Cdr6p lacks the N-terminal regulatory sequences (NTE) found in Cdr1p/Cdr2p, suggesting a regulatory mechanism that is distinct from the Cdrp prototype transporters. Furthermore, unlike all other full-length transporters of the fungal ABCG family, Cdr6p contains two 'symmetrical' NBDs identified by the presence of the typical Walker A motif GxGK instead of the atypical NBD1 GxGC motif (Chapter I.5.2.5). Finally, recent phylogenic analyses showed that orthologous genes of Cdr6p are found in many fungal species belonging to the Saccharomycotina as well as the Basidiomycota phyla (Lamping *et al.* 2010). Taken together, it is tempting to propose that the Cdr6p-type transporter is an ancestral full-length

transporter of the yeast ABCG family with the NBD_1-TMD_1-NBD_2-TMD_2 organization since this transporter possesses two typical NBDs.

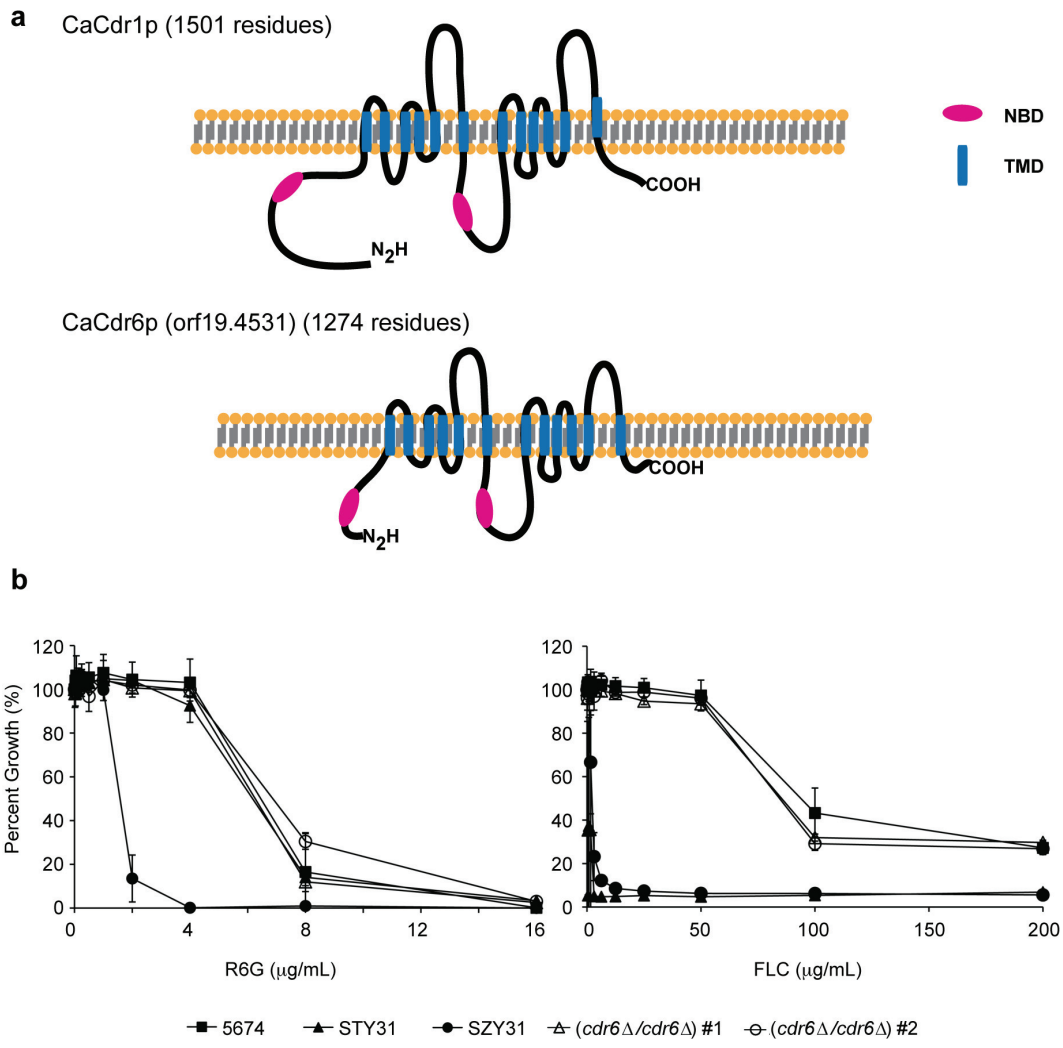

Figure V. 2 Characterization of *C. albicans* Cdr6p

(**a**) Schematic representation of Cdr1p and Cdr6 predicted topology. (**b**) Rhodamine 6G and fluconazole resistance profiles of 5674-derived *cdr6*Δ/*cdr6*Δ mutant strains were analyzed in MIC assays. STY31, 5674-derived *cdr1*Δ/*cdr1*Δ *cdr2*Δ/*cdr2*Δ. SZY31, 5674-derived *tac1*Δ/*tac1*Δ.

In the azole-resistant strain 5674, Cdr1p, Cdr2p and Cdr6p are up-regulated in a Tac1p-dependent manner, and deletion of Tac1p resulted in a significantly reduced resistance to rhodamine 6G (a fluorescent substrate of many ABC

transporters). These results suggest that Tac1p-regulated ABC transporters could be responsible for mediating the rhodamine 6G resistance in this strain. Surprisingly, deletion of Cdr1p and Cdr2p did not result in reduced resistance to rhodamine 6G (Chapter II, (Tsao *et al.* 2009)). These findings suggest that other Tac1p-regulated protein(s) besides Cdr1p and Cdr2p is involved in rhodamine 6G efflux in *C. albicans*. As Cdr6p is the third ABC transporter indentified in the Tac1p regulon, we considered that Cdr6p could be the rhodamine 6G transporter. In collaboration with Dr. P. David Rogers at the University of Tennessee, we began to characterize the function of this transporter by deleting the two alleles of *CDR6* from the azole resistant strain 5674 followed by drug susceptibility analyses (Fig. V.2b, unpublished data). Our result showed that deletion of this transporter did not affect cell susceptibility to rhodamine 6G, indicating that Cdr6p is not involved in rhodamine 6G transport. Rhodamine 6G hypersusceptibility in the *tac1Δ/tac1Δ* mutant is thus unlikely to be solely due to the lost of ABC transporters function. Instead, we favor the explanation that the increased rhodamine 6G sensitivity in the *tac1Δ/tac1Δ* mutant is due to the changes in the lipid or phospholipid composition of the plasma membrane. Additionally, our result showed that deletion of *CDR6* from strain 5674 did not reduce its azole resistance, suggesting that the contribution of Cdr6p to the overall azole resistance phenotype maybe negligible. However, we cannot exclude the possibility that the effect of *CDR6* deletion may be masked by the presence of strong Cdr1p activity. Future experiments will include investigations of Cdr6p function by deleting *CDR6* from the *cdr1Δ/cdr1Δ cdr2Δ/cdr2Δ* mutant strain and test the new mutant strain against a panel of different compounds with antifungal properties.

Genes involved in sphingolipid biosynthesis

We also investigated the function of another Tac1p-regulated gene, *RTA3*, which expression is strongly induced in several azole-resistant clinical isolates (Liu *et al.* 2007). Rta3p is a putative phospholipid floppase and sequence annotation suggests it could be the homolog of *S. cerevisiae* Rta1p (involved in 7-

aminocholesterol resistance, a cholesterol derivative with antibacterial and antifungal properties) or Rsb1p (involved in sphingoid long-chain base, LCB, export and its expression is induced in the *pdr5Δ* mutant strain; see below [(Kihara *et al.* 2002; Soustre *et al.* 1996); www.candidagenome.org)]. Using a protein domain prediction program and hydropathy analysis software, I propose that *C. albicans* Rta3p is an integral membrane protein with 7 transmembrane (TM) segments (Fig. V.3a). Furthermore, based on sequence alignment and phylogeny analyses, I found that the 7-TM Rta family contains an additional three members in *C. albicans*, Orf19.6244 (Rta1p), Rta2p and Rta4p. Interestingly, our analyses showed that all members of the *C. albicans* Rta family exhibit a closer evolutionary relationship to *S. cerevisiae* Rsb1p than Rta1p (Fig. V.3b). Nevertheless, experimental validations are required to confirm whether these proteins are indeed the functional homologs of *S. cerevisiae* Rsb1p. As already mentioned, *S. cerevisiae* Rsb1p is involved in the sphingolipid pathway by acting as a LCB exporter. LCBs can be cytotoxic if allowed to accumulate, and expression of Rsb1p prevents the inappropriate buildup of these sphingolipid intermediates. Interestingly, loss of Pdr5p (and Yor1p) from cells strongly elevates LCB resistance in a Rsb1p-dependent manner, linking the interconnections between sphingolipid biosynthesis and the function of these ABC transporters (Kihara *et al.* 2004).

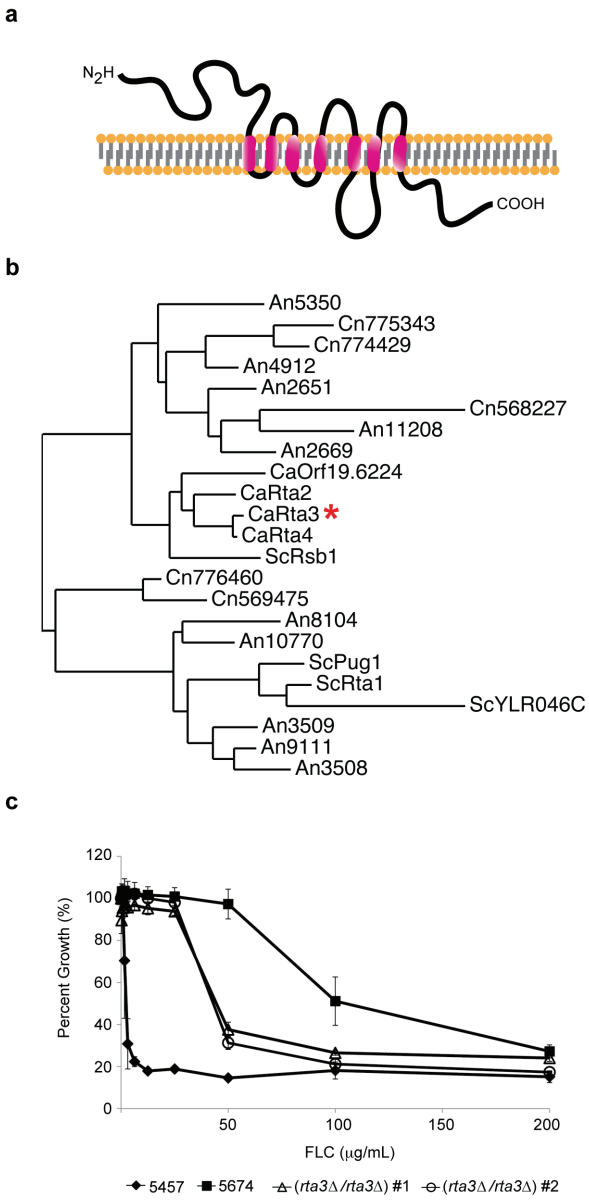

Figure V. 3 Characterization of *C. albicans* Rta3p

(**a**) Schematic representation of *C. albicans* Rta3p predicted topology. (**b**) Phylogenic analyses of Rta3p and fungal homologs. First, the sequence of CaRta3p has been used to blast against fungal databases to obtain a list of hit proteins. The sequences of these hit proteins were analyzed using SMART program (http://smart.embl-heidelberg.de/) to select the ones that contain at least 6 or preferred 7 transmembrane segments. There were 4 proteins of this family found in *S. cerevisiae*; 2 in *C. glabrata*; 4 in *C. albicans*, 5 in *C. neoformans*, 5 in *P. stipitis* and 10 in *A. nidulans*, (www. phylogeny.fr; with the default 'one click' mode). CaRta3p and CaRta4p are most homologous, sharing ~80% sequence identity. (**c**) Fluconazole resistance profiles of 5674-derived *rta3*Δ/*rta3*Δ mutants were analyzed in MIC assay.

Recently, *C. albicans RTA2* has been characterized (Jia *et al.* 2008; Jia *et al.* 2009). Although *RTA2* is not a Tac1p-dependent gene, its expression has been associated with azole resistant phenotype of *C. albicans* (Karababa *et al.* 2006; Xu *et al.* 2006). Moreover, deletion of *RTA2* increases, and overexpression of *RTA2* decreases the azole susceptibility in *C. albicans*, demonstrating its role in azole resistance (Jia *et al.* 2008; Jia *et al.* 2009). Since Rta2p and Rta3p are two homologous proteins sharing ~48% sequence identity, it is possible that Rta3p could, directly or indirectly contributes to the overall azole resistance in strain 5674. Indeed, our preliminary result showed that the deletion of the two alleles of *RTA3* from strain 5674 reduced the fluconazole resistance by two-fold, demonstrating that in addition to Cdr1p, Cdr2p and Pdr16p, Rta3p also contributes to azole resistance in strain 5674 (Fig. V.3c). It is possible that the reduced growth of the *rta3Δ/rta3Δ* mutant in the presence of fluconazole is the consequence of an increased accumulation of fluconazole, as lost of Rta3p function probably affects the levels of sphingolipid in the plasma membrane and enhances plasma membrane permeability. On the other hand, we cannot exclude the possibility that the contribution of Rta3p to overall azole resistance is through other yet unidentified mechanisms. A very recent report proposed that *S. cerevisiae* Rsb1p modulates the endocytosis pathway of the membrane protein tyrosine permease and potentially other membrane proteins as well (Johnson *et al.* 2010). According to this proposed model, one could imagine that Rta3p could also modulate the stability of membrane proteins in *C. albicans*, by affecting candidate proteins that are directly involved in azole export, for example, the Cdr1p/Cdr2p transporters. It would be interesting to investigate whether Rta3p could stabilize Cdr1p/Cdr2p levels in *C. albicans* azole-resistant strains. Protein levels of Cdr1p/Cdr2p can be compared in WT and the *rta3Δ/rta3Δ* mutant by Western blot analyses. In addition, to examine whether the contribution of Rta3p function to azole resistance is dependent of Cdr1p/Cdr2p function, deletion of *RTA3* in strain STY31 (*cdr1Δ/cdr1Δ cdr2Δ/cdr2Δ*) followed by azole susceptibility testing could be performed.

Finally, another gene that is involved in sphingolipid homeostasis and co-regulated with *CDR1/CDR2* by Tac1p is *LCB4*, which encodes a putative sphingosine kinase (Liu *et al.* 2007). The function of *LCB4* has not been characterized in *C. albicans*. In *S. cerevisiae*, regulation of Lcb4p has been linked to the ergosterol biosynthesis pathway and the lost of plasma membrane-localization of Lcb4p was found in an ergosterol biosynthesis mutant (*erg6Δ*) strain (Sano *et al.* 2005). This result highlights a potential extensive genetic interaction between the sphingolipid biosynthesis pathway and the ergosterol biosynthesis pathway, which in turn, indicates that the disruption of either pathway could affect the overall azole susceptibility of *C. albicans* cells. Sphingolipids are important constituents for the lipid rafts, where the Cdrp transporters are thought to be preferentially localized. Disruption of sphingolipid biosynthesis, namely, deletion of *LCB4* from *C. albicans*, could potentially result in the mislocalization of the Cdrp transporters and consequently cause reduction in azole resistance (Pasrija *et al.* 2008; Pasrija *et al.* 2005). Future experiments are required to characterize the function of *LCB4* and determine the contribution of Lcb4p to the overall azole resistance in strain 5674.

Taken together, I propose that the physiological role of the Tac1p regulon pathway is to regulate the function of the plasma membrane at the level of both lipids and membrane transporters. Identification and characterization of Tac1p targets reveal an intimate relationship between the ergosterol and the sphingolipid biosynthesis pathways, which are both necessary to overcome azole stress.

V.3 Discovery of novel antifungal targets

The ideal antifungal agent would meet the following criteria: effectiveness against a broad spectrum of fungi, low toxicity to human and low rates of resistance development. In line with this, preferences are given to drugs with a rapidly

acting fungicidal mode of action, as these drugs in principal do not allow the selection of resistant variants; hence, essential gene products would make better targets than non-essential gene products. In addition, extracellular targets are perhaps more favorable than intracellular targets as the intracellular action of drugs could elicit cellular responses for drug inactivation, sequestration and efflux pump-mediated resistance.

V.3.1 Inhibitors of ABC transporters

Azoles provide unique clinical advantages over the antifungal agents echinocandins and amphotericin B, as some azoles offer a flexible routes of administration (oral administration) and fewer associated adverse effects (Chapter I). Often encountered in the clinic, overexpression of ABC transporters Cdr1p and Cdr2p represents one of the major obstacles in effective azole chemotherapy; therefore, finding inhibitors to block the efflux capability of Cdr1p/Cdr2p appears to be an attractive therapeutic strategy to reverse and prevent the development of ABC transporter-mediated azole resistance. Moreover, such inhibitors could be used in combination with azoles to enhance their efficacy. In fact, we have shown that genetic inhibition of both Cdr1p and Cdr2p rendered azole hypersusceptibility in clinical *C. albicans* strains (Chapter II), providing genetic evidence supporting this approach.

To date, experimentally tested chemical modulators of yeast ABC transporters include Disulfiram (a drug clinically used for the treatment of alcoholism) and Curcumin (a natural product of the popular Indian spice turmeric). Both compounds have been shown to be potent modulators of the mammalian ABC transporter P-gp (Chearwae *et al.* 2004; Loo *et al.* 2000; Sharma *et al.* 2009; Shukla *et al.* 2004b). These compounds demonstrate synergistic activities with several antifungal agents against the growth of *S. cerevisiae* strains expressing Cdr1p by either directly interfering with the Cdr1p drug binding or inhibiting its ATPase activity (Sharma *et al.* 2009; Shukla *et al.* 2004b). Similarly, using

Cdr1p- or Cdr2p-expressing *S. cerevisiae* strains, researchers identified other chemosensitizers, such as milbemycins (insecticide macrolide), unnarmicin (cyclic peptide from marine bacterium) or synthetic D-octapeptides, which could be used to revert Cdr1p(/Cdr2p)-mediated azole resistance (Lamping *et al.* 2007; Niimi *et al.* 2004a; Tanabe *et al.* 2007). Taken together, these studies provided data supporting further investigation to find ABC transporter modulators those with specific affinity to both Cdr1p and Cdr2p in order to reverse the ABC transporter-mediated azole resistance. The next steps will be to test whether these compounds can also effectively sensitize *C. albicans* azole-resistant strains and if they can be used for treatment in human.

Besides the direct target inhibition of Cdr1p and Cdr2p, alternative strategy would involve the design of inhibitors that interrupt pathways involved in the modulation of the function of these transporters. For example, since phosphorylation of Cdr1p is important for its function (Chapter III), identification of the kinase(s) and of the signaling pathways involved in Cdr1p phosphorylation could potentially represent new and fungal-specific targets for Cdr1p inhibition. Alternatively, diminishing the overexpression of these transporters by targeting the transcription factor Tac1p could represent another strategy (see below).

In practical terms, there are considerations that argue against the pursuit of the development of Cdrp inhibitor as a therapeutic strategy. First, there are other mechanisms contributing to azole resistance and it is not uncommon to find azole-resistant strains carrying multiple resistance mechanisms, such as overexpression of Mdr1p and/or overexpression or mutation of Erg11p alone, or in combination with Cdr1p/Cdr2p overexpression (Chapter I.4.2). Because of this, the use of Cdrp-inhibitors would likely be ineffective in such cases. The second issue is linked to the fungal-specificity of these inhibitors. Ideal fungal ABC transporter inhibitors should offer high binding affinity to ABC transporters derived from different fungal origins for a broad spectrum of antifungal inhibition but present a low affinity to human ABC transporters. As ABC transporters are widely present

in human and contribute to various physiological functions, non-specific ABC transporter inhibitors could cause serious side effects in human. Extensive screening and counter screening for suitable inhibitor candidates will thus likely be necessary to avoid cross-reactivity with human transporters.

Taking into account the considerations discussed above in finding inhibitors directly against ABC transporters (azole resistance effectors), designing inhibitors targeting transcriptional regulations of these effector genes is perhaps a more attractive strategy. In fact, Tac1p belongs to a group of fungal-specific zinc cluster transcription factors, as members of this family bind to DNA in a zinc (or cadmium)-dependent manner (reviewed in (MacPherson *et al.* 2006)). In fungi, these transcription factors are involved in a wide variety of cellular processes including metabolism of sugar and amino acids, cellular morphogenesis, ergosterol biosynthesis. Importantly, there are at least three zinc cluster transcription factors demonstrated to be associated with multidrug resistance in *C. albicans* by controlling expression of various genes including those encoding drug efflux pumps (Cdr1p/Cdr2p and Mdr1p) and genes involved in ergosterol biosynthesis (Erg11p) (Chapter I.4.2). An efficient anti-zinc cluster compound could specifically target zinc binding and interfere with the DNA-binding activity of zinc cluster transcription factors. Such inhibitor would likely to cause cell growth inhibition by interfering with various cellular processes simultaneously. For example, inhibition of Tac1p could result in downregulation of Cdr1p/Cdr2p as well as factors involved in lipid metabolism. Since zinc cluster proteins are found in most, if not all, species of fungi and not in human, such inhibitor could provide a broad spectrum of antifungal actions without causing toxicity in human.

V.3.2 Histone modifications as targets for antifungal therapy

Histone modifications as novel anticancer/antifungal strategy

Chromatin is made of a complex of histone proteins and DNA. Chromatin structure is therefore recognized as an important regulator of various processes

such as gene expression, DNA repair and DNA replication. Acetylation state of specific lysine residues in histone proteins can alter chromatin structure and functions. Importantly, there are emerging data implicating these histone acetylations in the pathobiology of cancers and other diseases; therefore enzymes that catalyze histone acetylation (histone acetyltransferases, HATs) and that remove the acetyl groups from acetylated histones (histone deacetylases, HDACs) have become targets of choice for chemotherapy. Well-known examples of histone deacetylase inhibitor (HDACi) that have clinical implications include trichostatin A (TSA) and suberoylanilide hydroxamic acid (SAHA), which have been shown to exhibit anti-leukaemia and anti-cutaneous T cell lymphoma properties, respectively. Furthermore, there are a few other HDACi currently in clinical trials as anticancer drugs [reviewed in (Bolden *et al.* 2006; Mai 2007)].

Previous studies showed that HDACi could also be used in antifungal therapies. TSA has been shown to reduce the azole trailing effect through reduction in azole-dependent upregulation of *CDR*/*ERG* genes and can be used in combination therapy with azoles [(Smith *et al.* 2002); Chapter I.3.4.2]. We hypothesized that the study of chromatin dynamics, specifically HATs and HDACs and their roles in *C. albicans* biology, pathogenesis and survival could uncover potential targets for antifungal therapies.

Studies of chromatin biology and histone modifications in *C. albicans*

Current knowledge of chromatin biology in *C. albicans* is very limited. Although genes encoding histones as well as histone modifying enzymes have been annotated in *C. albicans* based on sequence homology with that in *S. cerevisiae*, their functional roles have largely been left undefined. One of the first studies on chromatin biology in *C. albicans* has recently been published. The *C. albicans* genome contains two genes (*HHF1* and *HHF22*, total four alleles) encoding identical histone H4 proteins. Deletion any three of these alleles showed severe growth defects and altered morphologies when grown under the standard growth condition (YPD, 30 ^{o}C). Interestingly, a small population of these cells would

counterbalance the low dosage of nucleosomal histone H4 by increasing histone H4 gene copy number through the formation of aneuploidies (Zacchi *et al.* 2010b). In *C. albicans*, altered morphological changes (yeast-to-hyphae transition) and aneuploidy formation have been demonstrated to be associated with virulence as well as antifungal resistance [see Chapter I.1.1.1 and the recent review (Selmecki *et al.* 2010)], linking chromatin biology with *C. albicans* pathogenesis. Another study demonstrated the deletion of genes encoding the Set3p/Hos2p histone deacetylase complex (SetC) from *C. albicans* leads to a constitutive hyper-filamentation phenotype at 37 ^{o}C. Specifically, this histone deacetylase complex has been shown to be involved in the negative regulation of the cAMP/PKA signaling, genetic deletion of this complex enhances the Efg1p-dependent constitutive hyperfilamentation and the mutant strain displays strongly attenuated virulence in a murine model of system infection (Hnisz *et al.* 2010). Interestingly, this morphological phenotype can also be mimicked by the addition of HDACi TSA. Taken together, these studies demonstrated that important cellular functions attributed to *C. albicans* virulence traits could be modulated at the level of nucleosomes and it is possible that the different HDACs and HDACi could have diverse effects on *C. albicans* pathogenesis (Hnisz *et al.* 2010; Zacchi *et al.* 2010a; Zacchi *et al.* 2010b). These studies support the idea of developing antifungal drugs that modulate the chromatin functions as a novel approach to antifungal therapy. In line with this, the pharmaceutical company MethylGene Inc. has recently discovered a HDACi small molecule (MGCD290) that inhibits the Hos2p function and showed that this compound increases the fungal sensitivity to azoles and broadens the spectrum of azole activity *in vitro*, including azole-resistant clinical isolates (Pfaller *et al.* 2009).

Characterization of H3K56 acetylation in *C. albicans*

While the most characterized histone modifications in *S. cerevisiae* and mammalian cells are those in the flexible N- and C-terminal tails (see reviews (Corpet *et al.* 2009; Kouzarides 2007), residues in the core domain are also modified. A series of studies have shown that histone H3 lysine 56 (H3K56), in

the H3 core domain, is a frequent site of acetylation in fungi (*S. cerevisiae* and *Schizosaccharomyces pombe*) (Masumoto *et al.* 2005; Xhemalce *et al.* 2007); more recently, this modification has also been discovered in flies and mammals (Das *et al.* 2009).

In *S. cerevisiae*, H3K56 acetylation (H3K56ac) is an abundant modification found in newly synthesized histones during the S-phase, but it disappears rapidly when cells enter the G2/M phase of the cell cycle (Masumoto *et al.* 2005). *S. cerevisiae* strains that lack this particular modification were genetically unstable and hypersusceptible to genotoxic agents, demonstrating that H3K56 acetylation plays an important role in DNA damage response (Masumoto *et al.* 2005). Enzymes involved in H3K56 acetylation, histone acetyltransferase Rtt109 and deacetylase Hst3p/Hst4p have been characterized (Celic *et al.* 2006; Driscoll *et al.* 2007). Deleting *RTT109* or expressing H3 with nonacetylable lysine 56 (H3K56R) in *S. cerevisiae* resulted in an increased frequency of spontaneous chromosome breaks and increased sensitivity to genotoxic agents (Driscoll *et al.* 2007). The strain lacking Hst3p/Hst4p also exhibited important phenotypes such as spontaneous DNA damage, chromosome loss, as well as increased genotoxic sensitivity (Celic *et al.* 2006). Taken together, these results support the notion that H3K56 acetylation is important to cells at least during the DNA replication to maintain genome stability.

Interestingly, Hst3p/Hst4p and Rtt109p exhibit fungal specific properties, thus representing potential antifungal targets. In the present thesis, we characterized H3K56ac in *C. albicans* and *C. albicans* Rtt109p and Hst3p involved in the H3K56 acetylation and deacetylation processes (Chapter IV; (Wurtele *et al.* 2010)). We found that deletion of *RTT109* led to an increased antifungal susceptibility against echinocandins but not azoles, a result that is due to an increased sensitivity to oxidative stress (which resulted in DNA damage) in the *rtt109Δ/rtt109Δ* strain. Indeed, a separate study published during the review process of our article also showed that *C. albicans rtt109Δ/rtt109Δ* cells exhibited

an increased sensitivity to reactive oxygen species (ROS)-mediated killing by macrophages and that genes involved in oxidative stress response were upregulated in these cells (Lopes da Rosa *et al.* 2010). Taken together, these results are consistent with findings in *S. cerevisiae* showing that H3K56 acetylation is important for protecting cells from DNA-damaging agents (Masumoto *et al.* 2005). In addition, both our study and the one from Lopes da Rosa *et al*. showed that *C. albicans rtt109Δ/rtt109Δ* mutant exhibit a slow growth phenotype accompanied by altered morphologies when grown under standard growth conditions, leading to significantly attenuated virulence in the mouse models of *Candida* infections [Chapter IV, (Lopes da Rosa *et al.* 2010; Wurtele *et al.* 2010)]. Since Rtt109p is a fungal-specific enzyme, compounds that could interfere with Rtt109p function could potentially diminish fungal pathogenesis while being less toxic to human. Also, Rtt109p inhibitors could sensitize cells to echinocandins.

We also characterized Hst3p, the fungal-specific HDAC enzyme for H3K56ac [Chapter IV; (Wurtele *et al.* 2010)]. Our data showed that loss of Hst3p function resulted in a severe loss of cell viability. Indeed, we showed that *HST3* is an essential gene and that downregulation of *HST3* resulted in accumulation of high H3K56ac levels, which subsequently led to a massive genomic DNA fragmentation and inevitable cell death. Although the exact mechanism of how an elevated level of H3K56 acetylation lead to cell death is not known, we have observed interesting phenotypes of these cells. As most of these phenotypes have already been extensively discussed in Chapter IV (Wurtele *et al.* 2010), here I would like to elaborate the discussion on the morphological changes observed in Hst3p-repression cells. The time course study of Hst3p-repression showed that at the beginning of Hst3p-repression (cell growth in the repressing condition for 3 hours), cells appeared to divide normally, as many dividing oval-shaped yeast cells were observed [Chapter IV, Fig. IV.3b; (Wurtele *et al.* 2010)]. However, at 6 hours, we observed a morphological change from oval budding yeast-like cells to cells with elongated shapes that resemble pseudohyphae. Finally, after 9 hours,

we observed that in majority, two extended rod-shape like cells attached to a round yeast cell, presenting as a 'V-shaped' filament [Chapter IV, Fig IV.3b; (Wurtele *et al.* 2010)]. Additionally, I also observed that the width of 'filament' (the extended rod-shape cells) appears to be roughly 2-times wider than that of the spider medium-induced *C. albicans* filament (Chapter IV, Fig IV.3a and b-panel 9 or 24 h). Since *C. albicans* morphogenesis and the control of cell size is closely linked to its cell cycle progression (Berman 2006), these results demonstrated that the altered cell cycle control could also be one of many consequences accompanied by downregulation of Hst3p. Future studies will be to investigate how elevated level of H3K56 acetylation could cause cell death in *C. albicans*. It would be interesting to perform immunofluorescence microscopy analyses of Hst3p-repressed cells with DNA damage markers (for example, the TUNEL staining) to determine the types of DNA damage that concomitantly occurred with increased H3K56 acetylation. Furthermore, microarray profiling of Hst3p-repressed cells could reveal changes of gene expression and their related function (gene ontology term), providing insights of which cellular pathways are most affected by downregulating Hst3p. Importantly, all these experiments should be performed in a time-course dependent manner and the levels of H3K56 acetylation in these cells would be monitored by quantitative mass spectrometry.

Our data demonstrated that the essentiality of Hst3p for cell survival argues that Hst3p may be a more suitable antifungal therapy target than Rtt109p. We also showed that the use of nicotinamide as an inhibitor of Hst3p phenocopied the effect downregulating Hst3p *in vitro*. Finally, we showed that short-term treatment of nicotinamide reduced fungal load in mice infected by wild-type *C. albicans* cells but not by the *rtt109Δ/rtt109Δ* mutant cells, indicating that nicotinamide exerts its therapeutic effect through inhibition of Hst3p-mediated H3K56 deacetylation. These proof-of-principle experiments demonstrated that inhibition of Hst3p by HDACi (nicotinamide or derivatives, see below) could be a novel therapeutic intervention against fungal pathogens, not limited to *C. albicans*.

Future studies will include long-term mouse experiments, which are required to evaluate the therapeutic effectiveness of nicotinamide against fungal infections. At present, our animal experiments are terminated at 24 hours after infection due to experimental limitations. The A/J mice (Chapter I.2.3) are extremely sensitive to fungal infections and allow a fast development of candidiasis within 24 hours after injection of *C. albicans* inoculum. Another major challenge in future experiments is the maintenance of sufficient nicotinamide concentrations *in vivo*. Nicotinamide is a form of vitamin B3 and the precursor for the coenzyme β-nicotinamide adenine dinucleotide (NAD^+); once nicotinamide is injected in the mice, it is quickly metabolized and has an estimated short half-life of approximately 2 hours (Horsman *et al.* 1997). Due to technical and ethical considerations, we injected nicotinamide into mice intra-peritoneally only twice and these two injections were 8 hours apart. It is likely that the potential protective effect of nicotinamide was incomplete under these conditions. Hence, we will try different methods, including lowering the initial *C. albicans* inoculum in order to allow a slower disease progression and change the route of nicotinamide administration by adding nicotinamide in the mice drinking water (Green *et al.* 2008). In parallel, we could also try to use nicotinamide derivatives that maybe more metabolically stable *in vivo* (Girgis *et al.* 2006).

Nicotinamide uptake

We showed that nicotinamide could inhibit the growth of several other pathogenic fungi to different extent [Chapter IV; (Wurtele *et al.* 2010)]. While the sequences encoding Hst3p homologs are found in the genome of these fungi and the catalytic motifs are also conserved across these species, their functions have not been characterized and their effect on H3K56 acetylation is not known. Assuming that H3K56 acetylation exists in these fungi and plays a similar crucial role in maintaining genome stability, the observed differential sensitivities to nicotinamide could be explained in part by the presence of different uptake systems in these fungi. Although it is not known how nicotinamide enters into the

cell, facilitated diffusion via transporters has been proposed. This proposition is based on the recent identification of transporters for NAD^+ precursors (nicotinamide, nicotinamide riboside or nicotinic acid) in *S. cerevisiae* and *C. glabrata*, suggesting that multi-membrane spanning Fur4p uracil permease-like transporters could be involved in nicotinamide import (Belenky *et al.* 2008; Ma *et al.* 2009). Identification of the nicotinamide uptake systems in these pathogenic fungi could help us developing a more efficient antifungal therapeutic strategy involving the use of nicotinamide. However, we cannot exclude the possibility that different fungi may adopt different metabolic pathways for processing NAD^+ precursors, which should also be taken into consideration.

Structural-function studies of Hst3p

Our data showed that fungal Hst3p appears to be highly substrate-specific (recognizes only H3K56 acetylation) since in *S. cerevisiae* and in *C. albicans*, acetylation of several sites in the N-terminal tails of H3 or H4 did not increase in the absence of Hst3p or Hst4p [Chapter IV, (Celic *et al.* 2006; Wurtele *et al.* 2010)]. Sequence alignment of fungal Hst3p and human homologs sirtuins SIRT1 and SIRT2 revealed the presence of conserved fungal Hst3p motifs that are absent from human sirtuins. Altogether, these findings suggest that it is conceivable that small molecules may inhibit only fungal Hst3p without affecting human sirtuins. We propose to perform large-scale chemical compound library screening for finding such inhibitor. The experiment will include the use of cell-based assays to screen for compounds that inhibit the growth of wild-type *C. albicans* cells but show no activity against the *rtt109Δ/rtt109Δ* mutant. This process will ensure the selection of compounds that exert their inhibitory activity in the Rtt109-dependent H3K56 acetylation manner, by most likely acting through the inhibition of Hst3p. In parallel, determine the structure of fungal Hst3p, for example, by X-ray crystallography, could aid in the rational design of inhibitors that specifically target Hst3p and also for performing structure-activity relationship analyses on putative hits identified in the large-scale screening.

would facilitate the virtual screening and/or rational design of inhibitors that specifically target Hst3p. Hst3p is a small (~50 kDa) cytosolic protein, unlike the large multi-membrane spanning ABC transporters, hence crystallization of Hst3p should be much less problematic. High-resolution human SIRT crystal structures are already available (Cosgrove *et al.* 2006; Finnin *et al.* 2001; Jin *et al.* 2009) and could serve as future references for comparison with the fungal Hst3p structure and contribute to our understanding of the substrate selectivity of Hst3p.

V.4 Conclusion

Azole resistance in *C. albicans* involves multiple transcriptional pathways governing different cellular mechanisms, Tac1p-dependent Cdr1p and Cdr2p overexpression contributing to high levels of azole resistance in clinical azole resistant isolates. I showed that genetic inhibition of Cdr1p and Cdr2p abolished azole resistance in a clinical azole-resistant strain and furthermore, it conferred hypersusceptibility of *C. albicans* to azoles. These data support the proposition that finding a pharmacological inhibitor against both Cdr1p and Cdr2p could be one of the future therapeutic options to circumvent azole resistance mediated by Cdr1p and Cdr2p. However, finding a specific inhibitor against fungal ABC transporters that will not affect human ABC transporters poses a major challenge. Hence, I began to study the phosphorylation-related regulatory pathway of these transporters, in the hope to understand how these transporters are regulated. Finally, I focused on the characterization of evolutionary conserved, fungal-specific genes involved in chromatin biology of *C. albicans*. I showed that *HST3*, encoding a histone deacetylase of an abundant fungal histone modification H3K56, has crucial functions for *C. albicans* survival. Based on results presented in this thesis, I favor future investigations focusing in the direction of finding Hst3p inhibitors as a novel, effective antifungal strategy.

Chapter VI

Bibliography

Chapter VI Bibliography

1 Abele, R. and Tampe, R. (2004). The ABCs of immunology: structure and function of TAP, the transporter associated with antigen processing. Physiology (Bethesda) **19**: 216-224.

2 Akins, R.A. (2005). An update on antifungal targets and mechanisms of resistance in *Candida albicans* Med Mycol **43**: 285-318.

3 Albertson, G.D., Niimi, M., Cannon, R.D. and Jenkinson, H.F. (1996). Multiple efflux mechanisms are involved in *Candida albicans* fluconazole resistance. Antimicrob Agents Chemother **40**: 2835-2841.

4 Albrecht, C. and Viturro, E. (2007). The ABCA subfamily--gene and protein structures, functions and associated hereditary diseases. Pflugers Arch **453**: 581-589.

5 Aller, S.G., Yu, J., Ward, A., Weng, Y., Chittaboina, S., Zhuo, R., Harrell, P.M., Trinh, Y.T., Zhang, Q., Urbatsch, I.L.*, et al.* (2009). Structure of P-glycoprotein reveals a molecular basis for poly-specific drug binding. Science **323**: 1718-1722.

6 Allikmets, R., Singh, N., Sun, H., Shroyer, N.F., Hutchinson, A., Chidambaram, A., Gerrard, B., Baird, L., Stauffer, D., Peiffer, A.*, et al.* (1997). A photoreceptor cell-specific ATP-binding transporter gene (ABCR) is mutated in recessive Stargardt macular dystrophy. Nat Genet **15**: 236-246.

7 Alvarez, F.J., Douglas, L.M. and Konopka, J.B. (2007). Sterol-rich plasma membrane domains in fungi. Eukaryot Cell **6**: 755-763.

8 Ambudkar, S.V., Dey, S., Hrycyna, C.A., Ramachandra, M., Pastan, I. and Gottesman, M.M. (1999). Biochemical, cellular, and pharmacological aspects of the multidrug transporter. Annu Rev Pharmacol Toxicol **39**: 361-398.

9 Anaissie, E.J., Stratton, S.L., Dignani, M.C., Summerbell, R.C., Rex, J.H., Monson, T.P., Spencer, T., Kasai, M., Francesconi, A. and Walsh, T.J. (2002). Pathogenic *Aspergillus* species recovered from a hospital water system: a 3-year prospective study. Clin Infect Dis **34**: 780-789.

10 Anderson, J.B. (2005). Evolution of antifungal-drug resistance: mechanisms and pathogen fitness. Nat Rev Microbiol **3**: 547-556.

11 Anderson, J.B., Sirjusingh, C., Syed, N. and Lafayette, S. (2009). Gene expression and evolution of antifungal drug resistance. Antimicrob Agents Chemother **53**: 1931-1936.

12 Asai, K., Tsuchimori, N., Okonogi, K., Perfect, J.R., Gotoh, O. and Yoshida, Y. (1999). Formation of azole-resistant Candida albicans by mutation of sterol 14-demethylase P450. Antimicrob Agents Chemother **43**: 1163-1169.

13 Ashman, R.B., Fulurija, A. and Papadimitriou, J.M. (1996). Strain-dependent differences in host response to *Candida albicans* infection in mice are related to organ susceptibility and infectious load. Infect Immun **64**: 1866-1869.

14 Ashman, R.B., Papadimitriou, J.M., Fulurija, A., Drysdale, K.E., Farah, C.S., Naidoo, O. and Gotjamanos, T. (2003). Role of complement C5 and T lymphocytes in pathogenesis of disseminated and mucosal candidiasis in susceptible DBA/2 mice. Microb Pathog **34**: 103-113.

15 Avalos, J.L., Bever, K.M. and Wolberger, C. (2005). Mechanism of sirtuin inhibition by nicotinamide: altering the NAD(+) cosubstrate specificity of a Sir2 enzyme. Mol Cell **17**: 855-868.

16 Avalos, J.L., Boeke, J.D. and Wolberger, C. (2004). Structural basis for the mechanism and regulation of Sir2 enzymes. Mol Cell **13**: 639-648.
17 Bain, J.M., Stubberfield, C. and Gow, N.A. (2001). Ura-status-dependent adhesion of Candida albicans mutants. FEMS Microbiol Lett **204**: 323-328.
18 Balan, I., Alarco, A.M. and Raymond, M. (1997). The *Candida albicans CDR3* gene codes for an opaque-phase ABC transporter. J Bacteriol **179**: 7210-7218.
19 Balzi, E., Wang, M., Leterme, S., Van, D.L. and Goffeau, A. (1994). *PDR5*, a novel yeast multidrug resistance conferring transporter controlled by the transcription regulator PDR1 J Biol Chem **269**: 2206-2214.
20 Banerjee, D., Martin, N., Nandi, S., Shukla, S., Dominguez, A., Mukhopadhyay, G. and Prasad, R. (2007). A genome-wide steroid response study of the major human fungal pathogen *Candida albicans* Mycopathologia **164**: 1-17.
21 Barker, K.S., Pearson, M.M. and Rogers, P.D. (2003). Identification of genes differentially expressed in association with reduced azole susceptibility in *Saccharomyces cerevisiae*. J Antimicrob Chemother **51**: 1131-1140.
22 Belenky, P.A., Moga, T.G. and Brenner, C. (2008). *Saccharomyces cerevisiae YOR071C* encodes the high affinity nicotinamide riboside transporter Nrt1. J Biol Chem **283**: 8075-8079.
23 Ben-Yaacov, R., Knoller, S., Caldwell, G.A., Becker, J.M. and Koltin, Y. (1994). *Candida albicans* gene encoding resistance to benomyl and methotrexate is a multidrug resistance gene. Antimicrob Agents Chemother **38**: 648-652.
24 Bennett, R.J. (2009). A *Candida*-based view of fungal sex and pathogenesis. Genome Biol **10**: 230.
25 Bennett, R.J. and Johnson, A.D. (2005). Mating in *Candida albicans* and the search for a sexual cycle. Annual review of microbiology **59**: 233-255.
26 Berman, J. (2006). Morphogenesis and cell cycle progression in *Candida albicans*. Curr Opin Microbiol **9**: 595-601.
27 Berman, J. and Sudbery, P.E. (2002). *Candida albicans*: a molecular revolution built on lessons from budding yeast. Nat Reviews **3**: 918-930.
28 Blanco, J.L. and Garcia, M.E. (2008). Immune response to fungal infections. Vet Immunol Immunopathol **125**: 47-70.
29 Blander, G., Olejnik, J., Krzymanska-Olejnik, E., McDonagh, T., Haigis, M., Yaffe, M.B. and Guarente, L. (2005). SIRT1 shows no substrate specificity in vitro. J Biol Chem **280**: 9780-9785.
30 Bodzioch, M., Orso, E., Klucken, J., Langmann, T., Bottcher, A., Diederich, W., Drobnik, W., Barlage, S., Buchler, C., Porsch-Ozcurumez, M*., et al.* (1999). The gene encoding ATP-binding cassette transporter 1 is mutated in Tangier disease. Nat Genet **22**: 347-351.
31 Bogan, K.L. and Brenner, C. (2008). Nicotinic acid, nicotinamide, and nicotinamide riboside: a molecular evaluation of NAD+ precursor vitamins in human nutrition. Annual review of nutrition **28**: 115-130.
32 Bohnert, J.A., Karamian, B. and Nikaido, H. (2010). Optimized Nile Red efflux assay of AcrAB-TolC multidrug efflux system shows competition between substrates. Antimicrob Agents Chemother **54**: 3770-3775.
33 Bolden, J.E., Peart, M.J. and Johnstone, R.W. (2006). Anticancer activities of histone deacetylase inhibitors. Nat Rev Drug Discov **5**: 769-784.
34 Braun, B.R., Head, W.S., Wang, M.X. and Johnson, A.D. (2000). Identification and characterization of TUP1-regulated genes in Candida albicans. Genetics **156**: 31-44.

35 Braun, B.R., van Het Hoog, M., d'Enfert, C., Martchenko, M., Dungan, J., Kuo, A., Inglis, D.O., Uhl, M.A., Hogues, H., Berriman, M*., et al.* (2005). A human-curated annotation of the *Candida albicans* genome. PLoS Genet **1**: 36-57.

36 Buchanan, K.L. and Murphy, J.W. (1998). What makes *Cryptococcus neoformans* a pathogen? Emerg Infect Dis **4**: 71-83.

37 Burke, M.A. and Ardehali, H. (2007). Mitochondrial ATP-binding cassette proteins. Transl Res **150**: 73-80.

38 Cannon, R.D., Lamping, E., Holmes, A.R., Niimi, K., Baret, P.V., Keniya, M.V., Tanabe, K., Niimi, M., Goffeau, A. and Monk, B.C. (2009). Efflux-mediated antifungal drug resistance. Clin Microbiol Rev **22**: 291-321.

39 Cannon, R.D., Lamping, E., Holmes, A.R., Niimi, K., Tanabe, K., Niimi, M. and Monk, B.C. (2007). *Candida albicans* drug resistance another way to cope with stress. Microbiology **153**: 3211-3217.

40 Cappelletty, D. and Eiselstein-McKitrick, K. (2007). The echinocandins. Pharmacotherapy **27**: 369-388.

41 Celic, I., Masumoto, H., Griffith, W.P., Meluh, P., Cotter, R.J., Boeke, J.D. and Verreault, A. (2006). The sirtuins hst3 and Hst4p preserve genome integrity by controlling histone h3 lysine 56 deacetylation. Curr Biol **16**: 1280-1289.

42 Chamilos, G., Lionakis, M.S., Lewis, R.E. and Kontoyiannis, D.P. (2007). Role of mini-host models in the study of medically important fungi. Lancet Infect Dis **7**: 42-55.

43 Chang, Y.C. and Kwon-Chung, K.J. (1994). Complementation of a capsule-deficient mutation of *Cryptococcus neoformans* restores its virulence. Molecular and cellular biology **14**: 4912-4919.

44 Chang, Y.C., Stins, M.F., McCaffery, M.J., Miller, G.F., Pare, D.R., Dam, T., Paul-Satyaseela, M., Kim, K.S. and Kwon-Chung, K.J. (2004). *Cryptococcal* yeast cells invade the central nervous system via transcellular penetration of the blood-brain barrier. Infect Immun **72**: 4985-4995.

45 Chayakulkeeree, M. and Perfect, J.R. (2006). Cryptococcosis. Infect Dis Clin North Am **20**: 507-544.

46 Chearwae, W., Anuchapreeda, S., Nandigama, K., Ambudkar, S.V. and Limtrakul, P. (2004). Biochemical mechanism of modulation of human P-glycoprotein (ABCB1) by curcumin I, II, and III purified from Turmeric powder. Biochem Pharmacol **68**: 2043-2052.

47 Cheung, J.C., Kim Chiaw, P., Pasyk, S. and Bear, C.E. (2008). Molecular basis for the ATPase activity of CFTR. Arch Biochem Biophys **476**: 95-100.

48 Chi, A., Huttenhower, C., Geer, L.Y., Coon, J.J., Syka, J.E., Bai, D.L., Shabanowitz, J., Burke, D.J., Troyanskaya, O.G. and Hunt, D.F. (2007). Analysis of phosphorylation sites on proteins from *Saccharomyces cerevisiae* by electron transfer dissociation (ETD) mass spectrometry. Proc Natl Acad Sci U S A **104**: 2193-2198.

49 Conseil, G., Perez-Victoria, J.M., Jault, J.M., Gamarro, F., Goffeau, A., Hofmann, J. and Di Pietro, A. (2001). Protein kinase C effectors bind to multidrug ABC transporters and inhibit their activity. Biochemistry **40**: 2564-2571.

50 Corpet, A. and Almouzni, G. (2009). Making copies of chromatin: the challenge of nucleosomal organization and epigenetic information. Trends Cell Biol **19**: 29-41.

51 Cosgrove, M.S., Bever, K., Avalos, J.L., Muhammad, S., Zhang, X. and Wolberger, C. (2006). The structural basis of sirtuin substrate affinity. Biochemistry **45**: 7511-7521.

52 Coste, A., Selmecki, A., Forche, A., Diogo, D., Bougnoux, M.E., d'Enfert, C., Berman, J. and Sanglard, D. (2007). Genotypic evolution of azole resistance mechanisms in sequential *Candida albicans* isolates. Eukaryot Cell **6**: 1889-1904.

53 Coste, A., Turner, V., Ischer, F., Morschhauser, J., Forche, A., Selmecki, A., Berman, J., Bille, J. and Sanglard, D. (2006). A mutation in Tac1p, a transcription factor regulating *CDR1* and *CDR2*, is coupled with loss of heterozygosity at chromosome 5 to mediate antifungal resistance in *Candida albicans* Genetics **172**: 2139-2156.

54 Coste, A.T., Crittin, J., Bauser, C., Rohde, B. and Sanglard, D. (2009). Functional analysis of cis- and trans-acting elements of the *Candida albicans CDR2* promoter with a novel promoter reporter system. Eukaryot Cell **8**: 1250-1267.

55 Coste, A.T., Karababa, M., Ischer, F., Bille, J. and Sanglard, D. (2004). *TAC1*, transcriptional activator of *CDR* genes, is a new transcription factor involved in the regulation of *Candida albicans* ABC transporters *CDR1* and *CDR2* Eukaryot Cell **3**: 1639-1652.

56 Cowen, L.E. (2008). The evolution of fungal drug resistance: modulating the trajectory from genotype to phenotype. Nat Rev Microbiol **6**: 187-198.

57 Cowen, L.E., Anderson, J.B. and Kohn, L.M. (2002). Evolution of drug resistance in *Candida albicans*. Annual review of microbiology **56**: 139-165.

58 Cowen, L.E. and Lindquist, S. (2005). Hsp90 potentiates the rapid evolution of new traits: drug resistance in diverse fungi. Science **309**: 2185-2189.

59 Cowen, L.E., Singh, S.D., Kohler, J.R., Collins, C., Zaas, A.K., Schell, W.A., Aziz, H., Mylonakis, E., Perfect, J.R., Whitesell, L.*, et al.* (2009). Harnessing Hsp90 function as a powerful, broadly effective therapeutic strategy for fungal infectious disease. Proc Natl Acad Sci U S A **106**: 2818-2823.

60 Cruz, M.C., Goldstein, A.L., Blankenship, J.R., Del Poeta, M., Davis, D., Cardenas, M.E., Perfect, J.R., McCusker, J.H. and Heitman, J. (2002). Calcineurin is essential for survival during membrane stress in *Candida albicans*. The EMBO journal **21**: 546-559.

61 Dagenais, T.R. and Keller, N.P. (2009). Pathogenesis of *Aspergillus fumigatus* in invasive aspergillosis. Clin Microbiol Rev **22**: 447-465.

62 Dahan, D., Evagelidis, A., Hanrahan, J.W., Hinkson, D.A., Jia, Y., Luo, J. and Zhu, T. (2001). Regulation of the CFTR channel by phosphorylation. Pflugers Arch **443**: S92-96.

63 Daleke, D.L. (2008). Regulation of phospholipid asymmetry in the erythrocyte membrane. Curr Opin Hematol **15**: 191-195.

64 Das, C., Lucia, M.S., Hansen, K.C. and Tyler, J.K. (2009). CBP/p300-mediated acetylation of histone H3 on lysine 56. Nature **459**: 113-117.

65 Davidson, A.L. and Chen, J. (2004). ATP-binding cassette transporters in bacteria. Annu Rev Biochem **73**: 241-268.

66 Dawson, R.J. and Locher, K.P. (2006). Structure of a bacterial multidrug ABC transporter. Nature **443**: 180-185.

67 De Backer, M.D., Magee, P.T. and Pla, J. (2000). Recent developments in molecular genetics of *Candida albicans*. Annual review of microbiology **54**: 463-498.

68 De, M.M., Bille, J., Schueller, C. and Sanglard, D. (2002). A common drug-responsive element mediates the upregulation of the *Candida albicans* ABC transporters *CDR1* and *CDR2*, two genes involved in antifungal drug resistance. Mol Microbiol **43**: 1197-1214.

69 Dean, M. and Allikmets, R. (2001a). Complete characterization of the human ABC gene family. J Bioenerg Biomembr **33**: 475-479.
70 Dean, M., Hamon, Y. and Chimini, G. (2001b). The human ATP-binding cassette (ABC) transporter superfamily. J Lipid Res **42**: 1007-1017.
71 Dean, M., Rzhetsky, A. and Allikmets, R. (2001c). The human ATP-binding cassette (ABC) transporter superfamily. Genome Res **11**: 1156-1166.
72 Decottignies, A. and Goffeau, A. (1997). Complete inventory of the yeast ABC proteins. Nat Genet **15**: 137-145.
73 Decottignies, A., Grant, A.M., Nichols, J.W., de Wet, H., McIntosh, D.B. and Goffeau, A. (1998). ATPase and multidrug transport activities of the overexpressed yeast ABC protein Yor1p. J Biol Chem **273**: 12612-12622.
74 Decottignies, A., Kolaczkowski, M., Balzi, E. and Goffeau, A. (1994). Solubilization and characterization of the overexpressed *PDR5* multidrug resistance nucleotide triphosphatase of yeast. J Biol Chem **269**: 12797-12803.
75 Decottignies, A., Lambert, L., Catty, P., Degand, H., Epping, E.A., Moye-Rowley, W.S., Balzi, E. and Goffeau, A. (1995). Identification and characterization of SNQ2, a new multidrug ATP binding cassette transporter of the yeast plasma membrane. J Biol Chem **270**: 18150-18157.
76 Decottignies, A., Owsianik, G. and Ghislain, M. (1999). Casein kinase I-dependent phosphorylation and stability of the yeast multidrug transporter Pdr5p. J Biol Chem **274**: 37139-37146.
77 Deeley, R.G., Westlake, C. and Cole, S.P. (2006). Transmembrane transport of endo- and xenobiotics by mammalian ATP-binding cassette multidrug resistance proteins. Physiological reviews **86**: 849-899.
78 Deere, D., Shen, J., Vesey, G., Bell, P., Bissinger, P. and Veal, D. (1998). Flow cytometry and cell sorting for yeast viability assessment and cell selection. Yeast **14**: 147-160.
79 Denning, D.W. (1998). Invasive aspergillosis. Clin Infect Dis **26**: 781-803; quiz 804-785.
80 Denning, D.W. (2003). Echinocandin antifungal drugs. Lancet **362**: 1142-1151.
81 Dizdaroglu, M. (2005). Base-excision repair of oxidative DNA damage by DNA glycosylases. Mutat Res **591**: 45-59.
82 Dogra, S., Krishnamurthy, S., Gupta, V., Dixit, B.L., Gupta, C.M., Sanglard, D. and Prasad, R. (1999). Asymmetric distribution of phosphatidylethanolamine in *C. albicans*: possible mediation by *CDR1*, a multidrug transporter belonging to ATP binding cassette (ABC) superfamily. Yeast **15**: 111-121.
83 Dominguez, J.M. and Martin, J.J. (1998). Identification of elongation factor 2 as the essential protein targeted by sordarins in *Candida albicans*. Antimicrob Agents Chemother **42**: 2279-2283.
84 Doyle, L.A., Yang, W., Abruzzo, L.V., Krogmann, T., Gao, Y., Rishi, A.K. and Ross, D.D. (1998). A multidrug resistance transporter from human MCF-7 breast cancer cells. Proc Natl Acad Sci U S A **95**: 15665-15670.
85 Driscoll, R., Hudson, A. and Jackson, S.P. (2007). Yeast Rtt109 promotes genome stability by acetylating histone H3 on lysine 56. Science **315**: 649-652.
86 Drogaris, P., Wurtele, H., Masumoto, H., Verreault, A. and Thibault, P. (2008). Comprehensive profiling of histone modifications using a label-free approach and its applications in determining structure-function relationships. Anal Chem **80**: 6698-6707.
87 Dunkel, N., Blass, J., Rogers, P.D. and Morschhauser, J. (2008a). Mutations in the multi-drug resistance regulator *MRR1*, followed by loss of heterozygosity, are

the main cause of *MDR1* overexpression in fluconazole-resistant *Candida albicans* strains. Mol Microbiol **69**: 827-840.

88 Dunkel, N., Liu, T.T., Barker, K.S., Homayouni, R., Morschhauser, J. and Rogers, P.D. (2008b). A gain-of-function mutation in the transcription factor Upc2p causes upregulation of ergosterol biosynthesis genes and increased fluconazole resistance in a clinical *Candida albicans* isolate. Eukaryot Cell **7**: 1180-1190.

89 Egner, R., Bauer, B.E. and Kuchler, K. (2000). The transmembrane domain 10 of the yeast Pdr5p ABC antifungal efflux pump determines both substrate specificity and inhibitor susceptibility. Mol Microbiol **35**: 1255-1263.

90 Egner, R., Rosenthal, F.E., Kralli, A., Sanglard, D. and Kuchler, K. (1998). Genetic separation of FK506 susceptibility and drug transport in the yeast Pdr5 ATP-binding cassette multidrug resistance transporter. Mol Biol Cell **9**: 523-543.

91 Eraso, P., Martinez-Burgos, M., Falcon-Perez, J.M., Portillo, F. and Mazon, M.J. (2004). Ycf1-dependent cadmium detoxification by yeast requires phosphorylation of residues Ser908 and Thr911. FEBS Lett **577**: 322-326.

92 Ernst, R., Kueppers, P., Klein, C.M., Schwarzmueller, T., Kuchler, K. and Schmitt, L. (2008). A mutation of the H-loop selectively affects rhodamine transport by the yeast multidrug ABC transporter Pdr5. Proc Natl Acad Sci U S A **105**: 5069-5074.

93 Ernst, R., Kueppers, P., Stindt, J., Kuchler, K. and Schmitt, L. (2010). Multidrug efflux pumps: substrate selection in ATP-binding cassette multidrug efflux pumps--first come, first served? FEBS J **277**: 540-549.

94 Feinberg, A.P. and Vogelstein, B. (1984). A technique for radiolabeling DNA restriction endonuclease fragments to high specific activity. Anal Biochem **137**: 266-267.

95 Felk, A., Kretschmar, M., Albrecht, A., Schaller, M., Beinhauer, S., Nichterlein, T., Sanglard, D., Korting, H.C., Schafer, W. and Hube, B. (2002). *Candida albicans* hyphal formation and the expression of the Efg1-regulated proteinases Sap4 to Sap6 are required for the invasion of parenchymal organs. Infect Immun **70**: 3689-3700.

96 Ferreira-Pereira, A., Marco, S., Decottignies, A., Nader, J., Goffeau, A. and Rigaud, J.L. (2003). Three-dimensional reconstruction of the *Saccharomyces cerevisiae* multidrug resistance protein Pdr5p. J Biol Chem **278**: 11995-11999.

97 Finley, K.R., Bouchonville, K.J., Quick, A. and Berman, J. (2008). Dynein-dependent nuclear dynamics affect morphogenesis in *Candida albicans* by means of the Bub2p spindle checkpoint. Journal of cell science **121**: 466-476.

98 Finnin, M.S., Donigian, J.R. and Pavletich, N.P. (2001). Structure of the histone deacetylase SIRT2. Nat Struct Biol **8**: 621-625.

99 Fitzpatrick, D.A., Logue, M.E., Stajich, J.E. and Butler, G. (2006). A fungal phylogeny based on 42 complete genomes derived from supertree and combined gene analysis. BMC Evol Biol **6**: 99.

100 Fletcher, J.I., Haber, M., Henderson, M.J. and Norris, M.D. (2010). ABC transporters in cancer: more than just drug efflux pumps. Nat Rev Cancer **10**: 147-156.

101 Fling, M.E., Kopf, J., Tamarkin, A., Gorman, J.A., Smith, H.A. and Koltin, Y. (1991). Analysis of a *Candida albicans* gene that encodes a novel mechanism for resistance to benomyl and methotrexate. Mol Gen Genet **227**: 318-329.

102 Fonzi, W.A. and Irwin, M.Y. (1993). Isogenic strain construction and gene mapping in *Candida albicans*. Genetics **134**: 717-728.

103 Forche, A., Alby, K., Schaefer, D., Johnson, A.D., Berman, J. and Bennett, R.J. (2008). The parasexual cycle in *Candida albicans* provides an alternative pathway to meiosis for the formation of recombinant strains. PLoS Biol **6**: 110.

104 Frank, M.M. and Fries, L.F. (1991). The role of complement in inflammation and phagocytosis. Immunol Today **12**: 322-326.

105 Franz, R., Michel, S. and Morschhauser, J. (1998). A fourth gene from the *Candida albicans CDR* family of ABC transporters. Gene **220**: 91-98.

106 Frye, R.A. (2000). Phylogenetic classification of prokaryotic and eukaryotic Sir2-like proteins. Biochemical and biophysical research communications **273**: 793-798.

107 G.S. de Hoog, J.G., J. Gene, M.J. Figueras (2001). Atlas of Clinical Fungi, ASM Press.

108 Ganesan, L.T., Manavathu, E.K., Cutright, J.L., Alangaden, G.J. and Chandrasekar, P.H. (2004). *In vitro* activity of nikkomycin Z alone and in combination with polyenes, triazoles or echinocandins against *Aspergillus fumigatus*. Clin Microbiol Infect **10**: 961-966.

109 Garske, A.L. and Denu, J.M. (2006). SIRT1 top 40 hits: use of one-bead, one-compound acetyl-peptide libraries and quantum dots to probe deacetylase specificity. Biochemistry **45**: 94-101.

110 Gauthier, C., Weber, S., Alarco, A.M., Alqawi, O., Daoud, R., Georges, E. and Raymond, M. (2003). Functional similarities and differences between *Candida albicans* Cdr1p and Cdr2p transporters. Antimicrob Agents Chemother **47**: 1543-1554.

111 Germann, U.A., Chambers, T.C., Ambudkar, S.V., Licht, T., Cardarelli, C.O., Pastan, I. and Gottesman, M.M. (1996). Characterization of phosphorylation-defective mutants of human P-glycoprotein expressed in mammalian cells. J Biol Chem **271**: 1708-1716.

112 Ghannoum, M.A. and Rice, L.B. (1999). Antifungal agents: mode of action, mechanisms of resistance, and correlation of these mechanisms with bacterial resistance. Clin Microbiol Rev **12**: 501-517.

113 Girgis, A.S., Hosni, H.M. and Barsoum, F.F. (2006). Novel synthesis of nicotinamide derivatives of cytotoxic properties. Bioorg Med Chem **14**: 4466-4476.

114 Glavy, J.S., Horwitz, S.B. and Orr, G.A. (1997). Identification of the in vivo phosphorylation sites for acidic-directed kinases in murine mdr1b P-glycoprotein. J Biol Chem **272**: 5909-5914.

115 Golin, J., Ambudkar, S.V., Gottesman, M.M., Habib, A.D., Sczepanski, J., Ziccardi, W. and May, L. (2003). Studies with novel Pdr5p substrates demonstrate a strong size dependence for xenobiotic efflux. J Biol Chem **278**: 5963-5969.

116 Golin, J., Barkatt, A., Cronin, S., Eng, G. and May, L. (2000). Chemical specificity of the *PDR5* multidrug resistance gene product of *Saccharomyces cerevisiae* based on studies with tri-n-alkyltin chlorides. Antimicrob Agents Chemother **44**: 134-138.

117 Gottesman, M.M. and Ambudkar, S.V. (2001). Overview: ABC transporters and human disease. J Bioenerg Biomembr **33**: 453-458.

118 Gottesman, M.M., Fojo, T. and Bates, S.E. (2002). Multidrug resistance in cancer: role of ATP-dependent transporters. Nat Rev Cancer **2**: 48-58.

119 Gottesman, M.M. and Ling, V. (2006). The molecular basis of multidrug resistance in cancer: the early years of P-glycoprotein research. FEBS Lett **580**: 998-1009.

120 Gottesman, M.M., Pastan, I. and Ambudkar, S.V. (1996). P-glycoprotein and multidrug resistance. Curr Opin Genet Dev **6**: 610-617.
121 Graybill, J.R., Najvar, L., Fothergill, A., Bocanegra, R. and de las Heras, F.G. (1999). Activities of sordarins in murine histoplasmosis. Antimicrob Agents Chemother **43**: 1716-1718.
122 Green, K.N., Steffan, J.S., Martinez-Coria, H., Sun, X., Schreiber, S.S., Thompson, L.M. and LaFerla, F.M. (2008). Nicotinamide restores cognition in Alzheimer's disease transgenic mice via a mechanism involving sirtuin inhibition and selective reduction of Thr231-phosphotau. J Neurosci **28**: 11500-11510.
123 Griac, P. (2007). Sec14 related proteins in yeast. Biochim Biophys Acta **1771**: 737-745.
124 Guggino, W.B. and Stanton, B.A. (2006). New insights into cystic fibrosis: molecular switches that regulate CFTR. Nat Rev Mol Cell Biol **7**: 426-436.
125 Gunjan, A. and Verreault, A. (2003). A Rad53 kinase-dependent surveillance mechanism that regulates histone protein levels in *S. cerevisiae*. Cell **115**: 537-549.
126 Haldar, D. and Kamakaka, R.T. (2008). *Schizosaccharomyces pombe* Hst4 functions in DNA damage response by regulating histone H3 K56 acetylation. Eukaryot Cell **7**: 800-813.
127 Han, J., Zhou, H., Horazdovsky, B., Zhang, K., Xu, R.M. and Zhang, Z. (2007). Rtt109 acetylates histone H3 lysine 56 and functions in DNA replication. Science **315**: 653-655.
128 Hanadate, T., Tomishima, M., Shiraishi, N., Tanabe, D., Morikawa, H., Barrett, D., Matsumoto, S., Ohtomo, K. and Maki, K. (2009). FR290581, a novel sordarin derivative: synthesis and antifungal activity. Bioorg Med Chem Lett **19**: 1465-1468.
129 Hazelwood, L.A., Tai, S.L., Boer, V.M., de Winde, J.H., Pronk, J.T. and Daran, J.M. (2006). A new physiological role for Pdr12p in *Saccharomyces cerevisiae*: export of aromatic and branched-chain organic acids produced in amino acid catabolism. FEMS Yeast Res **6**: 937-945.
130 Hector, R.F. (1993). Compounds active against cell walls of medically important fungi. Clin Microbiol Rev **6**: 1-21.
131 Hegedus, T., Aleksandrov, A., Mengos, A., Cui, L., Jensen, T.J. and Riordan, J.R. (2009). Role of individual R domain phosphorylation sites in CFTR regulation by protein kinase A. Biochim Biophys Acta **1788**: 1341-1349.
132 Hemenway, C.S. and Heitman, J. (1999). Calcineurin. Structure, function, and inhibition. Cell Biochem Biophys **30**: 115-151.
133 Herbrecht, R., Natarajan-Ame, S., Nivoix, Y. and Letscher-Bru, V. (2003). The lipid formulations of amphotericin B. Expert Opin Pharmacother **4**: 1277-1287.
134 Herreros, E., Martinez, C.M., Almela, M.J., Marriott, M.S., De Las Heras, F.G. and Gargallo-Viola, D. (1998). Sordarins: in vitro activities of new antifungal derivatives against pathogenic yeasts, *Pneumocystis carinii*, and filamentous fungi. Antimicrob Agents Chemother **42**: 2863-2869.
135 Higgins, C.F. (2007). Multiple molecular mechanisms for multidrug resistance transporters. Nature **446**: 749-757.
136 Hiller, D., Sanglard, D. and Morschhauser, J. (2006). Overexpression of the *MDR1* gene is sufficient to confer increased resistance to toxic compounds in *Candida albicans*. Antimicrob Agents Chemother **50**: 1365-1371.
137 Hirao, M., Posakony, J., Nelson, M., Hruby, H., Jung, M., Simon, J.A. and Bedalov, A. (2003). Identification of selective inhibitors of NAD+-dependent deacetylases using phenotypic screens in yeast. J Biol Chem **278**: 52773-52782.

138 Hnisz, D., Majer, O., Frohner, I.E., Komnenovic, V. and Kuchler, K. (2010). The Set3/Hos2 histone deacetylase complex attenuates cAMP/PKA signaling to regulate morphogenesis and virulence of *Candida albicans*. PLoS Pathog **6**: e1000889.

139 Hoehamer, C.F., Cummings, E.D., Hilliard, G.M. and Rogers, P.D. (2010). Changes in the proteome of *Candida albicans* in response to azole, polyene, and echinocandin antifungal agents. Antimicrobial agents and chemotherapy **54**: 1655-1664.

140 Hoffman, C.S. and Winston, F. (1987). A ten-minute DNA preparation from yeast efficiently releases autonomous plasmids for transformation of *Escherichia coli* Gene **57**: 267-272.

141 Holbrook, E.D. and Rappleye, C.A. (2008). Histoplasma capsulatum pathogenesis: making a lifestyle switch. Curr Opin Microbiol **11**: 318-324.

142 Hollenstein, K., Dawson, R.J. and Locher, K.P. (2007). Structure and mechanism of ABC transporter proteins. Current opinion in structural biology **17**: 412-418.

143 Holmes, A.R., Lin, Y.H., Niimi, K., Lamping, E., Keniya, M., Niimi, M., Tanabe, K., Monk, B.C. and Cannon, R.D. (2008). ABC transporter Cdr1p contributes more than Cdr2p does to fluconazole efflux in fluconazole-resistant *Candida albicans* clinical isolates. Antimicrob Agents Chemother **52**: 3851-3862.

144 Horsman, M.R. (1997). Tolerance to nicotinamide and carbogen with radiation therapy for glioblastoma. Radiother Oncol **43**: 109-110.

145 Horsman, M.R., Siemann, D.W., Chaplin, D.J. and Overgaard, J. (1997). Nicotinamide as a radiosensitizer in tumours and normal tissues: the importance of drug dose and timing. Radiother Oncol **45**: 167-174.

146 Huang, R.Y., Kowalski, D., Minderman, H., Gandhi, N. and Johnson, E.S. (2007). Small ubiquitin-related modifier pathway is a major determinant of doxorubicin cytotoxicity in *Saccharomyces cerevisiae*. Cancer Res **67**: 765-772.

147 Hyde, S.C., Emsley, P., Hartshorn, M.J., Mimmack, M.M., Gileadi, U., Pearce, S.R., Gallagher, M.P., Gill, D.R., Hubbard, R.E. and Higgins, C.F. (1990). Structural model of ATP-binding proteins associated with cystic fibrosis, multidrug resistance and bacterial transport. Nature **346**: 362-365.

148 Hyland, E.M., Cosgrove, M.S., Molina, H., Wang, D., Pandey, A., Cottee, R.J. and Boeke, J.D. (2005). Insights into the role of histone H3 and histone H4 core modifiable residues in Saccharomyces cerevisiae. Molecular and cellular biology **25**: 10060-10070.

149 Insenser, M., Nombela, C., Molero, G. and Gil, C. (2006). Proteomic analysis of detergent-resistant membranes from *Candida albicans*. Proteomics **6 Suppl 1**: S74-81.

150 Ivnitski-Steele, I., Holmes, A.R., Lamping, E., Monk, B.C., Cannon, R.D. and Sklar, L.A. (2009). Identification of Nile red as a fluorescent substrate of the *Candida albicans* ATP-binding cassette transporters Cdr1p and Cdr2p and the major facilitator superfamily transporter Mdr1p. Anal Biochem **394**: 87-91.

151 Janas, E., Hofacker, M., Chen, M., Gompf, S., van der Does, C. and Tampe, R. (2003). The ATP hydrolysis cycle of the nucleotide-binding domain of the mitochondrial ATP-binding cassette transporter Mdl1p. J Biol Chem **278**: 26862-26869.

152 Jha, S., Dabas, N., Karnani, N., Saini, P. and Prasad, R. (2004). ABC multidrug transporter Cdr1p of *Candida albicans* has divergent nucleotide-binding domains which display functional asymmetry. FEMS Yeast Res **5**: 63-72.

153 Jha, S., Karnani, N., Dhar, S.K., Mukhopadhayay, K., Shukla, S., Saini, P., Mukhopadhayay, G. and Prasad, R. (2003a). Purification and characterization of the N-terminal nucleotide binding domain of an ABC drug transporter of *Candida albicans* : uncommon cysteine 193 of Walker A is critical for ATP hydrolysis. Biochemistry **42**: 10822-10832.

154 Jha, S., Karnani, N., Lynn, A.M. and Prasad, R. (2003b). Covalent modification of cysteine 193 impairs ATPase function of nucleotide-binding domain of a *Candida* drug efflux pump. Biochemical and biophysical research communications **310**: 869-875.

155 Jia, X.M., Ma, Z.P., Jia, Y., Gao, P.H., Zhang, J.D., Wang, Y., Xu, Y.G., Wang, L., Cao, Y.Y., Cao, Y.B.*, et al.* (2008). *RTA2*, a novel gene involved in azole resistance in *Candida albicans*. Biochemical and biophysical research communications **373**: 631-636.

156 Jia, X.M., Wang, Y., Jia, Y., Gao, P.H., Xu, Y.G., Wang, L., Cao, Y.Y., Cao, Y.B., Zhang, L.X. and Jiang, Y.Y. (2009). *RTA2* is involved in calcineurin-mediated azole resistance and sphingoid long-chain base release in *Candida albicans*. Cell Mol Life Sci **66**: 122-134.

157 Jin, L., Wei, W., Jiang, Y., Peng, H., Cai, J., Mao, C., Dai, H., Choy, W., Bemis, J.E., Jirousek, M.R.*, et al.* (2009). Crystal structures of human SIRT3 displaying substrate-induced conformational changes. J Biol Chem **284**: 24394-24405.

158 Johnson, E., Espinel-Ingroff, A., Szekely, A., Hockey, H. and Troke, P. (2008). Activity of voriconazole, itraconazole, fluconazole and amphotericin B in vitro against 1763 yeasts from 472 patients in the voriconazole phase III clinical studies. Int J Antimicrob Agents **32**: 511-514.

159 Johnson, M.D., MacDougall, C., Ostrosky-Zeichner, L., Perfect, J.R. and Rex, J.H. (2004). Combination antifungal therapy. Antimicrob Agents Chemother **48**: 693-715.

160 Johnson, S.S., Hanson, P.K., Manoharlal, R., Brice, S.E., Cowart, L.A. and Moye-Rowley, W.S. (2010). Regulation of yeast nutrient permease endocytosis by ATP-binding cassette transporters and a seven-transmembrane protein, RSB1. J Biol Chem **285**: 35792-35802.

161 Kam, A.P. and Xu, J. (2002). Diversity of commensal yeasts within and among healthy hosts. Diagn Microbiol Infect Dis **43**: 19-28.

162 Karababa, M., Valentino, E., Pardini, G., Coste, A.T., Bille, J. and Sanglard, D. (2006). CRZ1, a target of the calcineurin pathway in *Candida albicans*. Mol Microbiol **59**: 1429-1451.

163 Karkowska-Kuleta, J., Rapala-Kozik, M. and Kozik, A. (2009). Fungi pathogenic to humans: molecular bases of virulence of *Candida albicans*, *Cryptococcus neoformans* and *Aspergillus fumigatus*. Acta Biochim Pol **56**: 211-224.

164 Katzmann, D.J., Hallstrom, T.C., Voet, M., Wysock, W., Golin, J., Volckaert, G. and Moye-Rowley, W.S. (1995). Expression of an ATP-binding cassette transporter-encoding gene (YOR1) is required for oligomycin resistance in *Saccharomyces cerevisiae*. Molecular and cellular biology **15**: 6875-6883.

165 Kauffman, C.A. (2007). Histoplasmosis: a clinical and laboratory update. Clin Microbiol Rev **20**: 115-132.

166 Kelly, J., Rowan, R., McCann, M. and Kavanagh, K. (2009). Exposure to caspofungin activates Cap and Hog pathways in *Candida albicans*. Med Mycol **5**: 1-10.

167 Kelly, S.L., Lamb, D.C., Corran, A.J., Baldwin, B.C. and Kelly, D.E. (1995). Mode of action and resistance to azole antifungals associated with the formation

of 14 alpha-methylergosta-8,24(28)-dien-3 beta,6 alpha-diol. Biochemical and biophysical research communications **207**: 910-915.

168 Kelm, K.B., Huyer, G., Huang, J.C. and Michaelis, S. (2004). The internalization of yeast Ste6p follows an ordered series of events involving phosphorylation, ubiquitination, recognition and endocytosis. Traffic **5**: 165-180.

169 Kerr, I.D., Jones, P.M. and George, A.M. (2010). Multidrug efflux pumps: the structures of prokaryotic ATP-binding cassette transporter efflux pumps and implications for our understanding of eukaryotic P-glycoproteins and homologues. FEBS J **277**: 550-563.

170 Kihara, A. and Igarashi, Y. (2002). Identification and characterization of a Saccharomyces cerevisiae gene, RSB1, involved in sphingoid long-chain base release. J Biol Chem **277**: 30048-30054.

171 Kihara, A. and Igarashi, Y. (2004). Cross talk between sphingolipids and glycerophospholipids in the establishment of plasma membrane asymmetry. Mol Biol Cell **15**: 4949-4959.

172 Kispal, G., Csere, P., Guiard, B. and Lill, R. (1997). The ABC transporter Atm1p is required for mitochondrial iron homeostasis. FEBS Lett **418**: 346-350.

173 Klis, F.M., de Groot, P. and Hellingwerf, K. (2001). Molecular organization of the cell wall of *Candida albicans*. Med Mycol **39 Suppl 1**: 1-8.

174 Klis, F.M., Mol, P., Hellingwerf, K. and Brul, S. (2002). Dynamics of cell wall structure in *Saccharomyces cerevisiae*. FEMS Microbiol Rev **26**: 239-256.

175 Koenekoop, R.K. (2003). The gene for Stargardt disease, ABCA4, is a major retinal gene: a mini-review. Ophthalmic Genet **24**: 75-80.

176 Kohler, S., Wheat, L.J., Connolly, P., Schnizlein-Bick, C., Durkin, M., Smedema, M., Goldberg, J. and Brizendine, E. (2000). Comparison of the echinocandin caspofungin with amphotericin B for treatment of histoplasmosis following pulmonary challenge in a murine model. Antimicrob Agents Chemother **44**: 1850-1854.

177 Kolaczkowski, M., van der Rest, M., Cybularz-Kolaczkowska, A., Soumillion, J.P., Konings, W.N. and Goffeau, A. (1996). Anticancer drugs, ionophoric peptides, and steroids as substrates of the yeast multidrug transporter Pdr5p. J Biol Chem **271**: 31543-31548.

178 Kolling, R. (2002). Mutations affecting phosphorylation, ubiquitination and turnover of the ABC-transporter Ste6. FEBS Lett **531**: 548-552.

179 Kolling, R. and Losko, S. (1997). The linker region of the ABC-transporter Ste6 mediates ubiquitination and fast turnover of the protein. The EMBO journal **16**: 2251-2261.

180 Kos, V. and Ford, R.C. (2009). The ATP-binding cassette family: a structural perspective. Cell Mol Life Sci **66**: 3111-3126.

181 Kouzarides, T. (2007). Chromatin modifications and their function. Cell **128**: 693-705.

182 Kovalchuk, A. and Driessen, A.J. (2010). Phylogenetic analysis of fungal ABC transporters. BMC Genomics **11**: 177.

183 Kozel, T.R. (1996). Activation of the complement system by pathogenic fungi. Clin Microbiol Rev **9**: 34-46.

184 Krishnamurthy, P. and Schuetz, J.D. (2006). Role of ABCG2/BCRP in biology and medicine. Annu Rev Pharmacol Toxicol **46**: 381-410.

185 Krishnan-Natesan, S. (2009). Terbinafine: a pharmacological and clinical review. Expert Opin Pharmacother **10**: 2723-2733.

186 Krsmanovic, T., Pawelec, A., Sydor, T. and Kolling, R. (2005). Control of Ste6 recycling by ubiquitination in the early endocytic pathway in yeast. Mol Biol Cell **16**: 2809-2821.
187 Kuchler, K., Sterne, R.E. and Thorner, J. (1989). *Saccharomyces cerevisiae STE6* gene product: a novel pathway for protein export in eukaryotic cells. The EMBO journal **8**: 3973-3984.
188 Kumamoto, C.A. and Vinces, M.D. (2005). Contributions of hyphae and hypha-co-regulated genes to *Candida albicans* virulence. Cell Microbiol **7**: 1546-1554.
189 Kushnirov, V.V. (2000). Rapid and reliable protein extraction from yeast. Yeast **16**: 857-860.
190 Kwon-Chung, K.J. and Sugui, J.A. (2009). What do we know about the role of gliotoxin in the pathobiology of *Aspergillus fumigatus*? Med Mycol **47**: S97-103.
191 Lacaille, V.G. and Androlewicz, M.J. (1998). Herpes simplex virus inhibitor ICP47 destabilizes the transporter associated with antigen processing (TAP) heterodimer. J Biol Chem **273**: 17386-17390.
192 Lamping, E., Baret, P.V., Holmes, A.R., Monk, B.C., Goffeau, A. and Cannon, R.D. (2010). Fungal PDR transporters: Phylogeny, topology, motifs and function. Fungal Genet Biol **47**: 127-142.
193 Lamping, E., Monk, B.C., Niimi, K., Holmes, A.R., Tsao, S., Tanabe, K., Niimi, M., Uehara, Y. and Cannon, R.D. (2007). Characterization of three classes of membrane proteins involved in fungal azole resistance by functional hyperexpression in *Saccharomyces cerevisiae* Eukaryot Cell **6**: 1150-1165.
194 Lankat-Buttgereit, B. and Tampe, R. (2002). The transporter associated with antigen processing: function and implications in human diseases. Physiol Rev **82**: 187-204.
195 Latge, J.P. (1999). Aspergillus fumigatus and aspergillosis. Clin Microbiol Rev **12**: 310-350.
196 Laverdiere, M., Lalonde, R.G., Baril, J.G., Sheppard, D.C., Park, S. and Perlin, D.S. (2006). Progressive loss of echinocandin activity following prolonged use for treatment of *Candida albicans* oesophagitis. J Antimicrob Chemother **57**: 705-708.
197 Lay, J., Henry, L.K., Clifford, J., Koltin, Y., Bulawa, C.E. and Becker, J.M. (1998). Altered expression of selectable marker URA3 in gene-disrupted Candida albicans strains complicates interpretation of virulence studies. Infect Immun **66**: 5301-5306.
198 Lelong-Rebel, I.H. and Cardarelli, C.O. (2005). Differential phosphorylation patterns of P-glycoprotein reconstituted into a proteoliposome system: insight into additional unconventional phosphorylation sites. Anticancer Res **25**: 3925-3935.
199 Levitz, S.M. (2010). Innate recognition of fungal cell walls. PLoS Pathog **6**: e1000758.
200 Lewis, R.E. (2009). Overview of the changing epidemiology of candidemia. Curr Med Res Opin **25**: 1732-1740.
201 Li, X., Gerber, S.A., Rudner, A.D., Beausoleil, S.A., Haas, W., Villen, J., Elias, J.E. and Gygi, S.P. (2007). Large-scale phosphorylation analysis of alpha-factor-arrested *Saccharomyces cerevisiae*. J Proteome Res **6**: 1190-1197.
202 Linton, K.J. (2007). Structure and function of ABC transporters. Physiology (Bethesda) **22**: 122-130.
203 Linton, K.J. and Higgins, C.F. (1998). The Escherichia coli ATP-binding cassette (ABC) proteins. Mol Microbiol **28**: 5-13.

204 Liu, T.T., Lee, R.E., Barker, K.S., Wei, L., Homayouni, R. and Rogers, P.D. (2005). Genome-wide expression profiling of the response to azole, polyene, echinocandin, and pyrimidine antifungal agents in *Candida albicans*. Antimicrob Agents Chemother **49**: 2226-2236.

205 Liu, T.T., Znaidi, S., Barker, K.S., Xu, L., Homayouni, R., Saidane, S., Morschhauser, J., Nantel, A., Raymond, M. and Rogers, P.D. (2007). Genome-wide expression and location analyses of the *Candida albicans* Tac1p regulon. Eukaryot Cell **6**: 2122-2138.

206 Lo, H.J., Kohler, J.R., DiDomenico, B., Loebenberg, D., Cacciapuoti, A. and Fink, G.R. (1997). Nonfilamentous *C. albicans* mutants are avirulent. Cell **90**: 939-949.

207 Locher, K.P. (2009). Review. Structure and mechanism of ATP-binding cassette transporters. Philos Trans R Soc Lond B Biol Sci **364**: 239-245.

208 Loffler, J., Einsele, H., Hebart, H., Schumacher, U., Hrastnik, C. and Daum, G. (2000). Phospholipid and sterol analysis of plasma membranes of azole-resistant *Candida albicans* strains. FEMS Microbiol Lett **185**: 59-63.

209 Lomovskaya, O. (2002). Interactions among Multiple Efflux Pumps: Additive and Synergistic Effects on Antimicrobial Resistance.

210 Loo, T.W. and Clarke, D.M. (2000). Blockage of drug resistance in vitro by disulfiram, a drug used to treat alcoholism. J Natl Cancer Inst **92**: 898-902.

211 Lopes da Rosa, J., Boyartchuk, V.L., Zhu, L.J. and Kaufman, P.D. (2010). Histone acetyltransferase Rtt109 is required for Candida albicans pathogenesis. Proc Natl Acad Sci U S A **107**: 1594-1599.

212 Lopez-Ribot, J.L., McAtee, R.K., Perea, S., Kirkpatrick, W.R., Rinaldi, M.G. and Patterson, T.F. (1999). Multiple resistant phenotypes of *Candida albicans* coexist during episodes of oropharyngeal candidiasis in human immunodeficiency virus-infected patients. Antimicrob Agents Chemother **43**: 1621-1630.

213 Lupetti, A., Danesi, R., van 't Wout, J.W., van Dissel, J.T., Senesi, S. and Nibbering, P.H. (2002). Antimicrobial peptides: therapeutic potential for the treatment of Candida infections. Expert Opin Investig Drugs **11**: 309-318.

214 Lupetti, A., Nibbering, P.H., Campa, M., Del Tacca, M. and Danesi, R. (2003). Molecular targeted treatments for fungal infections: the role of drug combinations. Trends Mol Med **9**: 269-276.

215 Lupo, P., Chang, Y.C., Kelsall, B.L., Farber, J.M., Pietrella, D., Vecchiarelli, A., Leon, F. and Kwon-Chung, K.J. (2008). The presence of capsule in *Cryptococcus neoformans* influences the gene expression profile in dendritic cells during interaction with the fungus. Infect Immun **76**: 1581-1589.

216 Lyon, F.L., Hector, R.F. and Domer, J.E. (1986). Innate and acquired immune responses against Candida albicans in congenic B10.D2 mice with deficiency of the C5 complement component. J Med Vet Mycol **24**: 359-367.

217 Ma, B., Pan, S.J., Domergue, R., Rigby, T., Whiteway, M., Johnson, D. and Cormack, B.P. (2009). High-affinity transporters for NAD+ precursors in *Candida glabrata* are regulated by Hst1 and induced in response to niacin limitation. Molecular and cellular biology **29**: 4067-4079.

218 Maas, N.L., Miller, K.M., DeFazio, L.G. and Toczyski, D.P. (2006). Cell cycle and checkpoint regulation of histone H3 K56 acetylation by Hst3 and Hst4. Mol Cell **23**: 109-119.

219 MacPherson, S., Larochelle, M. and Turcotte, B. (2006). A fungal family of transcriptional regulators: the zinc cluster proteins. Microbiol Mol Biol Rev **70**: 583-604.

220 Maebashi, K., Niimi, M., Kudoh, M., Fischer, F.J., Makimura, K., Niimi, K., Piper, R.J., Uchida, K., Arisawa, M., Cannon, R.D*., et al.* (2001). Mechanisms of fluconazole resistance in *Candida albicans* isolates from Japanese AIDS patients. J Antimicrob Chemother **47**: 527-536.

221 Maesaki, S., Marichal, P., Vanden Bossche, H., Sanglard, D. and Kohno, S. (1999). Rhodamine 6G efflux for the detection of *CDR1*-overexpressing azole-resistant *Candida albicans* strains. J Antimicrob Chemother **44**: 27-31.

222 Mahe, Y., Lemoine, Y. and Kuchler, K. (1996). The ATP binding cassette transporters Pdr5 and Snq2 of *Saccharomyces cerevisiae* can mediate transport of steroids in vivo. J Biol Chem **271**: 25167-25172.

223 Mai, A. (2007). The therapeutic uses of chromatin-modifying agents. Expert Opin Ther Targets **11**: 835-851.

224 Mai, A., Rotili, D., Massa, S., Brosch, G., Simonetti, G., Passariello, C. and Palamara, A.T. (2007). Discovery of uracil-based histone deacetylase inhibitors able to reduce acquired antifungal resistance and trailing growth in *Candida albicans*. Bioorg Med Chem Lett **17**: 1221-1225.

225 Maiese, K., Chong, Z.Z., Hou, J. and Shang, Y.C. (2009). The vitamin nicotinamide: translating nutrition into clinical care. Molecules **14**: 3446-3485.

226 Maligie, M.A. and Selitrennikoff, C.P. (2005). *Cryptococcus neoformans* resistance to echinocandins: (1,3)beta-glucan synthase activity is sensitive to echinocandins. Antimicrob Agents Chemother **49**: 2851-2856.

227 Mamnun, Y.M., Schuller, C. and Kuchler, K. (2004). Expression regulation of the yeast PDR5 ATP-binding cassette (ABC) transporter suggests a role in cellular detoxification during the exponential growth phase. FEBS Lett **559**: 111-117.

228 Manoharlal, R., Gaur, N.A., Panwar, S.L., Morschhauser, J. and Prasad, R. (2008). Transcriptional activation and increased mRNA stability contribute to overexpression of *CDR1* in azole-resistant *Candida albicans*. Antimicrob Agents Chemother **52**: 1481-1492.

229 Manoharlal, R., Gorantala, J., Sharma, M., Sanglard, D. and Prasad, R. (2010). *PAP1* [poly(A) polymerase 1] homozygosity and hyperadenylation are major determinants of increased mRNA stability of *CDR1* in azole-resistant clinical isolates of *Candida albicans*. Microbiology **156**: 313-326.

230 Marchal, C., Haguenauer-Tsapis, R. and Urban-Grimal, D. (2000). Casein kinase I-dependent phosphorylation within a PEST sequence and ubiquitination at nearby lysines signal endocytosis of yeast uracil permease. J Biol Chem **275**: 23608-23614.

231 Marchetti, O., Entenza, J.M., Sanglard, D., Bille, J., Glauser, M.P. and Moreillon, P. (2000). Fluconazole plus cyclosporine: a fungicidal combination effective against experimental endocarditis due to *Candida albicans*. Antimicrob Agents Chemother **44**: 2932-2938.

232 Marichal, P., Vanden Bossche, H., Odds, F.C., Nobels, G., Warnock, D.W., Timmerman, V., Van Broeckhoven, C., Fay, S. and Mose-Larsen, P. (1997). Molecular biological characterization of an azole-resistant *Candida glabrata* isolate. Antimicrob Agents Chemother **41**: 2229-2237.

233 Martin, S.W. and Konopka, J.B. (2004). Lipid raft polarization contributes to hyphal growth in *Candida albicans*. Eukaryot Cell **3**: 675-684.

234 Masumoto, H., Hawke, D., Kobayashi, R. and Verreault, A. (2005). A role for cell-cycle-regulated histone H3 lysine 56 acetylation in the DNA damage response. Nature **436**: 294-298.

235 Mathews, H.L., Witek-Jaunsek, L. and Calderone, R.A. (2002). Host Defense against Oral, Esophageal, and Gastrointestinal Candidiasis. *Candida* and Candidiasis, ASM Press**:** 179-192.
236 McGrath, J.P. and Varshavsky, A. (1989). The yeast STE6 gene encodes a homologue of the mammalian multidrug resistance P-glycoprotein. Nature **340**: 400-404.
237 Medoff, G., Sacco, M., Maresca, B., Schlessinger, D., Painter, A., Kobayashi, G.S. and Carratu, L. (1986). Irreversible block of the mycelial-to-yeast phase transition of *Histoplasma capsulatum*. Science **231**: 476-479.
238 Medzhitov, R. (2007). Recognition of microorganisms and activation of the immune response. Nature **449**: 819-826.
239 Mense, M., Vergani, P., White, D.M., Altberg, G., Nairn, A.C. and Gadsby, D.C. (2006). *in vivo* phosphorylation of CFTR promotes formation of a nucleotide-binding domain heterodimer. The EMBO journal **25**: 4728-4739.
240 Mitchell, T.G. and Perfect, J.R. (1995). Cryptococcosis in the era of AIDS--100 years after the discovery of *Cryptococcus neoformans*. Clin Microbiol Rev **8**: 515-548.
241 Mohr, J., Johnson, M., Cooper, T., Lewis, J.S. and Ostrosky-Zeichner, L. (2008). Current options in antifungal pharmacotherapy. Pharmacotherapy **28**: 614-645.
242 Mok, J., Kim, P.M., Lam, H.Y., Piccirillo, S., Zhou, X., Jeschke, G.R., Sheridan, D.L., Parker, S.A., Desai, V., Jwa, M*., et al.* (2010). Deciphering protein kinase specificity through large-scale analysis of yeast phosphorylation site motifs. Sci Signal **3**: ra12.
243 Morales, D.K. and Hogan, D.A. (2010). Candida albicans interactions with bacteria in the context of human health and disease. PLoS Pathog **6**: e1000886.
244 Moriya, H. and Johnston, M. (2004). Glucose sensing and signaling in Saccharomyces cerevisiae through the Rgt2 glucose sensor and casein kinase I. Proc Natl Acad Sci U S A **101**: 1572-1577.
245 Morschhauser, J. (2010). Regulation of multidrug resistance in pathogenic fungi. Fungal Genet Biol **47**: 94-106.
246 Morschhauser, J., Barker, K.S., Liu, T.T., BlaB-Warmuth, J., Homayouni, R. and Rogers, P.D. (2007). The transcription factor Mrr1p controls expression of the *MDR1* efflux pump and mediates multidrug resistance in *Candida albicans*. PLoS Pathog **3**: e164.
247 Moura, G.R., Paredes, J.A. and Santos, M.A. (2010). Development of the genetic code: insights from a fungal codon reassignment. FEBS Lett **584**: 334-341.
248 Moye-Rowley, W.S. (2003). Transcriptional control of multidrug resistance in the yeast *Saccharomyces*. Prog Nucleic Acid Res Mol Biol **73**: 251-279.
249 Mullick, A., Elias, M., Picard, S., Bourget, L., Jovcevski, O., Gauthier, S., Tuite, A., Harakidas, P., Bihun, C., Massie, B*., et al.* (2004). Dysregulated inflammatory response to *Candida albicans* in a C5-deficient mouse strain. Infect Immun **72**: 5868-5876.
250 Mullick, A., Leon, Z., Min-Oo, G., Berghout, J., Lo, R., Daniels, E. and Gros, P. (2006). Cardiac failure in C5-deficient A/J mice after *Candida albicans* infection. Infect Immun **74**: 4439-4451.
251 Munoz, M., Henderson, M., Haber, M. and Norris, M. (2007). Role of the MRP1/ABCC1 multidrug transporter protein in cancer. IUBMB Life **59**: 752-757.
252 Mylonakis, E. (2008). Galleria mellonella and the study of fungal pathogenesis: making the case for another genetically tractable model host. Mycopathologia **165**: 1-3.

253 Mylonakis, E. and Aballay, A. (2005). Worms and flies as genetically tractable animal models to study host-pathogen interactions. Infect Immun **73**: 3833-3841.
254 Nakamura, K., Niimi, M., Niimi, K., Holmes, A.R., Yates, J.E., Decottignies, A., Monk, B.C., Goffeau, A. and Cannon, R.D. (2001). Functional expression of *Candida albicans* drug efflux pump Cdr1p in a Saccharomyces cerevisiae strain deficient in membrane transporters. Antimicrob Agents Chemother **45**: 3366-3374.
255 Netea, M.G. and Marodi, L. (2010). Innate immune mechanisms for recognition and uptake of *Candida* species. Trends Immunol **31**: 346-353.
256 Niimi, K., Harding, D.R., Parshot, R., King, A., Lun, D.J., Decottignies, A., Niimi, M., Lin, S., Cannon, R.D., Goffeau, A*., et al.* (2004a). Chemosensitization of fluconazole resistance in *Saccharomyces cerevisiae* and pathogenic fungi by a D-octapeptide derivative. Antimicrob Agents Chemother **48**: 1256-1271.
257 Niimi, M., Niimi, K., Takano, Y., Holmes, A.R., Fischer, F.J., Uehara, Y. and Cannon, R.D. (2004b). Regulated overexpression of *CDR1* in *Candida albicans* confers multidrug resistance. J Antimicrob Chemother **54**: 999-1006.
258 Niren, N.M. (2006). Pharmacologic doses of nicotinamide in the treatment of inflammatory skin conditions: a review. Cutis **77**: 11-16.
259 Noble, S.M. and Johnson, A.D. (2005). Strains and strategies for large-scale gene deletion studies of the diploid human fungal pathogen *Candida albicans*. Eukaryot Cell **4**: 298-309.
260 Odds, F.C., Brown, A.J. and Gow, N.A. (2003). Antifungal agents: mechanisms of action. Trends Microbiol **11**: 272-279.
261 Olson, J.A., George, A., Constable, D., Smith, P., Proffitt, R.T. and Adler-Moore, J.P. (2010). Liposomal Amphotericin B and Echinocandins as Monotherapy or Sequential or Concomitant Therapy in Murine Disseminated and Pulmonary *Aspergillus fumigatus* Infections. Antimicrob Agents Chemother **54**: 3884-3894.
262 Onyewu, C., Blankenship, J.R., Del Poeta, M. and Heitman, J. (2003). Ergosterol biosynthesis inhibitors become fungicidal when combined with calcineurin inhibitors against *Candida albicans*, *Candida glabrata*, and *Candida krusei*. Antimicrob Agents Chemother **47**: 956-964.
263 Orlowski, S., Martin, S. and Escargueil, A. (2006). P-glycoprotein and 'lipid rafts': some ambiguous mutual relationships (floating on them, building them or meeting them by chance?). Cell Mol Life Sci **63**: 1038-1059.
264 Ostedgaard, L.S., Baldursson, O. and Welsh, M.J. (2001). Regulation of the cystic fibrosis transmembrane conductance regulator Cl- channel by its R domain. J Biol Chem **276**: 7689-7692.
265 Ostrosky-Zeichner, L., Casadevall, A., Galgiani, J.N., Odds, F.C. and Rex, J.H. (2010). An insight into the antifungal pipeline: selected new molecules and beyond. Nat Rev Drug Discov.
266 Oswald, C., Holland, I.B. and Schmitt, L. (2006). The motor domains of ABC-transporters. What can structures tell us? Naunyn Schmiedebergs Arch Pharmacol **372**: 385-399.
267 Ozdemir, A., Spicuglia, S., Lasonder, E., Vermeulen, M., Campsteijn, C., Stunnenberg, H.G. and Logie, C. (2005). Characterization of lysine 56 of histone H3 as an acetylation site in *Saccharomyces cerevisiae*. J Biol Chem **280**: 25949-25952.
268 Ozvegy, C., Litman, T., Szakacs, G., Nagy, Z., Bates, S., Varadi, A. and Sarkadi, B. (2001). Functional characterization of the human multidrug transporter, ABCG2, expressed in insect cells. Biochemical and biophysical research communications **285**: 111-117.

269 Ozvegy, C., Varadi, A. and Sarkadi, B. (2002). Characterization of drug transport, ATP hydrolysis, and nucleotide trapping by the human ABCG2 multidrug transporter. Modulation of substrate specificity by a point mutation. J Biol Chem **277**: 47980-47990.

270 Pappas, P.G., Kauffman, C.A., Andes, D., Benjamin, D.K., Jr., Calandra, T.F., Edwards, J.E., Jr., Filler, S.G., Fisher, J.F., Kullberg, B.J., Ostrosky-Zeichner, L.*, et al.* (2009). Clinical practice guidelines for the management of candidiasis: 2009 update by the Infectious Diseases Society of America. Clin Infect Dis **48**: 503-535.

271 Park, S., Kelly, R., Kahn, J.N., Robles, J., Hsu, M.J., Register, E., Li, W., Vyas, V., Fan, H., Abruzzo, G.*, et al.* (2005). Specific substitutions in the echinocandin target Fks1p account for reduced susceptibility of rare laboratory and clinical *Candida* sp. isolates. Antimicrob Agents Chemother **49**: 3264-3273.

272 Pasrija, R., Banerjee, D. and Prasad, R. (2007). Structure and function analysis of CaMdr1p, a major facilitator superfamily antifungal efflux transporter protein of *Candida albicans*: identification of amino acid residues critical for drug/H+ transport. Eukaryot Cell **6**: 443-453.

273 Pasrija, R., Panwar, S.L. and Prasad, R. (2008). Multidrug transporters CaCdr1p and CaMdr1p of *Candida albicans* display different lipid specificities: both ergosterol and sphingolipids are essential for targeting of CaCdr1p to membrane rafts. Antimicrob Agents Chemother **52**: 694-704.

274 Pasrija, R., Prasad, T. and Prasad, R. (2005). Membrane raft lipid constituents affect drug susceptibilities of *Candida albicans*. Biochem Soc Trans **33**: 1219-1223.

275 Patterson, J.E., Peters, J., Calhoon, J.H., Levine, S., Anzueto, A., Al-Abdely, H., Sanchez, R., Patterson, T.F., Rech, M., Jorgensen, J.H.*, et al.* (2000). Investigation and control of aspergillosis and other filamentous fungal infections in solid organ transplant recipients. Transpl Infect Dis **2**: 22-28.

276 Paumi, C.M., Chuk, M., Chevelev, I., Stagljar, I. and Michaelis, S. (2008). Negative regulation of the yeast ABC transporter Ycf1p by phosphorylation within its N-terminal extension. J Biol Chem **283**: 27079-27088.

277 Paumi, C.M., Chuk, M., Snider, J., Stagljar, I. and Michaelis, S. (2009). ABC transporters in *Saccharomyces cerevisiae* and their interactors: new technology advances the biology of the ABCC (MRP) subfamily. Microbiol Mol Biol Rev **73**: 577-593.

278 Paumi, C.M., Menendez, J., Arnoldo, A., Engels, K., Iyer, K.R., Thaminy, S., Georgiev, O., Barral, Y., Michaelis, S. and Stagljar, I. (2007). Mapping protein-protein interactions for the yeast ABC transporter Ycf1p by integrated split-ubiquitin membrane yeast two-hybrid analysis. Mol Cell **26**: 15-25.

279 Perfect, J.R., Dismukes, W.E., Dromer, F., Goldman, D.L., Graybill, J.R., Hamill, R.J., Harrison, T.S., Larsen, R.A., Lortholary, O., Nguyen, M.H.*, et al.* (2009). Clinical practice guidelines for the management of cryptococcal disease: 2010 update by the infectious diseases society of america. Clin Infect Dis **50**: 291-322.

280 Perlin, D.S. (2007). Resistance to echinocandin-class antifungal drugs. Drug Resist Updat **10**: 121-130.

281 Pfaller, M.A. and Diekema, D.J. (2007). Epidemiology of invasive candidiasis: a persistent public health problem. Clin Microbiol Rev **20**: 133-163.

282 Pfaller, M.A. and Diekema, D.J. (2010). Epidemiology of invasive mycoses in North America. Crit Rev Microbiol **36**: 1-53.

283 Pfaller, M.A., Messer, S.A., Georgopapadakou, N., Martell, L.A., Besterman, J.M. and Diekema, D.J. (2009). Activity of MGCD290, a Hos2 histone deacetylase inhibitor, in combination with azole antifungals against opportunistic fungal pathogens. J Clin Microbiol **47**: 3797-3804.

284 Phan, Q.T., Myers, C.L., Fu, Y., Sheppard, D.C., Yeaman, M.R., Welch, W.H., Ibrahim, A.S., Edwards, J.E., Jr. and Filler, S.G. (2007). Als3 is a *Candida albicans* invasin that binds to cadherins and induces endocytosis by host cells. PLoS Biol **5**: e64.

285 Piper, P., Mahe, Y., Thompson, S., Pandjaitan, R., Holyoak, C., Egner, R., Muhlbauer, M., Coote, P. and Kuchler, K. (1998). The *Pdr12* ABC transporter is required for the development of weak organic acid resistance in yeast. EMBO Journal **17**: 4257-4265.

286 Pomorski, T., Holthuis, J.C., Herrmann, A. and van Meer, G. (2004). Tracking down lipid flippases and their biological functions. J Cell Sci **117**: 805-813.

287 Poveda, A., Pamblanco, M., Tafrov, S., Tordera, V., Sternglanz, R. and Sendra, R. (2004). Hif1 is a component of yeast histone acetyltransferase B, a complex mainly localized in the nucleus. J Biol Chem **279**: 16033-16043.

288 Prasad, R., De Wergifosse, P., Goffeau, A. and Balzi, E. (1995). Molecular cloning and characterization of a novel gene of *Candida albicans*, *CDR1*, conferring multiple resistance to drugs and antifungals. Curr Genet **27**: 320-329.

289 Ptacek, J., Devgan, G., Michaud, G., Zhu, H., Zhu, X., Fasolo, J., Guo, H., Jona, G., Breitkreutz, A., Sopko, R.*, et al.* (2005). Global analysis of protein phosphorylation in yeast. Nature **438**: 679-684.

290 Rai, V., Shukla, S., Jha, S., Komath, S.S. and Prasad, R. (2005). Functional characterization of N-terminal nucleotide binding domain (NBD-1) of a major ABC drug transporter Cdr1p of *Candida albicans*: uncommon but conserved Trp326 of Walker B is important for ATP binding. Biochemistry **44**: 6650-6661.

291 Ramos, H., Valdivieso, E., Gamargo, M., Dagger, F. and Cohen, B.E. (1996). Amphotericin B kills unicellular leishmanias by forming aqueous pores permeable to small cations and anions. J Membr Biol **152**: 65-75.

292 Raychaudhuri, S. and Prinz, W.A. (2006). Uptake and trafficking of exogenous sterols in *Saccharomyces cerevisiae* Biochem Soc Trans **34**: 359-362.

293 Raymond, M., Dignard, D., Alarco, A.M., Mainville, N., Magee, B.B. and Thomas, D.Y. (1998). A Ste6p/P-glycoprotein homologue from the asexual yeast *Candida albicans* transports the a-factor mating pheromone in Saccharomyces cerevisiae. Mol Microbiol **27**: 587-598.

294 Raymond, M., Gros, P., Whiteway, M. and Thomas, D.Y. (1992). Functional complementation of yeast ste6 by a mammalian multidrug resistance mdr gene. Science **256**: 232-234.

295 Reuss, O., Vik, A., Kolter, R. and Morschhauser, J. (2004). The *SAT1* flipper, an optimized tool for gene disruption in *Candida albicans* Gene **341**: 119-127.

296 Rhodes, J.C., Polacheck, I. and Kwon-Chung, K.J. (1982). Phenoloxidase activity and virulence in isogenic strains of *Cryptococcus neoformans*. Infect Immun **36**: 1175-1184.

297 Riordan, J.R. (2008). CFTR function and prospects for therapy. Annu Rev Biochem **77**: 701-726.

298 Roemer, T., Jiang, B., Davison, J., Ketela, T., Veillette, K., Breton, A., Tandia, F., Linteau, A., Sillaots, S., Marta, C.*, et al.* (2003). Large-scale essential gene identification in *Candida albicans* and applications to antifungal drug discovery. Mol Microbiol **50**: 167-181.

299 Romani, L. (2004). Immunity to fungal infections. Nat Rev Immunol **4**: 1-23.

300 Romsicki, Y. and Sharom, F.J. (1999). The membrane lipid environment modulates drug interactions with the P-glycoprotein multidrug transporter. Biochemistry **38**: 6887-6896.
301 Rosser, M.F.N., Grove, D.E. and Cyr, D.M. (2009). The Use of Small Molecules to Correct Defects in CFTR Folding, Maturation, and Channel Activity. Curr Chem Biol **3**: 420-431.
302 Rust, S., Rosier, M., Funke, H., Real, J., Amoura, Z., Piette, J.C., Deleuze, J.F., Brewer, H.B., Duverger, N., Denefle, P.*, et al.* (1999). Tangier disease is caused by mutations in the gene encoding ATP-binding cassette transporter 1. Nat Genet **22**: 352-355.
303 Sable, C.A., Strohmaier, K.M. and Chodakewitz, J.A. (2008). Advances in antifungal therapy. Annu Rev Med **59**: 361-379.
304 Sachs, C.W., Chambers, T.C. and Fine, R.L. (1999). Differential phosphorylation of sites in the linker region of P-glycoprotein by protein kinase C isozymes alpha, betaI, betaII, gamma, delta, epsilon, eta, and zeta. Biochem Pharmacol **58**: 1587-1592.
305 Saidane, S., Weber, S., De Deken, X., St-Germain, G. and Raymond, M. (2006). *PDR16* -mediated azole resistance in *Candida albicans* Mol Microbiol **60**: 1546-1562.
306 Saini, P., Gaur, N.A. and Prasad, R. (2006). Chimeras of the ABC drug transporter Cdr1p reveal functional indispensability of transmembrane domains and nucleotide-binding domains, but transmembrane segment 12 is replaceable with the corresponding homologous region of the non-drug transporter Cdr3p. Microbiology **152**: 1559-1573.
307 Saito, K., Tautz, L. and Mustelin, T. (2007). The lipid-binding SEC14 domain. Biochim Biophys Acta **1771**: 719-726.
308 Sanglard, D., Ischer, F., Monod, M. and Bille, J. (1996). Susceptibilities of *Candida albicans* multidrug transporter mutants to various antifungal agents and other metabolic inhibitors. Antimicrob Agents Chemother **40**: 2300-2305.
309 Sanglard, D., Ischer, F., Monod, M. and Bille, J. (1997). Cloning of *Candida albicans* genes conferring resistance to azole antifungal agents: characterization of *CDR2* , a new multidrug ABC transporter gene. Microbiology **143**: 405-416.
310 Sanglard, D., Kuchler, K., Ischer, F., Pagani, J.L., Monod, M. and Bille, J. (1995). Mechanisms of resistance to azole antifungal agents in *Candida albicans* isolates from AIDS patients involve specific multidrug transporters. Antimicrob Agents Chemother **39**: 2378-2386.
311 Sanglard, D. and Odds, F.C. (2002). Resistance of *Candida* species to antifungal agents: molecular mechanisms and clinical consequences. Lancet Infect Dis **2**: 73-85.
312 Sano, T., Kihara, A., Kurotsu, F., Iwaki, S. and Igarashi, Y. (2005). Regulation of the sphingoid long-chain base kinase Lcb4p by ergosterol and heme: studies in phytosphingosine-resistant mutants. J Biol Chem **280**: 36674-36682.
313 Saunders, L.R. and Verdin, E. (2007). Sirtuins: critical regulators at the crossroads between cancer and aging. Oncogene **26**: 5489-5504.
314 Scannell, D.R., Butler, G. and Wolfe, K.H. (2007). Yeast genome evolution--the origin of the species. Yeast **24**: 929-942.
315 Schaller, M., Borelli, C., Korting, H.C. and Hube, B. (2005). Hydrolytic enzymes as virulence factors of Candida albicans. Mycoses **48**: 365-377.
316 Schmitt, M.E., Brown, T.A. and Trumpower, B.L. (1990). A rapid and simple method for preparation of RNA from *Saccharomyces cerevisiae*. Nucleic acids research **18**: 3091-3092.

317 Schubert, S., Rogers, P.D. and Morschhauser, J. (2008). Gain-of-function mutations in the transcription factor *MRR1* are responsible for overexpression of the *MDR1* efflux pump in fluconazole-resistant *Candida dubliniensis* strains. Antimicrob Agents Chemother **52**: 4274-4280.

318 Schuetzer-Muehlbauer, M., Willinger, B., Egner, R., Ecker, G. and Kuchler, K. (2003). Reversal of antifungal resistance mediated by ABC efflux pumps from *Candida albicans* functionally expressed in yeast. Int J Antimicrob Agents **22**: 291-300.

319 Sebghati, T.S., Engle, J.T. and Goldman, W.E. (2000). Intracellular parasitism by Histoplasma capsulatum: fungal virulence and calcium dependence. Science **290**: 1368-1372.

320 Seibert, F.S., Chang, X.B., Aleksandrov, A.A., Clarke, D.M., Hanrahan, J.W. and Riordan, J.R. (1999). Influence of phosphorylation by protein kinase A on CFTR at the cell surface and endoplasmic reticulum. Biochim Biophys Acta **1461**: 275-283.

321 Selmecki, A., Forche, A. and Berman, J. (2006). Aneuploidy and isochromosome formation in drug-resistant *Candida albicans.* Science **313**: 367-370.

322 Selmecki, A., Forche, A. and Berman, J. (2010). Genomic plasticity of the human fungal pathogen *Candida albicans*. Eukaryot Cell **9**: 991-1008.

323 Selmecki, A., Gerami-Nejad, M., Paulson, C., Forche, A. and Berman, J. (2008). An isochromosome confers drug resistance *in vivo* by amplification of two genes, *ERG11* and *TAC1* Mol Microbiol **68**: 624-641.

324 Selmecki, A.M., Dulmage, K., Cowen, L.E., Anderson, J.B. and Berman, J. (2009). Acquisition of aneuploidy provides increased fitness during the evolution of antifungal drug resistance. PLoS Genet **5**: e1000705.

325 Servos, J., Haase, E. and Brendel, M. (1993). Gene SNQ2 of Saccharomyces cerevisiae, which confers resistance to 4-nitroquinoline-N-oxide and other chemicals, encodes a 169 kDa protein homologous to ATP-dependent permeases. Mol Gen Genet **236**: 214-218.

326 Shahi, P. and Moye-Rowley, W.S. (2009). Coordinate control of lipid composition and drug transport activities is required for normal multidrug resistance in fungi. Biochim Biophys Acta **1794**: 852-859.

327 Shani, N. and Valle, D. (1996). A *Saccharomyces cerevisiae* homolog of the human adrenoleukodystrophy transporter is a heterodimer of two half ATP-binding cassette transporters. Proc Natl Acad Sci U S A **93**: 11901-11906.

328 Shapiro, A.B. and Ling, V. (1997). Positively cooperative sites for drug transport by P-glycoprotein with distinct drug specificities. Eur J Biochem **250**: 130-137.

329 Sharma, K.G., Kaur, R. and Bachhawat, A.K. (2003). The glutathione-mediated detoxification pathway in yeast: an analysis using the red pigment that accumulates in certain adenine biosynthetic mutants of yeasts reveals the involvement of novel genes. Arch Microbiol **180**: 108-117.

330 Sharma, M., Manoharlal, R., Shukla, S., Puri, N., Prasad, T., Ambudkar, S.V. and Prasad, R. (2009). Curcumin modulates efflux mediated by yeast ABC multidrug transporters and is synergistic with antifungals. Antimicrob Agents Chemother **53**: 3256-3265.

331 Shaw, C.E. and Kapica, L. (1972). Production of diagnostic pigment by phenoloxidase activity of *Cryptococcus neoformans*. Appl Microbiol **24**: 824-830.

332 Shukla, S., Ambudkar, S.V. and Prasad, R. (2004a). Substitution of threonine-1351 in the multidrug transporter Cdr1p of *Candida albicans* results in hypersusceptibility to antifungal agents and threonine-1351 is essential for

synergic effects of calcineurin inhibitor FK520. J Antimicrob Chemother **54**: 38-45.

333 Shukla, S., Rai, V., Saini, P., Banerjee, D., Menon, A.K. and Prasad, R. (2007). Candida drug resistance protein 1, a major multidrug ATP binding cassette transporter of *Candida albicans*, translocates fluorescent phospholipids in a reconstituted system. Biochemistry **46**: 12081-12090.

334 Shukla, S., Saini, P., Smriti, Jha, S., Ambudkar, S.V. and Prasad, R. (2003). Functional characterization of *Candida albicans* ABC transporter Cdr1p. Eukaryot Cell **2**: 1361-1375.

335 Shukla, S., Sauna, Z.E., Prasad, R. and Ambudkar, S.V. (2004b). Disulfiram is a potent modulator of multidrug transporter Cdr1p of *Candida albicans*. Biochemical and biophysical research communications **322**: 520-525.

336 Simonetti, G., Passariello, C., Rotili, D., Mai, A., Garaci, E. and Palamara, A.T. (2007). Histone deacetylase inhibitors may reduce pathogenicity and virulence in *Candida albicans*. FEMS Yeast Res **7**: 1371-1380.

337 Sims, C.R., Ostrosky-Zeichner, L. and Rex, J.H. (2005). Invasive candidiasis in immunocompromised hospitalized patients. Arch Med Res **36**: 660-671.

338 Singh, N. and Paterson, D.L. (2005). *Aspergillus* infections in transplant recipients. Clin Microbiol Rev **18**: 44-69.

339 Sloane, P.A. and Rowe, S.M. (2010). Cystic fibrosis transmembrane conductance regulator protein repair as a therapeutic strategy in cystic fibrosis. Curr Opin Pulm Med **16**: 591-597.

340 Smith, W.L. and Edlind, T.D. (2002). Histone deacetylase inhibitors enhance *Candida albicans* sensitivity to azoles and related antifungals: correlation with reduction in *CDR* and *ERG* upregulation. Antimicrob Agents Chemother **46**: 3532-3539.

341 Smolka, M.B., Albuquerque, C.P., Chen, S.H. and Zhou, H. (2007). Proteome-wide identification of *in vivo* targets of DNA damage checkpoint kinases. Proc Natl Acad Sci U S A **104**: 10364-10369.

342 Smriti, Krishnamurthy, S., Dixit, B.L., Gupta, C.M., Milewski, S. and Prasad, R. (2002). ABC transporters Cdr1p, Cdr2p and Cdr3p of a human pathogen *Candida albicans* are general phospholipid translocators. Yeast **19**: 303-318.

343 Smriti, Krishnamurthy, S.S. and Prasad, R. (1999). Membrane fluidity affects functions of Cdr1p, a multidrug ABC transporter of *Candida albicans* FEMS Microbiol Lett **173**: 475-481.

344 Soe, R., Mosley, R.T., Justice, M., Nielsen-Kahn, J., Shastry, M., Merrill, A.R. and Andersen, G.R. (2007). Sordarin derivatives induce a novel conformation of the yeast ribosome translocation factor eEF2. J Biol Chem **282**: 657-666.

345 Sokol-Anderson, M.L., Brajtburg, J. and Medoff, G. (1986). Amphotericin B-induced oxidative damage and killing of *Candida albicans*. J Infect Dis **154**: 76-83.

346 Soustre, I., Letourneux, Y. and Karst, F. (1996). Characterization of the Saccharomyces cerevisiae RTA1 gene involved in 7-aminocholesterol resistance. Curr Genet **30**: 121-125.

347 Spellberg, B., Ibrahim, A.S., Edwards, J.E., Jr. and Filler, S.G. (2005). Mice with disseminated candidiasis die of progressive sepsis. J Infect Dis **192**: 336-343.

348 Stark, C., Su, T.C., Breitkreutz, A., Lourenco, P., Dahabieh, M., Breitkreutz, B.J., Tyers, M. and Sadowski, I. (2010). PhosphoGRID: a database of experimentally verified *in vivo* protein phosphorylation sites from the budding yeast *Saccharomyces cerevisiae*. Database (Oxford) **2010**: bap026.

349 Steinbach, W.J., Juvvadi, P.R., Fortwendel, J.R. and Rogg, L.E. (2010). Newer combination antifungal therapies for invasive aspergillosis. Med Mycol.
350 Steinbach, W.J., Reedy, J.L., Cramer, R.A., Jr., Perfect, J.R. and Heitman, J. (2007). Harnessing calcineurin as a novel anti-infective agent against invasive fungal infections. Nat Rev Microbiol **5**: 418-430.
351 Subba Rao, G., Bachhawat, A.K. and Gupta, C.M. (2002). Two-hybrid-based analysis of protein-protein interactions of the yeast multidrug resistance protein, Pdr5p. Funct Integr Genomics **1**: 357-366.
352 Sudbery, P., Gow, N. and Berman, J. (2004). The distinct morphogenic states of *Candida albicans*. Trends Microbiol **12**: 317-324.
353 Szczypka, M.S., Wemmie, J.A., Moye-Rowley, W.S. and Thiele, D.J. (1994). A yeast metal resistance protein similar to human cystic fibrosis transmembrane conductance regulator (CFTR) and multidrug resistance-associated protein. J Biol Chem **269**: 22853-22857.
354 Taglicht, D. and Michaelis, S. (1998). *Saccharomyces cerevisiae* ABC proteins and their relevance to human health and disease. Methods Enzymol **292**: 130-162.
355 Tanabe, K., Lamping, E., Adachi, K., Takano, Y., Kawabata, K., Shizuri, Y., Niimi, M. and Uehara, Y. (2007). Inhibition of fungal ABC transporters by unnarmicin A and unnarmicin C, novel cyclic peptides from marine bacterium. Biochemical and biophysical research communications **364**: 990-995.
356 Thakur, J.K., Arthanari, H., Yang, F., Pan, S.J., Fan, X., Breger, J., Frueh, D.P., Gulshan, K., Li, D.K., Mylonakis, E.*, et al.* (2008). A nuclear receptor-like pathway regulating multidrug resistance in fungi. Nature **452**: 604-609.
357 Thaminy, S., Newcomb, B., Kim, J., Gatbonton, T., Foss, E., Simon, J. and Bedalov, A. (2007). Hst3 is regulated by Mec1-dependent proteolysis and controls the S phase checkpoint and sister chromatid cohesion by deacetylating histone H3 at lysine 56. J Biol Chem **282**: 37805-37814.
358 Tjeertes, J.V., Miller, K.M. and Jackson, S.P. (2009). Screen for DNA-damage-responsive histone modifications identifies H3K9Ac and H3K56Ac in human cells. The EMBO journal **28**: 1878-1889.
359 Tomee, J.F. and Kauffman, H.F. (2000). Putative virulence factors of *Aspergillus fumigatus*. Clin Exp Allergy **30**: 476-484.
360 Trunk, K., Gendron, P., Nantel, A., Lemieux, S., Roemer, T. and Raymond, M. (2009). Depletion of the cullin Cdc53p induces morphogenetic changes in Candida albicans. Eukaryot Cell **8**: 756-767.
361 Tsao, S., Rahkhoodaee, F. and Raymond, M. (2009). Relative contributions of the *Candida albicans* ABC transporters Cdr1p and Cdr2p to clinical azole resistance. Antimicrob Agents Chemother **53**: 1344-1352.
362 Tsubota, T., Berndsen, C.E., Erkmann, J.A., Smith, C.L., Yang, L., Freitas, M.A., Denu, J.M. and Kaufman, P.D. (2007). Histone H3-K56 acetylation is catalyzed by histone chaperone-dependent complexes. Mol Cell **25**: 703-712.
363 Tuite, A., Elias, M., Picard, S., Mullick, A. and Gros, P. (2005). Genetic control of susceptibility to *Candida albicans* in susceptible A/J and resistant C57BL/6J mice. Genes Immun **6**: 672-682.
364 Tuite, A., Mullick, A. and Gros, P. (2004). Genetic analysis of innate immunity in resistance to Candida albicans. Genes Immun **5**: 576-587.
365 Tutulan-Cunita, A.C., Mikoshi, M., Mizunuma, M., Hirata, D. and Miyakawa, T. (2005). Mutational analysis of the yeast multidrug resistance ABC transporter Pdr5p with altered drug specificity. Genes Cells **10**: 409-420.

366 van de Veerdonk, F.L., Kullberg, B.J. and Netea, M.G. (2010). Pathogenesis of invasive candidiasis. Curr Opin Crit Care **16**: 453-459.

367 van den Hazel, H.B., Pichler, H., do Valle Matta, M.A., Leitner, E., Goffeau, A. and Daum, G. (1999). *PDR16* and *PDR17*, two homologous genes of *Saccharomyces cerevisiae*, affect lipid biosynthesis and resistance to multiple drugs. J Biol Chem **274**: 1934-1941.

368 Venkateswarlu, K., Denning, D.W., Manning, N.J. and Kelly, S.L. (1995). Resistance to fluconazole in *Candida albicans* from AIDS patients correlated with reduced intracellular accumulation of drug. FEMS Microbiol Lett **131**: 337-341.

369 Vermes, A., Guchelaar, H.J. and Dankert, J. (2000). Flucytosine: a review of its pharmacology, clinical indications, pharmacokinetics, toxicity and drug interactions. J Antimicrob Chemother **46**: 171-179.

370 Verrier, P.J., Bird, D., Burla, B., Dassa, E., Forestier, C., Geisler, M., Klein, M., Kolukisaoglu, U., Lee, Y., Martinoia, E.*, et al.* (2008). Plant ABC proteins--a unified nomenclature and updated inventory. Trends Plant Sci **13**: 151-159.

371 Wada, S., Niimi, M., Niimi, K., Holmes, A.R., Monk, B.C., Cannon, R.D. and Uehara, Y. (2002). Candida glabrata ATP-binding cassette transporters Cdr1p and Pdh1p expressed in a *Saccharomyces cerevisiae* strain deficient in membrane transporters show phosphorylation-dependent pumping properties. J Biol Chem **277**: 46809-46821.

372 Wada, S., Tanabe, K., Yamazaki, A., Niimi, M., Uehara, Y., Niimi, K., Lamping, E., Cannon, R.D. and Monk, B.C. (2005). Phosphorylation of *Candida glabrata* ATP-binding cassette transporter Cdr1p regulates drug efflux activity and ATPase stability. J Biol Chem **280**: 94-103.

373 Walsh, T.J., Anaissie, E.J., Denning, D.W., Herbrecht, R., Kontoyiannis, D.P., Marr, K.A., Morrison, V.A., Segal, B.H., Steinbach, W.J., Stevens, D.A.*, et al.* (2008). Treatment of aspergillosis: clinical practice guidelines of the Infectious Diseases Society of America. Clin Infect Dis **46**: 327-360.

374 Wanders, R.J., Visser, W.F., van Roermund, C.W., Kemp, S. and Waterham, H.R. (2007). The peroxisomal ABC transporter family. Pflugers Arch **453**: 719-734.

375 Wang, L., Tang, Y., Cole, P.A. and Marmorstein, R. (2008). Structure and chemistry of the p300/CBP and Rtt109 histone acetyltransferases: implications for histone acetyltransferase evolution and function. Current opinion in structural biology **18**: 741-747.

376 Wang, Y., Aisen, P. and Casadevall, A. (1995). *Cryptococcus neoformans* melanin and virulence: mechanism of action. Infect Immun **63**: 3131-3136.

377 Waterhouse, A.M., Procter, J.B., Martin, D.M., Clamp, M. and Barton, G.J. (2009). Jalview Version 2--a multiple sequence alignment editor and analysis workbench. Bioinformatics **25**: 1189-1191.

378 Whelan, W.L. (1987). The genetic basis of resistance to 5-fluorocytosine in Candida species and *Cryptococcus neoformans*. Crit Rev Microbiol **15**: 45-56.

379 White, T.C., Marr, K.A. and Bowden, R.A. (1998). Clinical, cellular, and molecular factors that contribute to antifungal drug resistance. Clin Microbiol Rev **11**: 382-402.

380 White, T.C. and Silver, P.M. (2005). Regulation of sterol metabolism in *Candida albicans* by the *UPC2* gene. Biochem Soc Trans **33**: 1215-1218.

381 Whiteway, M. and Bachewich, C. (2007). Morphogenesis in *Candida albicans*. Annual review of microbiology **61**: 529-553.

382 Wilcox, L.J., Balderes, D.A., Wharton, B., Tinkelenberg, A.H., Rao, G. and Sturley, S.L. (2002). Transcriptional profiling identifies two members of the ATP-binding cassette transporter superfamily required for sterol uptake in yeast. J Biol Chem **277**: 32466-32472.

383 Wilson, R.B., Davis, D. and Mitchell, A.P. (1999). Rapid hypothesis testing with *Candida albicans* through gene disruption with short homology regions. J Bacteriol **181**: 1868-1874.

384 Winter, M.C. and Welsh, M.J. (1997). Stimulation of CFTR activity by its phosphorylated R domain. Nature **389**: 294-296.

385 Wirsching, S., Michel, S., Kohler, G. and Morschhauser, J. (2000a). Activation of the multiple drug resistance gene *MDR1* in fluconazole-resistant, clinical *Candida albicans* strains is caused by mutations in a trans-regulatory factor. J Bacteriol **182**: 400-404.

386 Wirsching, S., Michel, S. and Morschhauser, J. (2000b). Targeted gene disruption in *Candida albicans* wild-type strains: the role of the *MDR1* gene in fluconazole resistance of clinical *Candida albicans* isolates. Mol Microbiol **36**: 856-865.

387 Wirsching, S., Moran, G.P., Sullivan, D.J., Coleman, D.C. and Morschhauser, J. (2001). *MDR1*-mediated drug resistance in *Candida dubliniensis*. Antimicrob Agents Chemother **45**: 3416-3421.

388 Wisplinghoff, H., Bischoff, T., Tallent, S.M., Seifert, H., Wenzel, R.P. and Edmond, M.B. (2004). Nosocomial bloodstream infections in US hospitals: analysis of 24,179 cases from a prospective nationwide surveillance study. Clin Infect Dis **39**: 309-317.

389 Wolfger, H., Mamnun, Y.M. and Kuchler, K. (2004). The yeast Pdr15p ATP-binding cassette (ABC) protein is a general stress response factor implicated in cellular detoxification. J Biol Chem **279**: 11593-11599.

390 Woods, J.P. (2002). *Histoplasma capsulatum* molecular genetics, pathogenesis, and responsiveness to its environment. Fungal Genet Biol **35**: 81-97.

391 Wurtele, H., Tsao, S., Lepine, G., Mullick, A., Tremblay, J., Drogaris, P., Lee, E.H., Thibault, P., Verreault, A. and Raymond, M. (2010). Modulation of histone H3 lysine 56 acetylation as an antifungal therapeutic strategy. Nat Med **16**: 774-780.

392 Xhemalce, B., Miller, K.M., Driscoll, R., Masumoto, H., Jackson, S.P., Kouzarides, T., Verreault, A. and Arcangioli, B. (2007). Regulation of histone H3 lysine 56 acetylation in *Schizosaccharomyces pombe*. J Biol Chem **282**: 15040-15047.

393 Xie, W., Song, C., Young, N.L., Sperling, A.S., Xu, F., Sridharan, R., Conway, A.E., Garcia, B.A., Plath, K., Clark, A.T.*, et al.* (2009). Histone h3 lysine 56 acetylation is linked to the core transcriptional network in human embryonic stem cells. Mol Cell **33**: 417-427.

394 Xie, Y., Xu, K., Linn, D.E., Yang, X., Guo, Z., Shimelis, H., Nakanishi, T., Ross, D.D., Chen, H., Fazli, L.*, et al.* (2008). The 44-kDa Pim-1 kinase phosphorylates BCRP/ABCG2 and thereby promotes its multimerization and drug-resistant activity in human prostate cancer cells. J Biol Chem **283**: 3349-3356.

395 Xu, F., Zhang, K. and Grunstein, M. (2005). Acetylation in histone H3 globular domain regulates gene expression in yeast. Cell **121**: 375-385.

396 Xu, Z., Zhang, L.X., Zhang, J.D., Cao, Y.B., Yu, Y.Y., Wang, D.J., Ying, K., Chen, W.S. and Jiang, Y.Y. (2006). cDNA microarray analysis of differential gene expression and regulation in clinically drug-resistant isolates of *Candida albicans* from bone marrow transplanted patients. Int J Med Microbiol **296**: 421-434.

397 Young, L., Leonhard, K., Tatsuta, T., Trowsdale, J. and Langer, T. (2001). Role of the ABC transporter Mdl1 in peptide export from mitochondria. Science **291**: 2135-2138.

398 Young, L.Y., Hull, C.M. and Heitman, J. (2003). Disruption of ergosterol biosynthesis confers resistance to amphotericin B in *Candida lusitaniae*. Antimicrob Agents Chemother **47**: 2717-2724.

399 Yuan, J., Pu, M., Zhang, Z. and Lou, Z. (2009). Histone H3-K56 acetylation is important for genomic stability in mammals. Cell Cycle **8**: 1747-1753.

400 Zacchi, L.F., Schulz, W.L. and Davis, D.A. (2010a). HOS2 and HDA1 encode histone deacetylases with opposing roles in *Candida albicans* morphogenesis. PLoS One **5**: e12171.

401 Zacchi, L.F., Selmecki, A.M., Berman, J. and Davis, D.A. (2010b). Low dosage of histone H4 leads to growth defects and morphological changes in *Candida albicans*. PLoS One **5**: e10629.

402 Zhang, Z., Wu, J.Y., Hait, W.N. and Yang, J.M. (2004). Regulation of the stability of P-glycoprotein by ubiquitination. Mol Pharmacol **66**: 395-403.

403 Zheng, X. and Wang, Y. (2004). Hgc1, a novel hypha-specific G1 cyclin-related protein regulates *Candida albicans* hyphal morphogenesis. The EMBO journal **23**: 1845-1856.

404 Zhou, H., Madden, B.J., Muddiman, D.C. and Zhang, Z. (2006). Chromatin assembly factor 1 interacts with histone H3 methylated at lysine 79 in the processes of epigenetic silencing and DNA repair. Biochemistry **45**: 2852-2861.

405 Znaidi, S., De Deken, X., Weber, S., Rigby, T., Nantel, A. and Raymond, M. (2007). The zinc cluster transcription factor Tac1p regulates *PDR16* expression in *Candida albicans* Mol Microbiol **66**: 440-452.

406 Znaidi, S., Weber, S., Al-Abdin, O.Z., Bomme, P., Saidane, S., Drouin, S., Lemieux, S., De Deken, X., Robert, F. and Raymond, M. (2008). Genomewide location analysis of *Candida albicans* Upc2p, a regulator of sterol metabolism and azole drug resistance. Eukaryot Cell **7**: 836-847.